UNIVERSITÀ
DEGLI STUDI
DI PADOVA

Sede Amministrativa: Università degli Studi di Padova

Dipartimento di Biologia

SCUOLA DI DOTTORATO DI RICERCA IN: Bioscienze e Biotecnologie
INDIRIZZO: Biochimica e Biofisica
CICLO XXVIII

Investigation of mechanisms modulating photosynthetic efficiency in *Nannochloropsis gaditana*

Direttore della Scuola: Ch.mo Prof. Paolo Bernardi
Coordinatore d'indirizzo: Ch.mo Prof. Fabio di Lisa
Supervisore: Ch.mo Prof. Tomas Morosinotto

Dottorando: Andrea Meneghesso

TABLE OF CONTENTS

SUMMARY

Oxygenic photosynthesis is a crucial process for life on earth as it enables plants and algae to convert sunlight into chemical energy, generating molecular oxygen as a byproduct. Light can also be harmful and when in excess can drive to photosystems over-excitation and production of reactive oxygen species (ROS) with the consequent decrease of the overall photosynthetic efficiency. In a highly dynamic natural environment photosynthetic organisms have evolved sophisticated mechanisms to modulate their efficiency to capture and exploit light. For instance the so called *non photochemical quenching* of fluorescence (NPQ) acts dissipating excess energy as heat and it's used as short term response to high light in order to avoid oxidative damages. The carotenoid zeaxanthin belonging to the xanthophyll cycle enhances this thermal dissipation but also has a direct role in the scavenging of ROS generated in the membrane. Acclimation instead is a more complex long term process that acts directly modeling the composition of the photosynthetic apparatus in response to different light intensity, for example through modifications in protein composition. Photoregulation and photoprotection are strongly related also to modulations of flow of excitation energy and electrons across the thylakoid membrane. Indeed the major pathway for the light reactions of photosynthesis, the linear electron flow, can modulate its rate depending on metabolic demand and can be also supported by alternative electron pathway which affect the thylakoid gradient across the membrane and the ATP/NADPH ratio.

The general aim of this work is to investigate the different mechanisms modulating photosynthetic efficiency in the microalga *Nannochloropsis gaditana* in order to increase the limited knowledge about this interesting microalga and exploit it to optimize photosynthetic efficiency in a large-scale cultivation perspective, even through the development of computational models. The spectroscopic tools developed to untangle the complexity of the photosynthetic regulation in *Nannochloropsis* have been successfully applied to study photosynthesis in other photosynthetic organisms such as, *Chlamydomonas reinhardtii, Physcomitrella patens* and *Koliella antarctica.*

Nannochloropsis gaditana is an eukaryotic alga of the phylum of *heterokonta*, originating from a secondary endosymbiotic event. Species of this group have received increasing attention in the scientific community, reflecting their potential application in biofuel production, although the photosynthetic and physiological properties of these organisms remain poorly characterized. *Nannochloropsis* species have a peculiar photosynthetic apparatus characterized by the presence of chlorophyll a, violaxanthin and vaucheriaxanthin as the most abundant pigments.

The regulation of the photosynthetic apparatus in this interesting microalgae has been deeply discussed in Section B. Our study focused firstly on the acclimation response in *Nannochloropsis gaditana* subjected to prolonged exposition to low and high light. Intense illumination induces a decrease in the chlorophyll content and the antenna size of both Photosystem I and II. Cells grown in high light also show increased photosynthetic electron transport, paralleled by an increased contribution of cyclic electron transport around Photosystem I. Even when exposed to extreme light intensities, *Nannochloropsis* cells do not activate photo-protection responses, such as NPQ

and the xanthophyll cycle in a constitutive way. Conversely, these responses remained available for activation upon additional changes in illumination. These results suggest NPQ and the xanthophyll cycle in *Nannochloropsis gaditana* play exclusive roles in response to short-term changes in illumination but only play a slight role, if any, in responses to chronic light stress.

In order to further explore the short term response mediated by xanthophyll cycle the effect of zeaxanthin accumulation in the photosynthetic apparatus of *Nannochloropsis gaditana* was investigated revealing some peculiar aspects. Interestingly zeaxanthin molecules are found to be constitutively present in this microalga, even in conditions of very low light in which the xanthophyll cycle is not yet induced. In addition this xanthophyll does not show a specific binding site in the different protein components of the photosynthetic apparatus and, in addition, has a strong effect in the NPQ response. The influence on NPQ seems to be related mostly on *de novo* synthesis of zeaxanthin while the molecules already present in the photosynthetic apparatus are involved in a transient NPQ active only in the first minute after the dark-light transition.

The regulation of the photosynthetic apparatus has been assessed also in *N. salina* in a growing system more compatible with a large-scale production system, a continuous-flow flat-plate photobioreactor. Interestingly changing the residence time maintaining the same irradiation affects the biomass concentration leading to an acclimation response very similar to that observed for *N. gaditana* grown in batch system, as previously discussed. These results highlight the importance of the biomass concentration and its connection with light supply as parameter to optimize in order to increase the microalgal culture productivity.

The molecular investigation of the mechanisms at the basis of light exploitations in *Nannochloropsis* is the starting point for the development of computational models that aim to simulate and predict microalgae behavior in order to optimize their productivity in large-scale cultivation systems. Section C deals with the development and widespread application of these models, which integrate chlorophyll fluorescence measurements allowing also the representation of complex mechanisms such as NPQ. Such models prove especially useful in identifying which parameters have the largest impact on productivity, thereby providing a means for enhancing growth through design and operational changes. They can also provide guidance for genetic engineering by identifying those modifications having the largest potential impact on productivity.

In Section D the study of photosynthetic processes is expanded to other organisms focusing on the regulation of the photosynthetic electron chain through the employment of several spectroscopic approaches set up during my PhD thesis. In the first work reported we show that the introduction of a mitochondrial mutation in *Chlamydomonas reinhardtii* mutants depleted in the chloroplastic PGRL1 rescue its photosensitivity in high light. Detailed functional analysis of these cells showed that the mitochondria mutation alters the electron transport reactions increasing alternative electron pathways around PSI at the detriment of PSII-related photosynthesis. This work thus clearly shows how mitochondrial activity play a seminal influence on photosynthesis in algae.

The second work presented deals with another important mechanisms to modulate flow of excitation, the Mehler-like reactions mediated by Flavodiiron (FLV) proteins. These proteins were lost during evolution of land plants but are still present in non vascular plants, as the moss

Physcomitrella patens, the model organism employed for this study. *P. patens* mutants depleted in FLV show these proteins are active as an electron sink downstream of Photosystem I. Measurement of electron transport showed that they play a major role particularly in the first seconds after a sudden change in light intensity, when for a few seconds they are the major sink for electrons from PSI. When exposed to fluctuating light FLV mutants showed light sensitivity and PSI photoinhibition, demonstrating their biological role as a safety valve for excess electrons in dynamic light. FLV absence in mutants was, in part, compensated by increased cyclic electron flow, suggesting that their biological role may have been substituted in vascular plants by this other mechanism of alternative electron flow.

Finally we analyzed the time course of physiological and morphological responses to different irradiances in *Koliella antarctica*, a green antarctic microalga isolated from Ross Sea. *K. antarctica* not only modulates cell morphology and composition of its photosynthetic apparatus on a long-term acclimation, but also shows the ability of a very fast response to light fluctuations. The ability to activate such responses is fundamental for survival in its natural extreme environment.

RIASSUNTO

La fotosintesi ossigenica è un processo fondamentale per la vita sulla terra in quanto consente a piante e alghe di convertire la luce solare in energia chimica generando ossigeno molecolare come sottoprodotto. La luce può anche essere dannosa e quando è in eccesso può portare alla sovreccitazione dei fotosistemi e alla produzione di specie reattive dell'ossigeno (ROS) con un conseguente calo dell'efficienza fotosintetica. In un ambiente naturale estremamente dinamico gli organismi fotosintetici hanno evoluto meccanismi sofisticati in grado di modulare la loro efficienza per catturare e sfruttare al meglio la luce. Per esempio il cosiddetto *quenching* non fotochimico della fluorescenza (NPQ) agisce dissipando l'energia in eccesso sotto forma di calore ed è utilizzato come sistema di risposta a breve termine agi stress luminosi col fine di evitare danni ossidativi. Il carotenoide zeaxantina appartenente al ciclo delle xantofille partecipa attivamente a questa risposta di dissipazione termica mantenendo però anche un ruolo diretto nello scavenging dei ROS generati nella membrana tilacoidale. L'acclimatazione invece è un processo a lungo termine che agisce direttamente modellando la composizione dell'apparato fotosintetico in risposta all'intensità della luce ad esempio attraverso modifiche nella composizione proteica. I meccanismi di regolazione e protezione indotti dalla luce sono spesso legati anche a modulazioni dei flussi elettronici attraverso la membrana tilacoidale. La via principale per le reazioni alla luce della fotosintesi infatti, il flusso elettronico lineare, è in grado di modulare la sua attività a seconda della richiesta metabolica e può essere sostenuto anche da pathways elettronici alternativi che influenzano il gradiente tilacoidale e il rapporto ATP / NADPH.

L'obiettivo generale di questo lavoro è quello di indagare i diversi meccanismi che modulano l'efficienza fotosintetica nella microalga *Nannochloropsis gaditana* al fine di aumentare la conoscenza ancora limitata di questa microalga e sfruttarla per ottimizzare l'efficienza fotosintetica in un ottica di coltivazione su larga scala, anche attraverso lo sviluppo modelli di calcolo. Gli strumenti spettroscopici sviluppati per districare la complessità dei meccanismi di regolazione della fotosintesi in *Nannochloropsis* sono stati applicati con successo anche per lo studio di altri organismi fotosintetici quali, *Chlamydomonas reinhardtii*, *Physcomitrella patens* e *Koliella antarctica*.

Nannochloropsis gaditana è un'alga eucariotica del phylum *heterokonts* originata da un evento di endosimbiosi secondaria. Specie di questo gruppo hanno ricevuto una crescente attenzione nella comunità scientifica che riflette la loro potenziale applicazione nella produzione di biocarburanti. Nonostante questo le proprietà fotosintetici e fisiologiche di questi organismi rimangono ancora poco caratterizzate. La specie *Nannochloropsis* possiede un apparato fotosintetico peculiare contenente come pigmenti più abbondanti clorofilla a, violaxantina e vaucheriaxantina. La regolazione dell'apparato fotosintetico in questa microalga è stato approfondito nella Sezione B. Il nostro studio si è concentrato in primo luogo sulla risposta di acclimatazione in *Nannochloropsis gaditana* sottoposta a prolungate esposizioni a luce bassa e alta. L'illuminazione intensa induce una diminuzione del contenuto di clorofilla e delle dimensioni della taglia d'antenna del PSI e II. Cellule coltivate in alta luce mostrano anche un aumento del

trasporto fotosintetico degli elettroni di pari passo con un maggior contributo da parte del trasporto alternativo ciclico. Anche quando esposte a intensità di luce estreme, le cellule di *Nannochloropsis* non attivano le risposte di foto-protezione, come ad esempio NPQ e il ciclo delle xantofille, in modo costitutivo. Al contrario, queste risposte rimangono a disposizione per l'attivazione in risposta a ulteriori modifiche dell' illuminazione. Questi risultati suggeriscono che l'NPQ e il ciclo delle xantofille in *Nannochloropsis gaditana* giocano un ruolo esclusivo in risposta alle variazioni luminose a breve termine, ma solo un ruolo marginale nelle risposte al stress luminosi cronico.

Al fine di esplorare ulteriormente la risposta a breve termine mediata dal ciclo delle xantofille è stato studiato l'effetto dell' accumulo di zeaxantina nell'apparato fotosintetico di *Nannochloropsis gaditana* rivelando alcuni aspetti peculiari. E' interessante notare che le molecole di zeaxantina si trovano ad essere sintetizzate costitutivamente in questa microalga, anche in condizioni di scarsa illuminazione in cui il ciclo delle xantofille non viene indotto. Inoltre questa xantofilla ha dimostrato di non avere un sito di legame specifico nelle diverse componenti proteiche dell'apparato fotosintetico e ha in aggiunta un forte effetto nella risposta di NPQ. L'effetto legato all' NPQ sembra legato principalmente alla sintesi *de novo* di zeaxantina mentre le molecole già presenti nel'apparato fotosintetico sono coinvolte in un NPQ transitorio attivo solo nel primo minuto dopo la transizione luce-buio.

La regolazione dell'apparato fotosintetico è stata valutata anche in *N. salina* in un sistema di coltivazione più compatibile con la produzione su larga scala, un fotobioreattore a flusso continuo. È interessante notare che modificare il tempo di permanenza mantenendo la stessa irradiazione influisce sulla concentrazione di biomassa e produce una risposta di acclimatazione molto simile a quella osservata in *N. gaditana* coltivata in sistema a *batch*, come precedentemente discusso. Questi risultati evidenziano l'importanza della concentrazione della biomassa e la sua connessione con la luce somministrata come parametro da ottimizzare per aumentare la produttività delle colture microalgali.

L'indagine molecolare sui meccanismi alla base dell'utilizzo della luce in *Nannochloropsis* è il punto di partenza per lo sviluppo di modelli computazionali che mirano a simulare e prevedere il comportamento delle microalghe nell'ottica di ottimizzare la produttività in sistemi di coltivazione su larga scala. La Sezione C tratta dello sviluppo e dell'applicazione di questi modelli, che integrano misure di fluorescenza della clorofilla e consentono anche la rappresentazione di meccanismi complessi come l'NPQ. Tali modelli risultano particolarmente utili per identificare i parametri che hanno il maggiore impatto sulla produttività algale fornendo inoltre una guida per individuare quelle modifiche genetiche che hanno il maggiore potenziale impatto sulla produttività.

Nella sezione D lo studio dei processi fotosintetici si espande ad altri organismi focalizzandosi in particolare sui meccanismi di regolazione della catena fotosintetica di trasposto degli elettroni. Questo studio si avvale dell'impiego di diverse tecniche spettroscopiche che ho messo a punto durante la mia tesi di dottorato. Nel primo lavoro riportato viene mostrato come l'introduzione di una mutazione mitocondriale nella microalga *Chlamydomonas reinhardtii* priva della proteina cloroplastica PGRL1 porti ad un recupero delle performance di crescita in condizioni di alta luce. Analisi fotosintetiche effettuate in queste cellule mutanti ha mostrato che la mutazione

mitocondriale altera le reazioni di trasporto degli elettroni aumentando i pathways elettronici alternativi che coinvolgono il PSI e limitando fortemente l'attività del PSII. Questo lavoro dimostra come l'attività mitocondriale abbia un'influenza fondamentale sulla fotosintesi delle microalghe.

Il secondo lavoro presentato si occupa di un importante meccanismo volto a modulare il flusso di eccitazione, le reazioni Mehler-like mediate dalle proteine Flavodiiron (FLV). Queste proteine sono state perse durante l'evoluzione delle piante terrestri, ma sono ancora presenti nelle piante non vascolari, come nel muschio *Physcomitrella patens*, l'organismo modello utilizzato per questo studio. Mutanti di *P. patens* deprivati della proteina FLV mostrano come quest'ultima abbia un ruolo di *sink* degli elettroni a valle del PSI. Misure di trasporto elettronico hanno dimostrato che le FLV svolgono un ruolo importante in particolare nei primi secondi dopo una rapida variazione dell'intensità luminosa, quando per alcuni secondi essi agiscono da principale *sink* degli elettroni provenienti dal PSI. Quando esposti ad una condizione di luce fluttuante i mutanti FLV mostrano fotosensibilità e inibizione del PSI, dimostrando il loro ruolo biologico come valvola di sicurezza in caso di sovrariduzione della catena fotosintetica. L'assenza delle FLV nei mutanti è in parte compensata da un aumento del flusso ciclico degli elettroni, suggerendo che quest'ultimo possa avere sostituito il ruolo biologico delle FLV nelle piante vascolari.

Infine abbiamo analizzato l'andamento nel tempo delle risposte fisiologiche e morfologiche a diverse intensità luminose in *Koliella antarctica*, una microalga verde antartica isolata nel Mare di Ross. *K. antarctica* modula non solo la morfologia cellulare e il suo apparato fotosintetico tramite una risposta acclimatativa a lungo termine, ma mostra anche la capacità di rispondere rapidamente alle variazioni dell'intensità luminosa. La possibilità di attivare tali risposte è fondamentale per la sopravvivenza nel suo ambiente naturale estremo.

SECTION A

Introduction

1. Microalgae as a source of energy

In these last decades the irreversible depletion of traditional sources of fossil fuels coupled with accumulation of greenhouse gases produced by their combustion has led to a global energy crisis. (Amaro et al., 2012). The need to find alternative feedstock able to replace the traditional ones goes towards an eco-sustainable model and has become an absolute priority. One of the most promising renewable resources is represented by photosynthetic organisms able to convert solar energy in high value molecules for industrial exploitation. Therefore, these 'green' alternative forms of energy find in the sun and in the CO_2-fixing process their principal driving force. Among different photosynthetic organisms, the unicellular eukaryotic microalgae show several advantages that make them an optimal candidate for industrial exploitation. The high solar energy conversion efficiency, that is the ability to collect light and efficiently exploit it to feed all the cellular metabolisms (Dismukes et al., 2008), together with the high growth rates and oil productivities represent their most important features (Chisti, 2007; Schenk et al., 2008). In addition, microalgae are capable of sustaining all year round production, they use less water than land plants to grow and don't require agricultural land, thus not competing with food production (Searchinger et al., 2008; Dismukes et al., 2008). They can be cultivated in wastewater with the potential of bio-treatment of waste derived from municipal, agricultural and industrial activities (Pittman et al., 2011), providing an additional environmental benefit. Last but not least, microalgae can be grown at high yields even in large scale production system (Brennan and Owende, 2010) and can adapt to different environmental conditions, a capacity suitable with outdoor cultivation (Grobbelaar, 2011).

Despite this great potential, the green biofuel industry is still at the beginning due to the high costs involved compared to the current petroleum prices (Norsker et al., 2011). For this reason at present microalgae are mainly used for production of high-value molecules in the chemical, nutraceutical, pharmaceutical and cosmetic industries (Wijffels et al., 2013; Brennan and Owende, 2010). One major drawback in the production of algal biomass is the limited knowledge of the mechanisms that control photosynthesis and the overall cellular metabolisms (Amaro et al., 2012). The absorption and exploitation of light, for example, play a pivotal role in the overall biomass productivity and need to be maximized (Carvalho et al., 2011).

The study of the biological principles governing photosynthesis has thus a seminal role for the development of microalgal-based technologies. In this scenario, a new promising approach is also found in the development of mathematical models able to describe the extreme complexity of the biological processes (Bernardi et al., 2014; García-Camacho et al., 2012; Papadakis et al., 2012). This innovative strategy can predict the growth performances in different conditions allowing the optimization of operating conditions in large scale production system.

1.1 *Nannochloropsis*: an interesting model for photosynthetic study

In the last few years, species belonging to the *Nannochloropsis* genus have gained increasing interest for their possible exploitation for biodiesel production due to their rapid growth rate and ability to accumulate a large amount of lipids (Bondioli et al., 2012; Rodolfi et al., 2009; Sforza et al., 2012; Simionato et al., 2011). These microalgae belong to the *Eustigmatophyceae* class within *Heterokonta*, which also includes diatoms and brown algae (Cavalier-Smith, 2004; Riisberg et al., 2009). They originated from a secondary endosymbiotic event in which an eukaryotic host cell engulfed a red alga (Archibald and Keeling, 2002). *Nannochloropsis* genus includes six species, one grows in fresh water, while the others are all found in marine environment. In particular *Nannochloropsis gaditana*, the marine species chosen for this work, has a cell size of 2-5 µm with a chloroplast that occupies most of the cell volume (Simionato et al., 2013).
Despite the growing attention related to its industrial exploitation, little molecular information is available on the photosynthetic apparatus of *Nannochloropsis*. *Nannochloropsis* presents distinct features with respect to other photosynthetic organisms and this makes it an interesting model for photosynthetic study. First of all *Nannochloropsis* presents only Chl a, lacking Chl b and c or any other accessory Chl at difference with other *Heterokonta* (Guillard and Lorenzen, 1972; Preisig and Wilhelm, 1989). Moreover the amount of carotenoid violaxanthin in control conditions is significantly higher compared to vascular plants, moss and green algae but also to the evolutionary closer diatoms containing diadinoxanthin xanthophyll (Lubián et al., 2000; Lavaud et al., 2002). This atypical pigmentation and the endosymbiotic origin suggest a peculiar photosynthetic regulatory system that still needs to be understood in detail.

2. Oxygenic Photosynthesis

Photosynthesis is the biological process used by plants, algae and cyanobacteria to convert light energy into chemical energy stored in the form of organic carbon compounds. Light energy is first used to synthesize high energy molecules (ATP, NADPH) through the so-called Light Phase. Afterward these molecules are employed to fix CO_2 in organic compounds during the light-independent phase of photosynthesis, the so-called Dark Phase. In eukaryotic algae and terrestrial plants photosynthesis occurs in specialized organelles known as chloroplasts. Chloroplasts entered the eukaryotic lineage through an endosymbiotic event over one billion years ago. The photosynthetic endosymbiont, most likely the prokaryote cyanobacteria, lost its autonomy during the evolution by means of conspicuous translocation of genetic material to the host cells (Keeling, 2010; Dyall et al., 2004).
The plant chloroplast is delimited by a double layer of membrane, the inner and the outer membrane, that together constitute the *envelope* (Figure 1A). While the inner membrane contains specific transporters which control the flux of metabolites from the cytoplasm, the outer membrane is highly permeable. The double layered *envelope* is one of the lines of evidence that the single endosymbiotic

event happened in plants, green algae and red algae. Surrounded by the *envelope* and detached from it by a liquid space (*stroma*), a complex system of membranes forms the thylakoids. The thylakoid membranes contain protein complexes that catalyze the photosynthesis light reactions. The *stroma* solution contains the plastidial DNA, RNA, ribosomes and all the enzymes that catalyze the dark reactions. In higher plants thylakoids are organized in two physical and functional compartments: the *grana* and the *stroma lamellae*. The *grana* are formed of appressed and piled sacs connected to each other by non-appressed regions, the *stroma lamellae* (Figure 1A). The aqueous continuous space surrounded by thylakoid membranes is called *lumen*.

The chloroplast structure in the organisms belonging to the phylum of the *Heterokonta*, which includes diatoms, brown algae and Eustigmatophytes (Cavalier-Smith, 1986), shows several differences compared to higher plants as a consequence of the particular evolutionary history. Indeed this group of algae originated from a secondary endosymbiotic event in which an eukaryotic host cell engulfed a red alga (Archibald and Keeling, 2002). Accordingly, the chloroplast has an *envelope* with four membranes instead of two and the thylakoids are arranged in continuous stacks of three and are not segregated into stromal and granal regions, as observed in the eustigmatophycea *Nannochloropsis gaditana* (Figure 1B) (Lepetit et al., 2012; Simionato et al., 2013).

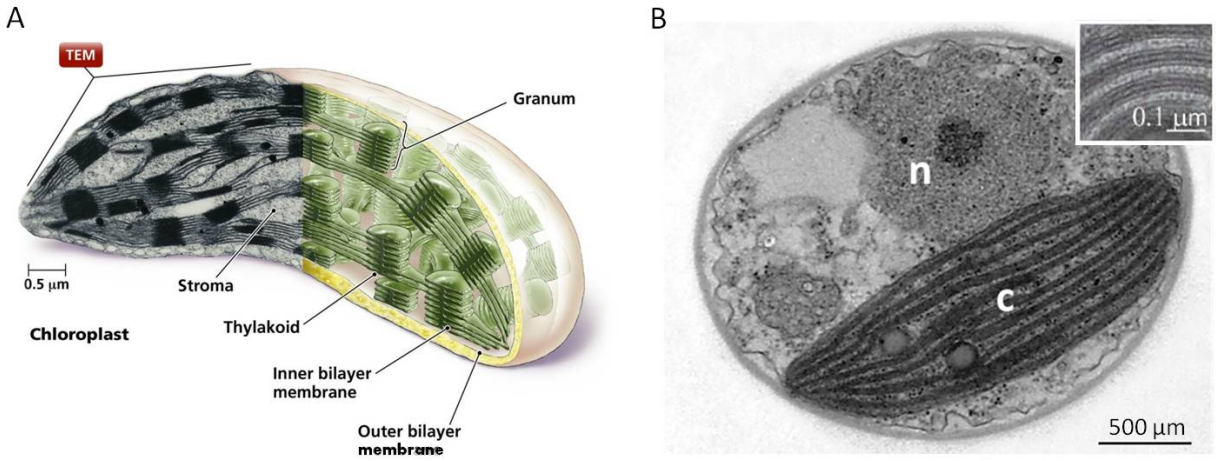

Figure 1. The chloroplast. A) The structure of plant chloroplast. Half chloroplast is a Transmission Electron Microscopy (TEM) picture, the other half a schematic representation (Pearson Education, Inc., publishing as Benjamin Cummings). B) Transmission Electron Microscopy of *Nannochloropsis gaditana* cells. Panel in the right shows magnifications focusing on the thylakoid membrane organization. The organelles are indicated as: n, nucleus; c, chloroplast (picture from Chapter 1, Section B).

2.1. The light absorbing complexes: Photosystem II and Photosystem I

Photosystems II and I (PSII and PSI) are protein complexes localized in the thylakoid membranes responsible for light harvesting and conversion into chemical energy. Although structurally different, they both are characterized by two moieties: a core complex, which includes the reaction centers in which the photochemical event occurred, and an antenna complex, formed of pigment binding proteins involved in light harvesting. The light absorbed in the antenna complex can be transferred between pigments by Förster resonance energy transfer. The absorbed light energy is then funneled into the photosystems reaction center moving preferentially from carotenoids to chlorophylls.
Among photosynthetic organisms the core complex of photosystems is highly conserved during evolution, accordingly to their common endosymbiotic origin (Archibald and Keeling, 2002). PSI and PSII core are composed by the products of the genes *Psa* and *Psb*, respectively. Both are encoded either by nuclear or chloroplast genomes. On the other hand, antenna complex exclusively composed of nuclear-encoded subunits, shows greater variability amongst different groups of organisms (Neilson and Durnford, 2010). In both photosystems antenna is composed by polypeptides members of a large multigene family, the Light Harvesting Complexes (LHC) family. These proteins have three transmembrane helices and bind chlorophylls and carotenoids (Green and Durnford, 1996).

2.1.1.Photosystem II: reaction center

PSII is a multisubunit protein complex also called water-splitting enzyme of photosynthesis because it catalyses the electron transfer from water to the downhill processes of light reactions. It is present in all types of oxygenic photosynthetic organisms like plants, algae and cyanobacteria (Barber, 2012). It is composed by different subunits encoded by *Psb* genes (PsbA-D, PsbO-Q). PsbA-D are large membrane intrinsic subunits that form the PSII core complex, the reaction centers containing moiety. In particular D2 (PsbD) and D1(PsbA) are two homologous proteins that bind all the redox-active cofactors involved in the energy conversion process. CP47(PsbB) and CP43(PsbC) are internal antennae of PSII (Figure 2) (Barber, 2012). PsbO-Q are three membrane extrinsic subunits attached to the lumenal side of PSII. These subunits compose the oxygen evolving complex (OEC) responsible for water oxidation, generation of protons, electrons and molecular oxygen (Figure 2) (Ferreira, 2004). In addition, there is a large number of small subunits, most of which with one transmembrane helix (Dekker and Boekema, 2005).
PSII contains a series of electron transport cofactors that mediate the different oxido-reduction reactions within its reaction center (Figure 2): the primary donor P680, a special Chl a pair with an absorption maximum at 680 nm; pheophytin (Phe), a Chl molecule lacking the central Mg2+; quinone A (Q_A), the first stable electron acceptor in PSII; quinone B (Q_B), converted into a mobile electron carrier after accepting two electrons from Q_A. The double protonated PQH_2 is released from the Q_B-binding site of PSII into the lipid bilayer, where it is subsequently oxidized by photosystem I (PSI) via the cytochrome b6f complex (Barber, 2012).

In cyanobacteria and photosynthetic eukaryotes, PSII core assembles as a dimer and forms a supercomplex with a variable number of antenna proteins (Nield et al., 2000; Dekker and Boekema, 2005; Umena et al., 2011).

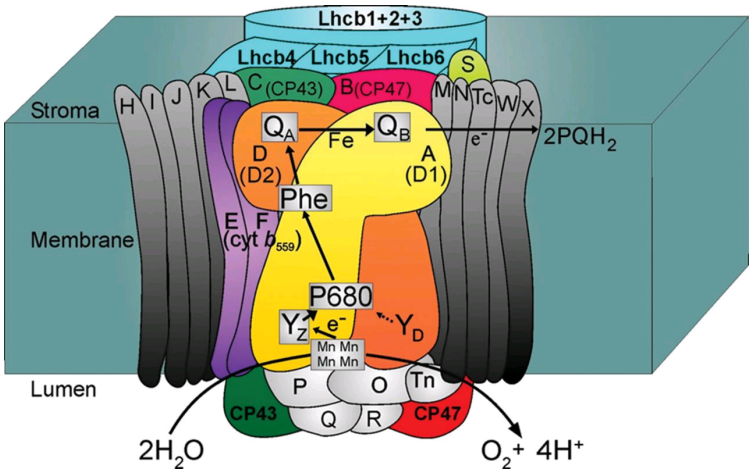

Figure 2. Structure and subunit composition of PSII of higher plants and green algae. PSII is composed of: core complex, mainly represented by the subunit PsbD (D2, orange) and PsbA (D1, yellow); antenna complex with Lhcb 1+2+3, the major antennas, and Lhcb 4, 5 and 6, the minor antennas (light blue); oxygen evolving complex (OEC) with the PsbO-Q subunits (white). Electron transfer pathway from water oxidation to plastoquinone reduction is indicated as arrows. (Barber, 2012)

2.1.2 Photosystem I: reaction center

PSI is a multisubunit protein complex that operates as a light dependent oxidoreductase transporting electrons from plastocyanin (PC) to $NADP^+$, through ferredoxin (Fd) (Figure 3). PC, a copper-containing protein, and Fd, an iron-sulfur protein, are two small soluble electron carriers located in the lumenal and stromal side of PSI, respectively. Upon excitation, the primary charge separation in PSI reaction center occurrs in P700, a Chl a dimer with an absorption maximum at 700 nm. Afterward electrons proceed through A_0 (chlorophyll *a*), Q_k (phylloquinone) and three 4Fe-4S clusters Fx, F_A, F_B and are finally transferred to Fd (Figure 3). The photoxidized P700 is successively reduced by PC.

The PSI core is highly conserved among plants, algae and cyanobacteria (Dekker and Boekema, 2005). Among 14 proteins constituting the PSI core, PsaA and PsaB coordinate most of the components of the electron transport chain, including the primary electron donor P700 (Jensen et al., 2007). Other subunits of the complex provide the docking site for Fd on PSI stromal side (PsaD and PsaE) and interact with PC (PsaF and PsaN) (Figure 3) (Jensen et al., 2007). At difference from PSII, PSI core in higher plants, green algae and diatoms is a monomer (Scheller et al., 2001; Germano et al.,

2002; Ikeda et al., 2008a; Veith and Büchel, 2007). On the contrary, in cyanobacteria, PSI can be both in a trimeric and a monomeric form (Kruip et al., 1994; Jordan et al., 2001).

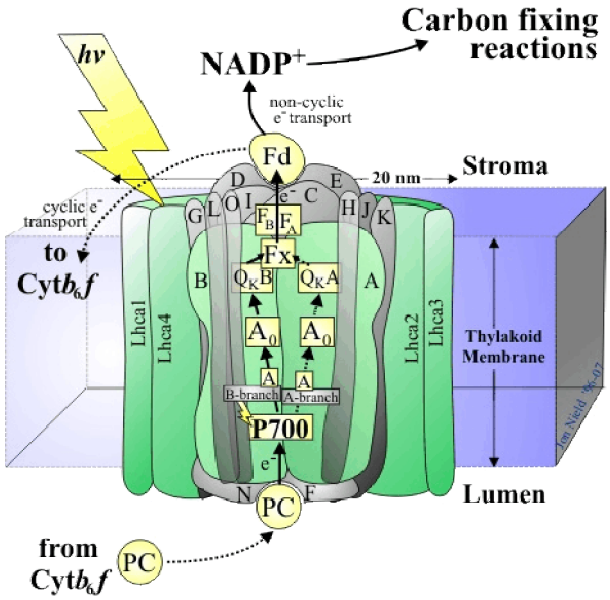

Figure 3. Structure and subunit composition of PSI of higher plants. PSI is mainly composed of: a core complex, mainly represented by the subunit PsaA and PsaB; antenna complex with four Lhca subunits (Lhca1-4). Electron transfer pathway from Plastocyanin (PC) to Ferredoxin (Fd) is indicated as arrows. (http://photosynthesis.sbcs.qmul.ac.uk/nield/downloads.htlm)

2.1.3 Light harvesting complex

Unlike the core complex of photosystems, antenna complex shows greater variability among the different groups of photosynthetic organisms. The higher variability in antenna system accounts for changes in the strategies for harvesting and dissipating light energy required to survive in extremely variable habitat (Neilson and Durnford, 2010). In the evolution of photosynthetic organisms there was a transition from phycobilisome-based antenna, probably owned by earliest photosynthetic eukaryotes, to membrane integral light-harvesting complexes (LHCs). The phycobilisome is an highly structured assembly bound extrinsically to the reaction center (Mullineaux, 2008; Grossman et al., 1993) and it is still the dominant antenna system in cyanobacteria. In the case of photosynthetic eukaryotes its absence has triggered diversification of the LHC antenna system (Neilson and Durnford, 2010).

In all photosynthetic eukaryotes the antenna system is composed of membrane proteins belonging to the multigenic Light Harvesting Complex (LHC) family which has diverged into different groups (Green and Durnford, 1996). In the green lineage, for example, the antenna complex of PSII and PSI is

composed by chlorophyll a/b-binding proteins belonging to LHCB and LHCA group, respectively (Klimmek et al., 2006; Jansson, 1999; Jensen et al., 2007). Also the light-harvesting system in *heterokonts* is formed by protein subunits belonging to the LHC family. In diatoms and brown algae, for example, these antenna complexes are characterized by Fucoxanthin-chlorophyll proteins (FCPs), also called LHCF (Durnford et al., 1996; Devaki and Grossman, 1993). Their pigment content differs considerably from plants light-harvesting complex and thus their absorption capabilities. FCPs do not possess Chl b but use Chl c as an accessory pigment and contain fucoxanthin as the major light-harvesting xanthophyll, not present in plants. Fucoxanthin bound to the proteins enables absorption between 460 and 570 nm, a range of wavelengths not used by higher plants and green algae (Beer et al., 2006). In addition, in FCP the Chl a:carotenoid ratio is 4:4 (Papagiannakis et al., 2005), much lower than for higher plants where it is around 14:4 (Liu et al., 2004). The association of the antenna system of this *heterokonts* with PSI or PSII has not been clearly demonstrated yet (Veith et al., 2009; Brakemann et al., 2006; Ikeda et al., 2008b). Among *heterokonts*, *Nannochloropsis* species are known to have a unique property of presenting only Chl a and lacking Chls b and c or any other accessory Chls (Preisig and Wilhelm, 1989; Basso et al., 2014). In the case of *N. gaditana*, a member of the LHC family was identified and named violaxanthin–Chl a-binding protein (VCP) because of its high violaxanthin content (Sukenik et al., 1992, 2000).
In addition to light harvesting, the different members of the multigenic family of LHC proteins are also involved in protection against excess illumination (Dittami et al., 2010; Zhu and Green, 2010). Indeed, LHC proteins are involved in several regulatory mechanisms in photosynthetic eukaryotes, including photosynthetic acclimation (Ballottari et al., 2007) and heat dissipation of excess energy (Niyogi and Truong, 2013; Peers et al., 2009).

2.2. The Light Phase

The light phase of photosynthesis includes all the reactions that take place in the thylakoids membrane of the chloroplast aimed at absorbing light and converting it into chemical energy. Once absorbed light drives a linear electron flow (LEF) from water to NADPH by two photosystems (PSI and PSII) powering the transfer of electrons to $NADP^+$. The proton gradient generated during this electron flowing across the membrane leads to the production of free energy in the form of ATP (Figure 4). These two molecules are the driving force for the dark phase described in the next paragraph.
The first step of light phase is the harvesting of solar energy by chlorophylls and carotenoids bound to light harvesting complexes (LHC). The light energy, once harvested, is transferred to the reaction center where the photochemical event takes place. This event involves a charge separation representing the beginning of an electron transfer across the membrane from PSII to PSI as described in the Z-scheme (HILL and BENDALL, 1960). The source of electrons is continuously maintained by water splitting performed in the OEC. The electron flow is mediated by intersystem electron carriers that consist of a pool of plastoquinone molecules (PQ), the $Cytb_6f$ complex and plastocyanin (PC) (Figure 4). PQ and PC are mobile electron carriers soluble in the thylakoid membrane and in the

thylakoid lumen, respectively. Cytb$_6$f is a transmembrane protein complex comprising a Fe-S cluster and four hemes. It functions by transferring electrons from PQ to PC and consequently from PSII to PSI. In the oxidized form, PQ is bound to PSII and accepts two electrons from water and two protons from the stroma, becoming in this way a mobile carrier (plastoquinol, PQH2). Cytb$_6$f oxidizes PQH2 and reduces PC transferring proton from stroma to lumen thus acting as a proton pump (Crofts and Meinhardt, 1982). The reduced PC transfers the electrons directly to PSI, thus reducing the reaction center previously oxidized by light. Through several intermediates, PSI reduces ferredoxin (Fd) in the stroma, which in turn donates electrons to $NADP^+$, in a reaction catalyzed by ferredoxin-NADPH-oxidoreductase (FNR).

During the entire photosynthetic pathway a proton gradient across the membrane is built up. This is due to the release of protons derived from oxidation of water (4 protons for each O_2 molecule) in the thylakoid lumen and Cytb$_6$f activity (3 protons for every 2 electrons transported to PSI) and their consumption in the stroma to produce NADPH (Figure 4). The electrical potential and the difference in proton concentration between the stromal and the lumenal side of the membrane leads to the formation of an electrochemical potential used by the transmembrane ATP synthase to drive ATP synthesis (MITCHELL, 1961; Hammes, 1982).

The linear electron flow, the chain of redox reactions starting from the splitting of water and ending with the production of NADPH and ATP, is widely accepted as the major pathway for the light reactions of photosynthesis (Figure 4) (Arnon et al., 1958). However, other alternative flows generate ATP without production of O_2 and NADPH (ARNON et al., 1954) (see paragraph 3).

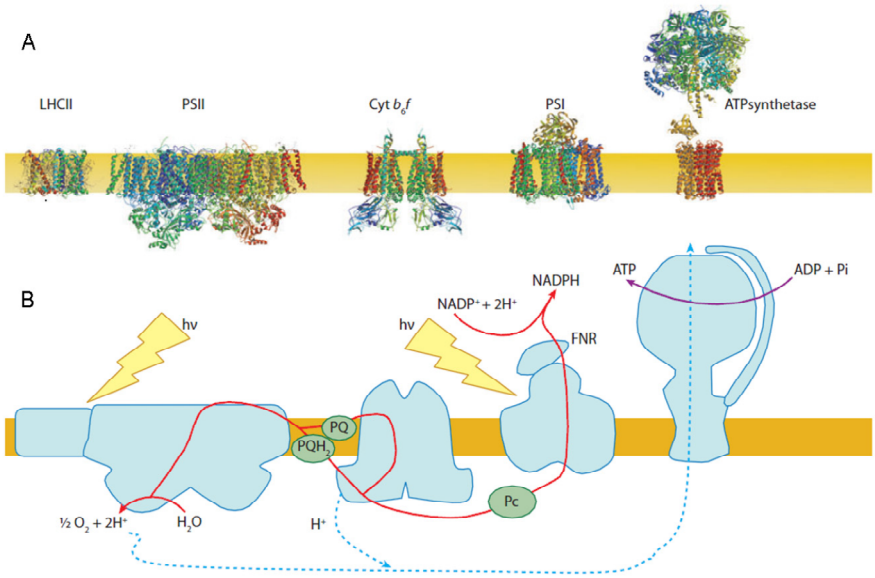

Figure 4. Representation of photosynthesis light reactions. A) Christallographic structure of the principal photosynthetic transmembrane complexes in their native oligomerization state. B) Schematic representation of the linear electron flow (red line) and proton translocation (blue dashed line) through major protein shown in A. LHCII (Light harvesting complex related to PSII); PSII (Photosystem II) ; Cytb$_6$f (Cytochrome b$_6$f); PSI (Photosystem I); hv (light energy); PQ/PQH2 (plastoquinone/plastoquinol); PC (plastocyanin); FNR (ferredoxin-NADPH-oxidoreductase). (Eberhard et al., 2008).

2.3. The Dark Phase

The dark phase of photosynthesis occur in the *stroma* of the chloroplast and involves all the reactions that assimilate atmospheric CO_2 in organic compounds using ATP and NADPH previously formed in the light phase. These reactions constitute the Calvin-Benson cycle (Calvin and Benson, 1948) which can be divided in three phases (Figure 5). The first one, called carboxylation, is catalyzed by the enzyme ribulose bisphosphate carboxylase/oxygenase (RuBisCO) which converts Ribulose 1,5-Bisphosphate (RuBP) into two molecules of 3-Phosphoglycerate in the presence of CO_2 and H_2O. In the following phase 3-phosphoglycerate is reduced to Glyceraldehyde-3-Phosphate (G3P) at the expense of ATP and NADPH. Finally RuBP is regenerated from G3P using ATP thus closing the cycle. At the end of the process 1 G3P is synthesized from 3 molecules of CO_2, 9 ATP and 6 NADPH (Figure 5). Part of G3P is also converted into sucrose or starch.

The principal enzyme of Calvin cycle is RuBisCO which catalyzes the CO_2 fixation. This enzyme is the most abundant enzyme on our planet and can be regulated by light through the Rubisco activase protein (Zhang and Portis, 1999). Moreover light-driven reactions in the thylakoids membrane lead to the formation of reduced ferredoxin that in turn reduces thioredoxin in a reaction catalyzed by ferredoxin-thioredoxin reductase. The reduced thioredoxin regulates enzymes from the Calvin cycle by reducing disulfide bridges that control their activity (Berg et al., 2002). Therefore, despite the name 'dark reactions', it is clear that this process occurs only when light is available.

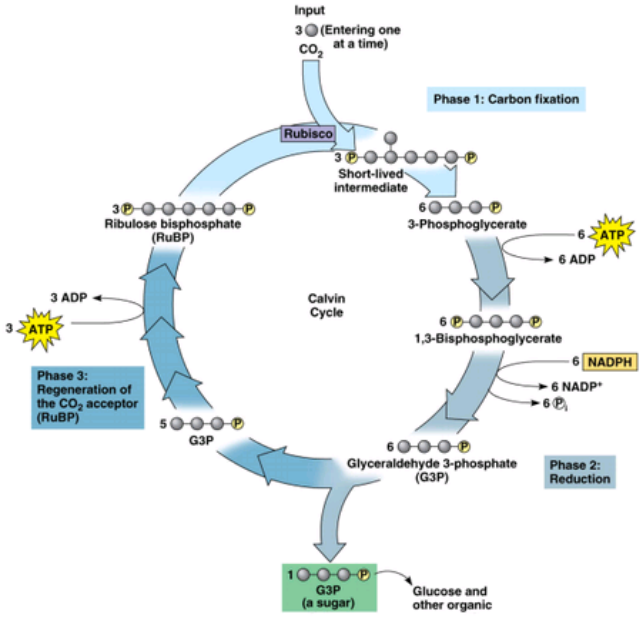

Figure 5. The Calvin cycle. Schematic representation of the three principal phases of Calvin-Benson cycle. G3P (Glyceraldehyde-3-Phosphate); RuBp (Ribulose 1,5-Bisphosphate). (Campbell Biology, Reece et al., 9th Edition)

3. Alternative pathway to LEF

The linear electron flow (LEF) is the major pathway for the light reactions of photosynthesis but other type of electron flows have been also identified. The so called alternative electron flows act modulating the thylakoid gradient across the membrane and the ATP/NADPH ratio depending on metabolic demand. It was also thought that they create futile cycles which avoid over-reduction of photosynthetic electron transport chain, preventing ROS production and photo-damage in case of excessive light intensity (Peltier et al., 2010; Eberhard et al., 2008).

3.1 Alternative pathway to LEF: Cyclic electron flow

3.1.1 Cyclic electron flow: two major pathways

Cyclic electron flow (CEF) was discovered in isolate chloroplasts, as a process that requires Fd to generate ATP without production of O_2. (ARNON et al., 1954). It is now well established that this process recycles electrons around PSI generating ATP without accumulation of NADPH (Shikanai, 2007). In plants, two partially redundant routes of CEF have been identified (Leister and Shikanai 2013). The first one, generally called AA-sensitive in higher plants, involves ferredoxin and the PGR5/PGRL1 complex, while the second route, referred as AA-insensitive, employs a thylakoid NDH complex (Figure 6).

In *A. thaliana*, a model organism for the study of these processes, mutants of the first (*pgr5)* and the second (*crr)* pathway have been generated. Both single mutants grew like wild type under standard conditions despite the decrease CEF activity. On the contrary, in the double mutant *crr pgr5,* growth and photosynthesis are severely impaired even to constant low light (Munekage et al., 2004). This underlines the significance of this alternative electron flow for the overall fitness of the organism.

- The antimycin A sensitive pathway (The PGR5/PGRL1 complex). This pathway is dependent on an unidentified activity called FQR (ferredoxin-quinone reductase), which mediates the reinjection of electrons from Fd to the PQ pool and so to the principal electron flow. In higher plants this pathway is sensitive to antimycin A (AA), an inhibitor known to interact with the Q_i binding pocket located on the stromal side of the cytochrome b_6/f complex (Bendall and Manasse, 1995).

One accredited hypothesis suggests that the activity of the elusive FQR enzyme could be partially executed by the PGR5/PGRL1 complex (Figure 6) (Shikanai, 2007). PGR5 is an extrinsic thylakoid protein that has been proposed to be bound to PGRL1 at the stroma-exposed surface of thylakoids (Munekage et al., 2002). The integral thylakoid protein PGRL1, in turn, anchored the complex to the membrane. In higher plants this complex transiently shuttle between PSI and the $Cytb_6f$ complex to allow efficient Fd-dependent CEF around PSI (DalCorso et al., 2008; Hertle et al., 2013). While in the green alga *C. reinhardtii* PGRL1 has been detected in a PSI–FNR–Cyt *bf* supercomplex that has intrinsic CEF activity (Figure 6) (Iwai et al., 2010; Terashima et al., 2012). In this organism this CEF pathway is

not sensitive to AA (Iwai et al., 2010). Although transcription of both PGR5 and PGRL1 genes was observed in *C. reinhardtii* (Petroutsos et al., 2009), only PGRL1 was detected in the active CEF supercomplex (Iwai et al., 2010). This data suggests a different role of PGR5 in plant and *C. reinhardtii* CEF (Minagawa and Tokutsu, 2015).

- The antimycin A insensitive pathway (The NADPH dehydrogenase complex). This CEF pathway, called in this way for the AA-insensitivity in higher plants, involves the activity of a NDH complex (NAD(P)H plastoquinone reductase) located in the thylakoid membrane. The thylakoidal NDH complex is a multi-protein complex which redirects electrons from NADPH (or NADH) to the PQ pool (Figure 6). It is analogous to NADH dehydrogenase complex (Complex I) of the mitochondrial respiratory chain and its mechanism of action has not been fully elucidated yet.

The first evidences that the NDH enzyme is involved in CEF have been found in the cyanobacterium *Synechocystis*. It was found that a mutant defective in chloroplastic gene *ndhB* (M55 mutant) has an impaired CEF around PSI (Ogawa, 1991). Afterward it has been shown that mutant plants defective in the NDH complex had a slightly reduced CEF, confirming a role of NDH in the electrons transport from the stromal electron pool to PQ (Hashimoto et al., 2003; Shikanai et al., 1998). In higher plants the subunit composition and the hypothetical role of the NDH complex was determined (Rumeau et al., 2005). In addition it was found to interact with PSI to form the NDH-PSI supercomplex (Peng and Shikanai, 2011). On the contrary, the NDH complex appears to be absent in *C. reinhardtii* (Peltier and Cournac, 2002). A type-2 NADPH dehydrogenase was shown to be active in cyclic electron transport in this green algae (Jans et al., 2008; Desplats et al., 2009).

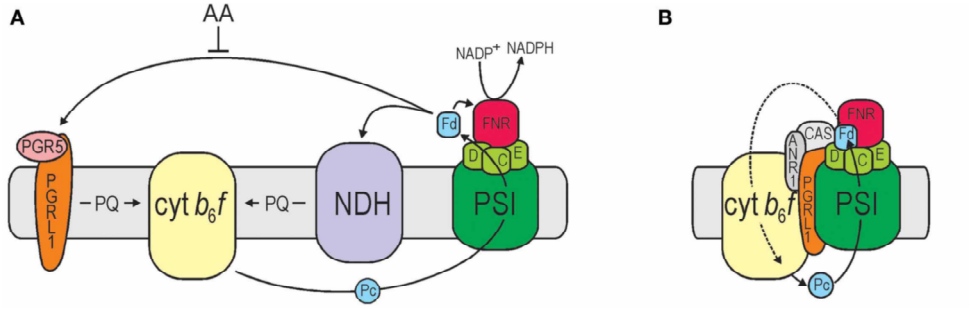

Figure 6. Schematic representation of CEF in two model organisms. A) CEF model in vascular plants operating via the PGRL1/PGR5-dependent (AA-sensitive) and NDH-dependent (AA-insensitive) pathway. B) CEF model in *C. reinhardtii* in which CEF could be mediated by a PSI-FNR-Cytb_6f -PGRL1 supercomplex. Fd (ferredoxin); Pc (plastocyanin); PQ (plastoquinone). (Leister and Shikanai, 2013)

3.1.2 Cyclic electron flow: molecular model

The lack of a generally accepted technique to measure CEF, the current technical limitations and the limited knowledge of the molecular mechanisms that drive CEF have prevented any clarifications of its function (Leister and Shikanai, 2013). At present four different models have been postulated to explain the interaction between linear and cyclic electron flow. The models proposals consider mostly experimental evidences collected in higher plants (Eberhard et al., 2008) and are described below :

- Restricted diffusion model. This model relies on the observations that the different photosynthetic protein complexes are distributed heterogeneously in the thylakoid membranes of higher plants, except for $Cytb_6f$. PSII and PSI are separated in two physically distinct compartments, the *grana* stack and the *stroma lamellae*, respectively (Albertsson, 2001). These two areas are energetically isolated as confirmed by restricted diffusion of the soluble electron carriers PQ (Lavergne and Joliot, 1991) and PC (Kirchhoff et al., 2004). According to the model, LEF and CEF processes are limited in the *grana* and *stroma lamellae*, respectively. PSII transfers electrons only to those $Cytb_6f$ and PSI complexes located in the *grana* and in their periphery, while PSI and NDH complexes only to $Cytb_6f$ in the *stroma lamellae* to drive CEF. Therefore there is no competition between the two electron flow because of the spatial separation.

- The super-complex model. This model represents an extreme case of the previous one, in which the domain where CEF occurs, the *stroma lamellae*, is further reduced to a supercomplex. According to this model, CEF in plants occurs in PSI-$Cytb_6f$ supercomplexes containing PC and Fd (Joliot and Joliot, 2002). In this way Fd involved in CEF would be trapped within supercomplex and thus not shared and accessible to LEF (DalCorso et al., 2008). The existence of this supercomplex has not been yet confirmed experimentally (Breyton et al., 2006).

- Competitive model As suggested by its name this model relies on a competition between CEF and LEF for the same reducing equivalents in the form of Fd. Fd can bind to FNR driving LEF transport or to Cyb6f thus fostering CEF (Breyton et al., 2006). The Fd binding site depends on the reduction state of the photosynthetic electron chain and in particular on the $NADPH/NADP^+$ ratio, strongly related on the balance between light and dark photosynthetic phase. Therefore when over-reduction of the PSI electron acceptor is induced (high $NADPH/NADP^+$ ratio), for example during a dark-light transition, high rate of CEF can be detected (Golding et al., 2004). Dark adapted leaves has an inactive Calvin cycle and consequently, at the onset of illumination, maintains its upstream electron carriers in a reduced form until its activation (Johnson, 2005). In this situation LEF is blocked and reduced Fd recycles through $Cytb_6f$. On the contrary, in steady-state illumination LEF was shown to be favored (see paragraph 4.4).

- The FNR model. This model is based on the observation that ferredoxin-NADPH-oxidoreductase (FNR) can be found associated with both PSI (Andersen et al., 1992) and $Cytb_6f$ complex (Zhang et al., 2001). The formation of the PSI-FNR complex would favor the LEF fostering Fd binding and the

consequent efficient $NADP^+$ reduction (Figure 7). The $Cytb_6f$-FNR complex instead would mainly work in cyclic flow attracting Fd from FNR-free PSI (Breyton et al., 2006; Joliot and Joliot, 2005).

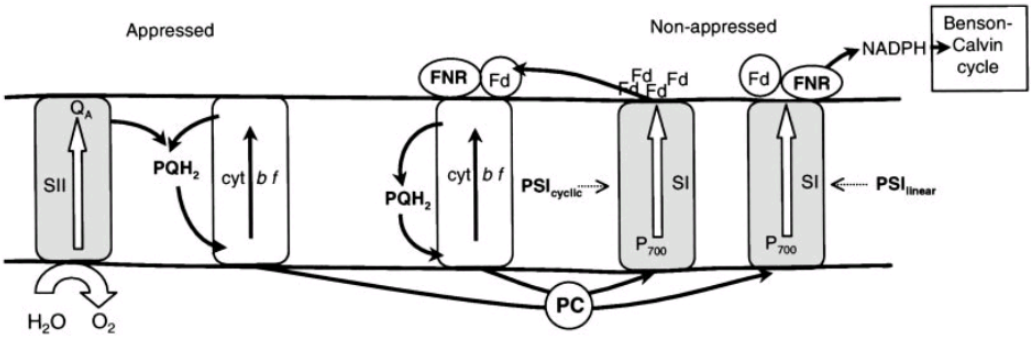

Figure 7. The FNR model to explain the repartition between LEF and CEF activity. The model proposes two possible routes followed by the electron carrier ferredoxin (Fd). One relies on the formation of the PSI-FNR-Fd ternary complex (LEF active) the other on the $Cytb_6f$-FNR complex (CEF active). SII (Photosystem II); SI (Photosystem I); PQH_2 (plastoquinone); PC (plastocyanin); FNR (ferredoxin-NADPH-oxidoreductase). (Joliot and Joliot, 2005)

3.2 Alternative pathway to LEF: Mehler and Mehler-like reaction

Photoreduction of O_2 to H_2O_2 by the photosynthetic electron transport chain was described for the first time in chloroplasts by Mehler (Mehler, 1951), and is therefore known as the Mehler reaction. In this process reduced Fd from PSI can be directly oxidized by O_2. The reaction leads to the production of superoxide anions (O_2^-), which are rapidly converted into H_2O_2 by a superoxide dismutase (SOD) located in the chloroplast. Consequently the H_2O_2 produced by SOD may be converted to O_2 and H_2O by the activity of catalase (Eberhard et al., 2008). Therefore in this process the electrons derived from water oxidation by PSII subsequently flow through PSI to produce water again. Thus, it has been termed the water–water cycle (Asada, 2000). The Mehler reaction in plant performs two physiological functions. It has a photoprotective role and helps balance the ratio NADPH/ATP (Allahverdiyeva et al., 2015).

Another similar strategy alternative to LEF, called Mehler-like reaction, was found for the first time in cyanobacteria. They can photoreduce O_2 using NADPH by means of soluble FLV1 and FLV3 proteins. The final product of this O_2 photoreduction is water without, however, the production of ROS (Helman et al., 2003). This reaction is active in the PSI photoprotection and occurs in nearly all cyanobacteria and additionally in green algae, mosses and lycophytes (Allahverdiyeva et al., 2015; Dang et al., 2014).

4. Regulation of light harvesting and photoprotection

Light is fundamental for photosynthesis but it might also be harmful when it exceeds the capacity of the photosynthetic electron chain. If the absorbed radiation exceeds the saturation level of photosynthesis, photochemical reactions do not readily use excitation energy. This excess of absorbed light causes photo-oxidative damage and inhibits photosynthesis (Figure 8) (Niyogi, 1999; Demmig-Adams and Adams, 2000). The intensity of light considered in excess and detrimental for the photosynthetic organism is very variable and relates to the environmental condition. Additional stress such as heat, cold, drought and nutrient deprivation can impair photosynthetic electron transport chain decreasing the light use efficiency (Figure 8) (Demmig-Adams and Adams, 1992).

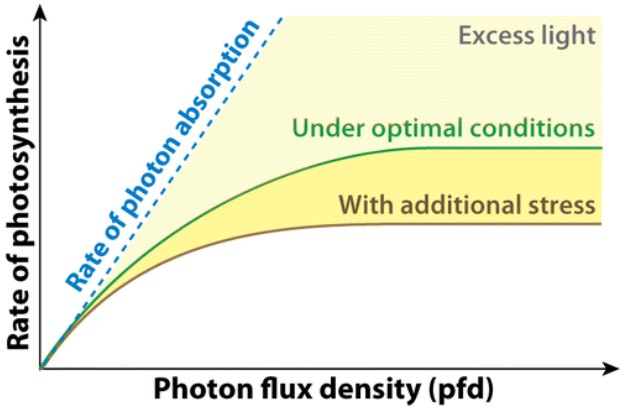

Figure 8. Photosynthesis light response curve. Photosynthetic performance related to the light employed during growth expressed as photon flux density (pfd). The dashed blue line represents the rate of light absorption. Two light response curves are represented for photosynthetic organism grown under optimal and stressful condition. Excess light is the light absorbed by the photosynthetic organism that exceeds its photosynthetic capacity. (Li et al., 2009)

In this condition chlorophylls singlet excited state (^{1}Chl*) aren't efficiently quenched by photochemistry, increasing the probability of intersystem crossing and leading to chlorophylls triplet (^{3}Chl*) formation (Vass et al., 1992). ^{3}Chl* are not intrinsically harmful but due to their long life they can transfer energy to oxygen creating reactive species (ROS) (Figure 9). The overproduction of these oxidative species has a deleterious effect in the overall photosynthetic machinery. The first photosynthetic component affected is PSII reaction center (RC) (LEDFORD and NIYOGI, 2005; Eberhard et al., 2008). PSII RC is localized in a hyperoxic environment due to the high amount of oxygen produced during the water splitting event (Durrant et al., 1990). The increased probability to generate ROS in this environment, in particular $^1O_2$ from the triplet state of P680, characterizes the high photosensitivity of PSII (Murata et al., 2007; Mellis, 1999). A repair cycle for D1 protein of PSII exists at all light intensities, even at low light (Keren et al., 1997). Other ROS such as superoxide, hydrogen peroxide, and hydroxyl radical are generated around PSI due to the transfer of electrons from

ferredoxin and NADPH to oxygen species (Asada, 2006). Thylakoid membrane represents a susceptible target to these ROS because of its enrichment in polyunsaturated fatty acids easily subjected to lipid peroxidation.

Photoinhibition represents all those effects detrimental for the photosynthetic efficiency that arise when the rate of light energy conversion is lower than the rate of light energy absorption. This phenomenon is very common in a natural environment where light intensity can often experience variations of several orders of magnitude.

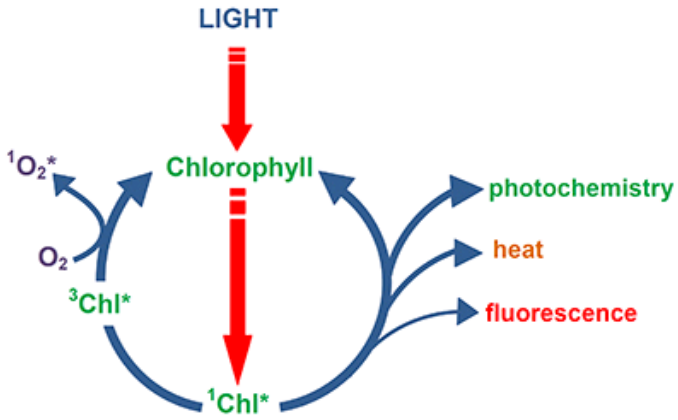

Figure 9. Different way to quench excited chlorophyll. After photon excitation, chlorophyll in the singlet state (^{1}Chl*) can be quenched according to three different competitive pathway: photochemical quenching, when light energy is used to drive photosynthesis; non-photochemical quenching (NPQ) or more commonly called heat dissipation; fluorescence emission. However an alternative pathway increases its yield in high light conditions: it's the production of chlorophyll triplet (^{3}Chl*) through intersystem crossing. ^{3}Chl* can react with O_2 to form ROS. (Gina Mohammed / P&M Technologies)

In a natural environment, changes in light intensity occur with different rates, spanning from seconds to weeks. Light intensity can change as a consequence of passing clouds or of leaves movement in a tree canopy, but also for slow seasonal changes. In aquatic environment, in particular, light variation are even exacerbated by scattering processes of the water, depth of the water column and presence of suspended particles (including photosynthetic organisms themselves) (Depauw et al., 2012). Additionally, natural water movements (tides, streams) cause relevant spatial displacements of marine microorganisms, which have no equivalent in the terrestrial environment (Falkowski and Raven, 2013).

To thrive in a highly variable environment photosynthetic organisms have evolved multiple regulatory mechanisms with different activation timescales, enabling responses to short- and long-term variations (Eberhard et al., 2008; Walters, 2005). When exposed to short–term stress photosynthetic organism activates quenching mechanisms aimed at decrease the light harvesting efficiency such as

the Non Photochemical Quenching (NPQ). The short term response is also dependent on the fast activation of xanthophyll cycle aimed at synthesize photoprotective carotenoids (Li et al., 2009). On the contrary, if the light stress is prolonged, cells adapt their overall metabolism to the new condition, a response called long-term response or acclimation (Niyogi, 1999). This is achieved modulating the organization of the photosynthetic apparatus by means of gene expression and protein content regulation. In many photosynthetic organisms when solar radiation is constantly high, acclimation response downsizes light-harvesting apparatus increasing the light use efficiency (Eberhard et al., 2008). The long term response involves also thylakoid structure that can dynamically change according to the light intensity. Moreover photosynthetic organisms respond to short and long term stress also modulating their electron transport efficiency, for example activating the cyclic electron flow around PSI.

4.1. Short term regulation of photosynthetic apparatus

As previously discussed PSII reaction center can be easily damaged by formation of the triplet state of P680 and consequent singlet O_2 production. These damages appears to be an inevitable consequence of PSII function, strictly related to a O_2 enriched environment. On the contrary PSI is less susceptible to light stress because is considered an effective energy quencher (Horton et al., 1996)**.** The high rate PSII RC damage can be only partially solved by repair mechanisms. Indeed they are energetically costly and too slow to respond to fast light variation (Chow, 1994). In addition light absorption is not modifiable in a short lapse of time modifying the pigment or protein composition. To reduce this detrimental photosensitivity, PSII evolved several mechanisms that activate suddenly and allow a fast response to light stress. These mechanisms, acting mostly at the level of PSII, involve generally a fine regulation of the light-harvesting efficiency of LHC. They are collectively called non-photochemical quenching (NPQ) because measured by quantifying the light induced quenching of Chl fluorescence (Figure 10) (Demmig-Adams and Adams, 1992). Indeed, since the three possible energy dissipation pathway (photochemistry, heat (NPQ) and fluorescence) are complementary (Figure 9), their yield can be easily extrapolated following fluorescence variation. NPQ can be divided in different components based on its different relaxation kinetics (qE, qT, qZ and qI). In Figure 10 it is possible to see the protocol employed to distinguish these different components based on a light treatment to induce NPQ (fluorescence quenching) followed by a dark period. The dark recovery of NPQ allow the identification of different relaxation kinetics. qE, qT, qZ and qI represent the fast, two intermediate and slow relaxing NPQ components, respectively, as described below (Horton et al., 1996).

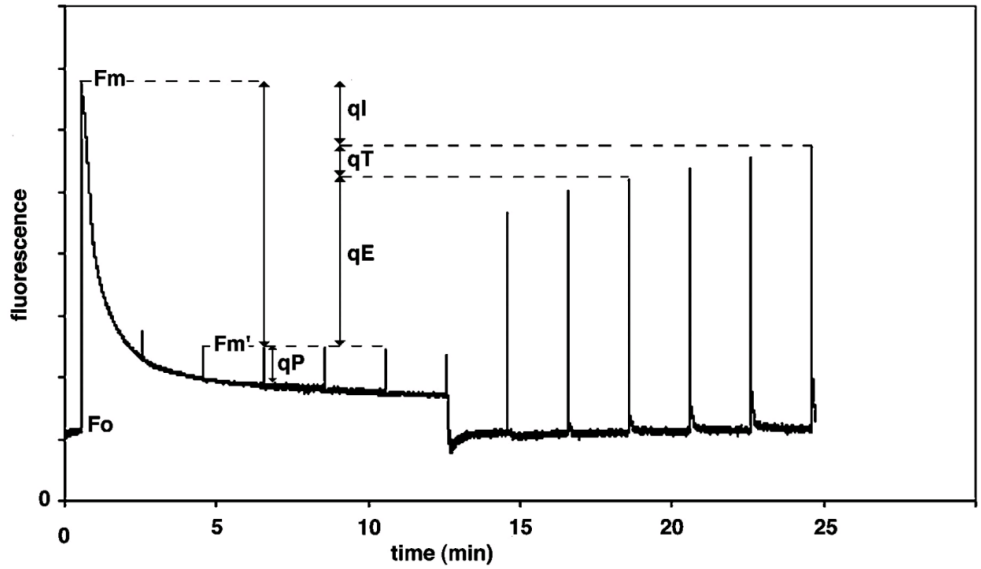

Figure 10. Chl fluorescence measurement from an *A. thaliana* leaf. In the fluorescence measurement reported the sample is exposed to 12 minutes of high actinic light to induce an NPQ response. In the remaining 12 minutes the light is switched off to follow the NPQ relaxation kinetic. In the presence of only weak measuring light the minimal fluorescence (Fo) is seen. When a saturating light pulse is given, the photosynthetic light reactions are saturated and fluorescence reaches a maximum level (Fm or Fm′). Upon continuous illumination with high light, a combination of photochemical (qP) and non photochemical (NPQ) quenching lowers the fluorescence yield. This decrease is quantified by the NPQ parameter. Upon dark adaptation, NPQ relaxes with multiphasic kinetics, which allows the identification of three kinetic components (qE, qT, qI). qZ is not reported in this graph. (Müller et al., 2001)

- Energy dependent component of NPQ (qE). The qE mechanism is conserved in many organisms from higher plant to algae and represents the major component of NPQ. It is the more fast activated component, inducible and reversible in the range of seconds, and the principal responsible to heat dissipation when the energy harvested exceed cell photosynthetic capacity (Figure 10). In excess light condition this mechanism can dissipate up to 80% of total absorbed photons. qE is called also ΔpH-dependent quenching because its activation is strictly dependent on a pH gradient generation across the thylakoid membranes (Müller et al., 2001; Niyogi, 2000). The drop in lumenal pH is a result of photosynthetic activity and increases in the presence of excessive light as a result of an increase in the overall electron transport through the membrane. The ΔpH generated can trigger two main processes: activation of the conversion of carotenoid violaxanthin to zeaxanthin via xanthophyll cycle and activation of members of the light-harvesting complex (LHC) protein superfamily. A decrease in lumen pH activates the enzyme violaxanthin de-epoxidase (VDE) that catalyzes the de-epoxidation of violaxanthin to zeaxanthin. The accumulation of zeaxanthin enhances qE, mainly in the first phase of its activation (Pfundel and Dilley, 1993). In addition the increased gradient leads to protonation of residues in the lumenal loops of LHC proteins, such as PsbS (in plants) or LHCSR (in algae) (Li et al., 2000; Peers et al., 2009; Li et al., 2004). It was hypothesized that all these processes induce a

conformational change in the PSII antenna with the consequent transition to a quenching state. This quenching conformation could be characterized by an LCHII aggregation or a dissociation of antenna subcomplex resulting anyhow in quenching amplification (Horton et al., 2005; Betterle et al., 2009).
To confirm the pivotal role of proton gradient for qE response several mutants have been generated in the model *A. thaliana. M*utants in linear or cyclic electron transport are defective in generate ΔpH and show lower qE than wild type (Munekage et al., 2001). Furthermore if the thylakoid gradient collapses chemically with the addition of uncoupler the qE drastically decreases (Jahns and Heyde, 1999). On the other hand plants over-expressing protein related to cyclic electron transport enhance qE even in low light (Okegawa et al., 2007). The reduced fitness of qE mutant exposed to naturally fluctuating conditions underlines the physiological relevance of qE in photosynthetic organisms (Külheim et al., 2002). The basis of this mechanisms are very similar in different photosynthetic organisms. Despite this, some peculiarities can be found in the group of diatoms in which the extent of qE, that dominate the overall algal NPQ, is far more pronounced than in higher plants (Goss and Jakob, 2010) .

- State transitions component of NPQ (qT). The qT component represents the quenching of fluorescence due to a reversible detachment of LHCII antenna from PSII and migration toward PSI and *vice versa*, a process called state transition. The fluorescence yield decreases as a consequence of the decreased energy input to PSII. This mechanism, activated by the redox state of the plastoquinone pool, presents a slower activation and relaxation kinetic (in the minute range) than the qE mechanism and is activated to rebalance the excitation pressure upon the two photosystems (Wollman, 2001; Eberhard et al., 2008). Its contribution in the overall NPQ is usually limited if compared with qE (Figure 10). Sate transition has been observed in higher plant (Wollman, 2001), green algae (Allen, 1992) and cyanobacteria (Kirilovsky, 2015). In diatoms and Eustigmatophytes, instead, no evidence for state transition was observed yet (Owens, 1986).

- Zeaxanthin-dependent component of NPQ (qZ). qZ is a NPQ component correlated with the amount of zeaxanthin (Nilkens et al., 2010). Its activation depends on the conversion of more slowly convertible violaxanthin in zeaxanthin, at difference from the faster conversion that occurred in the qE component. Its relaxation kinetic are in the range of minutes and coincides with reconversion of zeaxanthin, synthesized during the light stress, in violaxanthin. qZ was originally attributed to qT (Quick and Stitt, 1989) for their similar kinetics and later considered a part of the qI component sensitive to uncouplers and zeaxanthin-dependent. At difference with the known qI related to damaged RC, this new qI component was more related to PSII photoprotection in LHCII antenna (Ruban and Horton, 1995; Dall'Osto et al., 2005). At present zeaxanthin-dependent NPQ component represents a separate mechanism clearly not related to qE, qT or qI. It is independent of ΔpH once zeaxanthin is synthesized and independent of PsbS, as demonstrated in *A. thaliana* (Nilkens et al., 2010; Brooks et al., 2013; Ware et al., 2014).

- Photoinhibition component of NPQ (qI). The slowest quenching mechanism is known as qI, relaxing in the range of hours (Figure 10). The decreased fluorescence yield that characterizes this component is associated with the damage of the D1 protein in the PSII RC. The slow recovery is due to the slow

PSII repair cycle that involves partial disassembly of inactive PSII, proteolytic degradation of the damaged D1, and insertion of newly synthesized D1 into PSII (Aro et al., 1993).
While a part of qI occurs because the damaged RC quenches fluorescence, in the other hand a significant proportion has been referred to as a "sustained quenching" and has an active role in photoprotection (Horton et al., 1996; Demmig-Adams, 1990). This proportion arises even in the absence of any loss of PSII activity and may be associated to the qZ mechanism previously described. There is not a general consensus regarding the different processes controlling the slow phase of NPQ.
Assessment of qI based on fluorescence recovery kinetics can be difficult in particular conditions in which the intermediate and slow NPQ components (qT, qZ and qI) are overlapping and so not easily discernible. In this scenario invasive techniques, such as the tracking of D1 protein degradation, can be useful to estimate the qI-related RCII damage.
qI is widely present among photosynthetic organisms. Its extent depends on the illumination time, the light intensity, but in particular on the photosynthetic organism. It is often significantly smaller compared to qE in cells in standard condition. Organisms with higher NPQ capacity generally develop smaller qI due to their enhanced photoprotection (Nilkens et al., 2010). In diatoms, for example, known for their ability to develop extremely high level of NPQ, the qI component is strongly reduced (Ting and Owens, 1994).

4.2. Photoprotection by carotenoids and xanthophyll cycle

Carotenoids are pigment molecules that can be divided in two major groups, xanthophylls and carotenes, depending on the presence or absence of oxygen. These molecules are mostly located in photosystems but can be found also in the thylakoid membrane lipid phase with variable extent. They act principally as accessory light-harvesting pigments and in protection of the photosyntetic apparatus from excess light stress (Young, 1991).
The absorbed energy can be transferred between pigments by FRET moving preferentially from carotenoids to chlorophylls due to differences in their electronic energetic levels. Thus, during the light absorption event, carotenoids play a primary function in the energy funneling towards photosystems RC. In additions they have a photoprotective role that results in quenching chlorophyll triplet state and scavenging ROS species formed within the chloroplast (Young, 1991). Their photoprotective role involves also a modulation of the thylakoid structure leading to a decrease in membrane fluidity, an increase in membrane thermostability and a lowered susceptibility to lipid peroxidation (Havaux, 1998).
Some of them are constitutively present in the photosynthetic apparatus, such as carotenoids bound to photosystems. For example the efficient scavenging of excited triplet Chl (^{3}Chl*) and singlet oxygen ($^1O_2$) in the photosystems RC is constitutively provided by tightly bound β-carotenes (Krieger-Liszkay et al.). On the contrary some carotenoids, such as xanthophylls, are exclusively induced by light stress and thus play a fundamental role in the short-term response.

Xanthophyll cycle is a mechanisms that acts responding to fast changes in environmental conditions widely present in many phothosynthetic organisms. In higher plants, green and brown algae, it involves the reversible conversion of violaxanthin into zeaxanthin by the intermediate antheraxanthin (Figure 11) (Arnoux et al., 2009; Jahns et al., 2009).This conversion is activated in strong illumination and it is catalyzed by the VDE enzyme (violaxanthin de-epoxidase) a soluble monomeric enzyme localized in the thylakoid lumen (Hager and Holocher, 1994). Under strong illumination the lumenal pH decreases, inducing the enzyme dimerization and association in regions of the thylakoids membrane enriched in MGDG, where the substrate violaxanthin is found (Rockholm, 1996; Pfundel et al., 1994; Schaller et al., 2010; Saga et al., 2010; Arnoux et al., 2009). Indeed the same condition also induce the release of violaxanthin substrate from its binding site in light harvesting complexes and its diffusion in the thylakoid membranes to reach VDE (Jahns et al., 2009). When illumination decreases, zeaxanthin is back converted to violaxanthin by the ZE (zeaxanthin epoxidase) constitutively active in the stromal side of the thylakoid membrane (Figure 11) (Schaller et al., 2012). The ZE enzyme in plants, although active both during darkness and illumination (Gilmore et al., 1994), catalyzes the epoxidation reaction with much lower rates if compared to the de-epoxidation. In that way the fast accumulation of zeaxanthin during period of high light is not impaired (Siefermann and Yamamoto, 1975).

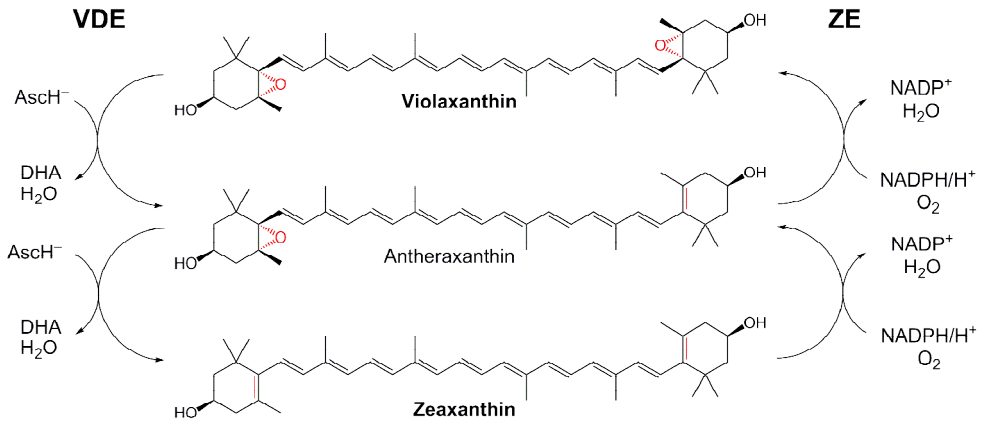

Figure 11. Scheme of the xanthophyll cycle and its regulation. Stepwise removal of two epoxy groups in violaxanthin results in the production of zeaxanthin, with the intermediate product antheraxanthin. This de-epoxidation reaction is catalyzes in the lumen by the VDE enzyme, activated at pH 5-6. The enzyme requires reduced ascorbate (AscH) as co-substrate to reduce the epoxy group. The reverse epoxidation reaction is mediated by ZE, located at the stromal side of the thylakoid membrane. This enzyme has a pH optimum at 7.5 and utilizes O_2, NADPH and FAD as co-substrates.

Once synthesized, zeaxanthin plays a central role in photoprotection. Indeed it is involved in the fast response to excess energy triggering the qE mechanism and so enhancing thermal dissipation (Jahns et al., 2009; Niyogi et al., 1998). Furthermore it is involved in slower photoprotection processes as the

qZ intermediate component of NPQ (Nilkens et al., 2010). The mechanism by which zeaxanthin is involved in qE is still under debate. It is thought that zeaxanthin may directly acts as a quencher of excited chlorophylls generating a heterodimer with chlorophyll and performing charge transfer (Holt et al., 2005). Alternatively it could have an allosteric role triggering a conformational change in the light-harvesting antenna and consequently leading to energy quenching (Pascal et al., 2005). Furthermore zeaxanthin is also active in the scavenging of Chl triplets (Mozzo et al., 2008; Dall'Osto et al., 2012) and when accumulated as a free pool in the thylakoids membrane it is an effective ROS scavenger to avoid lipids peroxidation (Havaux et al., 2007; Jahns et al., 2009). For what concern its role in the thylakoid membrane structure it is thought that its accumulation in the lipid bilayer decreases the fluidity of the lipid bilayer thus lowering its permeability to oxygen (Gruszecki et al., 1999; Tardy and Havaux, 1997). All these mechanisms described are interconnected and together belong to the same diversified photoprotective response related to zeaxanthin accumulation.

The pivotal role of zeaxanthin in the photoprotection was demonstrated generating mutants not able to produce it, as the *npq1* in *A. thaliana*. The *npq1* mutant shows reduced NPQ capacity, increased PSII damage and lipid peroxidation; all features that decrease drastically its fitness in stress condition (Niyogi et al., 1998; Havaux and Niyogi, 1999). On the contrary, when zeaxanthin is constitutively expressed, as in the *npq2* mutant in *A. thaliana*, it induces high NPQ level also in low light condition. The constitutive high energy dissipation leads to strong impairment in growth performance even in limiting light (Dall'Osto et al., 2005; Niyogi et al., 1998). This evidence confirms that zeaxanthin presence must to be temporally limited and exclusively linked to a short term response due to its strong impact to the overall light harvesting efficiency.

Other xanthophyll cycles mediate similar responses in other organisms such as the lutein-epoxide cycle in some plant species (Bungard et al., 1999; García-Plazaola et al., 2007) and the diadinoxanthin (Dd) – diatoxanthin (Dt) cycle in diatoms, phaeophytes, dinophytes and haptophytes (Coesel et al., 2008). The lutein epoxide cycle involves the de-epoxidation of lutein epoxide to lutein and the reverse reaction. In higher plants it has reported to operate in parallel with the analogous violaxanthin-zeaxanthin cycle with which share the VDE and ZE enzymes (García-Plazaola et al., 2007). The xanthophyll lutein has been shown to be important in qE induction and replace zeaxanthin function, as observed in *A. thaliana* mutants (Pogson et al., 1998). In diatoms a single step reaction turns diadinoxanthin into diatoxanthin by means of the VDE and ZE homologues enzymes, diadinoxanthin de-epoxidase (DDE) and diatoxanthin epoxidase (DE), respectively. The quenching properties of diatoxanthin are similar to those of zeaxanthin in higher plants (Olaizola et al., 1994; Young and Frank, 1996). Some differences between the two xanthophyll cycle are found mostly in de-epoxidation and epoxidation reactions, faster in diatoms. This is in part due to the broader pH range in which the DDE and DE operate in these organisms (Goss and Jakob, 2010). The physiological meaning of the faster activation rate compared to other xanthophyll cycle could derived from the extremely variable natural environment in which diatoms live. Therefore to survive to continue displacement in the turbulent water and fast light variation, diatoms had evolved faster response mechanism.

4.3. Long term regulation of photosynthetic apparatus

To respond to prolonged stress exposition in their natural environment, photosynthetic organisms have evolved long-term mechanisms that involve modulation of the composition of the photosynthetic apparatus. This response, called acclimation, involves mostly changes in expression of a diversity of photosynthesis-related genes with the consequent modifications in protein composition. In most photosynthetic organisms, this regulation involves a reduction in the chlorophyll content and an increase in photoprotective xanthophylls when exposed to high irradiance (Rodríguez et al., 2005; Demmig-Adams and Adams, 1992). In addition, two categories of long-term acclimation responses have been proposed based on microalgae behavior to changes in growth irradiance (Falkowski and Owens, 1980): the modulation of the antenna absorption cross-section (antenna size), a strategy termed σ-type photoacclimation observed in the diatom *Skeletonema costatum*; the modulation of the number of reaction centers (RC) through a strategy termed n-type photoacclimation, as observed in the green algae *Dunaliella tertiolecta*.

The regulation of the antenna size, σ-type photoacclimation, is a strategy used to protect RC against photodamage reducing the light harvested and thus the energetic pressure on it. In most photosynthetic organisms it involves mostly modulation of LHCII proteins which are subjected to marked changed in their expression, easily followed with transcriptomic approach. Plants and green algae transferred from low to strong illumination decrease their PSII antenna to reduce light absorption and avoid photoinhibition. On the contrary when exposed to limiting light intensity they increase the antenna system to increase the probability to harvest photons (Melis, 1991; Smith et al., 1990). In higher plant such as *A. thaliana* this dynamic process is controlled by Lhcb 1-2-3-6 proteins whereas the levels of Lhcb4-5 remain unaltered (Ballottari et al., 2007). In *C. reinhardtii*, instead, the contribution of major and minor LHCII proteins was shown to be the same and therefore they are coordinately repressed when the alga is transferred to high light (Teramoto et al., 2002).

The study realized in plants and green algae have shown that the downsizing of the antenna system can be fulfilled through two principal strategies: a proteolytic degradation of existing proteins, as observe in spinach (Jackowski et al., 2003; Yang et al., 1998) and A. thaliana (Zelisko et al., 2005) or a downregulation of Lhcb proteins translation, mostly observed in *C. reinhardtii* (Durnford et al., 2003). The protein degradation followed likely by re-synthesis at the end of the light stress, make the first strategy the more expensive in terms of energy cost. This σ-type photoacclimation is highly variable even in species of the same phylum suggesting that the acclimation mechanisms are species-specific and often associated with the growth environment (Perry et al., 1981; Bonente et al., 2012; Lepetit et al., 2012).

Whereas PSII undergoes to an intense antenna variation, PSI with its tightly bound antennas seems to remain almost unchanged in response to variations in growth light intensity. In *A. thaliana* and *C. reinhardtii* for example, Lhca antenna proteins are not affected by growth conditions (Ballottari et al., 2007; Bonente et al., 2012). In these organisms the PSI response to high irradiances relies on different

mechanisms like state transition and variation in photosystems stoichiometry. LHCI remodeling, instead, seems to respond to other kind of environmental changes such as Fe availability. Indeed, in irons starved *C. reinhardtii* cells PSI antenna size decrease significantly probably due to a disconnection of the LHCI antenna from PSI (Moseley et al., 2002). The stability of the PSI antenna size in different irradiances has consistently been observed in green algae and plants, while the information for other photosynthetic organisms remains incomplete.

The n-type photoacclimation strategy leads to a variations in the stoichiometry of photosystems to balance the redox state of photosynthetic electron chain. In plant for example PSII/PSI ratio increases under far-red enriched light (PSI light) whereas decreases under illumination favoring PSII excitation (PSII light) (Melis, 1991). This response to changes in light quality restores a balanced light absorption by the two photosystems decreasing the reaction center overexcited. In this way the organism maintain a high quantum efficiency of photosynthesis also in stressful conditions. The same sort of mechanism is involved also in response to high irradiances. Plants grown under low light intensity have fewer PSII units relative to PSI, while plants in high light have higher PSII/PSI ratios (Fan et al., 2007; Chow et al., 1990).

The same increase in PSII/PSI ratio under high light was observed also for the green algae *Dunaliella salina* (Smith et al., 1990). This response is present in many other organisms (Lepetit et al., 2012; Strzepek and Harrison, 2004) even if, in some cases, acts in the opposite directions thus decreasing the PSII/PSI ratio in response to high light (Smith and Melis, 1988).

It is worth mentioning that the two strategies of photoacclimation, the n-type and σ-type, are often mutually related. Mutation in PSII light harvesting complex, for example, increase consequently the PSII/PSI ratio. Therefore in this scenario the effect of mutation is correct restoring the balance of light absorption between PSII and PSI (Melis, 1991).

In addition to the major strategies described, other acclimation responses are also commonly observed such as the variation of the chloroplast morphology, of the photosynthetic capacity and of the overall amount of sinks of photosynthetic electron flow. In the first case plant chloroplasts increase the area of thylakoid membranes creating larger grana stacks when grown in limiting light condition. Conversely in high light the ratio of appressed to non-appressed membrane decreases (Anderson et al., 1988). Furthermore, it was showed that high light stress in plant leads to a lateral shrinkage of grana diameter and increased protein mobility (Herbstová et al., 2012). These structural modulations are presumably aimed at improve the accessibility between damaged PSII in grana and its repair machinery in stroma lamellae. Plant chloroplasts can also move along the cell to avoid or follow incident light, a light response called chloroplast avoidance movement (Li et al., 2009). Also diatoms respond to high light lowering the thylakoid area per chloroplast and maintaining, however, the triple structure of the membranes (Lepetit et al., 2012; Wilhelm et al., 2014). During the acclimation process also the overall capacity of the photosynthetic apparatus can be modulated to optimize the exploitation of absorbed light. For example high-light acclimated cells of the diatom *Phaeodactylum tricornutum* and the green algae *C. reinhardtii* show an increased photosynthetic electron transport rate (Nymark et al., 2009; Bonente et al., 2012). Moreover, the long term

responses can act also changing the overall amount of sinks of photosynthetic. In high light, an increased accumulation of Calvin-Benson cycle enzymes, particularly RuBisCO, have been observed in different species (Fisher et al., 1989; Simionato et al., 2011; Niyogi, 1999).

4.4. The regulatoty role of CEF in photosynthesis

The CEF process contributes to proton translocation into the lumen without net NADPH production. This cyclic activity, fundamental for photosynthetic organisms, can be activated both in stress condition, as a photoprotective response, but also to support LEF to maintain the basal metabolisms. The different conditions in which the activation of CEF was shown are the following:

- Steady-state illumination. ATP and NADPH ratio needed for Calvin cycle reactions (Allen, 2002) can't be satisfied by LEF, which generates a pH gradient insufficient for the required ATP. The additional ATP are provided by CEF activity which generate ΔpH without NADPH accumulation. This CEF activity, essential to sustain the basal metabolisms, explains why mutants defective in CEF present decreased fitness compared to wild type (Munekage et al., 2004).

- Transition dark-to-light. As described in the 'competitive model' paragraph a significant CEF increase it was observed at the onset of illumination in dark adapted leaves (Golding et al., 2004). The physiological reason behind this result can be found in the Calvin cycle reactions, inactive in the dark and slowing activated in the light. The consequent higher NADPH/$NADP^+$ ratio blocks the major linear pathway due to the lack of the final electron acceptor (Johnson, 2005). The over-reduction of the overall photosynthetic chain could lead to photoinhibitory effects. In this scenario the electron recycling performed by CEF rebalances the redox state of the photosynthetic chain limiting photodamage.

- State transition. The unbalanced excitation of PSs perturbs the redox state of the PQ pool which acts as a signal triggering reversible association of LHCII antenna to PSII or PSI, the so-called state transition (see paragraph 4.1). In *C. reinhardtii* this phenomenon is more marked than in higher plant (Wollman, 2001). It was observed that, in the presence of PSII exciting light, antenna migration to PSI causes a switch between LEF and CEF in this green alga (G. Finazzi 2002).The activation of CEF would increase the reduction of PQ pool rebalancing the redox state of the photosynthetic apparatus (Finazzi and Forti, 2004).

- Stress condition. As discussed CEF has a constitutive activity, but there are consolidate evidences that relate this electron transport to different stress responses. CEF activation indeed is involved in the response to drought, high temperature, CO_2 limitation and high light. In all these different kind of stresses CEF is activated by an over-reduction of the stromal electron carriers that leads to a down-regulation of LEF. Under drought, for example, CO_2 fixation is decreased with the consequent increase in the NADPH/$NADP^+$ ratio. As a consequence a down-regulation of LEF was observed with an overall over-reduction of the photosynthetic electron chain. In this scenario CEF is activated increasing proton gradient across the membrane. Accordingly thermal dissipation (NPQ) is induced alleviating the excitation pressure on PSII (Golding and Johnson, 2003). The same kind of response also occurs

under conditions of low CO_2 (Golding and Johnson, 2003). Higher CEF activity was shown also for high temperature (Egorova and Bukhov, 2002) and anaerobiosis (Joët et al., 2002) stresses probably linked in both cases to a decrease of RuBisCO activity (Crafts-Brandner and Salvucci, 2000).
In high light stress the activation of CEF avoid over-reduction of photosynthetic electron transport chain, preventing ROS production and photo-damage (Peltier et al., 2010). Futhermore CEF contributes to activate the photoprotective NPQ response increasing the ΔpH across the membrane (Miyake et al., 2005). The NPQ phenotype related to CEF impairment for example was been the base for the identification of *pgr5* in *A. thaliana*. An altered ability to develop NPQ was observed also in *pgr5* and *pgrl1* mutant in *C. reinhardtii* (Tolleter et al., 2011; Dang et al., 2014). In high light stress CEF activity is also been related to direct protection of PSI from photoinhibition, as described in *A. thaliana* and *C. reinhardtii* (Munekage et al., 2002; Dang et al., 2014; Johnson et al., 2014). In this situation CEF could be considered as a safety valve acting at relieving the electronic pressure on PSI recycling electrons.

References

Albertsson, P. (2001). A quantitative model of the domain structure of the photosynthetic membrane. Trends Plant Sci. **6**: 349–58.

Allahverdiyeva, Y., Isojärvi, J., Zhang, P., and Aro, E.-M. (2015). Cyanobacterial Oxygenic Photosynthesis is Protected by Flavodiiron Proteins. Life **5**: 716–743.

Allen, J. (2002). Photosynthesis of ATP-electrons, proton pumps, rotors, and poise. Cell **110**: 273–6.

Allen, J.F. (1992). Protein phosphorylation in regulation of photosynthesis. Biochim. Biophys. Acta **1098**: 275–335.

Amaro, H.M., Macedo, Â.C., and Malcata, F.X. (2012). Microalgae: An alternative as sustainable source of biofuels? Energy **44**: 158–166.

Andersen, B., Scheller, H. V, and Møller, B.L. (1992). The PSI-E subunit of photosystem I binds ferredoxin:NADP+ oxidoreductase. FEBS Lett. **311**: 169–73.

Anderson, J., Chow, W., and Goodchild, D. (1988). Thylakoid Membrane Organisation in Sun/Shade Acclimation. Aust. J. Plant Physiol. **15**: 11.

Archibald, J.M. and Keeling, P.J. (2002). Recycled plastids: a “green movement” in eukaryotic evolution. Trends Genet. **18**: 577–584.

ARNON, D.I., ALLEN, M.B., and WHATLEY, F.R. (1954). Photosynthesis by Isolated Chloroplasts. Nature **174**: 394–396.

Arnon, D.I., Whatley, F.R., and Allen, M.B. (1958). Assimilatory Power in Photosynthesis: Photosynthetic phosphorylation by isolated chloroplasts is coupled with TPN reduction. Science **127**: 1026–34.

Arnoux, P., Morosinotto, T., Saga, G., Bassi, R., and Pignol, D. (2009). A structural basis for the pH-dependent xanthophyll cycle in Arabidopsis thaliana. Plant Cell **21**: 2036–44.

Aro, E.-M., Virgin, I., and Andersson, B. (1993). Photoinhibition of Photosystem II. Inactivation, protein damage and turnover. Biochim. Biophys. Acta - Bioenerg. **1143**: 113–134.

Asada, K. (2006). Production and scavenging of reactive oxygen species in chloroplasts and their functions. Plant Physiol. **141**: 391–6.

Asada, K. (2000). The water-water cycle as alternative photon and electron sinks. Philos. Trans. R. Soc. B Biol. Sci. **355**: 1419–1431.

Ballottari, M., Dall’Osto, L., Morosinotto, T., and Bassi, R. (2007). Contrasting behavior of higher plant

photosystem I and II antenna systems during acclimation. J. Biol. Chem. **282**: 8947–8958.

Barber, J. (2012). Photosystem II: the water-splitting enzyme of photosynthesis. Cold Spring Harb. Symp. Quant. Biol. **77**: 295–307.

Basso, S., Simionato, D., Gerotto, C., Segalla, A., Giacometti, G.M., and Morosinotto, T. (2014). Characterization of the photosynthetic apparatus of the Eustigmatophycean Nannochloropsis gaditana: evidence of convergent evolution in the supramolecular organization of photosystem I. Biochim. Biophys. Acta **1837**: 306–14.

Beer, A., Gundermann, K., Beckmann, J., and Büchel, C. (2006). Subunit composition and pigmentation of fucoxanthin-chlorophyll proteins in diatoms: evidence for a subunit involved in diadinoxanthin and diatoxanthin binding. Biochemistry **45**: 13046–53.

Bendall, D.S. and Manasse, R.S. (1995). Cyclic photophosphorylation and electron transport. Biochim. Biophys. Acta - Bioenerg. **1229**: 23–38.

Berg, J.M., Tymoczko, J.L., and Stryer, L. (2002). The Activity of the Calvin Cycle Depends on Environmental Conditions.

Bernardi, A., Perin, G., Sforza, E., Galvanin, F., Morosinotto, T., and Bezzo, F. (2014). An Identifiable State Model To Describe Light Intensity Influence on Microalgae Growth. Ind. Eng. Chem. Res. **53**: 6738–6749.

Betterle, N., Ballottari, M., Zorzan, S., de Bianchi, S., Cazzaniga, S., Dall'Osto, L., Morosinotto, T., and Bassi, R. (2009). Light-induced dissociation of an antenna hetero-oligomer is needed for non-photochemical quenching induction. J. Biol. Chem. **284**: 15255–15266.

Bondioli, P., Della Bella, L., Rivolta, G., Chini Zittelli, G., Bassi, N., Rodolfi, L., Casini, D., Prussi, M., Chiaramonti, D., and Tredici, M.R. (2012). Oil production by the marine microalgae Nannochloropsis sp. F&M-M24 and Tetraselmis suecica F&M-M33. Bioresour. Technol. **114**: 567–72.

Bonente, G., Pippa, S., Castellano, S., Bassi, R., and Ballottari, M. (2012). Acclimation of Chlamydomonas reinhardtii to different growth irradiances. J. Biol. Chem. **287**: 5833–47.

Brakemann, T., Schlörmann, W., Marquardt, J., Nolte, M., and Rhiel, E. (2006). Association of fucoxanthin chlorophyll a/c-binding polypeptides with photosystems and phosphorylation in the centric diatom Cyclotella cryptica. Protist **157**: 463–75.

Brennan, L. and Owende, P. (2010). Biofuels from microalgae—A review of technologies for production, processing, and extractions of biofuels and co-products. Renew. Sustain. Energy Rev. **14**: 557–577.

Breyton, C., Nandha, B., Johnson, G.N., Joliot, P., and Finazzi, G. (2006). Redox modulation of cyclic electron flow around photosystem I in C3 plants. Biochemistry **45**: 13465–75.

Brooks, M.D., Sylak-Glassman, E.J., Fleming, G.R., and Niyogi, K.K. (2013). A thioredoxin-like/β-propeller protein maintains the efficiency of light harvesting in Arabidopsis. Proc. Natl. Acad. Sci. U. S. A. **110**: E2733–40.

Bungard, R.A., Ruban, A. V, Hibberd, J.M., Press, M.C., Horton, P., and Scholes, J.D. (1999). Unusual carotenoid composition and a new type of xanthophyll cycle in plants. Proc. Natl. Acad. Sci. U. S. A. **96**: 1135–9.

Calvin, M. and Benson, A.A. (1948). The Path of Carbon in Photosynthesis. Science **107**: 476–80.

Carvalho, A.P., Silva, S.O., Baptista, J.M., and Malcata, F.X. (2011). Light requirements in microalgal photobioreactors: an overview of biophotonic aspects. Appl. Microbiol. Biotechnol. **89**: 1275–88.

Cavalier-Smith, T. (2004). Only six kingdoms of life. Proc. Biol. Sci. **271**: 1251–62.

Cavalier-Smith, T. (1986). The kingdoms of organisms. Nature **324**: 416–417.

Chisti, Y. (2007). Biodiesel from microalgae. Biotechnol. Adv. **25**: 294–306.

Chow, W.S. (1994). Molecular Processes of Photosynthesis (Elsevier).

Chow, W.S., Melis, A., and Anderson, J.M. (1990). Adjustments of photosystem stoichiometry in chloroplasts improve the quantum efficiency of photosynthesis. Proc. Natl. Acad. Sci. U. S. A. **87**: 7502–6.

Coesel, S., Oborník, M., Varela, J., Falciatore, A., and Bowler, C. (2008). Evolutionary origins and functions of the carotenoid biosynthetic pathway in marine diatoms. PLoS One **3**: e2896.

Crafts-Brandner, S.J. and Salvucci, M.E. (2000). Rubisco activase constrains the photosynthetic potential of

leaves at high temperature and CO2. Proc. Natl. Acad. Sci. U. S. A. **97**: 13430–5.

Crofts, A.R. and Meinhardt, S.W. (1982). A Q-cycle mechanism for the cyclic electron-transfer chain of Rhodopseudomonas sphaeroides. Biochem. Soc. Trans. **10**: 201–3.

DalCorso, G., Pesaresi, P., Masiero, S., Aseeva, E., Schünemann, D., Finazzi, G., Joliot, P., Barbato, R., and Leister, D. (2008). A complex containing PGRL1 and PGR5 is involved in the switch between linear and cyclic electron flow in Arabidopsis. Cell **132**: 273–85.

Dall'Osto, L., Caffarri, S., and Bassi, R. (2005). A mechanism of nonphotochemical energy dissipation, independent from PsbS, revealed by a conformational change in the antenna protein CP26. Plant Cell **17**: 1217–32.

Dall'Osto, L., Holt, N.E., Kaligotla, S., Fuciman, M., Cazzaniga, S., Carbonera, D., Frank, H.A., Alric, J., and Bassi, R. (2012). Zeaxanthin protects plant photosynthesis by modulating chlorophyll triplet yield in specific light-harvesting antenna subunits. J. Biol. Chem. **287**: 41820–34.

Dang, K.-V., Plet, J., Tolleter, D., Jokel, M., Cuiné, S., Carrier, P., Auroy, P., Richaud, P., Johnson, X., Alric, J., Allahverdiyeva, Y., and Peltier, G. (2014). Combined increases in mitochondrial cooperation and oxygen photoreduction compensate for deficiency in cyclic electron flow in Chlamydomonas reinhardtii. Plant Cell **26**: 3036–50.

Dekker, J.P. and Boekema, E.J. (2005). Supramolecular organization of thylakoid membrane proteins in green plants. Biochim. Biophys. Acta **1706**: 12–39.

Demmig-Adams, B. (1990). Carotenoids and photoprotection in plants: A role for the xanthophyll zeaxanthin. Biochim. Biophys. Acta - Bioenerg. **1020**: 1–24.

Demmig-Adams, B. and Adams, W.W. (2000). Harvesting sunlight safely. Nature **403**: 371, 373–4.

Demmig-Adams, B. and Adams, W.W. (1992). Photoprotection and Other Responses of Plants to High Light Stress. Annu. Rev. Plant Physiol. Plant Mol. Biol. **43**: 599–626.

Depauw, F.A., Rogato, A., Ribera d'Alcalá, M., and Falciatore, A. (2012). Exploring the molecular basis of responses to light in marine diatoms. J. Exp. Bot. **63**: 1575–91.

Desplats, C., Mus, F., Cuiné, S., Billon, E., Cournac, L., and Peltier, G. (2009). Characterization of Nda2, a plastoquinone-reducing type II NAD(P)H dehydrogenase in chlamydomonas chloroplasts. J. Biol. Chem. **284**: 4148–57.

Devaki, B. and Grossman, A.R. (1993). Characterization of gene clusters encoding the fucoxanthin chlorophyll proteins of the diatom Phaeodactylum tricornutum. Nucleic Acids Res. **21**: 4458–4466.

Dismukes, G.C., Carrieri, D., Bennette, N., Ananyev, G.M., and Posewitz, M.C. (2008). Aquatic phototrophs: efficient alternatives to land-based crops for biofuels. Curr. Opin. Biotechnol. **19**: 235–40.

Dittami, S.M., Michel, G., Collén, J., Boyen, C., and Tonon, T. (2010). Chlorophyll-binding proteins revisited--a multigenic family of light-harvesting and stress proteins from a brown algal perspective. BMC Evol. Biol. **10**: 365.

Durnford, D.G., Aebersold, R., and Green, B.R. (1996). The fucoxanthin-chlorophyll proteins from a chromophyte alga are part of a large multigene family: structural and evolutionary relationships to other light harvesting antennae. MGG Mol. Gen. Genet. **253**: 377.

Durnford, D.G., Price, J.A., McKim, S.M., and Sarchfield, M.L. (2003). Light-harvesting complex gene expression is controlled by both transcriptional and post-transcriptional mechanisms during photoacclimation in Chlamydomonas reinhardtii. Physiol. Plant. **118**: 193–205.

Durrant, J.R., Giorgi, L.B., Barber, J., Klug, D.R., and Porter, G. (1990). Characterisation of triplet states in isolated Photosystem II reaction centres: Oxygen quenching as a mechanism for photodamage. Biochim. Biophys. Acta - Bioenerg. **1017**: 167–175.

Dyall, S.D., Brown, M.T., and Johnson, P.J. (2004). Ancient invasions: from endosymbionts to organelles. Science **304**: 253–7.

Eberhard, S., Finazzi, G., and Wollman, F.-A. (2008). The dynamics of photosynthesis. Annu. Rev. Genet. **42**: 463–515.

Egorova, E.A. and Bukhov, N.G. (2002). Effect of Elevated Temperatures on the Activity of Alternative

Pathways of Photosynthetic Electron Transport in Intact Barley and Maize Leaves. Russ. J. Plant Physiol. **49**: 575–584.

Falkowski, P.G. and Owens, T.G. (1980). Light-Shade Adaptation : TWO STRATEGIES IN MARINE PHYTOPLANKTON. Plant Physiol. **66**: 592–595.

Falkowski, P.G. and Raven, J.A. (2013). Aquatic Photosynthesis: (Second Edition).

Fan, D.-Y., Hope, A.B., Smith, P.J., Jia, H., Pace, R.J., Anderson, J.M., and Chow, W.S. (2007). The stoichiometry of the two photosystems in higher plants revisited. Biochim. Biophys. Acta **1767**: 1064–72.

Ferreira, K.N. (2004). Architecture of the Photosynthetic Oxygen-Evolving Center. Science (80-.). **303**: 1831–1838.

Finazzi, G. (2002). Involvement of state transitions in the switch between linear and cyclic electron flow in Chlamydomonas reinhardtii. EMBO Rep. **3**: 280–285.

Finazzi, G. and Forti, G. (2004). Metabolic Flexibility of the Green Alga Chlamydomonas reinhardtii as Revealed by the Link between State Transitions and Cyclic Electron Flow. Photosynth. Res. **82**: 327–38.

Fisher, T., Shurtz-swirski, R., Gepstein, S., and Dubinsky, Z. (1989). Changes in the levels of ribulose-l,5-bisphosphate carboxylase/oxygenase (rubisco) in tetraedron minimum (chlorophyta) during light and shade adaptation. Plant Cell Physiol. **30**: 221–228.

García-Camacho, F., Sánchez-Mirón, A., Molina-Grima, E., Camacho-Rubio, F., and Merchuck, J.C. (2012). A mechanistic model of photosynthesis in microalgae including photoacclimation dynamics. J. Theor. Biol. **304**: 1–15.

García-Plazaola, J.I., Matsubara, S., and Osmond, C.B. (2007). The lutein epoxide cycle in higher plants: its relationships to other xanthophyll cycles and possible functions. Funct. Plant Biol. **34**: 759.

Germano, M., Yakushevska, A.E., Keegstra, W., van Gorkom, H.J., Dekker, J.P., and Boekema, E.J. (2002). Supramolecular organization of photosystem I and light-harvesting complex I in Chlamydomonas reinhardtii. FEBS Lett. **525**: 121–5.

Gilmore, A.M., Mohanty, N., and Yamamoto, H.Y. (1994). Epoxidation of zeaxanthin and antheraxanthin reverses non-photochemical quenching of photosystem II chlorophyll a fluorescence in the presence of trans-thylakoid ΔpH. FEBS Lett. **350**: 271–274.

Golding, A.J., Finazzi, G., and Johnson, G.N. (2004). Reduction of the thylakoid electron transport chain by stromal reductants--evidence for activation of cyclic electron transport upon dark adaptation or under drought. Planta **220**: 356–63.

Golding, A.J. and Johnson, G.N. (2003). Down-regulation of linear and activation of cyclic electron transport during drought. Planta **218**: 107–14.

Goss, R. and Jakob, T. (2010). Regulation and function of xanthophyll cycle-dependent photoprotection in algae. Photosynth. Res. **106**: 103–122.

Green, B.R. and Durnford, D.G. (1996). The chlorophyll-carotenoid proteins of oxygenic photosynthesis. Annu. Rev. Plant Physiol. Plant Mol. Biol. **47**: 685–714.

Grobbelaar, J.U. (2011). Microalgae mass culture: the constraints of scaling-up. J. Appl. Phycol. **24**: 315–318.

Grossman, A.R., Schaefer, M.R., Chiang, G.G., and Collier, J.L. (1993). The phycobilisome, a light-harvesting complex responsive to environmental conditions. Microbiol. Rev. **57**: 725–49.

Gruszecki, W.I., Sujak, A., Strzalka, K., Radunz, A., and Schmid, G.H. (1999). Organisation of xanthophyll-lipid membranes studied by means of specific pigment antisera, spectrophotometry and monomolecular layer technique lutein versus zeaxanthin. Zeitschrift fur Naturforsch. - Sect. C J. Biosci. **54**: 517–525.

Guillard, R.R.L. and Lorenzen, C.J. (1972). YELLOW-GREEN ALGAE WITH CHLOROPHYLLIDE C 2. J. Phycol. **8**: 10–14.

Hager, A. and Holocher, K. (1994). Localization of the xanthophyll-cycle enzyme violaxanthin de-epoxidase within the thylakoid lumen and abolition of its mobility by a (light-dependent) pH decrease. Planta **192**: 581–589.

Hammes, G.G. (1982). Unifying concept for the coupling between ion pumping and ATP hydrolysis or synthesis. Proc. Natl. Acad. Sci. U. S. A. **79**: 6881–4.

Hashimoto, M., Endo, T., Peltier, G., Tasaka, M., and Shikanai, T. (2003). A nucleus-encoded factor, CRR2, is essential for the expression of chloroplast ndhB in Arabidopsis. Plant J. **36**: 541–9.

Havaux, M. (1998). Carotenoids as membrane stabilizers in chloroplasts. Trends Plant Sci. **3**: 147–151.

Havaux, M., Dall'osto, L., and Bassi, R. (2007). Zeaxanthin has enhanced antioxidant capacity with respect to all other xanthophylls in Arabidopsis leaves and functions independent of binding to PSII antennae. Plant Physiol. **145**: 1506–20.

Havaux, M. and Niyogi, K.K. (1999). The violaxanthin cycle protects plants from photooxidative damage by more than one mechanism. Proc. Natl. Acad. Sci. **96**: 8762–8767.

Helman, Y., Tchernov, D., Reinhold, L., Shibata, M., Ogawa, T., Schwarz, R., Ohad, I., and Kaplan, A. (2003). Genes Encoding A-Type Flavoproteins Are Essential for Photoreduction of O2 in Cyanobacteria. Curr. Biol. **13**: 230–235.

Herbstová, M., Tietz, S., Kinzel, C., Turkina, M. V, and Kirchhoff, H. (2012). Architectural switch in plant photosynthetic membranes induced by light stress. Proc. Natl. Acad. Sci. U. S. A. **109**: 20130–5.

Hertle, A.P., Blunder, T., Wunder, T., Pesaresi, P., Pribil, M., Armbruster, U., and Leister, D. (2013). PGRL1 is the elusive ferredoxin-plastoquinone reductase in photosynthetic cyclic electron flow. Mol. Cell **49**: 511–23.

HILL, R. and BENDALL, F. (1960). Function of the Two Cytochrome Components in Chloroplasts: A Working Hypothesis. Nature **186**: 136–137.

Holt, N.E., Zigmantas, D., Valkunas, L., Li, X.-P., Niyogi, K.K., and Fleming, G.R. (2005). Carotenoid cation formation and the regulation of photosynthetic light harvesting. Science **307**: 433–6.

Horton, P., Ruban, A. V., and Walters, R.G. (1996). REGULATION OF LIGHT HARVESTING IN GREEN PLANTS. Annu. Rev. Plant Physiol. Plant Mol. Biol. **47**: 655–684.

Horton, P., Wentworth, M., and Ruban, A. (2005). Control of the light harvesting function of chloroplast membranes: the LHCII-aggregation model for non-photochemical quenching. FEBS Lett. **579**: 4201–6.

Ikeda, Y., Komura, M., Watanabe, M., Minami, C., Koike, H., Itoh, S., Kashino, Y., and Satoh, K. (2008a). Photosystem I complexes associated with fucoxanthin-chlorophyll-binding proteins from a marine centric diatom, Chaetoceros gracilis. Biochim. Biophys. Acta **1777**: 351–61.

Ikeda, Y., Komura, M., Watanabe, M., Minami, C., Koike, H., Itoh, S., Kashino, Y., and Satoh, K. (2008b). Photosystem I complexes associated with fucoxanthin-chlorophyll-binding proteins from a marine centric diatom, Chaetoceros gracilis. Biochim. Biophys. Acta **1777**: 351–61.

Iwai, M., Takizawa, K., Tokutsu, R., Okamuro, A., Takahashi, Y., and Minagawa, J. (2010). Isolation of the elusive supercomplex that drives cyclic electron flow in photosynthesis. Nature **464**: 1210–3.

Jackowski, G., Olkiewicz, P., and Zelisko, A. (2003). The acclimative response of the main light-harvesting chlorophyll a/b-protein complex of photosystem II (LHCII) to elevated irradiances at the level of trimeric subunits. J. Photochem. Photobiol. B. **70**: 163–70.

Jahns, P. and Heyde, S. (1999). Dicyclohexylcarbodiimide alters the pH dependence of violaxanthin de-epoxidation. Planta **207**: 393–400.

Jahns, P., Latowski, D., and Strzalka, K. (2009). Mechanism and regulation of the violaxanthin cycle: the role of antenna proteins and membrane lipids. Biochim. Biophys. Acta **1787**: 3–14.

Jans, F., Mignolet, E., Houyoux, P.-A., Cardol, P., Ghysels, B., Cuiné, S., Cournac, L., Peltier, G., Remacle, C., and Franck, F. (2008). A type II NAD(P)H dehydrogenase mediates light-independent plastoquinone reduction in the chloroplast of Chlamydomonas. Proc. Natl. Acad. Sci. U. S. A. **105**: 20546–51.

Jansson, S. (1999). A guide to the Lhc genes and their relatives in Arabidopsis. Trends Plant Sci. **4**: 236–240.

Jensen, P.E., Bassi, R., Boekema, E.J., Dekker, J.P., Jansson, S., Leister, D., Robinson, C., and Scheller, H.V. (2007). Structure, function and regulation of plant photosystem I. Biochim. Biophys. Acta **1767**: 335–52.

Joët, T., Cournac, L., Peltier, G., and Havaux, M. (2002). Cyclic electron flow around photosystem I in C(3) plants. In vivo control by the redox state of chloroplasts and involvement of the NADH-dehydrogenase complex. Plant Physiol. **128**: 760–9.

Johnson, G.N. (2005). Cyclic electron transport in C3 plants: fact or artefact? J. Exp. Bot. **56**: 407–16.

Johnson, X. et al. (2014). Proton gradient regulation 5-mediated cyclic electron flow under ATP- or redox-limited conditions: a study of ΔATpase pgr5 and ΔrbcL pgr5 mutants in the green alga Chlamydomonas reinhardtii. Plant Physiol. **165**: 438–52.

Joliot, P. and Joliot, A. (2002). Cyclic electron transfer in plant leaf. Proc. Natl. Acad. Sci. U. S. A. **99**: 10209–14.

Joliot, P. and Joliot, A. (2005). Quantification of cyclic and linear flows in plants. Proc. Natl. Acad. Sci. U. S. A. **102**: 4913–8.

Jordan, P., Fromme, P., Witt, H.T., Klukas, O., Saenger, W., and Krauss, N. (2001). Three-dimensional structure of cyanobacterial photosystem I at 2.5 A resolution. Nature **411**: 909–17.

Keeling, P.J. (2010). The endosymbiotic origin, diversification and fate of plastids. Philos. Trans. R. Soc. Lond. B. Biol. Sci. **365**: 729–48.

Keren, N., Berg, A., van Kan, P.J.M., Levanon, H., and Ohad, I. (1997). Mechanism of photosystem II photoinactivation and D1 protein degradation at low light: The role of back electron flow. Proc. Natl. Acad. Sci. **94**: 1579–1584.

Kirchhoff, H., Schöttler, M.A., Maurer, J., and Weis, E. (2004). Plastocyanin redox kinetics in spinach chloroplasts: evidence for disequilibrium in the high potential chain. Biochim. Biophys. Acta **1659**: 63–72.

Kirilovsky, D. (2015). Modulating energy arriving at photochemical reaction centers: orange carotenoid protein-related photoprotection and state transitions. Photosynth. Res. **126**: 3–17.

Klimmek, F., Sjödin, A., Noutsos, C., Leister, D., and Jansson, S. (2006). Abundantly and rarely expressed Lhc protein genes exhibit distinct regulation patterns in plants. Plant Physiol. **140**: 793–804.

Krieger-Liszkay, A., Fufezan, C., and Trebst, A. Singlet oxygen production in photosystem II and related protection mechanism. Photosynth. Res. **98**: 551–64.

Kruip, J., Bald, D., Boekema, E., and Rögner, M. (1994). Evidence for the existence of trimeric and monomeric Photosystem I complexes in thylakoid membranes from cyanobacteria. Photosynth. Res. **40**: 279–86.

Külheim, C., Agren, J., and Jansson, S. (2002). Rapid regulation of light harvesting and plant fitness in the field. Science **297**: 91–3.

Lavaud, J., Rousseau, B., and Etienne, A.-L. (2002). In diatoms, a transthylakoid proton gradient alone is not sufficient to induce a non-photochemical fluorescence quenching. FEBS Lett. **523**: 163–6.

Lavergne, J. and Joliot, P. (1991). Restricted diffusion in photosynthetic membranes. Trends Biochem. Sci. **16**: 129–34.

LEDFORD, H.K. and NIYOGI, K.K. (2005). Singlet oxygen and photo-oxidative stress management in plants and algae. Plant, Cell Environ. **28**: 1037–1045.

Leister, D. and Shikanai, T. (2013). Complexities and protein complexes in the antimycin A-sensitive pathway of cyclic electron flow in plants. Front. Plant Sci. **4**: 161.

Lepetit, B., Goss, R., Jakob, T., and Wilhelm, C. (2012). Molecular dynamics of the diatom thylakoid membrane under different light conditions. Photosynth. Res. **111**: 245–57.

Li, X.P., Björkman, O., Shih, C., Grossman, A.R., Rosenquist, M., Jansson, S., and Niyogi, K.K. (2000). A pigment-binding protein essential for regulation of photosynthetic light harvesting. Nature **403**: 391–5.

Li, X.-P., Gilmore, A.M., Caffarri, S., Bassi, R., Golan, T., Kramer, D., and Niyogi, K.K. (2004). Regulation of Photosynthetic Light Harvesting Involves Intrathylakoid Lumen pH Sensing by the PsbS Protein. J. Biol. Chem. **279**: 22866–22874.

Li, Z., Wakao, S., Fischer, B.B., and Niyogi, K.K. (2009). Sensing and responding to excess light. Annu. Rev. Plant Biol. **60**: 239–60.

Liu, Z., Yan, H., Wang, K., Kuang, T., Zhang, J., Gui, L., An, X., and Chang, W. (2004). Crystal structure of spinach major light-harvesting complex at 2.72 Å resolution. Nature **428**: 287–292.

Lubián, L.M., Montero, O., Moreno-Garrido, I., Huertas, I.E., Sobrino, C., González-Del Valle, M., and Parés, G. (2000). Nannochloropsis (Eustigmatophyceae) as source of commercially valuable pigments. In Journal of Applied Phycology, pp. 249–255.

Mehler, A.H. (1951). Studies on reactions of illuminated chloroplasts. Arch. Biochem. Biophys. **33**: 65–77.

Melis, A. (1991). Dynamics of photosynthetic membrane composition and function. Biochim. Biophys. Acta -

Bioenerg. **1058**: 87–106.

Mellis, A. (1999). Photosystem-II damage and repair cycle in chloroplasts: What modulates the rate of photodamage in vivo? Trends Plant Sci. **4**: 130–135.

Minagawa, J. and Tokutsu, R. (2015). Dynamic regulation of photosynthesis in Chlamydomonas reinhardtii. Plant J. **82**: 413–28.

MITCHELL, P. (1961). Coupling of phosphorylation to electron and hydrogen transfer by a chemi-osmotic type of mechanism. Nature **191**: 144–8.

Miyake, C., Horiguchi, S., Makino, A., Shinzaki, Y., Yamamoto, H., and Tomizawa, K. (2005). Effects of light intensity on cyclic electron flow around PSI and its relationship to non-photochemical quenching of Chl fluorescence in tobacco leaves. Plant Cell Physiol. **46**: 1819–30.

Moseley, J.L., Allinger, T., Herzog, S., Hoerth, P., Wehinger, E., Merchant, S., and Hippler, M. (2002). Adaptation to Fe-deficiency requires remodeling of the photosynthetic apparatus. EMBO J. **21**: 6709–20.

Mozzo, M., Dall'Osto, L., Hienerwadel, R., Bassi, R., and Croce, R. (2008). Photoprotection in the antenna complexes of photosystem II: role of individual xanthophylls in chlorophyll triplet quenching. J. Biol. Chem. **283**: 6184–92.

Müller, P., Li, X.P., and Niyogi, K.K. (2001). Non-photochemical quenching. A response to excess light energy. Plant Physiol. **125**: 1558–1566.

Mullineaux, C.W. (2008). Phycobilisome-reaction centre interaction in cyanobacteria. Photosynth. Res. **95**: 175–82.

Munekage, Y., Hashimoto, M., Miyake, C., Tomizawa, K., Endo, T., Tasaka, M., and Shikanai, T. (2004). Cyclic electron flow around photosystem I is essential for photosynthesis. Nature **429**: 579–82.

Munekage, Y., Hojo, M., Meurer, J., Endo, T., Tasaka, M., and Shikanai, T. (2002). PGR5 is involved in cyclic electron flow around photosystem I and is essential for photoprotection in Arabidopsis. Cell **110**: 361–71.

Munekage, Y., Takeda, S., Endo, T., Jahns, P., Hashimoto, T., and Shikanai, T. (2001). Cytochrome b6f mutation specifically affects thermal dissipation of absorbed light energy in Arabidopsis. Plant J. **28**: 351–359.

Murata, N., Takahashi, S., Nishiyama, Y., and Allakhverdiev, S.I. (2007). Photoinhibition of photosystem II under environmental stress. Biochim. Biophys. Acta **1767**: 414–21.

Neilson, J.A.D. and Durnford, D.G. (2010). Structural and functional diversification of the light-harvesting complexes in photosynthetic eukaryotes. Photosynth. Res. **106**: 57–71.

Nield, J., Kruse, O., Ruprecht, J., da Fonseca, P., Büchel, C., and Barber, J. (2000). Three-dimensional structure of Chlamydomonas reinhardtii and Synechococcus elongatus photosystem II complexes allows for comparison of their oxygen-evolving complex organization. J. Biol. Chem. **275**: 27940–6.

Nilkens, M., Kress, E., Lambrev, P., Miloslavina, Y., Müller, M., Holzwarth, A.R., and Jahns, P. (2010). Identification of a slowly inducible zeaxanthin-dependent component of non-photochemical quenching of chlorophyll fluorescence generated under steady-state conditions in Arabidopsis. Biochim. Biophys. Acta **1797**: 466–75.

Niyogi, K.K. (1999). PHOTOPROTECTION REVISITED: Genetic and Molecular Approaches. Annu. Rev. Plant Physiol. Plant Mol. Biol. **50**: 333–359.

Niyogi, K.K. (2000). Safety valves for photosynthesis. Curr. Opin. Plant Biol. **3**: 455–460.

Niyogi, K.K., Grossman, A.R., and Björkman, O. (1998). Arabidopsis mutants define a central role for the xanthophyll cycle in the regulation of photosynthetic energy conversion. Plant Cell **10**: 1121–1134.

Niyogi, K.K. and Truong, T.B. (2013). Evolution of flexible non-photochemical quenching mechanisms that regulate light harvesting in oxygenic photosynthesis. Curr. Opin. Plant Biol. **16**: 307–14.

Norsker, N.-H., Barbosa, M.J., Vermuë, M.H., and Wijffels, R.H. (2011). Microalgal production--a close look at the economics. Biotechnol. Adv. **29**: 24–7.

Nymark, M., Valle, K.C., Brembu, T., Hancke, K., Winge, P., Andresen, K., Johnsen, G., and Bones, A.M. (2009). An integrated analysis of molecular acclimation to high light in the marine diatom Phaeodactylum tricornutum. PLoS One **4**: e7743.

Ogawa, T. (1991). A gene homologous to the subunit-2 gene of NADH dehydrogenase is essential to inorganic carbon transport of Synechocystis PCC6803. Proc. Natl. Acad. Sci. U. S. A. **88**: 4275–9.

Okegawa, Y., Long, T.A., Iwano, M., Takayama, S., Kobayashi, Y., Covert, S.F., and Shikanai, T. (2007). A Balanced PGR5 Level is Required for Chloroplast Development and Optimum Operation of Cyclic Electron Transport Around Photosystem I. Plant Cell Physiol. **48**: 1462–1471.

Olaizola, M., La Roche, J., Kolber, Z., and Falkowski, P.G. (1994). Non-photochemical fluorescence quenching and the diadinoxanthin cycle in a marine diatom. Photosynth. Res. **41**: 357–370.

Owens, T.G. (1986). Light-Harvesting Function in the Diatom Phaeodactylum tricornutum: II. Distribution of Excitation Energy between the Photosystems. Plant Physiol. **80**: 739–46.

Papadakis, I.A., Kotzabasis, K., and Lika, K. (2012). Modeling the dynamic modulation of light energy in photosynthetic algae. J. Theor. Biol. **300**: 254–64.

Papagiannakis, E., H M van Stokkum, I., Fey, H., Büchel, C., and van Grondelle, R. (2005). Spectroscopic characterization of the excitation energy transfer in the fucoxanthin-chlorophyll protein of diatoms. Photosynth. Res. **86**: 241–50.

Pascal, A.A., Liu, Z., Broess, K., van Oort, B., van Amerongen, H., Wang, C., Horton, P., Robert, B., Chang, W., and Ruban, A. (2005). Molecular basis of photoprotection and control of photosynthetic light-harvesting. Nature **436**: 134–7.

Peers, G., Truong, T.B., Ostendorf, E., Busch, A., Elrad, D., Grossman, A.R., Hippler, M., and Niyogi, K.K. (2009). An ancient light-harvesting protein is critical for the regulation of algal photosynthesis. Nature **462**: 518–21.

Peltier, G. and Cournac, L. (2002). Chlororespiration. Annu. Rev. Plant Biol. **53**: 523–50.

Peltier, G., Tolleter, D., Billon, E., and Cournac, L. (2010). Auxiliary electron transport pathways in chloroplasts of microalgae. Photosynth. Res. **106**: 19–31.

Peng, L. and Shikanai, T. (2011). Supercomplex formation with photosystem I is required for the stabilization of the chloroplast NADH dehydrogenase-like complex in Arabidopsis. Plant Physiol. **155**: 1629–39.

Perry, M.J., Talbot, M.C., and Alberte, R.S. (1981). Photoadaption in marine phytoplankton: Response of the photosynthetic unit. Mar. Biol. **62**: 91–101.

Petroutsos, D., Terauchi, A.M., Busch, A., Hirschmann, I., Merchant, S.S., Finazzi, G., and Hippler, M. (2009). PGRL1 participates in iron-induced remodeling of the photosynthetic apparatus and in energy metabolism in Chlamydomonas reinhardtii. J. Biol. Chem. **284**: 32770–81.

Pfundel, E.E. and Dilley, R.A. (1993). The pH Dependence of Violaxanthin Deepoxidation in Isolated Pea Chloroplasts. Plant Physiol. **101**: 65–71.

Pfundel, E.E., Renganathan, M., Gilmore, A.M., Yamamoto, H.Y., and Dilley, R.A. (1994). Intrathylakoid pH in Isolated Pea Chloroplasts as Probed by Violaxanthin Deepoxidation. Plant Physiol. **106**: 1647–1658.

Pittman, J.K., Dean, A.P., and Osundeko, O. (2011). The potential of sustainable algal biofuel production using wastewater resources. Bioresour. Technol. **102**: 17–25.

Pogson, B.J., Niyogi, K.K., Bjorkman, O., and DellaPenna, D. (1998). Altered xanthophyll compositions adversely affect chlorophyll accumulation and nonphotochemical quenching in Arabidopsis mutants. Proc. Natl. Acad. Sci. **95**: 13324–13329.

Preisig, H.R. and Wilhelm, C. (1989). Ultrastructure, pigments and taxonomy of Botryochloropsis similis gen. et sp. nov. (Eustigmatophyceae). Phycologia **28**: 61–69.

Quick, W.P. and Stitt, M. (1989). An examination of factors contributing to non-photochemical quenching of chlorophyll fluorescence in barley leaves. Biochim. Biophys. Acta - Bioenerg. **977**: 287–296.

Riisberg, I., Orr, R.J.S., Kluge, R., Shalchian-Tabrizi, K., Bowers, H.A., Patil, V., Edvardsen, B., and Jakobsen, K.S. (2009). Seven gene phylogeny of heterokonts. Protist **160**: 191–204.

Rockholm, D. (1996). Violaxanthin de-epoxidase. PLANT Physiol. **110**: 697–703.

Rodolfi, L., Chini Zittelli, G., Bassi, N., Padovani, G., Biondi, N., Bonini, G., and Tredici, M.R. (2009). Microalgae for oil: strain selection, induction of lipid synthesis and outdoor mass cultivation in a low-cost photobioreactor. Biotechnol. Bioeng. **102**: 100–12.

Rodríguez, F., Chauton, M., Johnsen, G., Andresen, K., Olsen, L.M., and Zapata, M. (2005). Photoacclimation in phytoplankton: implications for biomass estimates, pigment functionality and chemotaxonomy. Mar. Biol. **148**: 963–971.

Ruban, A. V. and Horton, P. (1995). An Investigation of the Sustained Component of Nonphotochemical Quenching of Chlorophyll Fluorescence in Isolated Chloroplasts and Leaves of Spinach. Plant Physiol. **108**: 721–726.

Rumeau, D., Bécuwe-Linka, N., Beyly, A., Louwagie, M., Garin, J., and Peltier, G. (2005). New subunits NDH-M, -N, and -O, encoded by nuclear genes, are essential for plastid Ndh complex functioning in higher plants. Plant Cell **17**: 219–32.

Saga, G., Giorgetti, A., Fufezan, C., Giacometti, G.M., Bassi, R., and Morosinotto, T. (2010). Mutation analysis of violaxanthin de-epoxidase identifies substrate-binding sites and residues involved in catalysis. J. Biol. Chem. **285**: 23763–70.

Schaller, S., Latowski, D., Jemioła-Rzemińska, M., Wilhelm, C., Strzałka, K., and Goss, R. (2010). The main thylakoid membrane lipid monogalactosyldiacylglycerol (MGDG) promotes the de-epoxidation of violaxanthin associated with the light-harvesting complex of photosystem II (LHCII). Biochim. Biophys. Acta **1797**: 414–24.

Schaller, S., Wilhelm, C., Strzałka, K., and Goss, R. (2012). Investigating the interaction between the violaxanthin cycle enzyme zeaxanthin epoxidase and the thylakoid membrane. J. Photochem. Photobiol. B. **114**: 119–25.

Scheller, H. V, Jensen, P.E., Haldrup, A., Lunde, C., and Knoetzel, J. (2001). Role of subunits in eukaryotic Photosystem I. Biochim. Biophys. Acta **1507**: 41–60.

Schenk, P.M., Thomas-Hall, S.R., Stephens, E., Marx, U.C., Mussgnug, J.H., Posten, C., Kruse, O., and Hankamer, B. (2008). Second Generation Biofuels: High-Efficiency Microalgae for Biodiesel Production. BioEnergy Res. **1**: 20–43.

Searchinger, T., Heimlich, R., Houghton, R.A., Dong, F., Elobeid, A., Fabiosa, J., Tokgoz, S., Hayes, D., and Yu, T.-H. (2008). Use of U.S. croplands for biofuels increases greenhouse gases through emissions from land-use change. Science **319**: 1238–40.

Sforza, E., Simionato, D., Giacometti, G.M., Bertucco, A., and Morosinotto, T. (2012). Adjusted light and dark cycles can optimize photosynthetic efficiency in algae growing in photobioreactors. PLoS One **7**: e38975.

Shikanai, T. (2007). Cyclic electron transport around photosystem I: genetic approaches. Annu. Rev. Plant Biol. **58**: 199–217.

Shikanai, T., Endo, T., Hashimoto, T., Yamada, Y., Asada, K., and Yokota, A. (1998). Directed disruption of the tobacco ndhB gene impairs cyclic electron flow around photosystem I. Proc. Natl. Acad. Sci. U. S. A. **95**: 9705–9.

Siefermann, D. and Yamamoto, H.Y. (1975). Properties of NADPH and oxygen-dependent zeaxanthin epoxidation in isolated chloroplasts. A transmembrane model for the violaxanthin cycle. Arch. Biochem. Biophys. **171**: 70–7.

Simionato, D., Block, M.A., La Rocca, N., Jouhet, J., Maréchal, E., Finazzi, G., and Morosinotto, T. (2013). The response of Nannochloropsis gaditana to nitrogen starvation includes de novo biosynthesis of triacylglycerols, a decrease of chloroplast galactolipids, and reorganization of the photosynthetic apparatus. Eukaryot. Cell **12**: 665–76.

Simionato, D., Sforza, E., Corteggiani Carpinelli, E., Bertucco, A., Giacometti, G.M., and Morosinotto, T. (2011). Acclimation of Nannochloropsis gaditana to different illumination regimes: effects on lipids accumulation. Bioresour. Technol. **102**: 6026–32.

Smith, B.M. and Melis, A. (1988). Photochemical Apparatus Organization in the Diatom Cylindrotheca fusiformis: Photosystem Stoichiometry and Excitation Distribution in Cells Grown under High and Low Irradiance. Plant Cell Physiol. **29**: 761–769.

Smith, B.M., Morrissey, P.J., Guenther, J.E., Nemson, J.A., Harrison, M.A., Allen, J.F., and Melis, A. (1990). Response of the Photosynthetic Apparatus in Dunaliella salina (Green Algae) to Irradiance Stress. Plant

Physiol. **93**: 1433–40.

Strzepek, R.F. and Harrison, P.J. (2004). Photosynthetic architecture differs in coastal and oceanic diatoms. Nature **431**: 689–92.

Sukenik, A., Livne, A., Apt, K.E., and Grossman, A.R. (2000). CHARACTERIZATION OF A GENE ENCODING THE LIGHT-HARVESTING VIOLAXANTHIN-CHLOROPHYLL PROTEIN OF NANNOCHLOROPSIS SP. (EUSTIGMATOPHYCEAE). J. Phycol. **36**: 563–570.

Sukenik, A., Livne, A., Neori, A., Yacobi, Y.Z., and Katcoff, D. (1992). Purification and characterization of a light-harvesting chlorophyll-protein complex from the marine eustigmatophyte nannochloropsis sp. Plant Cell Physiol. **33**: 1041–1048.

Tardy, F. and Havaux, M. (1997). Thylakoid membrane fluidity and thermostability during the operation of the xanthophyll cycle in higher-plant chloroplasts. Biochim. Biophys. Acta **1330**: 179–93.

Teramoto, H., Nakamori, A., Minagawa, J., and Ono, T. (2002). Light-intensity-dependent expression of Lhc gene family encoding light-harvesting chlorophyll-a/b proteins of photosystem II in Chlamydomonas reinhardtii. Plant Physiol. **130**: 325–33.

Terashima, M., Petroutsos, D., Hüdig, M., Tolstygina, I., Trompelt, K., Gäbelein, P., Fufezan, C., Kudla, J., Weinl, S., Finazzi, G., and Hippler, M. (2012). Calcium-dependent regulation of cyclic photosynthetic electron transfer by a CAS, ANR1, and PGRL1 complex. Proc. Natl. Acad. Sci. U. S. A. **109**: 17717–22.

Ting, C.S. and Owens, T.G. (1994). The Effects of Excess Irradiance on Photosynthesis in the Marine Diatom Phaeodactylum tricornutum. Plant Physiol. **106**: 763–770.

Tolleter, D. et al. (2011). Control of hydrogen photoproduction by the proton gradient generated by cyclic electron flow in Chlamydomonas reinhardtii. Plant Cell **23**: 2619–30.

Umena, Y., Kawakami, K., Shen, J.-R., and Kamiya, N. (2011). Crystal structure of oxygen-evolving photosystem II at a resolution of 1.9 Å. Nature **473**: 55–60.

Vass, I., Styring, S., Hundal, T., Koivuniemi, A., Aro, E., and Andersson, B. (1992). Reversible and irreversible intermediates during photoinhibition of photosystem II: stable reduced QA species promote chlorophyll triplet formation. Proc. Natl. Acad. Sci. **89**: 1408–1412.

Veith, T., Brauns, J., Weisheit, W., Mittag, M., and Büchel, C. (2009). Identification of a specific fucoxanthin-chlorophyll protein in the light harvesting complex of photosystem I in the diatom Cyclotella meneghiniana. Biochim. Biophys. Acta **1787**: 905–12.

Veith, T. and Büchel, C. (2007). The monomeric photosystem I-complex of the diatom Phaeodactylum tricornutum binds specific fucoxanthin chlorophyll proteins (FCPs) as light-harvesting complexes. Biochim. Biophys. Acta **1767**: 1428–35.

Walters, R.G. (2005). Towards an understanding of photosynthetic acclimation. J. Exp. Bot. **56**: 435–47.

Ware, M.A., Belgio, E., and Ruban, A. V. (2014). Comparison of the protective effectiveness of NPQ in Arabidopsis plants deficient in PsbS protein and zeaxanthin. J. Exp. Bot. **66**: 1259–1270.

Wijffels, R.H., Kruse, O., and Hellingwerf, K.J. (2013). Potential of industrial biotechnology with cyanobacteria and eukaryotic microalgae. Curr. Opin. Biotechnol. **24**: 405–13.

Wilhelm, C., Jungandreas, A., Jakob, T., and Goss, R. (2014). Light acclimation in diatoms: from phenomenology to mechanisms. Mar. Genomics **16**: 5–15.

Wollman, F.A. (2001). State transitions reveal the dynamics and flexibility of the photosynthetic apparatus. EMBO J. **20**: 3623–30.

Yang, D., Webster, J., Adam, Z., Lindahl, M., and Andersson, B. (1998). Induction of acclimative proteolysis of the light-harvesting chlorophyll a/b protein of photosystem II in response to elevated light intensities. Plant Physiol. **118**: 827–34.

Young, A.J. (1991). The photoprotective role of carotenoids in higher plants. Physiol. Plant. **83**: 702–708.

Young, A.J. and Frank, H.A. (1996). Energy transfer reactions involving carotenoids: quenching of chlorophyll fluorescence. J. Photochem. Photobiol. B Biol. **36**: 3–15.

Zelisko, A., García-Lorenzo, M., Jackowski, G., Jansson, S., and Funk, C. (2005). AtFtsH6 is involved in the degradation of the light-harvesting complex II during high-light acclimation and senescence. Proc. Natl.

Acad. Sci. U. S. A. **102**: 13699–704.

Zhang, H., Whitelegge, J.P., and Cramer, W.A. (2001). Ferredoxin:NADP+ oxidoreductase is a subunit of the chloroplast cytochrome b6f complex. J. Biol. Chem. **276**: 38159–65.

Zhang, N. and Portis, A.R. (1999). Mechanism of light regulation of Rubisco: a specific role for the larger Rubisco activase isoform involving reductive activation by thioredoxin-f. Proc. Natl. Acad. Sci. U. S. A. **96**: 9438–43.

Zhu, S.-H. and Green, B.R. (2010). Photoprotection in the diatom Thalassiosira pseudonana: role of LI818-like proteins in response to high light stress. Biochim. Biophys. Acta **1797**: 1449–57.

SECTION B

CHAPTER B1

REGULATION OF PHOTOSYNTHESIS IN RESPONSE TO SHORT-TERM AND PROLONGED LIGHT STRESS IN THE EUSTIGMATOPHYCEA *NANNOCHLOROPSIS GADITANA*

Submitted in
PLoS ONE

REGULATION OF PHOTOSYNTHESIS IN RESPONSE TO SHORT-TERM AND PROLONGED LIGHT STRESS IN THE EUSTIGMATOPHYCEA *NANNOCHLOROPSIS GADITANA*

Andrea Meneghesso[1], Diana Simionato[1], Caterina Gerotto[1], Nicoletta La Rocca[1], Giovanni Finazzi[2] and Tomas Morosinotto[1,*]

[1] Dipartimento di Biologia, Università di Padova, Via U. Bassi 58/B, 35121 Padova, Italy
[2] Laboratoire de Physiologie Cellulaire et Végétale, UMR 5168, Centre National de la Recherche Scientifique (CNRS), Commissariat à l'Energie Atomique et aux Energies Alternatives (CEA), Université Grenoble Alpes, Institut National Recherche Agronomique (INRA), Institut de Recherche en Sciences et Technologies pour le Vivant (iRTSV), CEA Grenoble, F-38054 Grenoble cedex 9, France

* Corresponding author:
E-mail: tomas.morosinotto@unipd.it (TM)

Abstract

Nannochloropsis gaditana is an eukaryotic alga of the phylum of *heterokonta*, originating from a secondary endosymbiotic event. Species of this group have received increasing attention in the scientific community, reflecting their potential application in biofuel production, although the photosynthetic and physiological properties of these organisms remain poorly characterized. *Nannochloropsis* species have a peculiar photosynthetic apparatus characterized by the presence of chlorophyll a, violaxanthin and vaucheriaxanthin as the most abundant pigments.

The regulation of the photosynthetic apparatus was investigated in *Nannochloropsis gaditana* cells exposed to different light regimes. Intense illumination induces a decrease in the chlorophyll content and the antenna size of both Photosystem I and II. Cells grown in high light also show increased photosynthetic electron transport, paralleled by an increased contribution of cyclic electron transport around Photosystem I. Even when exposed to extreme light intensities, *Nannochloropsis* cells do not activate photo-protection responses, such as Non Photochemical Quenching and the xanthophyll cycle in a constitutive way. Conversely, these responses remained available for activation upon additional changes in illumination. These results suggest NPQ and the xanthophyll cycle in *Nannochloropsis gaditana* play exclusive roles in response to short-term changes in illumination but only play a slight role, if any, in responses to chronic light stress.

Introduction

Oxygenic photosynthesis catalyzes the conversion of solar light into chemical energy to assimilate CO_2 and release molecular oxygen. The complex redox activity of photosystems in the presence of oxygen easily induces the production of Reactive Oxygen Species (ROS), leading to oxidative damage of the photosynthetic apparatus (photoinhibition) (Szabó et al., 2005; Li et al., 2009; Murata et al., 2007). This phenomenon becomes particularly relevant when the absorbed radiation exceeds the saturation level of photosynthesis, and thus photochemical reactions do not readily use excitation energy (Li et al., 2009; Demmig-Adams and Adams, 2000; Barber and Andersson, 1992). To survive and thrive in a highly variable environment, photosynthetic organisms evolved the ability to maximize light-harvesting efficiency when solar radiation is limited, while dissipating energy when irradiance exceeds photosynthetic capacity.

In a natural environment, changes in light intensity occur with different rates, spanning from seconds to weeks, and photosynthetic organisms have evolved multiple regulatory mechanisms with different activation timescales, enabling responses to short- and long-term variations (Eberhard et al., 2008; Savitch et al., 2001; Walters, 2005). The long term acclimation response involves the modulation the composition of the photosynthetic apparatus according to irradiance intensity (Falkowski and LaRoche, 1991; Walters, 2005; Falkowski and Owens, 1980; Zou and Richmond, 2000). In most photosynthetic organisms, this regulation involves a reduction in the chlorophyll (Chl) content and an increase in photoprotective xanthophylls when exposed to high irradiance (Rodriguez et al., 2006; Johnsen and Sakshaug, 2007). In some organisms, the photosystem antenna size, i.e., the number of light harvesting complexes associated with each reaction center also changes according to light irradiance (Falkowski and LaRoche, 1991; Walters, 2005; Falkowski and Owens, 1980; Zou and Richmond, 2000). For example, in the green algae *Dunaliella salina,* the diatom *Skeletonema costatum* and most vascular plants, the functional antenna size of photosystems is significantly reduced in response to high irradiance during cell growth (Smith et al., 1990; Perry et al., 1981; Kurasová et al., 2002). However, the same behavior has not been observed in other green algae (*Chlamydomonas reinhardtii* and *Dunaliella euchlora*) and in most diatoms (*Phaeodactylum tricornutum* and *Cyclotella meneghiniana),* in which the antenna size in the photosystems is not modulated by light acclimation (Bonente et al., 2012; Perry et al., 1981; Lepetit et al., 2012). This heterogeneity, even within the same phylum, suggests that the acclimation mechanisms in photosynthetic organisms are species-specific and often associated with the growth environment.

Another common feature of acclimation is the modulation of the photosynthetic capacity. The high-light acclimated cells of the diatom *Phaeodactylum tricornutum* and the green algae *Chlamydomonas reinhardtii* showed an increased photosynthetic electron transport rate (Nymark et al., 2009; Bonente et al., 2012). Moreover, the overall amount of sinks of photosynthetic electron flow is typically modulated. In high light, an increased accumulation of Calvin-Benson cycle enzymes, particularly RuBisCO, have been observed in different species (Simionato et al., 2011; Fisher et al., 1989). The

effects of light acclimation were also observed in some cases at the chloroplast ultrastructural level, with the modulation of the number and reorganization of thylakoid membranes (La Rocca et al., 2015; Wilhelm et al., 2014).

While these acclimation responses represent long-term phenomena, requiring the *de novo* synthesis or degradation of proteins, photosynthetic organisms possess faster mechanisms to manage sudden changes in illumination. In this latter case, photosynthetic organisms activate the dissipation of a fraction of absorbed energy, thereby reducing ROS production. The fastest known mechanism for the modulation of light harvesting efficiency is called Non Photochemical Quenching (NPQ), involving the dissipation of excess energy as heat (Li et al., 2009). In several eukaryotic algae, NPQ activation depends on the presence of a protein called LHCSR/LHCX, as demonstrated in the green microalga *Chlamydomonas reinhardtii,* the pycoeukaryote *Ostreococcus tauri* and some diatoms (Peers et al., 2009; Zhu and Green, 2010; Bailleul et al., 2010b; Gerotto and Morosinotto, 2013). In different species, NPQ intensity is modulated under different growth conditions through the regulation of LHCSR/LHCX accumulation (Peers et al., 2009; Zhu and Green, 2010; Gerotto et al., 2011). In minutes, strong illumination also activates the synthesis of the xanthophyll zeaxanthin from pre-existing violaxanthin through the activation of Violaxanthin De-Epoxidase (VDE) (Arnoux et al., 2009; Jahns et al., 2009). The reverse reaction is mediated through the enzyme Zeaxanthin Epoxidase, leading to the reconversion of zeaxanthin into violaxanthin. Zeaxanthin, not only enhances NPQ and retards the relaxation of this process in the dark, but this enzyme also plays a direct role in ROS scavenging (Demmig-Adams, 1990; Havaux et al., 2007; Niyogi et al., 1998). The Violaxanthin (Vx)-Zeaxanthin (Zx) cycle is widely distributed in photosynthetic organisms spanning from green algae and plants to *eustigmatophytes* or brown algae, and other xanthophyll cycles mediate similar responses in other organisms, such as the diadinoxanthin (Dd)-diatoxanthin (Dt) cycle in diatoms (Coesel et al., 2008). The Dd-Dt cycle undergoes faster activation compared with the Vx-Zx cycle and plays a major role in the induction of the NPQ typical in diatoms (Ruban et al., 2004; Lavaud and Kroth, 2006; Lavaud et al., 2002).

Although these basic regulatory mechanisms are widespread in photosynthetic organisms, differences are seen in different species, likely depending on the colonization of specific ecological niches (Quaas et al., 2014; Goss and Lepetit, 2015; La Rocca et al., 2015). For example, the trans-thylakoid proton gradient, seminal for NPQ activation in plants and chlorophytes, does not play a direct role in diatoms, where the activation of the response only depends on the xanthophyll cycle (Goss et al., 2006; Lavaud and Kroth, 2006). Exploring the variability of photosynthesis regulatory responses and understanding how these responses are adapted to different environmental conditions represents a valuable source of information for a better understanding of the physiological role of these mechanisms. *Nannochloropsis gaditana* is a microalga of the *Eustigmatophyceae* class within *Heterokonta*, a group which also includes diatoms and brown algae (Cavalier-Smith, 2004; Riisberg et al., 2009). These species originated from a secondary endosymbiotic event in which an eukaryotic host cell engulfed a red alga, thus acquiring a different evolutionary history with respect to plants and green algae (Archibald and Keeling, 2002). In recent years, species belonging to the *Nannochloropsis* genus have

gained increasing interest for their potential exploitation for biodiesel production, reflecting the rapid growth rate and accumulation of lipids in these species (Rodolfi et al., 2009; Bondioli et al., 2012; Sforza et al., 2012). Despite this increased attention, information on the *Nannochloropsis* photosynthetic apparatus and its regulation remain elusive. Available studies have shown that *Nannochloropsis* species have a unique pigment composition, presenting only Chl *a* and lacking any other accessory Chl molecules, while presenting violaxanthin and vaucheriaxanthin esters as the most abundant carotenoids (Basso et al., 2014; Sukenik et al., 1992; Lubián et al., 2000).

In the present study, the response of *Nannochloropsis gaditana* cells to different growth irradiances was investigated. We found that high light-acclimated cells modulated the composition of their photosynthetic apparatus to increase photosynthetic electron transport, showing an increased contribution from cyclic electron transport. In contrast, no constitutive activation of the xanthophyll cycle and NPQ could be observed, even in extreme light excess. This shows that these mechanisms play a specific role in response to rapid changes in illumination conditions.

Materials and Methods

Culture conditions

Nannochloropsis gaditana from CCAP, strain 849/5, was grown in sterile F/2 medium containing 32 g/l sea salts, 40 mM TRIS-HCl, pH 8, and Guillard's (F/2) marine water enrichment solution (Sigma-Aldrich). The cultures were maintained and propagated using the same medium supplemented with 10 g/l of Plant Agar (Duchefa Biochemie). The growth experiments were performed in Erlenmeyer flasks through mechanical agitation, starting from a pre-culture grown at 100 μmoles of photons $m^{-2}s^{-1}$ at the exponential phase, which was diluted to an Optical Density (OD) at 750 nm equal to 0.2 in a final volume of 200 ml. Illumination was provided through a 16 hours photoperiod (16 hours light, 8 hours dark) at intensities of 10 (Low Light), 100 (Medium Light) and 1000 (High Light) μmoles of photons $m^{-2}s^{-1}$, using a fluorescent lamp or a LED Light Source SL 3500 (Photon Systems Instruments, Brno, Czech Republic). The temperature was maintained at 22 ± 1 °C in a growth chamber. Growth experiments with additional CO_2 were performed using a Multicultivator MC 1000-OD system (Photon Systems Instruments, Czech Republic) in which temperature was maintained at 21°C and illumination was provided through a 16 hours photoperiod (16 hours light, 8 hours dark) at intensities of 10, 100 and 1000 μmoles of photons $m^{-2}s^{-1}$ using an array of white LEDs. The Multicultivator experiments was performed using two different types of media: the F/2 medium described above and a F/2 medium modified to guarantee non-limiting nutrient conditions (10 times more $NaNO_3$ and NaH_2PO_4 and 2 times more $FeCl_3 \cdot 6H_2O$ and EDTA). The suspension culture was constantly mixed and aerated through air bubbling. The growth curves in the Multicultivator system were initiated using a pre-culture grown at 100 μmol of photons $m^{-2}s^{-1}$ in 0.25-L Drechsel bottles under continuous air flow enriched with 5% CO_2. Algal growth was measured through daily changes in the optical density (OD_{750}), and the cell number was monitored using a Cellometer Auto X4 cell counter (Nexcelom Bioscience). All curves were repeated at least five independent times. All analyses were performed on the fifth day of the

growth curve when the cells were still actively growing but had enough time to acclimate to different conditions. On the sampling day, the optical density for flask growth curves in LL, ML and HL conditions was 0.510±0.038, 0.469±0.032 and 0.395±0.044, respectively.

Pigments analysis

Chlorophyll (Chl) and total Carotenoids (Car) were directly extracted from intact cells using 100 % N,N'-dimethylformamide for at least 48 hours in the dark at 4°C after centrifugation of *Nannochloropsis* cells at 15000 ×*g* for 10 minutes. The pigment concentrations were spectrophotometrically determined using specific extinction coefficients (Wellburn, 1994). The content of individual carotenoids was determined using high-pressure liquid chromatography (HPLC) as previously described [38]. To perform this analysis pigments were extracted from *Nannochloropsis* cell using 80% acetone after mechanical lysis using a Mini Bead Beater (Biospec Products) in the presence of glass beads (150–212 μm diameter). The HPLC system comprised a reverse-phase column (5 μm particle size; 25x0.4 cm; 250/4 RP 18 Lichrocart, Darmstadt, Germany) and a diode-array detector to record the absorbance spectra (1100 series, Agilent, 141 Waldbronn, Germany). The peaks of each sample were identified based on the retention time and absorption spectrum. The vaucheriaxanthin retention factor was estimated after correcting that of violaxanthin for differences in absorption at 440 nm.

Thylakoid isolation

To obtain isolated thylakoids, *Nannochloropsis* cells were broken using a Mini Bead Beater (Biospec Products), according to the protocol of Basso *et al.* (2014). The thylakoids in the appropriate buffer were immediately frozen in liquid nitrogen and stored at − 80 °C until further use. All steps were performed at 4 °C in dim light. Total pigments were extracted using 80% acetone, and the chlorophyll concentration of the samples was spectrophotometrically determined.

Spectroscopic analysis

The spectroscopic analysis was performed on the fifth day of growth *in vivo* using a Joliot-type spectrophotometer (JTS-10, Biologic, France) as previously described for *Nannochloropsis gaditana* cells (Simionato et al., 2013). Changes in the amount of functional photosynthetic complexes were evaluated after measuring the Electrochromic Shift (ECS) spectral change in intact cells, representing a shift in the pigment absorption bands associated with changes in the membrane potential (Witt, 1979). Upon illumination, the charge separation occurring in photosystems generates a transmembrane electric field, which induces a change in the carotenoid absorption spectrum. These absorption changes are linearly related to changes in the transmembrane electric field potential, which, in turn, reflects the transmembrane change separation in PSI, PSII and the cytochrome b_6f complex (Bailleul et al., 2010a). ECS was measured as the difference between the signals at 520 and 498 nm (the positive and negative peaks of the ECS signal, respectively) to eliminate minor additional spectral changes that were associated with the membrane potential (Simionato et al., 2013). Upon

exposure to a saturating single turnover flash, the ECS kinetics present rather complex features: a fast signal, which is not kinetically resolved in the measurements, is observed, which reflects charge separation in the two photosystems. This fast phase is followed by a slower one, reflecting electron flow in the cytochrome b_6f complex. On a longer time scale, the signal decreases because the ATPase-synthase CF_0-Fi dissipated the transmembrane potential (Bailleul et al., 2010a). The fastest signal solely depending on PSI and PSII photochemical activity, it is possible to evaluate the relative contribution of each photosystem by comparing the amplitude of this phase in the absence and presence of PSII inhibitors. The PSII contribution was evaluated as the decrease in the amplitude of the signal measured in samples poisoned with DCMU (3-(3,4-dichlorophenyl)-1,1-dimethylurea, 80 µM) and HA (hydroxylamine, 4 mM). These molecules irreversibly block PSII charge separation, respectively acting as acceptor and donor side inhibitors of PSII. PSI was estimated as the fraction of the signal that was insensitive to these inhibitors (e.g., (Bailleul et al., 2010a)). ECS measurements were performed in intact cells using a final concentration of 200 x 10^6 cell/ml.

The spectroscopic quantification of the electron flows through the photosynthetic electron transport chain was performed measuring P_{700} (the primary electron donor to PSI) at 705 nm in intact cells. Analysis was conducted exposing the samples (final concentration 300 10^6cells/ml) to saturating actinic light (2050 µmoles of photons $m^{-2}s^{-1}$, 630 nm) for 15 seconds to maximize P_{700} oxidation and reach a steady state. At the end of the treatment, the light was switched off to follow the P_{700}^+ rereduction in the dark. The total electron flow (TEF) was deduced after measuring the P_{700}^+ re-reduction rates after illumination in untreated cells. Subsequently, the samples were treated with DCMU (80 µM) to evaluate the contribution of cyclic and other alternative electron flow (CEF + AEF) and with DCMU in combination with DBMIB (dibromothymoquinone, 300 µM) to measure the alternative electron flow (AEF), independent from cyt b_6f activity. The DCMU treatment blocks linear flow through the inhibition of PSII, while the treatment with DCMU in combination with DBMIB (inhibitor of the cytochrome b_6f) blocks both linear and cyclic flows. Cyclic electron flow was therefore evaluated as the residual rate of P_{700}^+ reduction observed in the presence of DCMU, but abolished after DBMIB addition. The electron transport rate was calculated assuming a single exponential decay of P_{700}^+. This allowed calculating the rate constant of P_{700}^+ reduction as 1/□. By multiplying the rate constant times the fraction of P_{700} oxidized, considering this value as 1 in DCMU- and DBMIB-poisoned cells (see below) we could evaluate the number of electrons transferred per unit of time electron flux (Simionato et al., 2013).

The PSI content was evaluated based on the maximum change in the absorption of P_{700}^+ in cells treated with DCMU and DBMIB at a saturating actinic light (2050 µmoles of photons $m^{-2}s^{-1}$, 630 nm) in an equal number of cells. Under these conditions, re-reduction of P_{700}^+ through photosynthetic electron flow is largely slowed down, thereby allowing to evaluate the full extent of photo-oxidizable P_{700} is likely (Simionato et al., 2013; Alric, 2010). To verify whether the light treatments used were indeed sufficient to completely oxidize $P_{700,}$ we examined several light intensities, as shown in Fig S3.

The PSI antenna size was assessed after measuring the kinetics of P_{700} oxidation at 705 nm in isolated dark-adapted thylakoids incubated with methylviologen (375 µM) and ascorbate (2 mM) for 5

minutes (Bonente et al., 2012; Swingley et al., 2010). The photo-oxidation kinetics was measured upon excitation with 150 µmoles of photons m^{-2} s^{-1} of actinic light at 630 nm (a wide range of actinic light were tested as presented in S4 Figure). The presence of a strong final electron acceptor, such as methylviologen, facilitated P_{700} oxidation at a given actinic light. The antenna size was quantified from the rate constant of the kinetics, calculated again assuming a single exponential character of the kinetics. The thylakoids were analyzed based on a total Chl amount of 40 µg.

Fluorescence measurements

On the fifth day of growth, the microalgae were collected and dark adapted for 20 minutes to achieve the complete oxidation of the primary electron acceptor Q_A, reaching a state in which all PSII reaction centers are 'open'. Chlorophyll fluorescence was determined *in vivo* using a Dual PAM 100 (Heinz-Walz, Effeltrich, Germany). Photosynthetic parameters were assessed using a Light Curve protocol, where the cells were stepwise exposed to increasing light intensities every 1 minute. After this light treatment cells were exposed to dim light for 30 minutes to estimate the dark recovery of fluorescence. The parameters Fv/Fm, NPQ and qL were calculated, respectively as (Fm-Fo)/Fm, (Fm-Fm')/Fm' and (Fm'-F')Fo'/(Fm'-Fo')F', respectively (Demmig-Adams et al., 2008).

The PSII antenna size was measured according to the fluorescence induction kinetics using a JTS-10 spectrophotometer in the fluorescence mode. Samples with a final concentration of 200 x 10^6 cell/ml after 20 minutes of dark adaptation were incubated with DCMU (80 µM) for 10 minutes to prevent the oxidation of the primary quinone acceptor Q_A. The induction kinetics was measured upon excitation with 320 µmoles of photons m^{-2} s^{-1} of actinic light at 630 nm. In the presence of this inhibitor, an average of 1 photon *per* PSII center is absorbed at time t. This parameter was estimated for every fluorescence induction trace to evaluate the number of absorbed photons by photosystems II, *i.e.* their antenna size.

Electron microscopy analysis

For transmission electron microscopy analysis, aliquots of algal cultures, sampled on the fifth day, were gently centrifuged (2000 x *g*) for 10 minutes at room temperature, and the pellets were fixed overnight at 4°C in 3% glutaraldehyde in 0.1 M sodium cacodylate buffer (pH 6.9) and post fixed for 2 hours in 1% osmium tetroxide in the same buffer. The specimens were dehydrated in a graded series of ethyl alcohol and propylene oxide and embedded in araldite. Ultrathin sections (800 nm) cut using an ultramicrotome (Ultracut; Reichert-Jung, Vienna, Austria) and stained with uranyl acetate and lead citrate were subsequently analyzed under a transmission electron microscope (TEM, Tecnai G2,FEI, Oregon) at 100 kV.

Results

Light intensity has little influence on Nannochloropsis growth under CO_2-limiting conditions

In the present study *Nannochloropsis gaditana* cultures were grown in conditions with artificial seawater and atmospheric CO_2, with slow mechanic agitation and a 16 hours light/8 hours dark photoperiod. The illumination intensity was instead set to three highly different intensities ranging from 10, 100 and 1000 µmoles of photons m^{-2} s^{-1} (hereafter, respectively referred to as LL, ML and HL). The illumination intensity has little influence on the growth kinetics, suggesting that light availability is not a limiting factor under the culture conditions tested (Figure 1A).

This hypothesis was confirmed when the cells were cultivated in a Multicultivator MC 1000-OD system with air bubbling, providing an additional carbon dioxide supply with respect to cultures grown in Erlenmeyer flasks. Notably, although the same external light intensities were applied, the geometry of the growing system was different in experiments with air bubbling, suggesting that the light absorbed by the cells was not identical. As shown in Figure 1C, for ML and HL, higher CO_2 availability resulted in faster growth compared with LL under the same conditions, demonstrating that the algae in flasks are limited by CO_2 and not by light. ML and HL with higher CO_2 availability grew faster but showed only a slight increase of the final biomass concentration. However, when the nutrient contents was also increased, ML and HL cells showed higher rates and much larger higher final biomass concentrations (Figure 1D). Under non-limiting nutrient conditions, HL cells grew faster than cells grown in flasks, but were not able to exploit the additional light energy available with respect to ML, suggesting that these cells achieved light saturation. LL cultures, however, did not benefit from the additional carbon and nutrient supply, suggesting in this case that these cells were indeed limited by light availability. The cell mortality in the different cultures was also evaluated based on the difference between the cells counted according to the bright field and fluorescence signals, where only Chl-containing living cells were visible. As shown in Figure 1B, in flask cultures HL showed a clearly higher number of bleached cells, ranging from 1-2% in LL to 2 % in ML and 14 % in HL. Such a strong increase in the concentration of dead cells suggests that HL cultures experience significant stress associated with intense illumination, reflecting growth kinetics similar to ML cells.

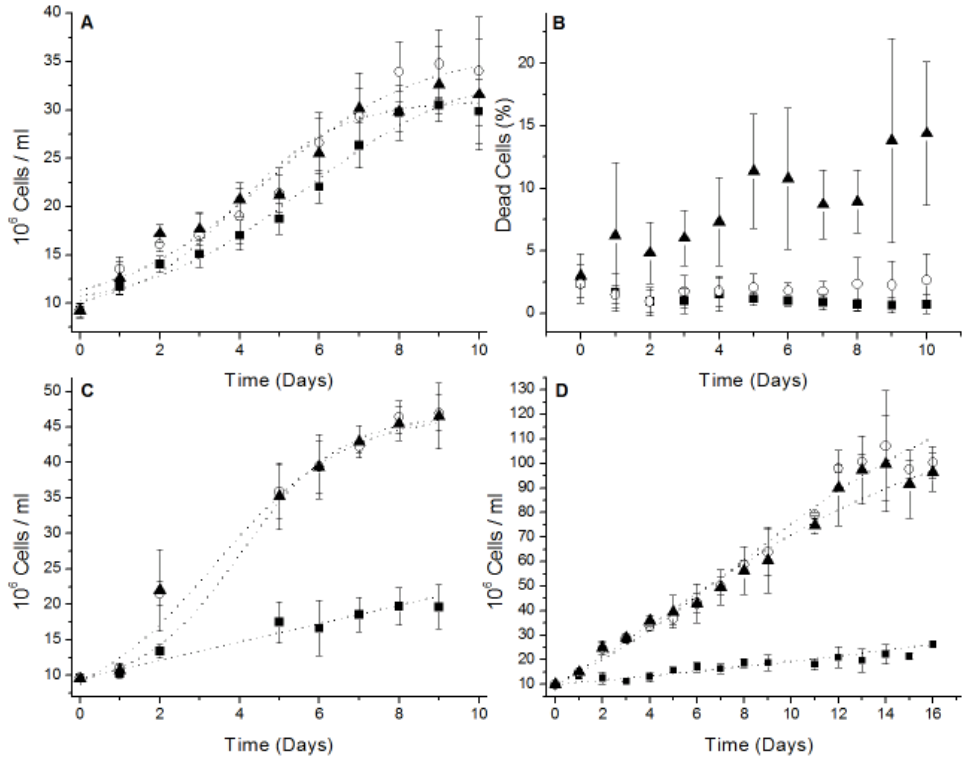

Figure 1. Cell growth with different illumination. *Nannochloropsis* cells grown under a 16-hour photoperiod (16 hours light/8 hours dark) at intensities of 10 (LL), 100 (ML), and 1000 (HL) µmoles of photons m^{-2} s^{-1} are shown, respectively, as black squares, empty circles and black triangles. A) The growth rate (Erlenmeyer flasks) in F/2 medium was evaluated after monitoring living fluorescent cells. B) The dead cells in the cultures shown in A were quantified as the difference between cell counts using a bright field and fluorescence microscopy. C-D) The growth rate under different light intensities with the external CO_2 supply provided through air bubbling in a MC 1000-OD system in F/2 medium (C) and a nutrient-enriched medium (D). Note the different Y axis between panels C and D due to the higher growth. All growth curves were repeated at least five independent times.

The increased stress under increasing light irradiance is consistent with transmission electron microscopy images of microalgae grown under different light intensities (Figure 2). LL cells are well organized, and in the chloroplast thylakoids, these cells consistently form groups of three membranes linearly distributed in the stroma (Figs. 2A and B). In contrast, HL cells and to a smaller extent ML cells showed the presence of storage lamellar vesicles and alterations in the thylakoid membranes structure (Figs. 2C and E). These effects were better evidenced at higher magnification, where chloroplast membranes displayed a variable number of thylakoids membranes (Figure 2F). Furthermore, EM pictures showed the presence of a number of highly damaged cells, consistent with higher cell mortality, in HL cultures.

To assess whether the cells had sufficient time to acclimate to the growth conditions, flask cultures were re-inoculated under the same conditions for multiple generations. As shown in S2 Figure, even after several generations, cell growth was not significantly altered under different light intensities, although a slightly higher final cell concentration was observed in HL cultures. The pigment composition and other functional analyses showed no significant differences with the cells maintained at different light intensities for multiple generations. Thus, we concluded that five days were sufficient to activate responses to different light intensities under these culture conditions and thus all analyses described below were performed after five days of growth under different light conditions, providing enough time for acclimation while maintaining the cells in the exponential growth phase.

Modulation of the photosynthetic apparatus composition under different light intensities.

Photosynthetic organisms show long-term responses to different light intensities through the modulation of the composition of the photosynthetic apparatus. Every species, however, shows specific responses in this respect, associated with adaptations to specific growing conditions during evolution. Among the acclimation strategies to different light regimes, changes in the content or composition of pigments are likely the most common effects observed. Consistently, *Nannochloropsis* cultures grown under different light conditions showed marked changes in the cell pigment content, and the Chl per cell content was four times higher in LL than in HL (Table 1). In addition, we observed a relative increase in the Car/Chl ratio, consistent with the role of carotenoids in photo-protective responses. The analysis of individual carotenoid species showed that the vaucheriaxanthin content, normalized to Chl, remained stable, and there was a slight increase in cantaxanthin and β-carotene in HL cells. The strongest increase involved violaxanthin, which, in absolute values, is be a major factor responsible for the carotenoid increase observed in HL cells. Overall, we observed the remarkable behavior of the carotenoids participating in the xanthophyll cycle (violaxanthin, antheraxanthin and zeaxanthin). On one side, these pigments are present in significant amounts, even in cells growing under light-limiting conditions (1.8 and 2.9% of total carotenoids are zeaxanthin and antheraxanthin, respectively). In ML cells, the de-epoxidized carotenoids content increased to 3.5 and 6.2% for zeaxanthin and antheraxanthin, respectively, clearly suggesting the activation of the xanthophyll cycle. However, a further increase in illumination by an order of magnitude (from 100 to 1000 µmol m^{-2} s^{-1}) did not induce any additional conversion of violaxanthin into zeaxanthin, evidenced as the unchanged de-epoxidation index (Table 1). Thus, violaxanthin represented by far the most abundant carotenoid in *Nannochloropsis* cells under all growth conditions, even in cells chronically exposed to excess light.

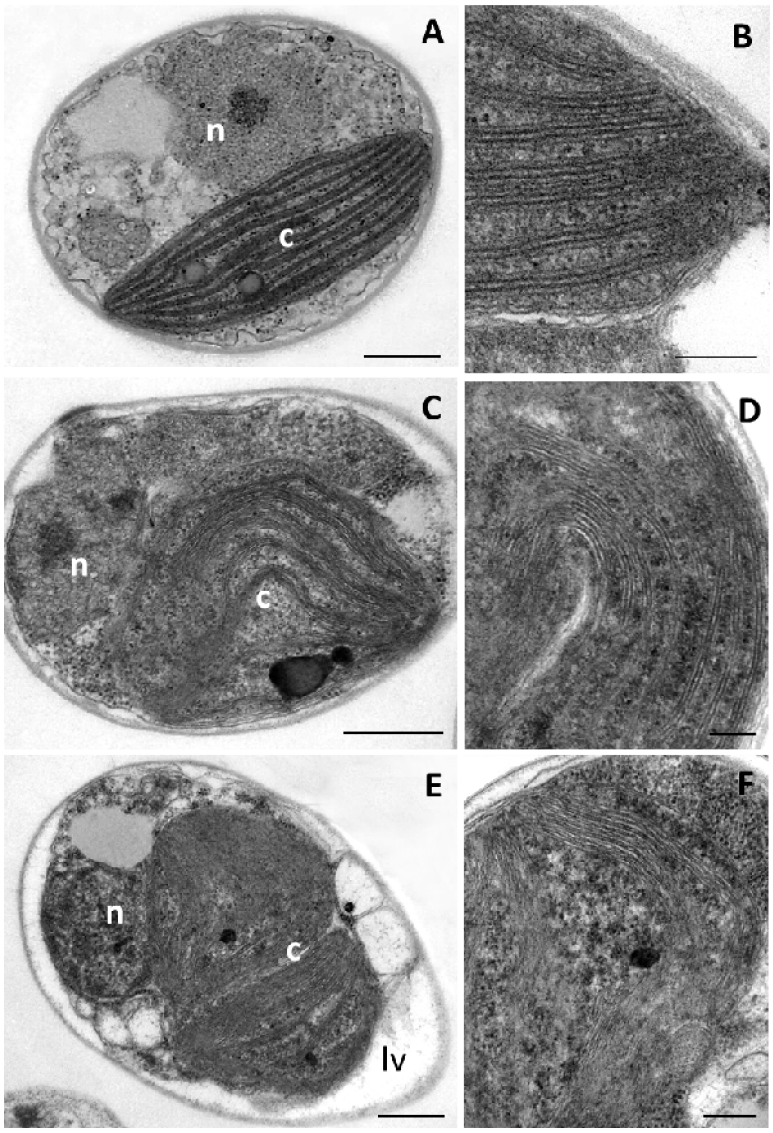

Figure 2. Transmission Electron Microscopy of *Nannochloropsis gaditana* cells. Representative transmission electron microscopy of *Nannochloropsis gaditana* cells in LL (A, B), ML (C, D) and HL conditions (E, F). Panels B, D and F show magnifications focusing on the thylakoid membrane organization. The organelles are indicated as: n, nucleus; c, chloroplast; lv, lamellar vesicles. Bars, A, C, E = 500 µm; B, D, F = 200 µm.

Table 1. Pigment composition of *Nannochloropsis* cells acclimated to different light intensities. The cells were collected after 5 days of growth under different illumination intensities, when the cells were still actively growing. The carotenoids data are reported as mol/100 mol of Chl. The data represent the average ± SD of 5 independent experiments. The de-epoxidation index (DI) was calculated as (2Z+A)/(V+A+Z).

	µg Chl / 10^6 cells	Tot Car	Viola-xanthin	Vaucher-a-xanthin	Antera-xanthin	Zea-xanthin	Canta-xanthin	β-carotene	DI
LL	0.151 ± 0.011	35.1 ± 3.4	21.5 ± 2.9	8.2 ± 2.6	1.0 ± 0.2	0.6 ± 0.2	0.3 ± 0.1	5.5 ± 0.3	0.10
ML	0.082 ± 0.005	40.2 ± 3.6	22.9 ± 3.7	8.5 ± 2.1	2.5 ± 0.5	1.4 ± 0.7	0.9 ± 0.2	5.6 ± 0.2	0.20
HL	0.039 ± 0.007	51.1 ± 4.4	32.3 ± 4.6	6.9 ± 1.1	3.5 ± 0.4	2.1 ± 0.3	1.8 ± 0.2	6.8 ± 0.3	0.20

Chl and carotenoids are bound to Photosystem I and II supercomplexes, comprising a reaction center and an associated antenna system. The observed changes in the pigment content strongly suggest that the accumulation of some PS components was modified under different growth conditions. To verify this hypothesis, we combined spectroscopic approaches with biochemical quantifications to evaluate the content of all components of the *Nannochloropsis* photosynthetic apparatus. The PSI content in LL, ML and HL treated cells was quantified after monitoring the P_{700}^{+} absorption signal in cells illuminated with saturating light in the presence of DCMU and DBMIB to inhibit PSI re-reduction (Figure 3A). The signal dependence on actinic light intensity was also verified to ensure the complete oxidation of the reaction centers in every sample (S3 Figure) and rule out the possibility that the different Chl content in the cells shade these effects, thereby altering the extent of P_{700}^{+} observed. Once verified this pre-requisite, the maximal P_{700} signal was exploited to quantify the PSI content in all samples. Figure 3B shows that the PSI content per cell was clearly progressively reduced with increasing growth light intensity from LL to ML and HL.

The PSII content was not directly quantifiable using spectrophotometric methods but could be indirectly assessed from the determination of the PSII/PSI ratio using ECS measurements (Bailleul et al., 2010a; Simionato et al., 2013). As shown in Figure 4B, the evaluation of this ratio in different cells showed a decrease in the PSII/PSI ratio in HL-acclimated cells, suggesting that even when the PSI absolute content decreased with illumination intensity in HL cells, the PSII decreased even further.

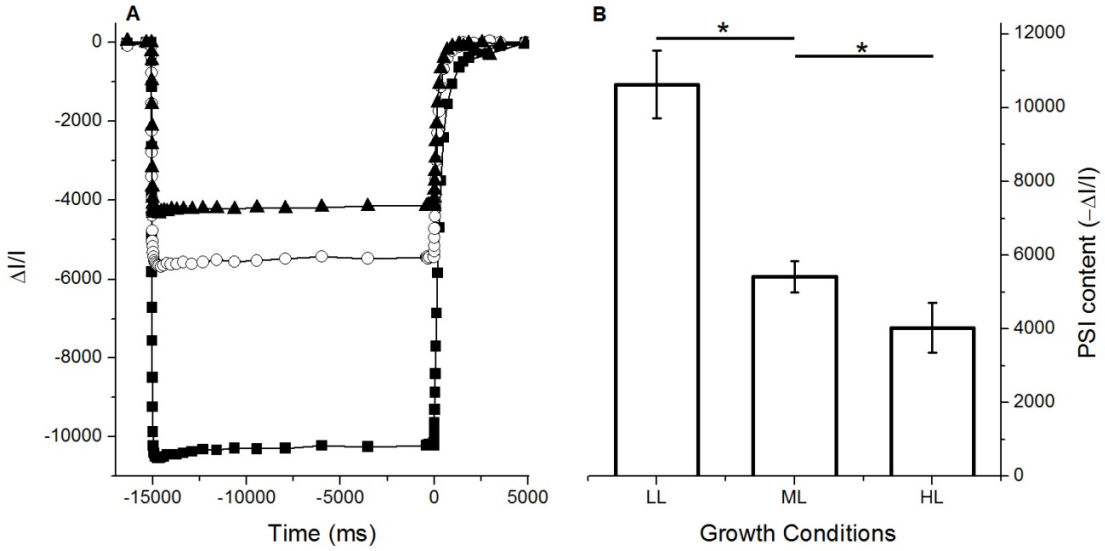

Figure 3. PSI quantification in *N. gaditana* intact cells. A) Representative traces of PSI quantification from oxidized P_{700} in the presence of DCMU and DBMIB and a saturating light of 2050 µmoles of photons m^{-2} s^{-1}; 300 10^6 cells/ml were employed for the measurement. Actinic light was verified to be sufficient to reach complete saturation of PSI reaction centers in all cells, as shown in S3 Figure LL, ML and HL conditions are shown, respectively, as black squares, empty circles and black triangles. B) PSI content in cells acclimated to different light conditions. The data are expressed as the means ±SD, n = 4. Significantly different values are indicated with an asterisk (ANOVA, p-value < 0.05).

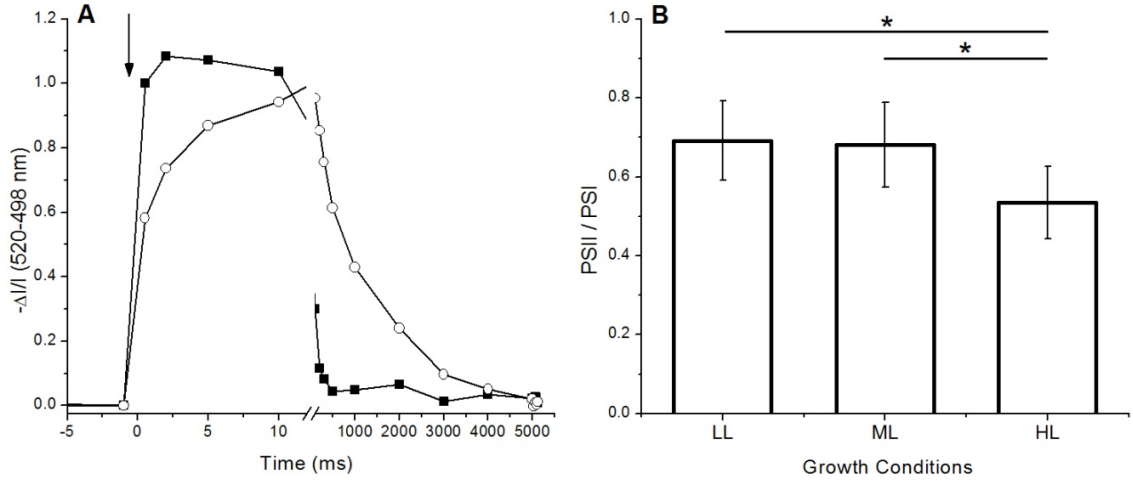

Figure 4. Evaluation of the PSII/PSI ratio in *Nannochloropsis* cells based on the ECS signal. A) ECS kinetics in *N. gaditana* cells grown under low light conditions (10 µE). The ECS signal is presented as the 520 nm minus the 498 nm absorption signal. The signal was induced using a saturating flash (arrow). The solid squares and empty circles represent, respectively, the kinetics of untreated cells (where PSII and PSI both contribute to the ECS signal) and of DCMU and HA-poisoned cells (where only PSI is responsible for the ECS signal). B) The PSII/PSI ratio obtained from the ECS signal in different acclimated cells with a final concentration of 200 x 10^6 cell/ml. The data are expressed as the means ±SD, n = 7. Significantly different values are indicated with an asterisk (ANOVA, p-value < 0.05).

The methods described above were used to quantify the content of functional PSI and PSII reaction centers, but did not provide information on the photosystems reorganization and the number of antenna complexes associated with each photosystem. To this aim, the PSI functional antenna size was evaluated after measuring the P_{700} oxidation kinetics in thylakoids treated with methylviologen and ascorbate (Bonente et al., 2012; Iwai et al., 2015), previously verifying that, as shown in S4 Figure, the employed actinic light intensities were limiting for the P_{700} oxidation rate. Thylakoids from different cells showed different kinetics (Figure 5), suggesting that these samples have a different functional antenna size and there is a consistent reduction of the PSI light-harvesting efficiency, gradually decreasing from LL to HL cells. Compared with the ML condition, LL showed a 20% increase, while HL showed a 40% decrease, of the antenna size value. Notably, the antenna size linearly increased with increasing light intensity used (20, 45, 80 and 150 µmol of photons $m^{-2} s^{-1}$), as shown in the S4A Fig, while maintaining the relative differences between different cells.

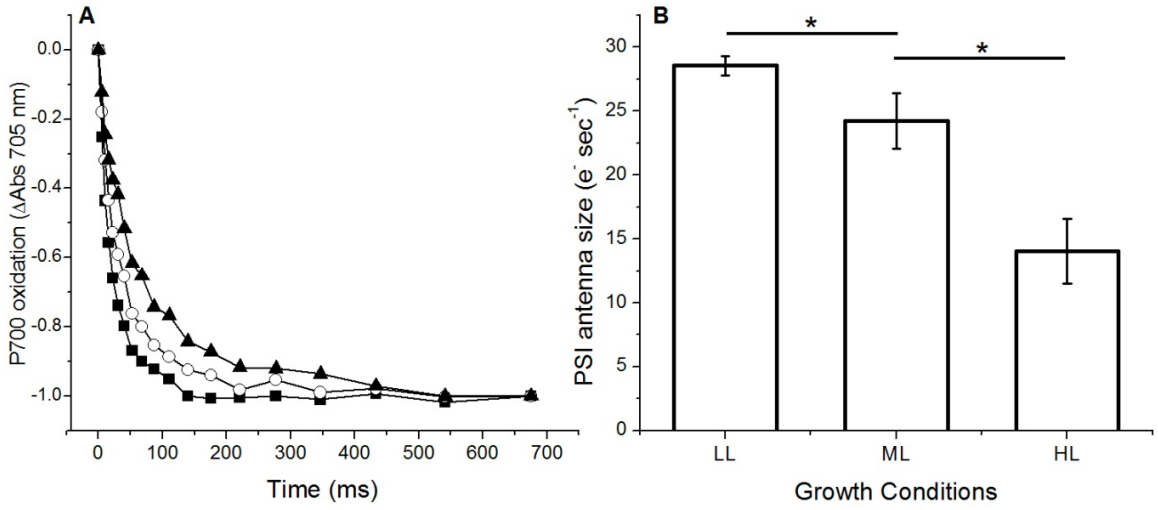

Figure 5. Modulation of the functional antenna size in PSI. A) Representative P_{700} oxidation kinetics at 705 nm from thylakoids treated with methylviologen and ascorbate. The measurements were performed with 150 µmoles of photons $m^{-2} s^{-1}$ of actinic light at 630 nm, and the data with other light intensities are shown in S4 Figure LL, ML and HL conditions are shown, respectively, as black squares, empty circles and black triangles. B) Average PSI antenna size for all samples. The data are expressed as the means ±SD, n = 4. Significantly different values are indicated with an asterisk (ANOVA, p-value < 0.05).

The PSII functional antenna size was instead evaluated based on the kinetics of the increased fluorescence in DCMU-treated cells at 320 µmoles of photons $m^{-2} s^{-1}$ (Figure 6) (Simionato et al., 2013; Bonente et al., 2012). Prior to the measurement, the cells were incubated overnight under dim light to facilitate the recovery of eventual photo-inhibited PSII reaction centers (Figure 7A), which otherwise could alter the antenna size determination. Using this caution, the PSII antenna size showed a clear decrease in response to growth light intensity, suggesting a modulation of the number

of light-harvesting complexes associated with each reaction center. Western blotting analysis with the available antibodies recognizing *Nannochloropsis* proteins showed a clear decrease in VCP, the main antenna complex in *Nannochloropsis* likely associated with PSII (Basso et al., 2014), upon shifting to high light. This was verified upon normalization to the Chl content (Figure 6C) and the cell number (S5 Figure), confirming the results obtained from the functional determination of the PSII antenna size.

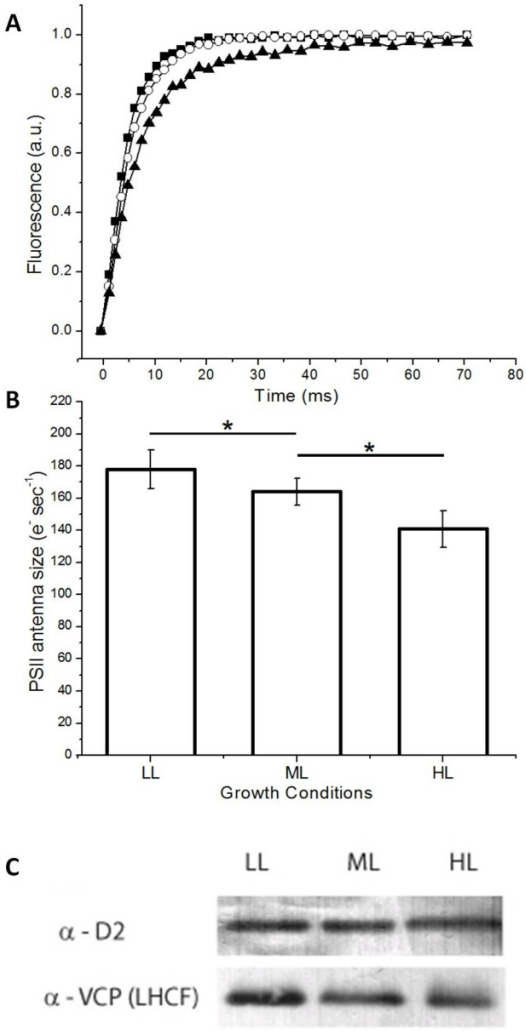

Figure 6. Modulation of the functional antenna size in PSII. A) Representative traces of the fluorescence kinetics of DCMU-treated cells in the presence of 320 µmoles of photons m^{-2} s^{-1} of actinic light at 630 nm. Prior to the measurement, the cells were incubated overnight under dim light. LL, ML and HL cells are shown, respectively, as black squares, empty circles and black triangles. B) Average PSII antenna size for all samples. The data are expressed as the means ±SD, n = 10. Significantly different values are indicated with an asterisk (ANOVA, p-value < 0.05). C) Western blotting analysis loading equal amounts of chlorophyll (1 and 0.2 µg Chl for α-D2 and α-VCP, respectively).

Modulation of the photosynthetic apparatus efficiency

The data presented thus far show a clear re-arrangement of the photosynthetic apparatus in *Nannochloropsis* in response to different light conditions, affecting both PSI and PSII. Further experiments were performed to investigate the consequences of these changes on the photosynthetic activity of this alga, exploiting for example *in vivo* fluorescence measurements. The determination of the maximum PSII quantum yield (Fv/Fm) provides an indication of light-induced damage. As shown in Figure 7A, Fv/Fm decreased from 0.65 in LL to 0.57 in ML and 0.51 in HL cells, suggesting the presence of substantial photo-damage in PSII, even under ML conditions. To verify this hypothesis, the cells were transferred to dim light (10 µmoles of photons m^{-2} s^{-1}). As shown in Figure 7A, the PSII activity required overnight recovery for efficient restoration, suggesting the decrease in activity indeed reflected photoinhibition.

Fluorescence measurements can also be exploited for determining PSII photochemical efficiency in illuminated cells, and the qL parameter estimates how cells use absorbed energy for photochemistry. As shown in Figure 7B, while LL and ML cells showed a similar dependence of this parameter on the light intensity, HL cells showed a higher photochemical efficiency at all irradiations, suggesting these cells had a higher ability to use light for photochemistry and that photosystems were open, even under strong illumination. Notably, the acclimation response observed under all growth conditions described was also substantially conserved in cells cultivated with extra CO_2 and nutrients (S1B and D Figs.).

Moreover, *in vivo* fluorescence kinetics also provides information on the intracellular dissipation of absorbed energy as heat through a mechanism called Non Photochemical Quenching (Figure 7C). LL cells reached higher NPQ values than other cells, but most of this additional NPQ did not relax after 30 minutes of dim light recovery, suggesting that this effect reflected photoinhibition induced during measurement (Figure 7D). The cells grown under different conditions showed no major differences in the fastest NPQ component (qE). However, the NPQ in different cell types showed a different dependence on light intensity, with HL cells activating NPQ only when exposed to light intensities over 700 µmoles of photons m^{-2} s^{-1}. The same correlation between the NPQ and the light intensity was observed also in cells grown in CO_2 and CO_2 and nutrient-enriched conditions (S1A and C Figs.).

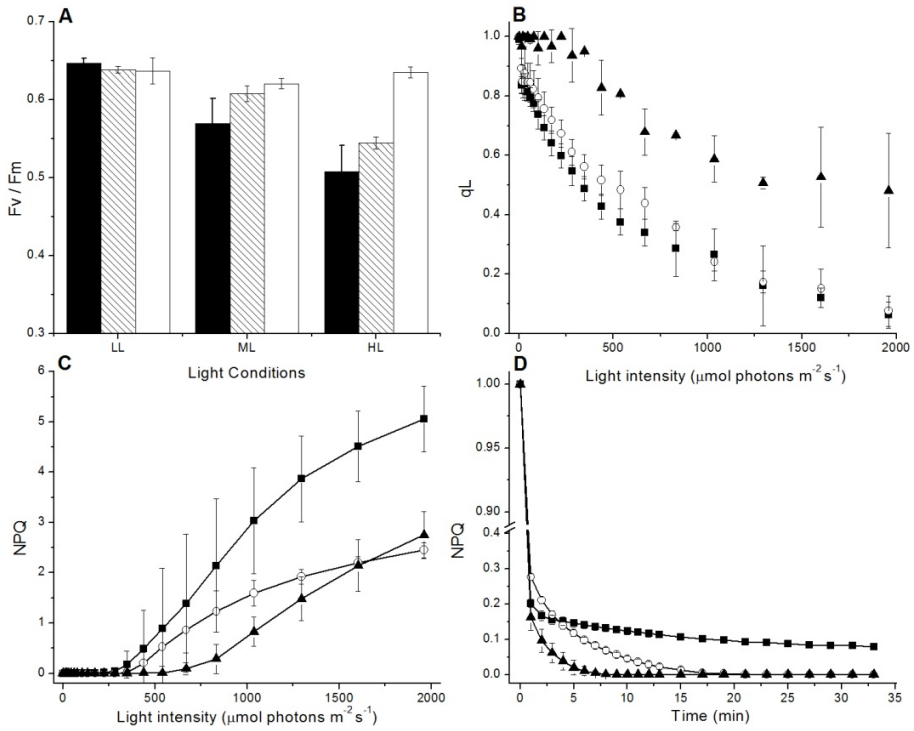

Figure 7. Photosystem II functionality monitored with PAM fluorimetry. A) Maximum Photosystem II quantum yield (Fv / Fm) in cells grown under different light conditions (LL, ML and HL) after 20 minutes of dark adaptation (dark bars). Fv/Fm of cells transferred for one hour or overnight under dim light are reported, respectively, as dashed and white bars. The data are expressed as the means ±SD, n = 2. B) Dependence of photochemical efficiency, estimated as the parameter qL, from the illumination intensity. The measurements were performed using one-minute steps of increasing light intensity. C) NPQ kinetics using one-minute steps of increasing light intensity. D) NPQ recovery during 30 minutes of dim light, after the light treatment in C. NPQ values are normalized to 1 at the maximal value, before light is decreased. In B-C-D LL, ML and HL cells are shown as black squares, white circles and black triangles, respectively. The data are expressed as the mean ± SD, n = 4.

Fluorescence-derived signals primarily reflect Photosystem II activity and therefore these data were complemented with measurements of total electron flow monitoring P_{700} re-reduction kinetics after a saturating light treatment that allows evaluating electron transport rates at the level of PSI (Figure 8A). In these samples, the P_{700}^{+} re-reduction in the dark was faster in HL cells with respect to cells acclimated to ML and LL (S6 Figure) and maximal total electron flow increased 50% in HL with respect to LL and ML cells (Figure 8B). Using inhibitors of PSII and cytochrome b_6f (DCMU and DBMIB, respectively), we evaluated the contribution of the linear (LEF) and cyclic (CEF) electron pathways to this total electron transport. As shown in Figure 8B, under all conditions, PSII inhibition through DCMU dramatically decreased electron transport, suggesting that linear flow is responsible for the largest fraction of electron transport under all conditions. Treatment with both DCMU and DBMIB also inhibits cyclic electron flow around PSI in addition to LEF, facilitating the estimation of the contribution of both pathways. We observed that the CEF contribution was significantly different in

the samples analyzed, and while this effect was hardly detectable in LL cells, the relevance increased in ML and HL cells, reaching ≈ 8 % of all Cyt b_6f-dependent electron transport (Figure 8C).

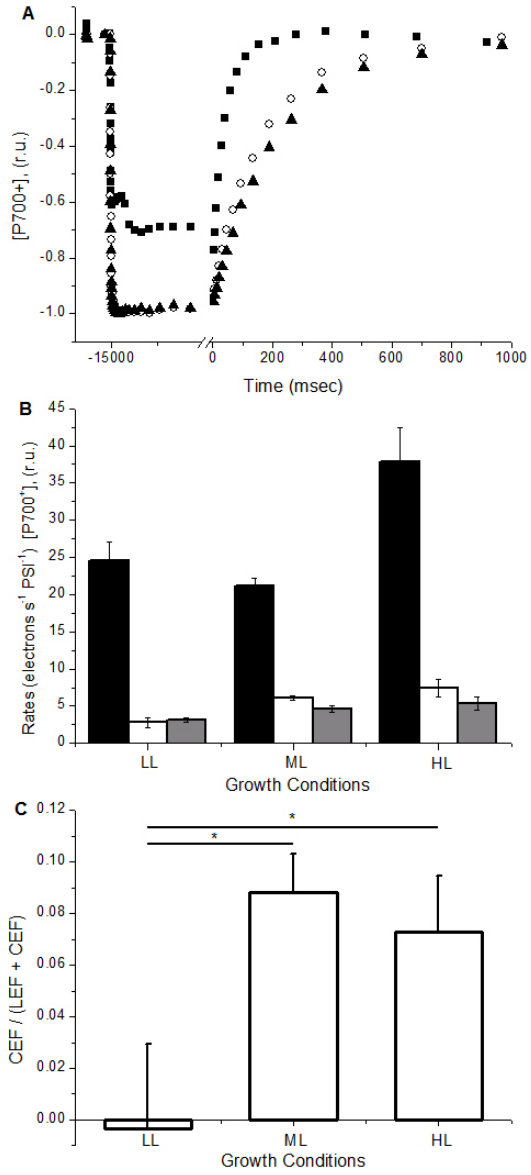

Figure 8. PSI Electron transport efficiency in cells acclimated to different conditions. A) P_{700} redox kinetics representing an electron transport quantification experiment. The cells acclimated to 100 µmoles of photons m^{-2} s^{-1} (ML) were exposed to a saturating light intensity (2050 µmoles of photons m^{-2} s^{-1}) for 15 seconds prior to the dark recovery kinetics. Untreated cells (solid squares), cells treated with DCMU (open circles) and cells treated with DCMU and DBMIB (solid triangles). The kinetics for LL and HL cells are reported in S6 Figure B) Electron transport rates evaluated from P_{700} re-reduction kinetics after illumination in different acclimated cells. The data refer to the rates measured in untreated cells (black column), DCMU treated cells (white column) and DCMU and DBMIB treated cells (gray column). The total electron flow values from the three conditions are all significantly different (ANOVA), n = 4, $p < 0.05$. C) Rate of cyclic electron flow (CEF) compared with the sum of linear and cyclic (LEF + CEF). Significantly different values are indicated with an asterisk (ANOVA, n=4, p-value < 0.05).

Discussion

Conserved features and peculiarities in the Nannochloropsis acclimation response

Nannochloropsis cultures under different light intensities respond to the environmental conditions through the reorganization of the photosynthetic apparatus and the modulation of its photosynthetic efficiency. HL cells show a higher capacity for electron transport (Figure 8), which does not translate into increased growth, reflecting a limitation in CO_2 and nutrient availability (Figure 1). Thus, we hypothesize that the "extra" capacity for electron transport likely is needed to compensate for the increased maintenance energy required for the continuous repair of the damaged photosynthetic apparatus (Figs. 1 and 2). Consistent with this hypothesis *Nannochloropsis gaditana* cultures showed Cyclic Electron Transport activation around PSI also under nitrogen depletion,(Simionato et al., 2013), suggesting that CEF activation contributes to photoprotection under stress conditions by reducing the electron pressure on PSI and preventing PSI photoinhibition.

Nannochloropsis cells acclimated to high light intensities show a decrease in the cell Chl content, reflecting a general decrease in all components of the photosynthetic apparatus. This observation was confirmed through transmission electron microscopy images showing a reduction of the number of thylakoid membrane in cells exposed to the highest light intensities (Figure 2, (Fisher et al., 1998; Lepetit et al., 2012)). In parallel to this general decrease, the photosynthetic apparatus showed internal reorganization, which is clearly evident at the level of the thylakoid structure. Reorganization of the photosynthetic activity is also evident at the level of the photosynthetic apparatus, with some components decreasing more than others. For example, while the Chl content per cell decreased to 25% in HL cells (Table 1), the PSI content per cell was only reduced to 38% of the LL content (Figure 3). This suggests a relative increase in the PSI content per Chl in HL cells, which was confirmed through the measured decrease in the PSII/PSI ratio. This conclusion is also supported by measurements of the total amount of P_{700} per Chl in isolated thylakoids (S4B Figure). Indeed compared with the other conditions, HL showed an approximately 30 % increase in P_{700}/µg Chl under all the light intensities examined. When the cells were exposed to the highest illumination used in the present study, PSII decreased more than PSI (Figure 4). An even larger decrease was observed for the light-harvesting complexes, as the functional antenna size decreased under HL for both PSI and PSII (Figs. 5 and 6). In the latter case, a diminished antenna content was also biochemically confirmed through Western blotting quantification of the VCP, a major component of PSII antenna in *Nannochloropsis* (Basso et al., 2014).

The seminal study by Falkowski and Owens (Falkowski and Owens, 1980) distinguished marine algal species, as the chlorophyte *Dunaliella tertiolecta*, that withstood changes in growth irradiance through changes in the number of reaction centers, a strategy termed n-type photoacclimation, and others, like the diatom *Skeletonema costatum*, that responded to decreasing growth irradiance through an increase of the antenna absorption cross-section serving reaction center, a strategy termed □-type photoacclimation. Indeed in *N. gaditana* both strategies were effective and both the

modulation of antenna size and changes in the reaction center stoichiometry were evidenced in response to light. The response of Nannochloropsis is also peculiar when compared to previous observation in *viridiplantae*. For example, in *Chlamydomonas reinhardtii* and *Arabidopsis thaliana*, the modulation of antenna size was only observed for PSII, while the PSI antenna composition remained stable (Bonente et al., 2012; Ballottari et al., 2007). Notably, however, the stability of the PSI antenna size in different irradiances has consistently been observed in green algae and plants, while the information for other photosynthetic organisms remains incomplete. LHC associated with PSI in these organisms shares a common evolutionary origin, and these structures all belong to a sub group of antennas called LHCA. The association of LHCA with the PSI core complex was particularly stable, potentially resulted in the loss of the flexibility required for regulation (Ballottari et al., 2004). In *Heterokonta*, like *Nannochloropsis* or diatoms, the precise composition of the PSI antenna system is not well described, although it is clear that in the genomes of these species, there are no proteins classified as LHCA (Ikeda et al., 2013; Vieler et al., 2012). Thus, it is likely that the modulation of the PSI antenna size is associated with the presence/absence of specific subunits associated with PSI. During evolution, these subunits diversified, and some organisms could have maintained the ability to modulate the Photosystem I antenna size, while in green algae and plants, subunits capable of forming stable super-complexes with PSI reaction center were selected. While this hypothesis is consistent with the available knowledge, additional information, such as studies on additional species from different phylogenetic groups, are still needed to confirm this hypothesis.

The prolonged exposition of *Nannochloropsis* to strong illumination also influenced the ability to use absorbed light for photochemistry and activate NPQ in response to different illumination intensities (Figure 7). HL cells showed a higher qL at all actinic light intensities, indicating that the overall modulation of the photosynthetic apparatus enables the cells to exploit higher light more efficiently than LL and ML cells. Moreover, HL cells showed the activation of the NPQ only when exposed to strong light, over 700 µmoles of photons m^{-2} s^{-1}. This value is comparable to the average illumination these cells are exposed to, suggesting that these cells do not constitutively activate NPQ under typical growth conditions. This response was closely replicated after removing the nutrients limitation, demonstrating that NPQ activation is not strictly associated with the growth conditions (S1 Figure). This observation is interesting, as the data in Figs. 1 and 7 clearly show that irradiation is in extreme excess in HL and cells are unable to use the largest fraction of absorbed energy for growth and sustain substantial damage to the photosynthetic apparatus (Figure 7). Nonetheless, these cells do not constitutively activate NPQ under the growth conditions but rely on other mechanisms (reduction of Chl content and antenna size) to reduce the light-harvesting efficiency.

Another mechanism for rapid protection from excess illumination is the xanthophyll cycle, involving the conversion of violaxanthin into zeaxanthin. *Nannochloropsis* has the potential for synthetizing large amounts of zeaxanthin, as violaxanthin is the major carotenoid representing ≈ 60 % of the carotenoids in the cell. However, when cells were chronically exposed to excess light, we observed a strong increase in the total violaxanthin content, which was not constitutively converted into zeaxanthin. Overall, the lack of zeaxanthin accumulation upon prolonged exposition to strong

illumination and the lack of NPQ induction indicated that HL-acclimated cells do not constitutively activate photo-protection responses. These results show that even in *Nannochloropsis* cells exposed to chronically excess light, both the NPQ and xanthophyll cycles respond to further eventual changes in illumination, thereby maintaining the ability to increase photo-protection mechanisms in cells, when needed. *Nannochloropsis* cells thus have a distinct set of mechanisms to respond to short-term or prolonged exposition to different light intensities that together modulate the efficiency of the photosynthetic apparatus in response to environmental conditions. The fast-responding mechanisms are not constitutively activated, even in cells chronically exposed to strong light excess, thereby maintaining the flexibility to respond to environmental conditions. Notably, for the HL cells analyzed in the present study, this strategy had a substantial drawback, as cells chronically exposed to extreme excess light clearly experienced significant radiation damage. This observation suggests that it was evolutionary preferable to sustain chronic damage to the photosynthetic apparatus than lose efficient and rapid responses to light changes, suggesting the biological relevance of these fast mechanisms in a natural variable environment (Külheim et al., 2002; Lavaud and Lepetit, 2013).

Acknowledgments

The authors would like to thank Vasil D'Ambrosio for the assistance with HPLC and Western blot analyses. GF acknowledges grants from Agence Nationale de la Recherche (ANR-12-BIME-0005, DiaDomOil); the Marie Curie Initial Training Network Accliphot (FP7-PEOPLE-2012-ITN; 316427); the CNRS Défi (ENRS 2013) and the CEA Bioénergies program.

References

Alric, J. (2010). Cyclic electron flow around photosystem I in unicellular green algae. Photosynth. Res. **106**: 47–56.

Archibald, J.M. and Keeling, P.J. (2002). Recycled plastids: a "green movement" in eukaryotic evolution. Trends Genet. **18**: 577–584.

Arnoux, P., Morosinotto, T., Saga, G., Bassi, R., and Pignol, D. (2009). A structural basis for the pH-dependent xanthophyll cycle in Arabidopsis thaliana. Plant Cell **21**: 2036–44.

Bailleul, B., Cardol, P., Breyton, C., and Finazzi, G. (2010a). Electrochromism: A useful probe to study algal photosynthesis. Photosynth. Res. **106**: 179–189.

Bailleul, B., Rogato, A., de Martino, A., Coesel, S., Cardol, P., Bowler, C., Falciatore, A., and Finazzi, G. (2010b). An atypical member of the light-harvesting complex stress-related protein family modulates diatom responses to light. Proc. Natl. Acad. Sci. U. S. A. **107**: 18214–9.

Ballottari, M., Dall'Osto, L., Morosinotto, T., and Bassi, R. (2007). Contrasting behavior of higher plant photosystem I and II antenna systems during acclimation. J. Biol. Chem. **282**: 8947–8958.

Ballottari, M., Govoni, C., Caffarri, S., and Morosinotto, T. (2004). Stoichiometry of LHCI antenna polypeptides and characterization of gap and linker pigments in higher plants Photosystem I. Eur. J. Biochem. **271**: 4659–65.

Barber, J. and Andersson, B. (1992). Too much of a good thing: light can be bad for photosynthesis. Trends Biochem. Sci. **17**: 61–66.

Basso, S., Simionato, D., Gerotto, C., Segalla, A., Giacometti, G.M., and Morosinotto, T. (2014). Characterization of the photosynthetic apparatus of the Eustigmatophycean Nannochloropsis gaditana: evidence of convergent evolution in the supramolecular organization of photosystem I. Biochim. Biophys. Acta **1837**: 306–14.

Bondioli, P., Della Bella, L., Rivolta, G., Chini Zittelli, G., Bassi, N., Rodolfi, L., Casini, D., Prussi, M., Chiaramonti, D., and Tredici, M.R. (2012). Oil production by the marine microalgae Nannochloropsis sp. F&M-M24 and Tetraselmis suecica F&M-M33. Bioresour. Technol. **114**: 567–72.

Bonente, G., Pippa, S., Castellano, S., Bassi, R., and Ballottari, M. (2012). Acclimation of Chlamydomonas reinhardtii to different growth irradiances. J. Biol. Chem. **287**: 5833–47.

Cavalier-Smith, T. (2004). Only six kingdoms of life. Proc. Biol. Sci. **271**: 1251–62.

Coesel, S., Oborník, M., Varela, J., Falciatore, A., and Bowler, C. (2008). Evolutionary origins and functions of the carotenoid biosynthetic pathway in marine diatoms. PLoS One **3**: e2896.

Demmig-Adams, B. (1990). Carotenoids and photoprotection in plants: A role for the xanthophyll zeaxanthin. Biochim. Biophys. Acta - Bioenerg. **1020**: 1–24.

Demmig-Adams, B., Adams III, W.W., Barker, D.H., Logan, B.A., Bowling, D.R., and Verhoeven, A.S. (2008). Using chlorophyll fluorescence to assess the fraction of absorbed light allocated to thermal dissipation of excess excitation. Physiol. Plant. **98**: 253–264.

Demmig-Adams, B. and Adams, W.W. (2000). Harvesting sunlight safely. Nature **403**: 371, 373–4.

Eberhard, S., Finazzi, G., and Wollman, F.-A. (2008). The dynamics of photosynthesis. Annu. Rev. Genet. **42**: 463–515.

Falkowski, P.G. and LaRoche, J. (1991). ACCLIMATION TO SPECTRAL IRRADIANCE IN ALGAE. J. Phycol. **27**: 8–14.

Falkowski, P.G. and Owens, T.G. (1980). Light-Shade Adaptation : TWO STRATEGIES IN MARINE PHYTOPLANKTON. Plant Physiol. **66**: 592–595.

Fisher, T., Berner, T., Iluz, D., and Dubinsky, Z. (1998). The kinetics of the photoacclimation response of Nannochloropsis sp. (Eustigmatophyceae): A study of changes in ultrastructure and PSU density. J. Phycol. **34**: 818–824.

Fisher, T., Shurtz-swirski, R., Gepstein, S., and Dubinsky, Z. (1989). Changes in the levels of ribulose-l,5-bisphosphate carboxylase/oxygenase (rubisco) in tetraedron minimum (chlorophyta) during light and shade adaptation. Plant Cell Physiol. **30**: 221–228.

Gerotto, C., Alboresi, A., Giacometti, G.M., Bassi, R., and Morosinotto, T. (2011). Role of PSBS and LHCSR in Physcomitrella patens acclimation to high light and low temperature. Plant. Cell Environ. **34**: 922–32.

Gerotto, C. and Morosinotto, T. (2013). Evolution of photoprotection mechanisms upon land colonization: evidence of PSBS-dependent NPQ in late Streptophyte algae. Physiol. Plant. **149**: 583–598.

Goss, R., Ann Pinto, E., Wilhelm, C., and Richter, M. (2006). The importance of a highly active and DeltapH-regulated diatoxanthin epoxidase for the regulation of the PS II antenna function in diadinoxanthin cycle containing algae. J. Plant Physiol. **163**: 1008–21.

Goss, R. and Lepetit, B. (2015). Biodiversity of NPQ. J. Plant Physiol. **172C**: 13–32.

Havaux, M., Dall'osto, L., and Bassi, R. (2007). Zeaxanthin has enhanced antioxidant capacity with respect to all other xanthophylls in Arabidopsis leaves and functions independent of binding to PSII antennae. Plant Physiol. **145**: 1506–20.

Ikeda, Y., Yamagishi, A., Komura, M., Suzuki, T., Dohmae, N., Shibata, Y., Itoh, S., Koike, H., and Satoh, K. (2013). Two types of fucoxanthin-chlorophyll-binding proteins I tightly bound to the photosystem I core complex in marine centric diatoms. Biochim. Biophys. Acta **1827**: 529–39.

Iwai, M., Yokono, M., Kono, M., Noguchi, K., Akimoto, S., and Nakano, A. (2015). Light-harvesting complex Lhcb9 confers a green alga-type photosystem I supercomplex to the moss Physcomitrella patens. Nat. Plants **1**: 14008.

Jahns, P., Latowski, D., and Strzalka, K. (2009). Mechanism and regulation of the violaxanthin cycle: the role of antenna proteins and membrane lipids. Biochim. Biophys. Acta **1787**: 3–14.

Johnsen, G. and Sakshaug, E. (2007). Biooptical characteristics of PSII and PSI in 33 species (13

pigment groups) of marine phytoplankton, and the relevance for pulse-amplitude-modulated and fast-. J. Phycol.

Külheim, C., Agren, J., and Jansson, S. (2002). Rapid regulation of light harvesting and plant fitness in the field. Science **297**: 91–3.

Kurasová, I., Cajánek, M., Kalina, J., Urban, O., and Spunda, V. (2002). Characterization of acclimation of Hordeum vulgare to high irradiation based on different responses of photosynthetic activity and pigment composition. Photosynth. Res. **72**: 71–83.

Lavaud, J. and Kroth, P.G. (2006). In diatoms, the transthylakoid proton gradient regulates the photoprotective non-photochemical fluorescence quenching beyond its control on the xanthophyll cycle. Plant Cell Physiol. **47**: 1010–6.

Lavaud, J. and Lepetit, B. (2013). An explanation for the inter-species variability of the photoprotective non-photochemical chlorophyll fluorescence quenching in diatoms. Biochim. Biophys. Acta **1827**: 294–302.

Lavaud, J., Rousseau, B., and Etienne, A.-L. (2002). In diatoms, a transthylakoid proton gradient alone is not sufficient to induce a non-photochemical fluorescence quenching. FEBS Lett. **523**: 163–6.

Lepetit, B., Goss, R., Jakob, T., and Wilhelm, C. (2012). Molecular dynamics of the diatom thylakoid membrane under different light conditions. Photosynth. Res. **111**: 245–57.

Li, Z., Wakao, S., Fischer, B.B., and Niyogi, K.K. (2009). Sensing and responding to excess light. Annu. Rev. Plant Biol. **60**: 239–60.

Lubián, L.M., Montero, O., Moreno-Garrido, I., Huertas, I.E., Sobrino, C., González-Del Valle, M., and Parés, G. (2000). Nannochloropsis (Eustigmatophyceae) as source of commercially valuable pigments. In Journal of Applied Phycology, pp. 249–255.

Murata, N., Takahashi, S., Nishiyama, Y., and Allakhverdiev, S.I. (2007). Photoinhibition of photosystem II under environmental stress. Biochim. Biophys. Acta **1767**: 414–21.

Niyogi, K.K., Grossman, A.R., and Björkman, O. (1998). Arabidopsis mutants define a central role for the xanthophyll cycle in the regulation of photosynthetic energy conversion. Plant Cell **10**: 1121–1134.

Nymark, M., Valle, K.C., Brembu, T., Hancke, K., Winge, P., Andresen, K., Johnsen, G., and Bones, A.M. (2009). An integrated analysis of molecular acclimation to high light in the marine diatom Phaeodactylum tricornutum. PLoS One **4**: e7743.

Peers, G., Truong, T.B., Ostendorf, E., Busch, A., Elrad, D., Grossman, A.R., Hippler, M., and Niyogi, K.K. (2009). An ancient light-harvesting protein is critical for the regulation of algal

photosynthesis. Nature **462**: 518–21.

Perry, M.J., Talbot, M.C., and Alberte, R.S. (1981). Photoadaption in marine phytoplankton: Response of the photosynthetic unit. Mar. Biol. **62**: 91–101.

Quaas, T., Berteotti, S., Ballottari, M., Flieger, K., Bassi, R., Wilhelm, C., and Goss, R. (2014). Non-photochemical quenching and xanthophyll cycle activities in six green algal species suggest mechanistic differences in the process of excess energy dissipation. J. Plant Physiol. **172**: 92–103.

Riisberg, I., Orr, R.J.S., Kluge, R., Shalchian-Tabrizi, K., Bowers, H.A., Patil, V., Edvardsen, B., and Jakobsen, K.S. (2009). Seven gene phylogeny of heterokonts. Protist **160**: 191–204.

La Rocca, N., Sciuto, K., Meneghesso, A., Moro, I., Rascio, N., and Morosinotto, T. (2015). Photosynthesis in extreme environments: responses to different light regimes in the Antarctic alga Koliella antarctica. Physiol. Plant. **153**: 654–67.

Rodolfi, L., Chini Zittelli, G., Bassi, N., Padovani, G., Biondi, N., Bonini, G., and Tredici, M.R. (2009). Microalgae for oil: strain selection, induction of lipid synthesis and outdoor mass cultivation in a low-cost photobioreactor. Biotechnol. Bioeng. **102**: 100–12.

Rodriguez, F., Chauton, M., and Johnsen, G. (2006). Photoacclimation in phytoplankton: implications for biomass estimates, pigment functionality and chemotaxonomy. Mar. Biol.

Ruban, A., Lavaud, J., Rousseau, B., Guglielmi, G., Horton, P., and Etienne, A.-L. (2004). The super-excess energy dissipation in diatom algae: comparative analysis with higher plants. Photosynth. Res. **82**: 165–75.

Savitch, L.L. V., Barker-Åstrom, J., Ivanov, A.G.A., Hurry, V., Öquist, G., Huner, N.P.A., Gardeström, P., and Barker-Astrom, J. (2001). Cold acclimation of Arabidopsis thaliana results in incomplete recovery of photosynthetic capacity, associated with an increased reduction of the chloroplast stroma. Planta **214**: 295–303.

Sforza, E., Simionato, D., Giacometti, G.M., Bertucco, A., and Morosinotto, T. (2012). Adjusted light and dark cycles can optimize photosynthetic efficiency in algae growing in photobioreactors. PLoS One **7**: e38975.

Simionato, D., Block, M.A., La Rocca, N., Jouhet, J., Maréchal, E., Finazzi, G., and Morosinotto, T. (2013). The response of Nannochloropsis gaditana to nitrogen starvation includes de novo biosynthesis of triacylglycerols, a decrease of chloroplast galactolipids, and reorganization of the photosynthetic apparatus. Eukaryot. Cell **12**: 665–76.

Simionato, D., Sforza, E., Corteggiani Carpinelli, E., Bertucco, A., Giacometti, G.M., and Morosinotto, T. (2011). Acclimation of Nannochloropsis gaditana to different illumination regimes: effects on

lipids accumulation. Bioresour. Technol. **102**: 6026–32.

Smith, B.M., Morrissey, P.J., Guenther, J.E., Nemson, J.A., Harrison, M.A., Allen, J.F., and Melis, A. (1990). Response of the Photosynthetic Apparatus in Dunaliella salina (Green Algae) to Irradiance Stress. Plant Physiol. **93**: 1433–40.

Sukenik, A., Livne, A., Neori, A., Yacobi, Y.Z., and Katcoff, D. (1992). Purification and characterization of a light-harvesting chlorophyll-protein complex from the marine eustigmatophyte nannochloropsis sp. Plant Cell Physiol. **33**: 1041–1048.

Swingley, W.D., Iwai, M., Chen, Y., Ozawa, S., Takizawa, K., Takahashi, Y., and Minagawa, J. (2010). Characterization of photosystem I antenna proteins in the prasinophyte Ostreococcus tauri. Biochim. Biophys. Acta **1797**: 1458–64.

Szabó, I., Bergantino, E., and Giacometti, G.M. (2005). Light and oxygenic photosynthesis: energy dissipation as a protection mechanism against photo-oxidation. EMBO Rep. **6**: 629–34.

Vieler, A. et al. (2012). Genome, functional gene annotation, and nuclear transformation of the heterokont oleaginous alga Nannochloropsis oceanica CCMP1779. PLoS Genet. **8**: e1003064.

Walters, R.G. (2005). Towards an understanding of photosynthetic acclimation. J. Exp. Bot. **56**: 435–47.

Wellburn, A.R. (1994). The spectral determination of chlorophylls a and b, as well as total carotenoids, using various solvents with spectrophotometers of different resolution. J. Plant Physiol. **144**: 307–313.

Wilhelm, C., Jungandreas, A., Jakob, T., and Goss, R. (2014). Light acclimation in diatoms: from phenomenology to mechanisms. Mar. Genomics **16**: 5–15.

Witt, H.T. (1979). Energy conversion in the functional membrane of photosynthesis. Analysis by light pulse and electric pulse methods. The central role of the electric field. BBA Rev. Bioenerg. **505**: 355–427.

Zhu, S.-H. and Green, B.R. (2010). Photoprotection in the diatom Thalassiosira pseudonana: role of LI818-like proteins in response to high light stress. Biochim. Biophys. Acta **1797**: 1449–57.

Zou, N. and Richmond, A. (2000). Light-path length and population density in photoacclimation of Nannochloropsis sp. (Eustigmatophyceae). In Journal of Applied Phycology, pp. 349–354.

Supporting Information

Figure S1. Photosynthetic parameters monitored using PAM fluorimetry under different growing conditions. NPQ (A,C) and qL (B,D) parameters monitored using increasing light intensity. Fluorescence measurements were performed in cells grown in a Multicultivator MC 1000-OD system in a F/2 medium (A,B) and in a enriched medium (C,D). After illumination three data point were recorded after 60, 120 and 180 seconds in dim light to evaluate NPQ recovery. LL, ML and HL cells are shown respectively in black squares, white circles and black triangles respectively. The data are expressed as the mean ± SD, n = 4.

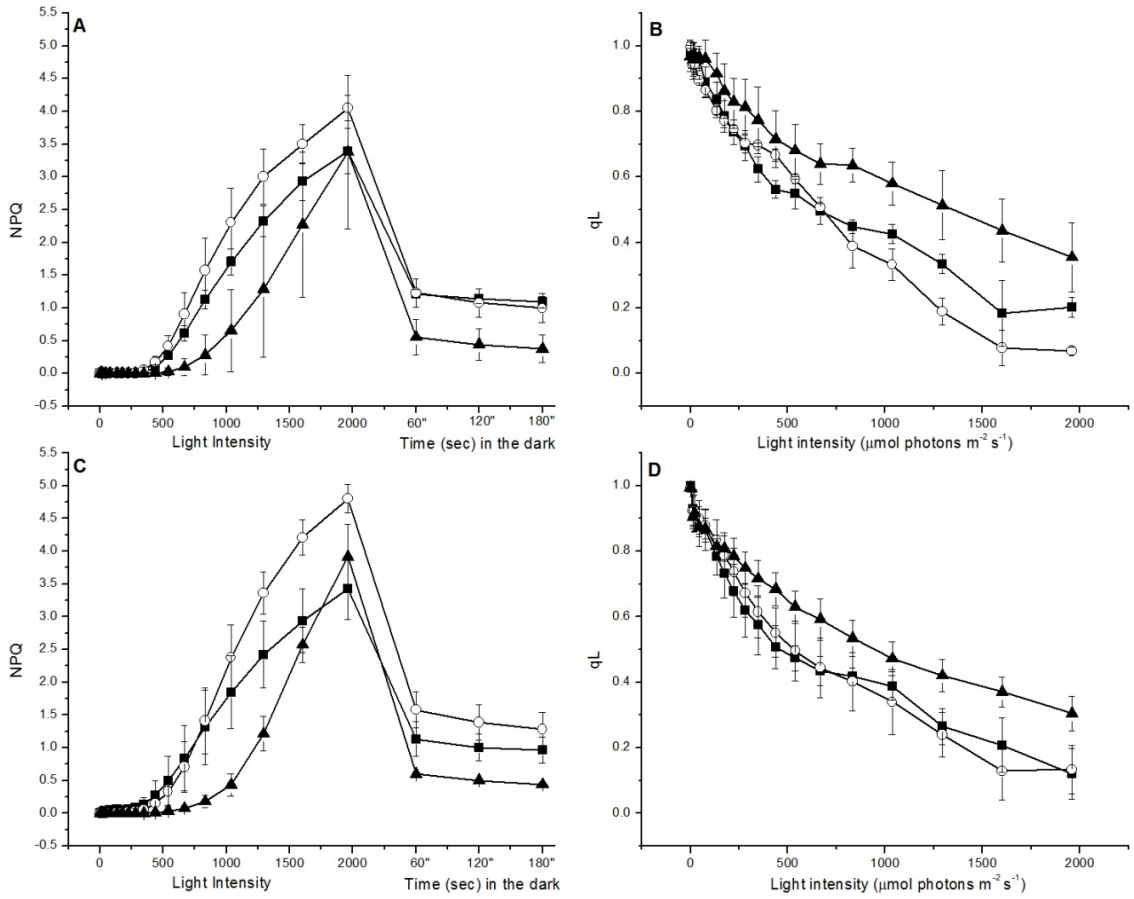

Figure S2. Growth rates in multiple generations under different growing conditions. Growth curves from Figure 1 (black squares) are compared with those in which cells have been harvested and resuspended in the same conditions (Erlenmeyer flasks, F/2 medium, LL or ML or HL) in order to extend the acclimation period. Red circles represent the average of curves after 3-9 generations (each 10 days long), and the blue triangles the one at the 9th generation, 8 days long. Cultures in LL, ML and HL conditions are shown in panels A, B and C respectively. The multiple generations experiment was repeated two independent times.

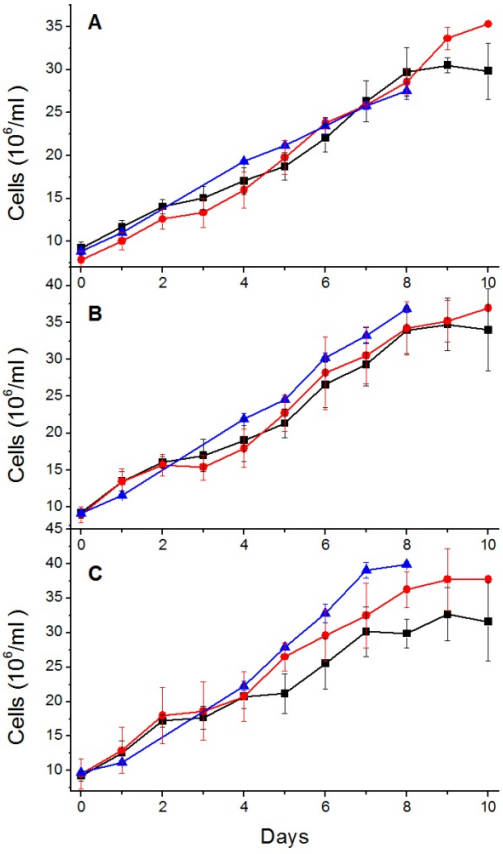

Figure S3. Dependence of P_{700} signal amplitude upon actinic light intensity. In *Nannochloropsis* cells P_{700} oxidation was measured at different light intensities (45, 80, 150, 320, 940, 2050 µmoles of photons m^{-2} s^{-1} at 630 nm) and the relative maximal P_{700} oxidation level reached at the steady state was plotted as a function of the intensity of the actinic light used for the measurement. All the measurements were performed at a final cellular concentration of 300 10^6 cell/ ml with the addition of DCMU and DBMIB to block both linear and cyclic electron flow at the level of the cytochrome b_6f complex, in order to allow the maximal P_{700} oxidation. LL, ML and HL conditions are shown respectively in black squares, empty circles and black triangles.

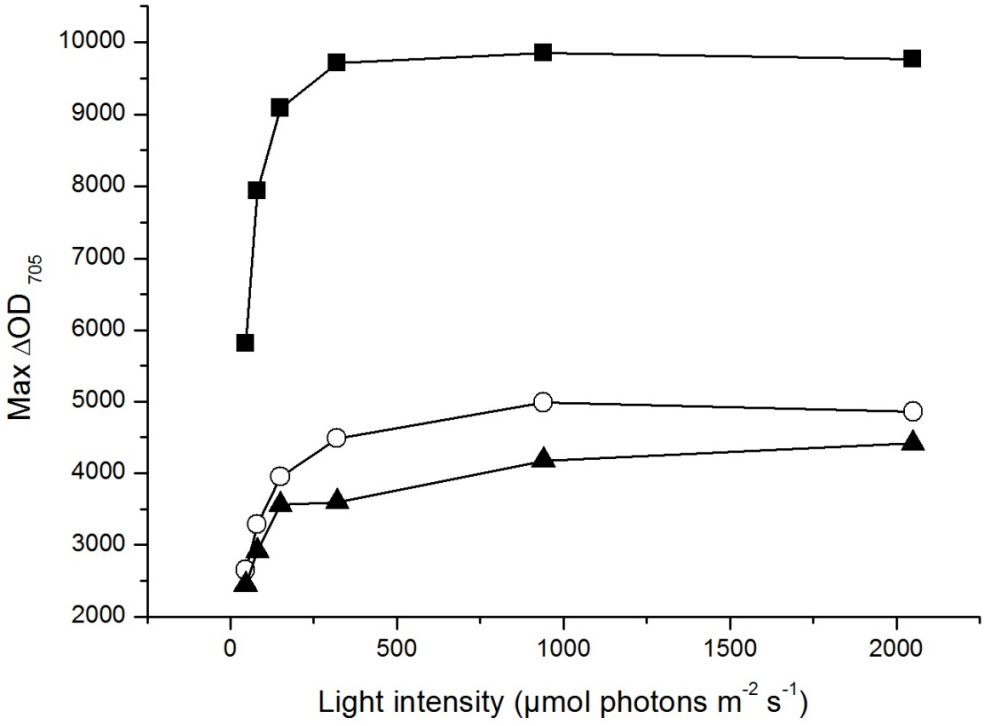

Figure S4. Dependence of the PSI Antenna Size upon actinic light intensity. P_{700} oxidation was measured at several actinic light (excitation light: 630 nm) in thylakoids extracted form LL, ML and HL acclimated cells. Photosynthetic membranes were treated with methylviologen and ascorbate. 40 µg Chl of each sample were analyzed. A) Correlation between PSI antenna size and the actinic light employed during the measurement. Significant differences between the three growth conditions were observed at all the actinic light employed (ANOVA), n = 4, $p < 0.05$. Dashed lines show the linear fitting of the antenna size values determined with the lowest actinic light intensities. Note that with the lower light intensities, we found a linear relationship between the amount of light provided and the rate of P_{700} oxidation. This confirms that light was limiting PSI turnover, as required for proper estimation of the antenna size of this complex. B) Correlation between the total amount of P_{700}^{+} divided for the Chl amount in the sample analyzed and the actinic light (630 nm) used for the measurement. The constant amplitude of the P_{700}^{+} signal indicates that all the PSI complexes could be oxidized in these experiments. The values obtained with the LL and ML conditions are significantly different from the HL condition (ANOVA, n=4, p-value < 0.05). LL, ML and HL conditions are shown respectively in black squares, empty circles and black triangles.

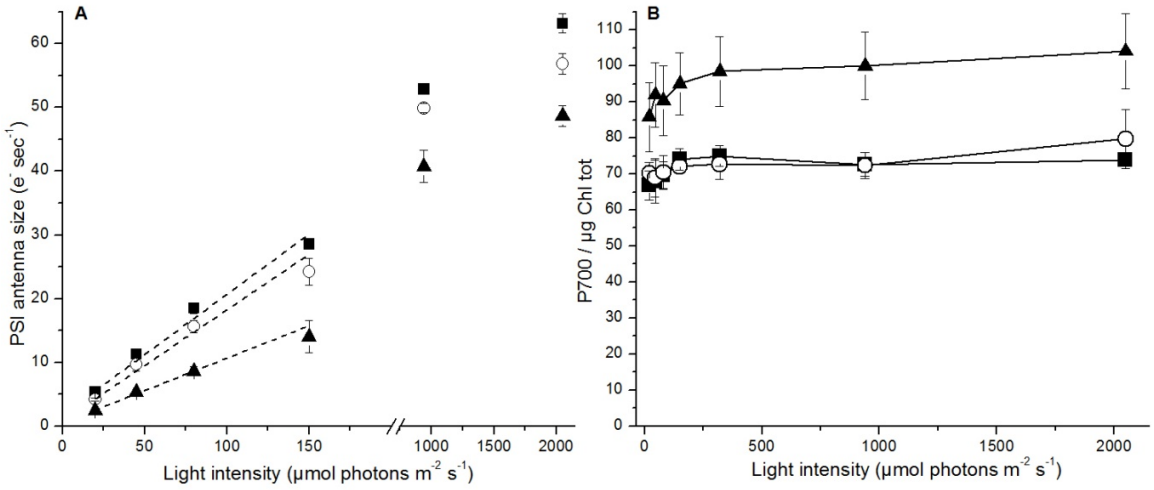

Figure S5. Western blotting loading an equal number of cells. Western blotting analysis was performed as in Figure 6C but loading equal amount of cells (8 and 2 10^6 cells for α-D2 and α-VCP respectively) for each sample.

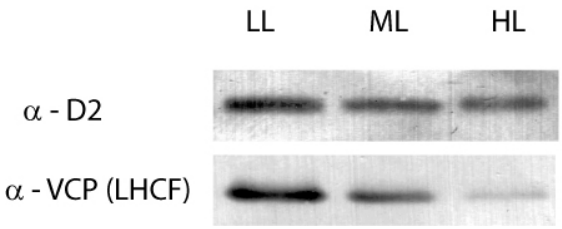

Figure S6. PSI electron transport efficiency in cells acclimated to different conditions. P_{700} redox kinetics employed for quantification of the photosynthetic electron transport in LL (A) and HL (B) acclimated cells. Cells were exposed to a saturating light intensity (2050 µmoles of photons m^{-2} s^{-1}) for 15 seconds before the dark recovery kinetics starting at time 0. Untreated cells (solid squares), cells treated with DCMU (open circles) and treated with DCMU and DBMIB (solid triangles). Kinetics for ML are shown in Figure 8A.

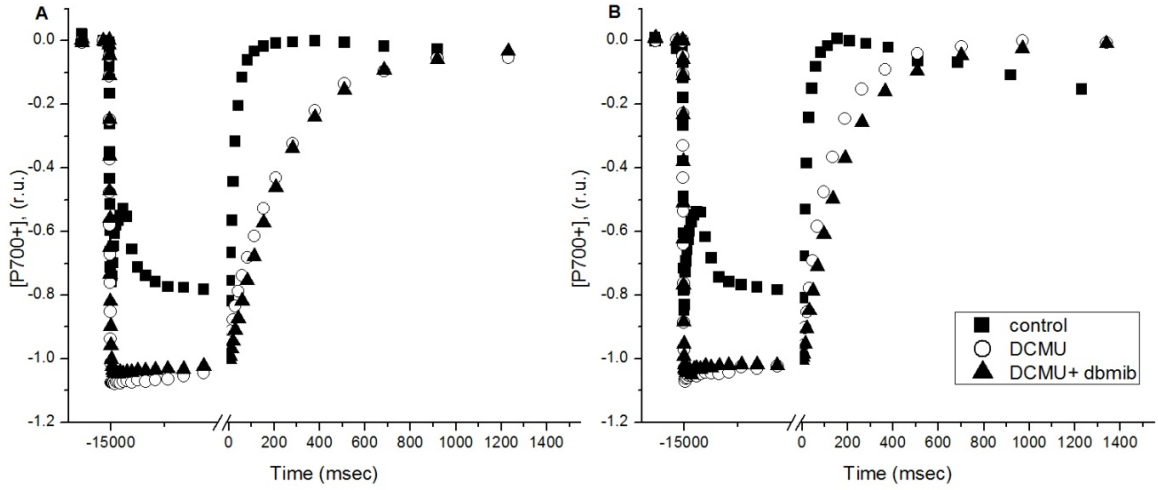

CHAPTER B2

EFFECT OF SPECIFIC LIGHT SUPPLY RATE ON PHOTOSYNTHETIC EFFICIENCY OF *NANNOCHLOROPSIS SALINA* IN A CONTINUOUS FLAT PLATE PHOTOBIOREACTOR

Published in
Applied Microbiology and Biotechnology

EFFECT OF SPECIFIC LIGHT SUPPLY RATE ON PHOTOSYNTHETIC EFFICIENCY OF *NANNOCHLOROPSIS SALINA* IN A CONTINUOUS FLAT PLATE PHOTOBIOREACTOR

Eleonora Sforza[1], Claudio Calvaruso[1], Andrea Meneghesso[2], Tomas Morosinotto[2], Alberto Bertucco[1]

1 Department of Industrial Engineering DII, University of Padova, Via Marzolo 9, 35131 Padova, Italy
2 Department of Biology, University of Padova, Via Bassi 58b, 35131 Padova, Italy

Received: 4 June 2015 /Revised: 16 July 2015 /Accepted: 18 July 2015 /Published online: 11 August 2015

Abstract

In this work, *Nannochloropsis salina* was cultivated in a continuous-flow flat-plate photobioreactor, working at different residence times and irradiations to study the effect of the specific light supply rate on biomass productivity and photosynthetic efficiency. Changes in residence times lead to different steady-state cell concentrations and specific growth rates. We observed that cultures at steady concentration were exposed to different values of light intensity per cell. This specific light supply rate was shown to affect the photosynthetic status of the cells, monitored by fluorescence measurements. High specific light supply rate can lead to saturation and photoinhibition phenomena if the biomass concentration is not optimized for the selected operating conditions. Energy balances were applied to quantify the biomass growth yield and maintenance requirements in *N. salina* cells.

Keywords:
Photosynthesis, Photosynthetic efficiency, Photoinhibition, Energy balance, Maintenance

1. LARGE-SCALE CULTIVATION OF MICROALGAE: LIMITS TO BE OVERCOME

About 90 % of energy is currently generated from fossil fuels, while only 10 % is produced from renewable energy sources (Maity et al., 2014). Such a massive use of fossil fuels has detrimental environmental consequences, making the development of alternative energy sources increasingly important. The exploitation of biomass is becoming relevant for the production of liquid fuels, and microalgae have a high potential for becoming a valuable feedstock for third-generation biofuels (Maity et al., 2014). The large-scale exploitation of microalgae for commercially sustainable biofuel production, however, still present several issues such as low productivity at the industrial scale, high costs and other technological hurdles (Brennan and Owende, 2010; Ho et al., 2014). The industrial production of microalgae is particularly limited by the decrease in photosynthetic efficiency (PE) moving from lab to large scale-cultivation systems which affects cultures productivity and, consequently, the net energy balance of the process.

Under phototrophic conditions, the increasing turbidity associated with microalgal concentration usually becomes a significant growth-limiting factor due to the self-shading effect (Ho et al., 2014). On the other hand, when exposed to high sunlight irradiances, the photosystems are not able to efficiently process the high flow rate of absorbed photons and this leads to photoinhibition (Simionato et al., 2013). As a consequence of both phenomena, photosystems are not able to efficiently process the high flow rate of absorbed photons when exposed to the high irradiances.

In the perspective of a large-scale cultivation of microalgae in industrial applications, a continuous process looks more suitable because it noticeably improves the growth rate; it is generally more efficient, has lower cost and is easier to operate (Ho et al., 2014). Cultivation of microalgae in continuous systems is quite established and studied for several species (Mazzuca Sobczuk and Chisti, 2010; Tang et al., 2012; Ruiz et al., 2013), but less information is available on species of *Nannochloropsis* genus, one interesting candidate for these applications thanks to its ability to accumulate lipids (Rodolfi et al., 2009; Sforza et al., 2012). Some interesting attempts to grow *Nannochloropsis* in outdoor continuous reactors were carried out and different reactor geometries were tested, analyzing both biomass productivity and biochemical composition (Zhang et al., 2014; San Pedro et al., 2014; Camacho-Rodríguez et al., 2014). However, little information is still available on the photosynthetic efficiency of *Nannochloropsis* cultures in photobioreactors and how the peculiar light environment here affects biomass productivity and cell physiology.

2. EFFECT OF RESIDENCE TIME ON *N. SALINA* CONCENTRATION AND PRODUCTIVITY

In order to understand the effect of the residence time on *N. salina* productivity, this species was cultivated in non-limiting nutrient conditions under constant incident light intensity of 150 $\mu E\ m^{-2}\ s^{-1}$, which was identified as the optimal light condition in batch cultures (Sforza et al., 2012). After the continuous mode of cultivation was set and steady-state operation reached, five flow rates were established under the same incident light condition, resulting in hydraulic residence times (τ) of 1.09,

1.69, 1.94, 2.64 and 4.3 days. The lipid content of the biomass was monitored under different residence times, but no significant differences were found, and the total lipid percentage was found to be about 10 % DW under all conditions (data not shown). Results of biomass concentration and productivity at steady-state were instead different, as reported in Figure 1A-B. The biomass concentration was found to increase with the residence time, as already reported for other microalgae (Barbosa et al., 2005; Zijffers et al., 2010) and for other species of the genus *Nannochloropsis* (Camacho-Rodríguez et al., 2014; San Pedro et al., 2014). This increase in concentration, however, was less than linear with the residence time, as a result of the increased self-shading effect at higher residence time values. The biomass productivity of the cultures displays a maximum of 0.66 g L^{-1} day^{1} at 1.94 days of residence time (Figure 1B). Such a productivity maximum is well known in literature also for other species (Ruiz et al., 2013; Sforza et al., 2014).

While the effect of residence time on biomass concentration and productivity is quite established, little information is available on the effect of this operating variable on the photosynthetic efficiency. The photosynthetic efficiency depicted in Figure 1C represents the fraction of light energy absorbed that is converted into biomass in a photobioreactor and it is shown to decrease increasing residence time. This suggests that, when biomass concentration increases, the actual light available per cell decreases as a result of self-shading.

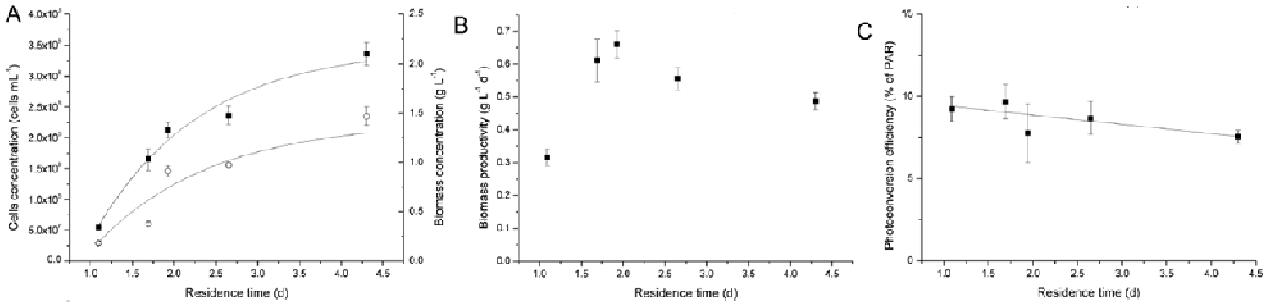

Figure 1. A) Biomass (dark squares) and cell (open circles) concentration as a function of residence time are reported (solid line are eye guides only). B) Biomass volumetric productivities data. C) The photosynthetic efficiency as % of PAR.

3. EFFECT OF RESIDENCE TIME ON PIGMENT CONTENT AND PHOTOSYNTHETIC PARAMETERS

In order to assess how cells responded to the cultivation in a continuous system, the pigment content was monitored for each residence time. As reported in Figure 2A, Chla content increased with the residence time. This is a typical response observed in low light acclimated cells and was likely the result of the higher cell concentration and, consequently, of the self shading (Simionato et al., 2011). Cultures with higher residence time also showed decreased Car/Chl ratio, another indication of cells acclimation to low light conditions (Simionato et al., 2011). Photosynthetic organisms regulate their pigments content in response to the intensity of the light they are exposed to, and while Chls are accumulated to increase light harvesting in light limiting conditions, carotenoids content is relatively increased for photoprotection mechanisms when light is in excess (Li et al., 2009). Interestingly, carotenoids content was found to increase (relatively to Chl) when the biomass concentration was lower even if the incident light was the same. The fluorescence parameter Fv/Fm (maximum PSII quantum yield) is commonly employed to evaluate the overall photosynthetic efficiency and to estimate the level of photoinhibition in PSII (Maxwell and Johnson, 2000). As shown in Figure 2B, this parameter monitored as a function of residence time showed a stable behavior at high residence times, while a significant reduction was observed decreasing τ, an indication of the presence of significant PSII photoinhibition in these cells. The presence of a photoacclimation can also be observed by the data of non-photochemical quenching (NPQ), an important protection mechanism consisting in the thermal dissipation of excitation energy which is activated upon exposition to excess illumination (Li et al., 2009). NPQ activation was measured in vivo by fluorescence (Maxwell and Johnson, 2000) on cells grown at different residence times, as a function of the actinic light intensity (Figure 2C). As can be observed in Figure 2C, cells grown at higher residence times showed an NPQ activation at very low illumination while at lower residence times, it is activated at higher actinic light intensities. This is a typical pattern observed for *Nannochloropsis* cells acclimated to respectively low and high light intensities. The presence of an acclimation to lower light intensity where the biomass concentration is higher is confirmed by the YII data. The YII parameter, quantum yield of Photosystem II, estimates the fraction of the light absorbed used in photochemistry. For cells grown at lower residence times, it is evident a higher capacity of light exploitation with increasing actinic light intensities. Taken together, both pigments content and photosynthetic parameters suggested that *N. salina* is responding to the different culture conditions by activating an acclimation response, similar to the one observed in batch cultures exposed to different light intensities (Sforza et al., 2012).

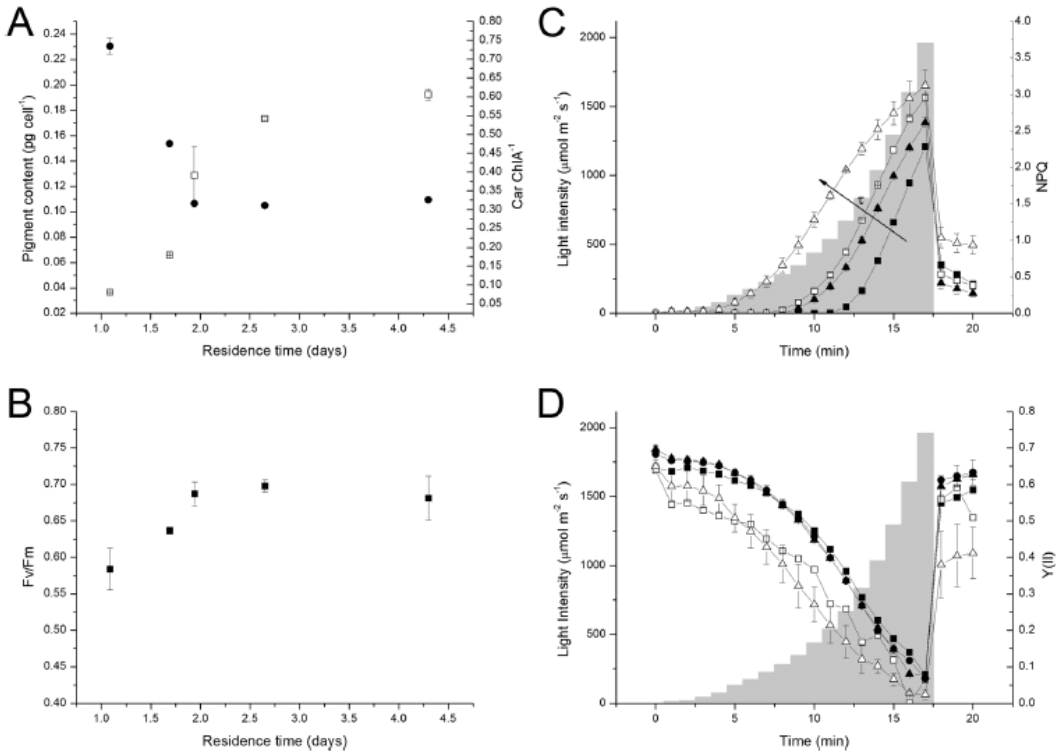

Figure 2. A) Chla (open squares) content is reported as a function of residence time, as well as the Car/Chla ratio (circles). B) The trend of Fv/Fm on residence time. C-D) Data of NPQ and YII measured under increasing light intensity, followed by a recovery under dark condition, for cell adapted at different residence times (filled squares for τ = 1.09 days, filled circles for τ = 1.69 days, filled triangles for τ = 1.94 days, open square for τ = 2.65 days, open triangles for τ = 4.30 days).The grey bars represent the light intensity of each step.

In this work *N. salina* was cultivated in a thin continuous-flow flat-plate reactor to test the effect of different residence time on biomass concentration identifying in particular a maximum in the biomass productivity of the cultures. Results obtained at different residence times suggest that, even though the incident light is similar, the light perceived per cell can be strongly different, and this activates an acclimatory response in *N. salina*. The acclimatory response activated by the cells allows them to maintain a stable photosynthetic efficiency under variable light supply rates, even if they experience some photoinhibition. This exemplifies the importance of this biological response to sustain algae productivity. To conclude setting a proper light supply rate, which depends on the incident light, the reactor depth and geometry and the biomass concentration, is the key factor to obtain a stable biomass productivity in a continuous system.

References

Barbosa, M.J., Zijffers, J.W., Nisworo, A., Vaes, W., van Schoonhoven, J., and Wijffels, R.H. (2005). Optimization of biomass, vitamins, and carotenoid yield on light energy in a flat-panel reactor using the A-stat technique. Biotechnol. Bioeng. **89**: 233–42.

Brennan, L. and Owende, P. (2010). Biofuels from microalgae—A review of technologies for production, processing, and extractions of biofuels and co-products. Renew. Sustain. Energy Rev. **14**: 557–577.

Camacho-Rodríguez, J., González-Céspedes, A.M., Cerón-García, M.C., Fernández-Sevilla, J.M., Acién-Fernández, F.G., and Molina-Grima, E. (2014). A quantitative study of eicosapentaenoic acid (EPA) production by Nannochloropsis gaditana for aquaculture as a function of dilution rate, temperature and average irradiance. Appl. Microbiol. Biotechnol. **98**: 2429–40.

Ho, S., Ye, X., Hasunuma, T., Chang, J., and Kondo, A. (2014). Perspectives on engineering strategies for improving biofuel production from microalgae—A critical review. Biotechnol. Adv.

Li, Z., Wakao, S., Fischer, B.B., and Niyogi, K.K. (2009). Sensing and responding to excess light. Annu. Rev. Plant Biol. **60**: 239–60.

Maity, J.P., Bundschuh, J., Chen, C.-Y., and Bhattacharya, P. (2014). Microalgae for third generation biofuel production, mitigation of greenhouse gas emissions and wastewater treatment: Present and future perspectives – A mini review. Energy **78**: 104–113.

Maxwell, K. and Johnson, G.N. (2000). Chlorophyll fluorescence - A practical guide. J. Exp. Bot. **51**: 659–668.

Mazzuca Sobczuk, T. and Chisti, Y. (2010). Potential fuel oils from the microalga Choricystis minor. J. Chem. Technol. Biotechnol. **85**: 100–108.

Rodolfi, L., Chini Zittelli, G., Bassi, N., Padovani, G., Biondi, N., Bonini, G., and Tredici, M.R. (2009). Microalgae for oil: strain selection, induction of lipid synthesis and outdoor mass cultivation in a low-cost photobioreactor. Biotechnol. Bioeng. **102**: 100–12.

Ruiz, J., Álvarez-Díaz, P.D., Arbib, Z., Garrido-Pérez, C., Barragán, J., and Perales, J.A. (2013). Performance of a flat panel reactor in the continuous culture of microalgae in urban wastewater: prediction from a batch experiment. Bioresour. Technol. **127**: 456–63.

San Pedro, A., González-López, C. V, Acién, F.G., and Molina-Grima, E. (2014). Outdoor pilot-scale production of Nannochloropsis gaditana: influence of culture parameters and lipid production rates in tubular photobioreactors. Bioresour. Technol. **169**: 667–76.

Sforza, E., Simionato, D., Giacometti, G.M., Bertucco, A., and Morosinotto, T. (2012). Adjusted light and dark cycles can optimize photosynthetic efficiency in algae growing in photobioreactors. PLoS One **7**: e38975.

Sforza, E., Urbani, S., and Bertucco, A. (2014). Evaluation of maintenance energy requirements in the cultivation of Scenedesmus obliquus: effect of light intensity and regime. J. Appl. Phycol. **27**: 1453–1462.

Simionato, D., Basso, S., Giacometti, G.M., and Morosinotto, T. (2013). Optimization of light use efficiency for biofuel production in algae. Biophys. Chem. **182**: 71–8.

Simionato, D., Sforza, E., Corteggiani Carpinelli, E., Bertucco, A., Giacometti, G.M., and Morosinotto, T. (2011). Acclimation of Nannochloropsis gaditana to different illumination regimes: effects on lipids accumulation. Bioresour. Technol. **102**: 6026–32.

Tang, H., Chen, M., Ng, K.Y.S., and Salley, S.O. (2012). Continuous microalgae cultivation in a photobioreactor. Biotechnol. Bioeng. **109**: 2468–74.

Zhang, D., Xue, S., Sun, Z., Liang, K., Wang, L., Zhang, Q., and Cong, W. (2014). Investigation of continuous-batch mode of two-stage culture of Nannochloropsis sp. for lipid production. Bioprocess Biosyst. Eng. **37**: 2073–82.

Zijffers, J.-W.F., Schippers, K.J., Zheng, K., Janssen, M., Tramper, J., and Wijffels, R.H. (2010). Maximum photosynthetic yield of green microalgae in photobioreactors. Mar. Biotechnol. (NY). **12**: 708–18.

CHAPTER B3

MULTIPLE BIOLOGICAL ROLES OF ZEAXANTHIN IN THE EUSTIGMATOPHYCEA *NANNOCHLOROPSIS GADITANA*

MULTIPLE BIOLOGICAL ROLES OF ZEAXANTHIN IN THE EUSTIGMATOPHYCEA *NANNOCHLOROPSIS GADITANA*[1]

Abstract

Light is the source of energy for photosynthetic organisms but when in excess it also drives the formation of reactive oxygen species and consequently photoinhibition. Photosynthetic organisms have evolved several mechanisms to regulate light harvesting efficiency in response to variable light intensity and to avoid oxidative damage. Xanthophyll cycle plays a fundamental role in photoprotection mechanisms synthesizing zeaxanthin, a xanthophyll with multiple role in the photosynthetic apparatus particularly affecting the thermal dissipative response. Although widespread among photosynthetic organisms, xanthophyll cycle shows important differences involving the role and localization of the same xanthophylls. In this work we investigate the biological role of zeaxanthin in *Nannochloropsis gaditana,* a microalgae mostly known for its industrial exploitation but still unknown for its peculiar photosynthetic apparatus. Indeed this microalga, belonging to Heterokonta together with diatoms and brown algae, accumulates atypical high amount of the xanthophyll violaxanthin that represents its major carotenoid.

Introduction

Light is fundamental for photosynthesis but it might also be harmful when exceeds the capacity of the photosynthetic electron chain. Indeed the presence of excess light leads to an overall over-reduction of the electron chain slowing down photochemical reactions (Li et al., 2009; Barber and Andersson, 1992). In this condition chlorophylls singlet excited state ($^1Chl^*$) are not efficiently quenched by photochemistry increasing the probability of intersystem crossing leading to chlorophylls triplet ($^3Chl^*$) formation (Vass et al., 1992). $^3Chl^*$ are not intrinsically harmful but due to their long life they can transfer energy to oxygen creating Reactive Species (ROS). The overproduction of these species leads to an extensive oxidative damage of the thylakoid membrane both in its lipid and protein components (Long et al., 1994). Indeed thylakoids membrane represent a susceptible target to lipid peroxidation due to their enrichment in polyunsaturated fatty acids (Müller et al., 2001). Moreover, the $^1O_2$ generated by the triplet state of P680 in the Photosystem II reaction center can directly damage structural protein (Mellis, 1999). Photoinhibition represents all those effects detrimental for the photosynthetic efficiency resulting from imbalance between the light absorption and its use (Raven, 2011).

[1] Andrea Meneghesso, Diana Simionato, Andrea Cailotto and Tomas Morosinotto contributed to the data reported in this work (Department of Biology, University of Padova).

In order to face this high variability in environmental conditions photosynthetic organisms evolved several mechanisms. Among all, the xanthophyll cycle is a widespread process fundamental to respond to fast changes in light intensities. Xanthophyll cycle involving the reversible conversion of violaxanthin into zeaxanthin by the intermediate antheraxanthin (Arnoux et al. 2009; Jahns, Latowski, and Strzalka 2009). This conversion is activated in strong illumination and it is catalyzed by the VDE enzyme (violaxanthin de-epoxidase), a soluble monomeric enzyme localized in the thylakoid lumen (Hager and Holocher, 1994). Under strong illumination the lumenal pH decreases, inducing the enzyme dimerization and association in regions of the thylakoids membrane enriched in MGDG, where the substrate violaxanthin is found (Rockholm, 1996; Pfundel et al., 1994; Schaller et al., 2010; Saga et al., 2010; Arnoux et al., 2009). Indeed the same condition also induce the release of violaxanthin substrate from its binding site in light harvesting complexes and its diffusion in the thylakoid membranes to reach VDE (Jahns et al., 2009). When illumination decreases back, zeaxanthin is back converted to violaxanthin by the ZE (zeaxanthin epoxidase) constitutively active in the stromal side of the thylakoid membrane (Schaller et al., 2012). The ZE enzyme, although active both during darkness and illumination (Gilmore et al., 1994), catalyzes the epoxidation reaction with much lower rates if compared to the de-epoxidation reaction. In this way the fast accumulation of zeaxanthin during period of high light is not impaired (Siefermann and Yamamoto, 1975; Goss et al., 2006b).

The xanthophylls discussed above have different role in the photosynthesis reactions. Violaxanthin, besides its role in photoprotection acting as reservoir to create de-epoxy carotenoids, is also active as harvesting pigments within antenna complexes (Basso et al., 2014; Owens et al., 2007). Antheraxanthin is commonly a reaction intermediate although if not fast converted into zeaxanthin can also play a photoprotective role, as demonstrated in some organisms (Frommolt et al., 2001; Gilmore and Yamamoto, 1993). At last zeaxanthin plays a central role in photoprotection being involved in several mechanisms often related to its localization in the photosynthetic apparatus (Jahns et al., 2009; Havaux and Niyogi, 1999). It contributes to the quenching of excess excitation energy enhancing thermal dissipation from $^{1}Chl^{*}$ (Non Photochemical Quenching, NPQ) (Horton et al., 1996). NPQ is composed by different components based on their activation kinetics (See Section A, paragraph 4.1). In higher plants the more rapidly activated component, the qE or energy-dependent component, is controlled primarily by the amplitude of ΔpH across the thylakoids but it is also enhanced by zeaxanthin accumulation (Holt et al., 2005; Niyogi et al., 1998). Zeaxanthin was also suggested to be involved in slower photoprotection processes components of NPQ (Nilkens et al., 2010; Dall'Osto et al., 2005). When bound to antenna complexes zeaxanthin is also active in the quenching of $^{3}Chl^{*}$ (Dall'Osto et al., 2012; Mozzo et al., 2008) and when accumulated free in the thylakoids membrane it is an effective antioxidant for the scavenging of ROS to avoid lipids peroxidation (Havaux et al., 2007; Jahns et al., 2009). Zeaxanthin triplets generated from the energy transfer with $^{3}Chl^{*}$ or $^{1}O_{2}{}^{*}$ decay harmlessly to the ground state by thermal dissipation. In addition to its role as direct quencher zeaxanthin could also decrease the fluidity of the lipid bilayer thus lowering its permeability to oxygen (Gruszecki et al., 1999; Tardy and Havaux, 1997). Among all the xanthophylls described, zeaxanthin is the only one that accumulates under excess light condition. Its presence must to be temporally limited and exclusively linked to a short term

response due to the strong impact to the light harvesting efficiency. A clear example of that is the *npq2* mutant in Arabidopsis accumulating constitutively zeaxanthin. The constitutive high energy dissipation leads to strong impairment in growth performance in limiting growing light (Dall'Osto et al., 2005).

Xanthophyll cycle is conserved in most photosynthetic eukaryotes with the remarkable exception of red algae, which are capable of synthesizing zeaxanthin but not violaxanthin and miss the VDE gene (Schubert et al., 2006; Goss and Jakob, 2010). Nevertheless several heterokonts which originated from a secondary endosymbiosis of a red algae still present VDE and the xanthophyll cycle, most likely as a result of a lateral gene transfer event. Eustigmatophyceae, including *Nannochloropsis* species, diatoms and brown algae belong all to the heterogeneous group of Heterokonta (Cavalier-Smith, 2004; Riisberg et al., 2009). All these organisms while having a conserved VDE they also display different xanthophyll pigments. Whereas brown algae and Eustigmatophyceae employ the violaxanthin-zeaxanthin cycle typical of higher plants and green algae, in diatoms violaxanthin and zeaxanthin pigments are substitutes by diadinoxanthin (Dd) and diatoxanthin (Dt), respectively (Stransky and Hager, 1970; Coesel et al., 2008; Basso et al., 2014). Moreover Heterokonts also display a different photosynthetic apparatus with different pigmentation and antenna complexes, formed by LHCF, LHCR and LHCX (or LHCSR) polypeptides (Goss and Jakob, 2010; Goss and Lepetit, 2015). How these complexes are affected by zeaxanthin synthesis is not clear and can provide interesting insights on how evolution shaped this regulatory mechanisms. To this aim we investigated the xanthophyll cycle regulation in the Eustigmatophycea *Nannochloropsis gaditana*, a microalgae still poorly characterized in the photosynthetic detail. This microalga with high potentiality in the biodiesel exploitation field presents several particularities that justify the scientific interest. For example the violaxanthin xanthophyll represents its major carotenoid present at particularly high content (Basso et al., 2014). This atypical xanthophyll content suggests a particularity in the photosynthetic regulatory mechanisms giving rise to questions regarding the zeaxanthin synthesis, localization and functionality in *Nannochloropsis*.

Materials and Methods

Culture conditions.

Nannochloropsis gaditana from the Culture Collection of Algae and Protozoa (CCAP), strain 849/5, was grown in sterile F/2 medium (Guillard and Ryther, 1962) using sea salts 32 g/l, 40 mM TRIS HCl (pH 8), and Guillard's (F/2) marine water enrichment solution (Sigma-Aldrich). Maintenance and propagation of cultures were performed using the same medium added with 10 g/l of Plant Agar (Duchefa Biochemie). All growth experiments started from a pre-culture grown in Erlenmeyer flasks at 100 μmoles of photons $m^2 s^{-1}$ ($\mu E\ m^{-2}\ s^{-1}$) with mechanical agitation. At exponential phase these cells were collected and employed as inoculum for following experiments. The initial experiments were focused on minimize or maximize zeaxanthin amount in *Nannochloropsis* cells. To do that, different cultures were submitted to a screening with different light intensities in a Multicultivator MC 1000-OD system (Photon Systems Instruments, Czech Republic). In this system, mixing and additional CO_2 were provided by constant air bubbling. Temperature was kept at 21°C

and different light intensities were provided using an array of white LEDs. For all the other experiments, cells were grown in 5 cm diameter Drechsel bottles with a 250 ml working volume and bubbled using air enriched with 5 % CO_2 (v/v). Cultures were exposed to 100 μmoles of photons m^{-2} s^{-1} of illumination and maintained at 22 ± 1 °C in a growth chamber. To guarantee non-limiting nutrient conditions F/2 medium was enriched with $NaNO_3$, NaH_2PO_4 and $FeCl_3$•6 H_2O at a final concentration of 0.75 g/L , 0.05 g/L and 0.0063 g/L respectively. Algal growth was measured by changes in optical density at 750 nm (OD_{750}, Cary Series 100 UV–VIS spectrophotometer, Agilent Technologies) and cells number monitored with a cell counter (Cellometer Auto X4, Nexcelom Bioscience). Once reached an OD_{750} of 2 a fed-batch culture was started and maintained in Drechsel bottle for months removing excess culture and adding fresh medium every 2 days to restore the starting optical density while maintaining cells in a constant active growing phase. The cells removed regularly were employed to perform other experiments discussed below.

High light treatments to induce zeaxanthin synthesis and accumulation were performed exposing the excess culture removed from the fed-batch to different light intensities, later described, using a LED Light Source SL 3500 (Photon Systems Instruments). During the high light treatment cells were magnetically mixed in a thin borosilicate cylinder placed in a water bath at 21 °C in order to get a homogeneous treatment and kept a constant temperature. Once treated, cells were moved to dim light for several hours magnetically mixed in a Erlenmeyer flasks. Every 30 minutes samples were collected for HPLC analysis until 4 hours.

Thylakoid isolation, solubilization and sucrose gradients.

To obtain isolated thylakoids, *Nannochloropsis* cells were broken using a Mini Bead Beater (Biospec Products), according to the protocol described by (Basso et al., 2014). The thylakoids were resuspended in B4 buffer (0.4 M sorbitol, 15 mM NaCl, 5 mM MgCl2 and 10 mM HEPES–KOH [pH 7.5]), immediately frozen in liquid nitrogen and stored at − 80 °C until use. All steps were performed at 4 °C and in dim light. The total pigments were extracted with 80% acetone and the chlorophyll concentration of the samples was determined spectrophotometrically using specific extinction coefficients (Porra et al., 1989) and the acetone spectra fitting previously described (Croce et al., 2002), which were modified to account for the unusual pigment content.

Thylakoid membranes corresponding to 500 μg of Chl were washed with 50 mM EDTA and then solubilized for 20 min on ice in 1 ml of final 0.4% α-DM and 10 mM HEPES (pH 7.5) after vortexing for 1 min. The solubilized samples were centrifuged at 15000 ×g for 20 min to eliminate any unsolubilized material, and the supernatant with the photosynthetic complexes was then fractionated by ultracentrifugation in a 0.1–1 M sucrose gradient containing 0.06% α-DM and 10 mM HEPES (pH 7.5) (280000 ×g, 18 h, 4 °C). The green fractions of the sucrose gradient were then harvested with a syringe. The identity of the different fractions have been confirmed through absorption spectra determined between 350 and 750 nm using a Cary Series 100 UV–VIS spectrophotometer (Agilent Technologies).

Pigments analysis.

The chlorophyll and total carotenoids were extracted from *Nannochloropsis* whole cells by 80% acetone preceded by cell mechanical lysis using a Mini Bead Beater in the presence of glass beads (150–212 μm diameter). The pigments of the gradient fractions were extracted using directly 80% acetone, and the quantification was determined by fitting the acetone spectra from 350 to 750 nm (Croce et al., 2002). The content of individual carotenoids was determined using a high-pressure liquid chromatography (HPLC) as described in (Färber and Jahns, 1998). The HPLC system consisted of a 139 reversed-phase column (5μm particle size; 25x0.4 cm; 250/4 RP 18 Lichrocart, Darmstadt, Germany) and a diode-array detector useful to record the absorbance spectra (1100 series, Agilent, 141 Waldbronn, Germany). The peaks of each sample were identified through the retention time and absorption spectrum (Jeffrey et al., 1997). The vaucheriaxanthin retention factor was estimated by correcting that of violaxanthin for their different absorption at 440 nm.

Fluorescence measurements.

In vivo chlorophyll fluorescence of *Nannochloropsis gaditana* grown in the fed-batch was measured with Dual PAM-100 fluorometer (Walz), using saturating light at 6000 μE m^{-2} s^{-1} and actinic light of 800 μE m^{-2} s^{-1}. Before measurements, cells were dark-adapted for 20 minutes. The parameters NPQ and qL were calculated respectively as (Fm-Fm')/Fm' and (Fm'-F')Fo'/(Fm'-Fo')F' (Demmig-Adams et al., 2008). Dithiotreitol (DTT) treatment was performed incubating the cells with 20 mM DTT during the 20 minutes of dark adaptation.

Results

Zeaxanthin is constitutively accumulated in Nannochloropsis gaditana

As described in (Basso et al., 2014), *Nannochloropsis gaditana* presents some biochemical peculiarities that distinguish it from most of the photosynthetic organisms known so far. *Nannochloropsis* antenna complexes display an unusual pigments composition with Chla as the only chlorophyll and with particularly high content in violaxanthin which represents its major carotenoid. To get a deep comprehension of the xanthophyll cycle in this particular microalgae, *Nannochloropsis* cells were initially cultivated at low illuminations in order to reduce as much as possible the basal level of zeaxanthin. The lights employed, from 23 to 100 μE m^{-2} s^{-1}, were limiting for *Nannochloropsis* growth and thus should be the best conditions to reduce as much as possible zeaxanthin (Figure 1A) (Sforza et al., 2012). Once acclimated completely to these growing conditions cells were collected and analyzed by HPLC to separate and quantify individual pigments (Figure 1B). Rather surprisingly at difference with plants, where undetectable zeaxanthin and antheraxanthin levels are easily achieved, here small amounts of zeaxanthin are always present, even in the cells grown in extreme limiting light.

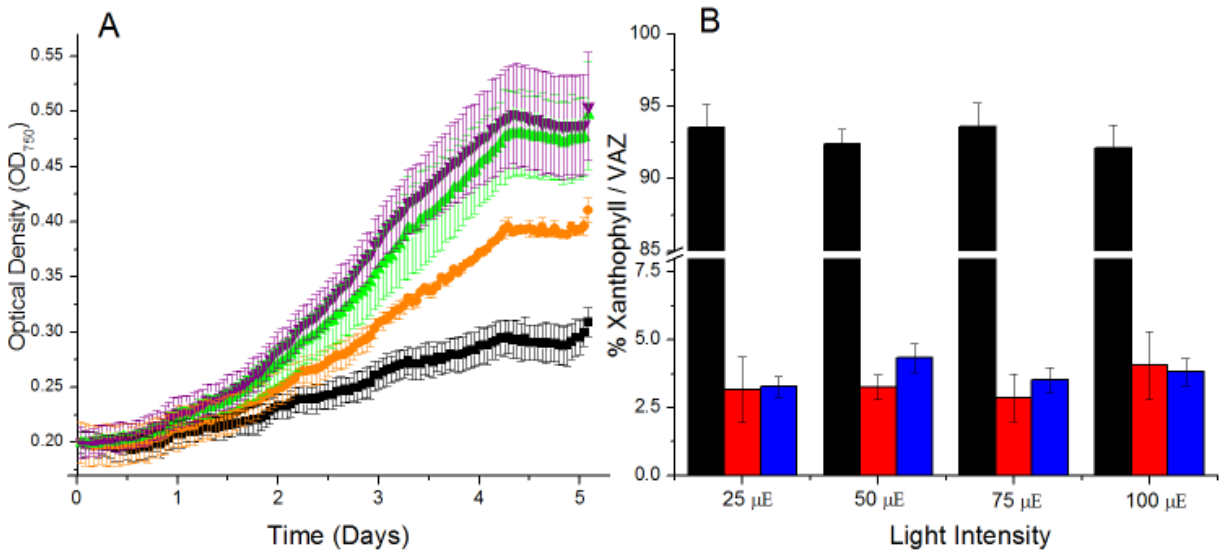

Figure 1. Kinetics of zeaxanthin formation in *Nannochloropsis gaditana*. A) *Nannochloropsis* cells grown under 25, 50 75 and 100 µE m^{-2} s^{-1} are shown, respectively, as black squares, orange circles, light green and purple triangles. The growth was evaluated using Optical Density (OD_{750}) measurements. B) Viola-, anthera- and zea- xanthin content in *Nannochloropsis* cells grown in the conditions described in A. Data are expressed as percentage of the single xanthophyll per their sum (VAZ). Black = violaxanthin, red = antheraxanthin, blue = zeaxanthin. Data are the average ± SD of 2 independent experiments.

Maximum zeaxanthin accumulation in Nannochloropsis gaditana

Cells cultivated at low light intensity were then moved to stronger illumination in order to evaluate light and time dependence of zeaxanthin formation kinetics (Figure 2A-B). In particular, cells were first exposed for 2.5 hours to different light intensities ranging from 25 to 1200 µE m^{-2} s^{-1} in order to identify the suitable light condition able to induce the maximal zeaxanthin synthesis (Figure 2A). Cells showed an increased zeaxanthin content with illumination associated with a decrease in violaxanthin, as expected. At 800 µE m^{-2} s^{-1} the conversion of violaxanthin in zeaxanthin reached a maximum maintained almost invariable for the further higher light intensity employed (Figure 2A). Afterward, to evaluate the maximal ratio of conversion in dependence of time, cells were exposed for a period of 0-2 hours at 1000 µE m^{-2} s^{-1} and sampled every 20 minutes (Figure 2B). The high light intensity 1000 µE m^{-2} s^{-1} was chosen since at this intensity there is the maximal zeaxanthin formation and it is also close to a hypothetical case of light stress in the natural environment. As shown in Figure 2B, the violaxanthin decreased prolonging the time exposition to strong illumination followed by a corresponding increase in the amount of antheraxanthin and zeaxanthin. The percentage of violaxanthin on the total xanthophylls pool after 2 hours at 1000 µE m^{-2} s^{-1} (HL condition) decreased about 25% with respect to the amount verified prior to treatment (Time 0, CTRL condition), while the concomitant amount of antheraxanthin and zeaxanthin almost triplicate (Figure 2B, Table 1). Vaucheriaxanthin and β-carotene, other important carotenoids with light harvesting and photoprotective functions, did not vary their amount in response to the light treatment (Table 1). This is consistent with a short-

term stress response that activates only the fastest mechanisms, as xanthophyll cycle, not changing the overall pigment composition.

Interestingly, as observed with time dependence, there was little tendency to saturation. In order to verify this point and induce zeaxanthin synthesis as much as possible cells were exposed to extreme illumination of 4000 µE m^{-2} s^{-1} also removing air bubbling to maximize photosynthesis saturation (Figure 2C). This induced an extreme zeaxanthin accumulation up to 80% of total viola-, anthera- and zea-xanthin (VAZ) pool. Although this condition was clearly not physiological this demonstrates that, if necessary, *Nannochloropsis* has the ability to convert almost completely its violaxanthin into zeaxanthin, at difference with plants.

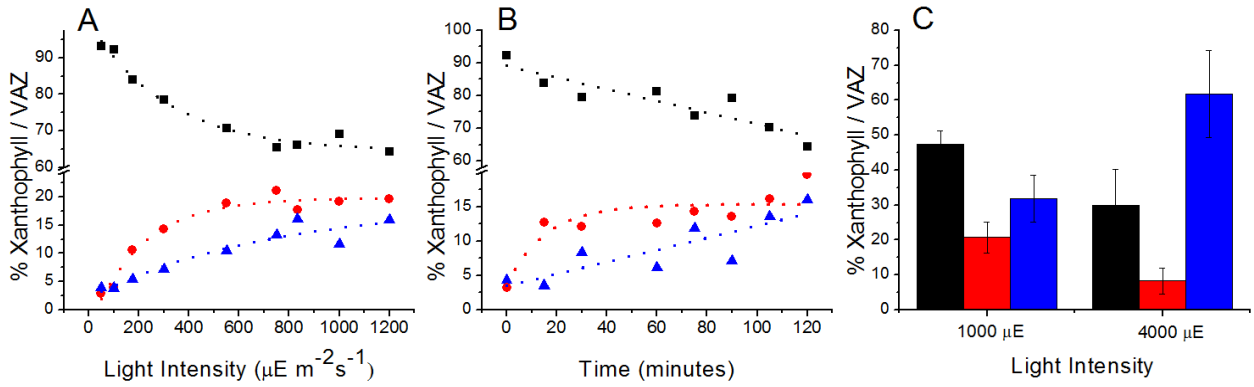

Figure 2. Kinetics of zeaxanthin formation in *Nannochloropsis gaditana*. A) Light intensity dependence of violaxanthin conversion into anthera- and zea- xanthin in sample exposed for 2.5 hours at different light intensities. B) Time dependence of violaxanthin conversion into anthera- and zea- xanthin in a sample exposed for 2 hours at 1000 µE m^{-2} s^{-1}. D) Viola-, anthera- and zea- xanthin content in *Nannochloropsis* cells grown in a Multicultivator system deprived of air bubbling at 1000 and 4000 µE m^{-2} s^{-1} for 2 hours. Data are expressed as percentage of the single xanthophyll per their sum (VAZ). Black = violaxanthin, red = antheraxanthin, blue = zeaxanthin. For A and B no replicates were performed for C data are the average ± SD of 2 independent experiments.

Table 1. Pigment content of *Nannochloropsis* cells in control and a high light conditions. Cells were collected from fed-batch cultures and then processed directly to perform HPLC analysis (CTRL cells) or after a high light treatment (2 hours at 1000 µE m^{-2} s^{-1}, HL cells). Carotenoids data are reported as mol/100 mol of chlorophyll. In the last three columns xanthophyll carotenoids, violaxanthin (Viola), antheraxanthin (Anthera) and zeaxanthin (Zea), are normalized for their sum (VAZ). Data are the average ± SD of 3 independent experiments.

	Viola-xanthin	Vaucheria-xanthin	Anthera-xanthin	Zea-xanthin	β–car	%Viola / VAZ	%Anthera / VAZ	%Zea / VAZ
CTRL cells	24.37 ± 2.41	4.88 ± 0.61	0.37 ± 0.53	0.99 ± 0.15	1.67 ± 2.37	93.84 ± 1.90	3.30 ± 0.33	3.96 ± 0.28
HL cells	18.12 ± 0.52	5.09 ± 0.76	4.69 ± 1.37	3.45 ± 0.83	1.17 ± 1.66	70.32 ± 4.09	17.72 ± 3.32	13.29 ± 1.47

Zeaxanthin is slowly converted to violaxanthin in Nannochloropsis gaditana

As already mentioned, the natural environment is characterized by sudden changes in light distribution that submit microalgae to quick transfer from low to high light and vice versa. After the experience of high light with the corresponding activation of xanthophyll cycle to dissipate excess energy and avoid photodamage, microalgal cells need to recovery their light harvesting ability when moved back to low light. For this reason the relaxation of xanthophyll cycle is as much as relevant as its activation. To this aim we investigated the kinetics of zeaxanthin relaxation in cultures first exposed to 1000 µE for 2 hours (HL) to maximize the activation of the xanthophyll cycle and then moved to a dim light of 25 µE m^{-2} s^{-1} (Figure 3). It has been decided to use dim light instead of dark because it stimulates epoxidation kinetics by means of photosynthesis products, such as O_2 and NADPH, which are needed during the ZE reaction (Hartel et al., 1996). After the shift to dim light, samples were collected every 30 minutes in order to verify the relaxation kinetic of zeaxanthin. This xanthophyll was completely reconverted in violaxanthin after almost 1 hour (Figure 3), coming back to levels already obtained for untreated cells (Figure 1, Table 1).

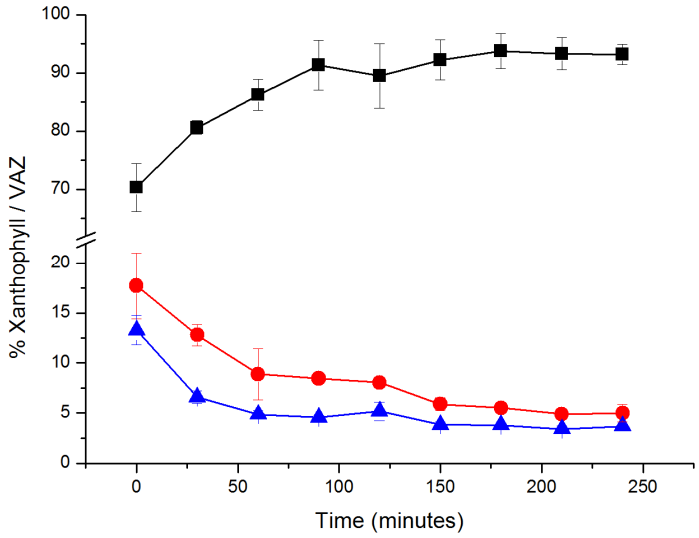

Figure 3. Epoxidation kinetics in N*annochloropsis gaditana* after HL treatment. The kinetic of zeaxanthin reconversion in violaxanthin was followed during dim light exposition after an illumination of 1000 µE m^{-2} s^{-1} for 2 hour (HL, Time 0). Data are expressed as percentage of the single xanthophylls per their sum (VAZ). Data are the average ± SD of 2 independent experiments.

Zeaxanthin localization in Nannochloropsis photosynthetic apparatus

Zeaxanthin biological role is played also by its association to specific protein complexes. In order to search for zeaxanthin specific binding site in the photosynthetic apparatus of *N gaditana*, thylakoids were purified from cells either harvested upon growth in control condition (100 µE m^{-2} s^{-1}, CTRL) or treated with excess light (2 hours at 1000 µE m^{-2} s^{-1}, HL) to maximize the zeaxanthin accumulation. Thylakoids were solubilized with mild detergent (0.4% α-DM) and loaded into a continuous sucrose gradient for ultracentrifugation. As reported in (Basso et al., 2014), five distinct fractions were recognizable with different migration rates, while a sixth was

present as pellet at the bottom of the tube (Figure 4A). The spectroscopic analysis of the different fractions allowed their identification. Fraction 1 (F1) represents free pigments and exhibits a maximum in the Qy region at 670 nm. F2–F3 are monomeric–oligomeric antenna complexes showing identical spectra with characteristic Chl maximum at 675 nm (Figure 4B-C). F4 is PSII core complex and F5 identifies PSI-LHC super-complexes, showing a typical red-shifted absorption over 700 nm. F6 band is very similar to the F5 and for that is considered characterized by PSI-LHC aggregates or PSI-enriched membrane particles (Figure 4D-E).

The migration pattern in the gradient and the spectral features of the different fractions were very similar between CTRL and HL sample suggesting that the high light treatment did not affect the overall organization of the photosynthetic apparatus (Figure 4). In order to identify the pattern of distribution of xanthophyll cycle pigments and their relative abundance, HPLC analysis of total pigments contained in F1, F2, F3 and F5 fractions were performed. As reported in Table 2, analysis of xanthophylls content in CTRL samples revealed a very similar pattern of accumulation among the different fractions. The same consideration can be done also for the HL condition where, despite the clear activation of the cycle, no significant differences between the different HL fractions were observed, suggesting no specific site of accumulation for this xanthophyll (Table 2). As expected the high light treatment did not change the amount of vaucheriaxanthin, widely distributed in the fractions, and β-carotene, mostly found associated with PSI core (Bassi et al, 1993) (Table 3).

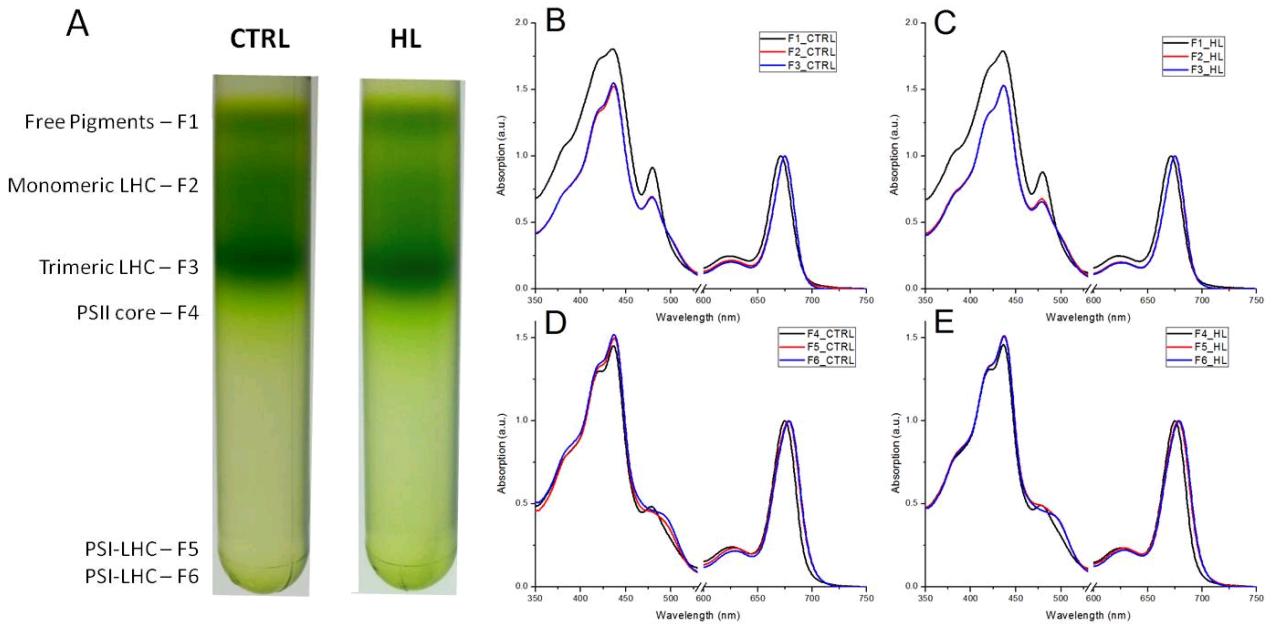

Figure 4. Sucrose gradient and relative absorption spectra in CTRL and HL samples. A) *Nannochloropsis* sucrose gradient after mild solubilization with 0.4% α-DM. Five distinct bands are distinguishable (F1–F5) while a sixth is present at the bottom of the tube (F6). Absorption spectra of sucrose gradient bands in CTRL (B,D) and HL samples (C,E). B,C) Free pigments (F1, black), monomeric and oligomeric antennas (F2, red and F3, blue). D,E) PSII core complex (F4, black), PSI-LHC (F5, red and F6, blue). All spectra are normalized to the Chl a maximum in the red part of the absorption spectra.

Table 2. Pigment data of sucrose gradient bands. Bands content in xanthophylls is reported. The CTRL and HL data refer to samples in a control condition and samples previously subjected to a high light treatment (2 hours at 1000 μE m^{-2} s^{-1}, HL). The values are normalized for the sum of the three xanthophylls violaxanthin (Viola), antheraxanthin (Anthera) and zeaxanthin (Zea). Data are the average ± SD of 2 independent experiments.

	CTRL			HL		
	Viola	**Anthera**	**Zea**	**Viola**	**Anthera**	**Zea**
Free pigments F1	95.1 ± 1.3	5.5 ± 0.6	0.8 ± 1.6	80.8 ± 3.4	16.2 ± 2.7	3.0 ± 4.2
Monomeric LHC F2	91.9 ± 2.7	3.9 ± 1.1	4.1 ± 1.6	79.7 ± 1.8	13.9 ± 1.4	6.4 ± 0.7
Trimeric LHC F3	94.5 ± 1.5	2.7 ± 1.0	2.9 ± 0.1	78.9 ± 1.1	13.7 ± 0.6	7.4 ± 1.5
PSI-LHC F5	90.4 ± 2.4	6.6 ± 1.9	6.5	73.0 ± 0.7	18.5 ± 1.1	9.3 ± 1.6

Table 3. Pigment data of sucrose gradient bands. Bands content in different carotenoids is reported. The CTRL and HL data refer to samples in a control condition and samples previously subjected to a high light treatment (2 hours at 1000 μE m^{-2} s^{-1}, HL cells). The value are normalized for the total amount of carotenoids and reported as average ± SD (n = 2).

	CTRL					HL				
	Viola-xanthin	**Vaucheria-xanthin**	**Anthera-xanthin**	**Zea-xanthin**	**β–car**	**Viola-xanthin**	**Vaucheria-xanthin**	**Anthera-xanthin**	**Zea-xanthin**	**β–car**
Free pigments F1	67.4 ± 1.7	12.4 ± 1.7	3.9 ± 0.4	2.1	3.9 ± 0.3	56.8 ± 1.9	12.8 ± 1.6	11.4 ± 1.8	5.4 ± 0.6	4.0 ± 1.1
Monomeric LHC F2	59.3 ±1.4	16.7 ± 1.0	2.5 ± 0.7	2.2 ± 0.6	1.7 ± 0.4	52.2 ± 1.0	16.4 ± 1.5	9.1 ± 0.9	4.2 ± 0.5	1.7 ± 0.4
Trimeric LHC F3	61.7 ± 1.0	16.6 ± 1.7	1.8 ± 0.6	1.9 ± 0.1	1.3 ± 0.4	52.2 ± 0.8	16.3 ± 1.9	9.0 ± 0.4	4.9 ± 1.0	1.2 ± 0.8
PSI-LHC F5	50.4 ± 2.3	9.6 ± 2.1	3.7 ± 1.2	4.2 ± 1.0	28.0 ± 3.5	46.8 ± 3.9	7.1 ± 1.1	11.7 ± 1.8	5.6 ± 0.6	2.2 ± 3.0

Biological Role of zeaxanthin in vivo: NPQ shows a DTT-insensitive component in N. gaditana

As mentioned above, zeaxanthin plays a role in both $^1Chl^*$ quenching and ROS/$^3Chl^*$ scavenging. The former activity can be monitored by monitoring NPQ. In order to investigate the influence of the synthesis of zeaxanthin on NPQ, we treated CTRL cells with different concentrations of a VDE inhibitor (DTT) before NPQ measurements. DTT inhibits zeaxanthin synthesis without affecting lumen acidification (Lavaud et al., 2002; Sokolove and Marsho, 1976) by reducing C-C bridges fundamental for its activity (Simionato et al., 2015). This treatment allowed to identifying which portion of NPQ activation was due to the accumulation of this xanthophyll. As shown in Figure 5A, when no DTT was added NPQ increased during the first minutes and showed a tendency to a saturation at the end of the light treatment. The maximum of NPQ was strongly affected by the

addition of DTT at concentrations higher than 5 mM, reducing its amplitude up to 10 % of the initial amount (Figure 5B). This suggest a strong influence of xanthophyll cycle in NPQ in *Nannochloropsis*. The DTT-insensitive component, representing NPQ non dependent from zeaxanthin synthesis, showed a rapid induction maintained till the end of the light treatment and then turned off just as rapidly (Figure 5A). This remaining NPQ represents probably the portion of the qE component not depended from zeaxanthin accumulation but principally related on the ΔpH gradient across the membrane (Müller et al., 2001).

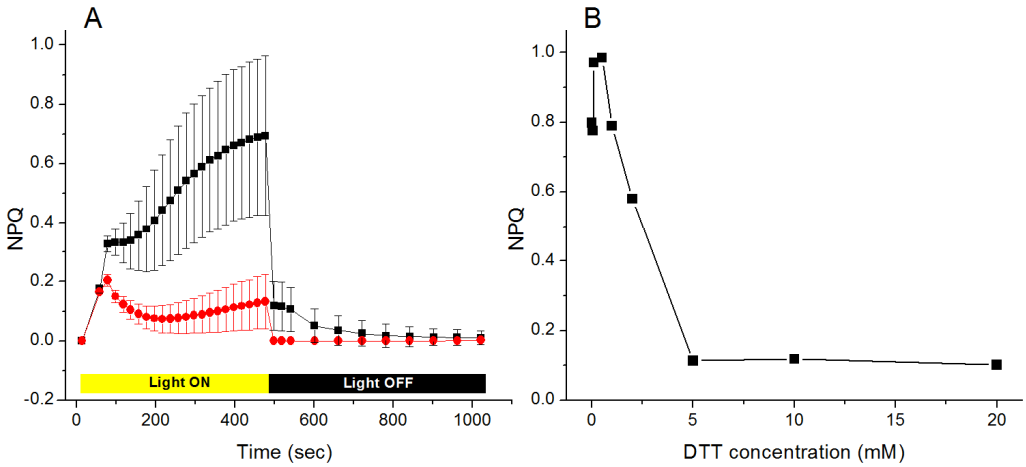

Figure 5. Effect of DTT on NPQ induction. A) NPQ induction analysis in *Nannochloropsis* cells grown at grown at 100 μE m^{-2} s^{-1} (CTRL condition). Induction kinetics of untreated (black squares) and 20mM DTT-treated (red circles) samples are shown. The induction protocol consists in 8 min of light at 800 μE m^{-2} s^{-1} and 15 min of dark recovery. Data are reported as average ± SD (n=5). B) NPQ versus DTT concentration derived from the same measurements as in A are reported.

Biological role of zeaxanthin in vivo: Zeaxanthin accumulation effect on NPQ induction in N. gaditana

One method to assess the zeaxanthin effect on NPQ is to repeat two NPQ measurements in series, separated by a short 10 minutes recovery. This allows ΔpH to relax but does not leave enough time to zeaxanthin to be back converted to violaxanthin. Therefore the second induction kinetic performed is influenced by the zeaxanthin synthesized during the previous 8 minutes treatment. This effect was evident in the CTRL sample, where the first points of the second induction were higher than the ones of the first induction indicating a faster activation of the NPQ response (Figure 6A). Although the different beginnings, the NPQ value reached at the end of each treatment were comparable. Performing the same measurements in the HL sample it is shown that the first kinetic presented a marked acceleration in the NPQ induction at the onset of illumination while, however, no significant differences were present between the first and the second induction kinetics (Figure 6B). Hence in the first minute of the first light treatment, HL sample showed a four time increase in the NPQ value compared to the CTRL one while no differences were observed between the CTRL and HL second kinetics (Figure 6A-B). The strong increase observed in the HL first kinetic was probably due to a significant amount of pre-accumulated zeaxanthin which has an active role in the NPQ induction. It's worth mentioning that,

despite the different amount of zeaxanthin at the beginning of each CTRL and HL induction and the consequent strong difference in the activation kinetics, NPQ reaches always similar steady state value at the end of the light treatment.

The NPQ response in HL sample was analyzed in detail to distinguish the different NPQ components. When DTT treatment was employed to remove the *de novo* synthesis of zeaxanthin, HL sample showed a fast component with similar kinetic already observed for the untreated sample (Figure 6C). This fastest components DTT-insensitive, probably related to pre-accumulated zeaxanthin, disappeared completely after the initial peak at difference for what described for the DTT CTRL analysis (Figure 5A).

For what concerns the photochemical quenching parameter, called qL, different behavior was observed in the NPQ induction between CTRL and HL cells (Figure 6D). This parameter assess the fraction of 'open' PSII RC (reaction center able to perform photochemistry), and could be employed as a index to monitor photosynthesis saturation. HL cells showed higher value in the first minute reaching at the end of light treatment the same CTRL value. The effect of higher zeaxanthin amount and the consequent NPQ peak at the onset of illumination seems to relieve PSII for excessive electronic pressure, temporally increasing the fraction of open PSII RC.

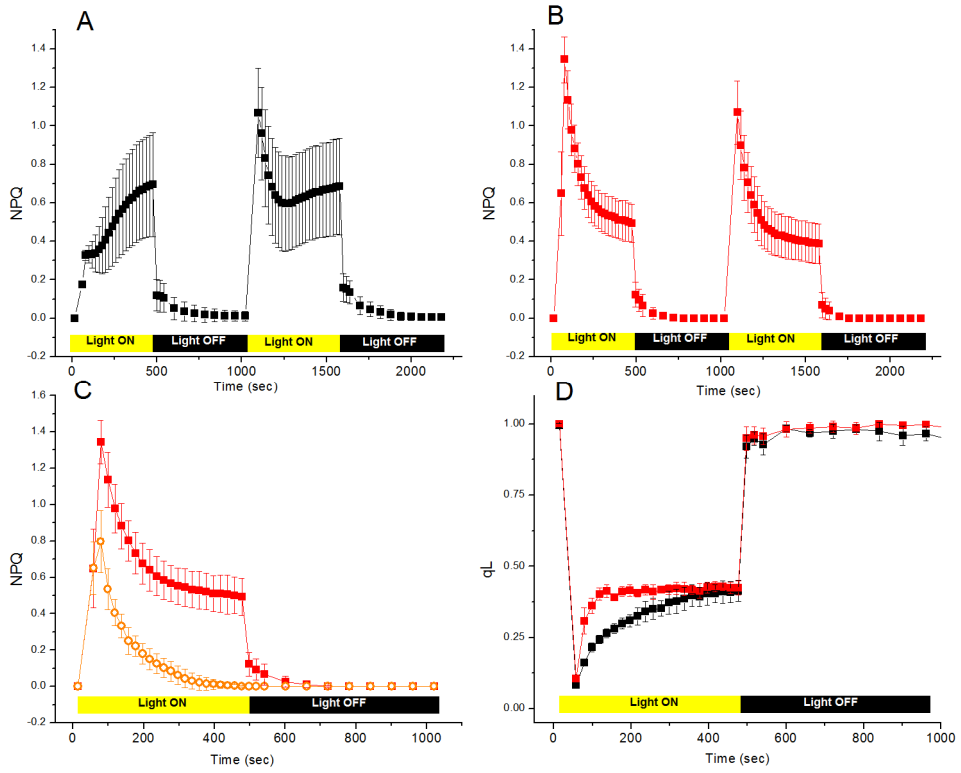

Figure 6. Zeaxanthin influence on NPQ. A-B) Two fluorescence kinetics were performed in rapid succession (8 minutes at 800 µE m^{-2} s^{-1}, yellow bars), separated by 10 minutes of dark relaxation (dark bars). NPQ kinetic in CTRL (A) and HL (B) samples are shown. C) Single NPQ induction kinetic performed in untreated (red) and DTT-treated (orange) HL samples. D) Single induction kinetic performed in CTRL and HL sample. Black curves, CTRL sample; Red curves, HL samples. Data are reported as average ± SD (n = 5).

DISCUSSION

Xanthophyll cycle has a crucial role in the response to excess light conditions in many photosynthetic organisms and its role is often related to thermal dissipation mechanisms as NPQ, ROS scavenging and thylakoid membrane reorganization (Havaux and Niyogi, 1999; Havaux et al., 2007; Betterle et al., 2009). *Nannochloropsis gaditana*, through its violaxanthin-zeaxanthin cycle, presents several features that distinguish it from other better known organisms. For instance the amount of violaxanthin found in this microalgae grown in control condition (Table 1) is significantly high if compared with vascular plant, moss and green algae grown in similar conditions but also with the evolutionary closer diatoms containing diadinoxanthin (Dd) xanthophyll (Lavaud et al., 2002; Goss et al., 2006a; Pinnola et al., 2013; Dall'Osto et al., 2005; Niyogi et al., 1997). This high amount of violaxanthin, in addition to the light harvesting function, could act as huge reservoir to synthesize zeaxanthin when needed. Indeed the most part of violaxanthin in *Nannochloropsis* could actually been converted in zeaxanthin even if, to reach such condition, non physiological treatment must be performed (Figure 2C). Moreover *Nannochloropsis* shows small amounts of zeaxanthin even if grown in the lowest light intensity (Figure 1) while in plants or moss, for instance, undetectable zeaxanthin and antheraxanthin levels are easily achieved (Ballottari et al., 2007; Pinnola et al., 2013). If we consider evolutionary closer species as diatoms the situation remains the same. Indeed no Dt was detected growing *P. tricornutum* cells in limiting light conditions (Lavaud et al., 2002). This atypical feature found in *Nannochloropsis* is possibly due to the carotenoids biosynthesis pathway where a small amount of zeaxanthin, precursor of violaxanthin, is always synthesized before being converted to violaxanthin. The same constitutive presence of zeaxanthin has been observed also in cyanobacteria and red algae, where zeaxanthin does not come from violaxanthin but is constitutively synthesized from beta-carotene (Schagerl and Müller, 2006; MacIntyre et al., 2002). Despite this high potential to produce zeaxanthin, as evidenced from high violaxanthin amount, and the sustained amount of zeaxanthin also in limiting light condition, the overall NPQ response in *Nannochloropsis* is similar to other NPQ xanthophyll-dependent organisms (Figure 5A).

Following the amount of xanthophylls after transferring cells from high light to low light it is clearly shown that the zeaxanthin epoxidation reaction in *Nannochloropsis* (Figure 3) has kinetics compatible to those already described in violaxanthin cycle containing organisms, such as plants, green algae but also for the evolutionary closer brown algae (Siefermann and Yamamoto, 1975; Goss et al., 2006a; Goss and Jakob, 2010). At contrary from what observed in Dd cycle containing algae, such as diatoms, capable instead of extremely high rates of de-epoxidation and epoxidation (Goss et al., 2006a). This strong difference between species belonging also to the same evolutionary group, as for Heterokonts, could be related to light environment in their natural habitat that forces the photosynthetic organisms to evolve suitable photoprotective mechanism. Diatoms, for example, differ from the other organisms for the extreme variability of the light environment in which they live and for they evolved faster xanthophyll cycle activation and relaxation (Lavaud and Lepetit, 2013). Interestingly *Nannochloropsis* in its marine environment has maintained the same xanthophyll cycle as higher plant, partially conserving also its reactions kinetic.

For what concerns xanthophylls localization in the different gradient fractions examined no difference is observed in CTRL cells. In HL cells violaxanthin, antheraxanthin and zeaxanthin behave accordingly to the xanthophyll cycle activation and so decreasing or increasing their amount as already observed in intact cells. Despite this, no specific binding site of zeaxanthin was detected after its strong accumulation. According to these results in *Nannochloropsis* free LHC (F2 and F3) in CTRL and in HL samples seems to bind the same amount of xanthophylls of PSI-bound LHC (F5) in CTRL and HL sample, respectively (Table 2,3), at difference from what observed in many other organisms. For example in the moss *Physcomitrella patens*, zeaxanthin is mostly bound to the free LHC (not associated with PSI or PSII) and less to PSI-LHC complex after HL exposition (Pinnola et al., 2013). Similar results were obtained also in diatoms, as in the species *Phaeodactylum tricornutum* where the free light-harvesting complex containing fucoxanthin (LHCF) in high light have a larger Dd content compared to those associated with the reaction centers and also a higher de-epoxidation state (Lavaud et al., 2003; Guglielmi et al., 2005). Evidences of specific LHC trimeric subunits engage in the binding of the most part of the xanthophyll cycle pigments pool were found also in the diatoms *Cyclotella meneghiniana*, after exposition to high light stress (Beer et al., 2006). These results highlight the peculiarity of *Nannochloropsis* photosynthetic apparatus among other photosynthetic organisms and open many questions regarding the relationship between the homogeneously distributed zeaxanthin and NPQ mechanism. To clarify these aspects a detailed analysis of the NPQ induction in *Nannochloropsis* has been performed.

As shown in Figure 5 zeaxanthin has a fundamental role for the full activation of energy dissipative mechanisms in *Nannochloropsis* as demonstrated from the strong NPQ decrease in DTT-treated sample. Despite this a small amount of zeaxanthin-independent NPQ remains always present. An analogues situation was observed also in *Chlamydomonas* and *Arabidopsis* where DTT inhibits the accumulation of de-epoxidized xanthophylls without totally suppress NPQ (Gilmore and Yamamoto, 1991; Niyogi et al., 1998, 1997). *Nannochloropsis* cells treated with DTT exhibit about 10% of the NPQ of control cells, a small amount if compared with 25 to 40% found in plants (Adams et al., 1990; Bilger and Björkman, 1990). The DTT-insensitive NPQ component found in *Nannochloropsis* is rapidly induced as observed in the induction kinetics depicted in Figure 5A. This suggest that the fastest component of NPQ, qE component, in *Nannochloropsis* can be triggered also in the absence of zeaxanthin, at contrary from what described in diatoms for example (Lavaud et al., 2002).

The NPQ induction kinetics performed in CTRL and HL cells allow to assess the effect on NPQ of higher amount of zeaxanthin accumulated after 2 hours of HL treatment (Figure 6). The only differences that could be found were during dark-to-light transitions in the first induction kinetics, in which HL cells developed an NPQ transient not observed in CTRL cells (Figure 6B). Interestingly the increase in zeaxanthin content does not result in any increase in steady-state NPQ. This suggests that the extra zeaxanthin in the HL cells may not be active in the overall stationary quenching response. This point was confirmed with the DTT measurements where it was shown that the effect of pre-accumulated zeaxanthin on NPQ response was restricted to the dark-light transition and totally disappeared at the end of the light treatment (Figure 6C). The stationary NPQ reached, instead, was mostly due to de novo zeaxanthin synthesis (Figure 6C). Furthermore

this same change in the initial development of NPQ in HL can be reproduced after treating the CTRL sample for 8 min in the PAM instrument, as shown in the second induction kinetics of CTRL cells (Figure 6A). Despite the different amount of zeaxanthin accumulated in the samples after the two different treatment, the effect on NPQ was the same. This suggests that only a small part of the zeaxanthin pool may be involved in NPQ response and that an accumulation of a large pool of zeaxanthin will not necessarily enhance thermal dissipation. The remaining part could act as direct scavenger of ROS as free pool in the lipid bilayer or bound to the antenna (Dall'Osto et al., 2010). This transient NPQ was previously described in diatoms (Grouneva et al., 2008) and vascular plant (Kalituho et al., 2007; Demmig-Adams et al., 1989). For example in the *Arabidopsis aba* mutant, which accumulates high amount of zeaxanthin because defective in zeaxanthin epoxidase activity, accelerated NPQ formation was described suggesting that the presence of zeaxanthin increases the sensitivity of NPQ to a given ΔpH (Hurry et al., 1997). Differently from what observed in the *aba* mutant, in which no difference in the photochemical capacity of PSII (qL) was observed with the wild type (Hurry et al., 1997), here zeaxanthin accumulation varies the initial development of NPQ affecting also the development of qL parameters (Figure 6D). Hence HL cells present higher fraction of open PSII reaction centers right after the onset of illumination. This is consistent with the hypothesis that higher energy dissipation leads to a decrease in the effective absorption cross section of PSII decreasing accordingly the electronic pressure on PSII. These results suggest that in *Nannochloropsis* cells, exposed to a short-term HL stress, zeaxanthin active in NPQ were neo-synthesized during illumination, while the molecules pre-accumulated manifest only an initial strong quenching effect. This transient NPQ seems to protect PSII from light-damage, as observe from the high qL parameters, and it is likely not related to the total amount of pre-accumulated zeaxanthin consistent with the hypothesis that only few zeaxanthin molecules can enhance NPQ depending on their binding site.

References

Adams, W.W., Demmig-Adams, B., and Winter, K. (1990). Relative contributions of zeaxanthin-related and zeaxanthin-unrelated types of "high-energy-state" quenching of chlorophyll fluorescence in spinach leaves exposed to various environmental conditions. Plant Physiol. **92**: 302–309.

Arnoux, P., Morosinotto, T., Saga, G., Bassi, R., and Pignol, D. (2009). A structural basis for the pH-dependent xanthophyll cycle in Arabidopsis thaliana. Plant Cell **21**: 2036–44.

Ballottari, M., Dall'Osto, L., Morosinotto, T., and Bassi, R. (2007). Contrasting behavior of higher plant photosystem I and II antenna systems during acclimation. J. Biol. Chem. **282**: 8947–8958.

Barber, J. and Andersson, B. (1992). Too much of a good thing: light can be bad for photosynthesis. Trends Biochem. Sci. **17**: 61–66.

Basso, S., Simionato, D., Gerotto, C., Segalla, A., Giacometti, G.M., and Morosinotto, T. (2014). Characterization of the photosynthetic apparatus of the Eustigmatophycean Nannochloropsis gaditana: evidence of convergent evolution in the supramolecular organization of photosystem I. Biochim. Biophys. Acta **1837**: 306–14.

Beer, A., Gundermann, K., Beckmann, J., and Büchel, C. (2006). Subunit composition and pigmentation of fucoxanthin-chlorophyll proteins in diatoms: evidence for a subunit involved in diadinoxanthin and diatoxanthin binding. Biochemistry **45**: 13046–53.

Betterle, N., Ballottari, M., Zorzan, S., de Bianchi, S., Cazzaniga, S., Dall'Osto, L., Morosinotto, T., and Bassi, R. (2009). Light-induced dissociation of an antenna hetero-oligomer is needed for non-photochemical quenching induction. J. Biol. Chem. **284**: 15255–15266.

Bilger, W. and Björkman, O. (1990). Role of the xanthophyll cycle in photoprotection elucidated by measurements of light-induced absorbance changes, fluorescence and photosynthesis in leaves of Hedera canariensis. Photosynth. Res. **25**: 173–85.

Cavalier-Smith, T. (2004). Only six kingdoms of life. Proc. Biol. Sci. **271**: 1251–62.

Coesel, S., Oborník, M., Varela, J., Falciatore, A., and Bowler, C. (2008). Evolutionary origins and functions of the carotenoid biosynthetic pathway in marine diatoms. PLoS One **3**: e2896.

Croce, R., Canino, G., Ros, F., and Bassi, R. (2002). Chromophore Organization in the Higher-Plant Photosystem II Antenna Protein CP26. Biochemistry **41**: 7334–7343.

Dall'Osto, L., Caffarri, S., and Bassi, R. (2005). A mechanism of nonphotochemical energy dissipation, independent from PsbS, revealed by a conformational change in the antenna protein CP26. Plant Cell **17**: 1217–32.

Dall'Osto, L., Cazzaniga, S., Havaux, M., and Bassi, R. (2010). Enhanced photoprotection by protein-bound vs free xanthophyll pools: a comparative analysis of chlorophyll b and xanthophyll biosynthesis mutants. Mol. Plant **3**: 576–93.

Dall'Osto, L., Holt, N.E., Kaligotla, S., Fuciman, M., Cazzaniga, S., Carbonera, D., Frank, H.A., Alric, J., and Bassi, R. (2012). Zeaxanthin protects plant photosynthesis by modulating chlorophyll triplet yield in specific light-harvesting antenna subunits. J. Biol. Chem. **287**: 41820–34.

Demmig-Adams, B., Adams III, W.W., Barker, D.H., Logan, B.A., Bowling, D.R., and Verhoeven, A.S. (2008). Using chlorophyll fluorescence to assess the fraction of absorbed light allocated to thermal dissipation of excess excitation. Physiol. Plant. **98**: 253–264.

Demmig-Adams, B., Winter, K., Kruger, A., and Czygan, F.-C. (1989). Zeaxanthin and the Induction and Relaxation Kinetics of the Dissipation of Excess Excitation Energy in Leaves in 2% O2, 0% CO2. PLANT Physiol. **90**: 887–893.

Färber, A. and Jahns, P. (1998). The xanthophyll cycle of higher plants: influence of antenna size and membrane organization. Biochim. Biophys. Acta - Bioenerg. **1363**: 47–58.

Frommolt, R., Goss, R., and Wilhelm, C. (2001). The de-epoxidase and epoxidase reactions of Mantoniella squamata (Prasinophyceae) exhibit different substrate-specific reaction kinetics compared to spinach. Planta **213**: 446–456.

Gilmore, A.M., Mohanty, N., and Yamamoto, H.Y. (1994). Epoxidation of zeaxanthin and antheraxanthin reverses non-photochemical quenching of photosystem II chlorophyll a fluorescence in the presence of trans-thylakoid ΔpH. FEBS Lett. **350**: 271–274.

Gilmore, A.M. and Yamamoto, H.Y. (1993). Linear models relating xanthophylls and lumen acidity to non-photochemical fluorescence quenching. Evidence that antheraxanthin explains zeaxanthin-independent quenching. Photosynth. Res. **35**: 67–78.

Gilmore, A.M. and Yamamoto, H.Y. (1991). Zeaxanthin Formation and Energy-Dependent Fluorescence Quenching in Pea Chloroplasts under Artificially Mediated Linear and Cyclic Electron Transport. PLANT Physiol. **96**: 635–643.

Goss, R., Ann Pinto, E., Wilhelm, C., and Richter, M. (2006a). The importance of a highly active and ΔpH-regulated diatoxanthin epoxidase for the regulation of the PS II antenna function in diadinoxanthin cycle containing algae. J. Plant Physiol. **163**: 1008–1021.

Goss, R. and Jakob, T. (2010). Regulation and function of xanthophyll cycle-dependent photoprotection in algae. Photosynth. Res. **106**: 103–122.

Goss, R. and Lepetit, B. (2015). Biodiversity of NPQ. J. Plant Physiol. **172C**: 13–32.

Goss, R., Lepetit, B., and Wilhelm, C. (2006b). Evidence for a rebinding of antheraxanthin to the light-harvesting complex during the epoxidation reaction of the violaxanthin cycle. J. Plant Physiol. **163**: 585–90.

Grouneva, I., Jakob, T., Wilhelm, C., and Goss, R. (2008). A new multicomponent NPQ mechanism in the diatom Cyclotella meneghiniana. Plant Cell Physiol. **49**: 1217–25.

Gruszecki, W.I., Sujak, A., Strzalka, K., Radunz, A., and Schmid, G.H. (1999). Organisation of xanthophyll-lipid membranes studied by means of specific pigment antisera, spectrophotometry and monomolecular layer technique lutein versus zeaxanthin. Zeitschrift fur Naturforsch. - Sect. C J. Biosci. **54**: 517–525.

Guglielmi, G., Lavaud, J., Rousseau, B., Etienne, A.-L., Houmard, J., and Ruban, A. V (2005). The light-harvesting antenna of the diatom Phaeodactylum tricornutum. Evidence for a diadinoxanthin-binding subcomplex. FEBS J. **272**: 4339–48.

Guillard, R.R.L. and Ryther, J.H. (1962). STUDIES OF MARINE PLANKTONIC DIATOMS: I. CYCLOTELLA NANA HUSTEDT, AND DETONULA CONFERVACEA (CLEVE) GRAN. Can. J. Microbiol. **8**: 229–239.

Hager, A. and Holocher, K. (1994). Localization of the xanthophyll-cycle enzyme violaxanthin de-epoxidase within the thylakoid lumen and abolition of its mobility by a (light-dependent) pH

decrease. Planta **192**: 581–589.

Hartel, H., Lokstein, H., Grimm, B., and Rank, B. (1996). Kinetic Studies on the Xanthophyll Cycle in Barley Leaves (Influence of Antenna Size and Relations to Nonphotochemical Chlorophyll Fluorescence Quenching). Plant Physiol. **110**: 471–482.

Havaux, M., Dall'osto, L., and Bassi, R. (2007). Zeaxanthin has enhanced antioxidant capacity with respect to all other xanthophylls in Arabidopsis leaves and functions independent of binding to PSII antennae. Plant Physiol. **145**: 1506–20.

Havaux, M. and Niyogi, K.K. (1999). The violaxanthin cycle protects plants from photooxidative damage by more than one mechanism. Proc. Natl. Acad. Sci. **96**: 8762–8767.

Holt, N.E., Zigmantas, D., Valkunas, L., Li, X.-P., Niyogi, K.K., and Fleming, G.R. (2005). Carotenoid cation formation and the regulation of photosynthetic light harvesting. Science **307**: 433–6.

Horton, P., Ruban, A. V., and Walters, R.G. (1996). REGULATION OF LIGHT HARVESTING IN GREEN PLANTS. Annu. Rev. Plant Physiol. Plant Mol. Biol. **47**: 655–684.

Hurry, V., Anderson, J.M., Chow, W.S., and Osmond, C.B. (1997). Accumulation of Zeaxanthin in Abscisic Acid-Deficient Mutants of Arabidopsis Does Not Affect Chlorophyll Fluorescence Quenching or Sensitivity to Photoinhibition in Vivo. Plant Physiol. **113**: 639–648.

Jahns, P., Latowski, D., and Strzalka, K. (2009). Mechanism and regulation of the violaxanthin cycle: the role of antenna proteins and membrane lipids. Biochim. Biophys. Acta **1787**: 3–14.

Jeffrey, S.W., Mantoura, R.F.C., and Wright, S.W. (1997). Phytoplankton pigments in oceanography: guidelines to modern methods. Monogr. Oceanogr. Methodol.

Kalituho, L., Beran, K.C., and Jahns, P. (2007). The Transiently Generated Nonphotochemical Quenching of Excitation Energy in Arabidopsis Leaves Is Modulated by Zeaxanthin. PLANT Physiol. **143**: 1861–1870.

Lavaud, J. and Lepetit, B. (2013). An explanation for the inter-species variability of the photoprotective non-photochemical chlorophyll fluorescence quenching in diatoms. Biochim. Biophys. Acta **1827**: 294–302.

Lavaud, J., Rousseau, B., and Etienne, A.-L. (2003). Enrichment of the light-harvesting complex in diadinoxanthin and implications for the nonphotochemical fluorescence quenching in diatoms. Biochemistry **42**: 5802–8.

Lavaud, J., Rousseau, B., and Etienne, A.-L. (2002). In diatoms, a transthylakoid proton gradient alone is not sufficient to induce a non-photochemical fluorescence quenching. FEBS Lett. **523**: 163–6.

Li, Z., Wakao, S., Fischer, B.B., and Niyogi, K.K. (2009). Sensing and responding to excess light. Annu. Rev. Plant Biol. **60**: 239–60.

Long, S.P., Humphries, S., and Falkowski, P.G. (1994). Photoinhibition of photosynthesis in nature. Annu. PHYSIOL.PLANT MOL.BIOL. **45**: 633–662.

MacIntyre, H.L., Kana, T.M., Anning, T., and Geider, R.J. (2002). PHOTOACCLIMATION OF PHOTOSYNTHESIS IRRADIANCE RESPONSE CURVES AND PHOTOSYNTHETIC PIGMENTS IN MICROALGAE AND CYANOBACTERIA1. J. Phycol. **38**: 17–38.

Matsubara, S., Krause, G.H., Seltmann, M., Virgo, A., Kursar, T.A., Jahns, P., and Winter, K. (2008). Lutein epoxide cycle, light harvesting and photoprotection in species of the tropical tree genus Inga. Plant. Cell Environ. **31**: 548–61.

Mellis, A. (1999). Photosystem-II damage and repair cycle in chloroplasts: What modulates the rate of photodamage in vivo? Trends Plant Sci. **4**: 130–135.

Mozzo, M., Dall'Osto, L., Hienerwadel, R., Bassi, R., and Croce, R. (2008). Photoprotection in the antenna complexes of photosystem II: role of individual xanthophylls in chlorophyll triplet quenching. J. Biol. Chem. **283**: 6184–92.

Müller, P., Li, X.P., and Niyogi, K.K. (2001). Non-photochemical quenching. A response to excess light energy. Plant Physiol. **125**: 1558–1566.

Nilkens, M., Kress, E., Lambrev, P., Miloslavina, Y., Müller, M., Holzwarth, A.R., and Jahns, P. (2010). Identification of a slowly inducible zeaxanthin-dependent component of non-photochemical quenching of chlorophyll fluorescence generated under steady-state conditions in Arabidopsis. Biochim. Biophys. Acta **1797**: 466–75.

Niyogi, K.K., Bjorkman, O., and Grossman, A.R. (1997). Chlamydomonas Xanthophyll Cycle Mutants Identified by Video Imaging of Chlorophyll Fluorescence Quenching. Plant Cell **9**: 1369–1380.

Niyogi, K.K., Grossman, A.R., and Björkman, O. (1998). Arabidopsis mutants define a central role for the xanthophyll cycle in the regulation of photosynthetic energy conversion. Plant Cell **10**: 1121–1134.

Owens, T.G., Gallagher, J.C., and Alberte, R.S. (2007). PHOTOSYNTHETIC LIGHT-HARVESTING FUNCTION OF VIOLAXANTHIN IN NANNOCHLOROPSIS SPP. (EUSTIGMATOPHYCEAE)1. J. Phycol. **23**: 79–85.

Pfundel, E.E., Renganathan, M., Gilmore, A.M., Yamamoto, H.Y., and Dilley, R.A. (1994). Intrathylakoid pH in Isolated Pea Chloroplasts as Probed by Violaxanthin Deepoxidation. Plant Physiol. **106**: 1647–1658.

Pinnola, A., Dall'Osto, L., Gerotto, C., Morosinotto, T., Bassi, R., and Alboresi, A. (2013). Zeaxanthin binds to light-harvesting complex stress-related protein to enhance nonphotochemical quenching in Physcomitrella patens. Plant Cell **25**: 3519–34.

Porra, R.J., Thompson, W.A., and Kriedemann, P.E. (1989). Determination of accurate extinction

coefficients and simultaneous equations for assaying chlorophylls a and b extracted with four different solvents: verification of the concentration of chlorophyll standards by atomic absorption spectroscopy. Biochim. Biophys. Acta - Bioenerg. **975**: 384–394.

Raven, J.A. (2011). The cost of photoinhibition. Physiol. Plant. **142**: 87–104.

Riisberg, I., Orr, R.J.S., Kluge, R., Shalchian-Tabrizi, K., Bowers, H.A., Patil, V., Edvardsen, B., and Jakobsen, K.S. (2009). Seven gene phylogeny of heterokonts. Protist **160**: 191–204.

Rockholm, D. (1996). Violaxanthin de-epoxidase. PLANT Physiol. **110**: 697–703.

Saga, G., Giorgetti, A., Fufezan, C., Giacometti, G.M., Bassi, R., and Morosinotto, T. (2010). Mutation analysis of violaxanthin de-epoxidase identifies substrate-binding sites and residues involved in catalysis. J. Biol. Chem. **285**: 23763–70.

Schagerl, M. and Müller, B. (2006). Acclimation of chlorophyll a and carotenoid levels to different irradiances in four freshwater cyanobacteria. J. Plant Physiol. **163**: 709–16.

Schaller, S., Latowski, D., Jemioła-Rzemińska, M., Wilhelm, C., Strzałka, K., and Goss, R. (2010). The main thylakoid membrane lipid monogalactosyldiacylglycerol (MGDG) promotes the de-epoxidation of violaxanthin associated with the light-harvesting complex of photosystem II (LHCII). Biochim. Biophys. Acta **1797**: 414–24.

Schaller, S., Wilhelm, C., Strzałka, K., and Goss, R. (2012). Investigating the interaction between the violaxanthin cycle enzyme zeaxanthin epoxidase and the thylakoid membrane. J. Photochem. Photobiol. B. **114**: 119–25.

Schubert, H., Andersson, M., and Snoeijs, P. (2006). Relationship between photosynthesis and non-photochemical quenching of chlorophyll fluorescence in two red algae with different carotenoid compositions. Mar. Biol. **149**: 1003–1013.

Sforza, E., Simionato, D., Giacometti, G.M., Bertucco, A., and Morosinotto, T. (2012). Adjusted light and dark cycles can optimize photosynthetic efficiency in algae growing in photobioreactors. PLoS One **7**: e38975.

Siefermann, D. and Yamamoto, H.Y. (1975). Properties of NADPH and oxygen-dependent zeaxanthin epoxidation in isolated chloroplasts. A transmembrane model for the violaxanthin cycle. Arch. Biochem. Biophys. **171**: 70–7.

Simionato, D., Basso, S., Zaffagnini, M., Lana, T., Marzotto, F., Trost, P., and Morosinotto, T. (2015). Protein redox regulation in the thylakoid lumen: the importance of disulfide bonds for violaxanthin de-epoxidase. FEBS Lett. **589**: 919–23.

Sokolove, P.M. and Marsho, T.V. (1976). Ascorbate-independent carotenoid de-epoxidation in intact spinach chloroplasts. Biochim. Biophys. Acta - Bioenerg. **430**: 321–326.

Stransky, H. and Hager, A. (1970). [The carotenoid pattern and the occurrence of the light-induced

xanthophyll cycle in various classes of algae. VI. Chemosystematic study]. Arch. für Mikrobiol. **73**: 315–23.

Tardy, F. and Havaux, M. (1997). Thylakoid membrane fluidity and thermostability during the operation of the xanthophyll cycle in higher-plant chloroplasts. Biochim. Biophys. Acta **1330**: 179–93.

Vass, I., Styring, S., Hundal, T., Koivuniemi, A., Aro, E., and Andersson, B. (1992). Reversible and irreversible intermediates during photoinhibition of photosystem II: stable reduced QA species promote chlorophyll triplet formation. Proc. Natl. Acad. Sci. **89**: 1408–1412.

SECTION C

CHAPTER C1

A MODEL OF CHLOROPHYLL FLUORESCENCE IN MICROALGAE INTEGRATING PHOTOPRODUCTION, PHOTOINHIBITION AND PHOTOREGULATION

Published in
Journal of Biotechnology

A MODEL OF CHLOROPHYLL FLUORESCENCE IN MICROALGAE INTEGRATING PHOTOPRODUCTION, PHOTOINHIBITION AND PHOTOREGULATION

Andreas Nikolaou[a,1], Andrea Bernardi[b,c,1], Andrea Meneghesso[d], Fabrizio Bezzo[b,c], Tomas Morosinotto[d], Benoit Chachuat[a,*]

[a]Centre for Process Systems Engineering, Department of Chemical Engineering, Imperial College London, UK
[b]CAPE-Lab: Computer-Aided Process Engineering Laboratory, Department of Industrial Engineering, University of Padova, Italy
[c]PAR-Lab: Padova Algae Research Laboratory, Department of Industrial Engineering, University of Padova, Italy
[d]PAR-Lab: Padova Algae Research Laboratory, Department of Biology, University of Padova, Italy

Article history: Received 6 August 2014. Received in revised form 26 November 2014. Accepted 1 December 2014. Available online 16 December 2014

Abstract

This paper presents a mathematical model capable of quantitative prediction of the state of the photo-synthetic apparatus of microalgae in terms of their open, closed and damaged reaction centers under variable light conditions. This model combines the processes of photoproduction and photoinhibition in the Han model with a novel mathematical representation of photoprotective mechanisms, including qE-quenching and qI-quenching. For calibration and validation purposes, the model can be used to simulate fluorescence fluxes, such as those measured in PAM fluorometry, as well as classical fluorescence indexes. A calibration is carried out for the microalga *Nannochloropsis gaditana*, whereby 9 out of the 13 model parameters are estimated with good statistical significance using the realized, minimal and maximal fluorescence fluxes measured from a typical PAM protocol. The model is further validated by considering a more challenging PAM protocol alternating periods of intense light and dark, showing a good ability to provide quantitative predictions of the fluorescence fluxes even though it was calibrated for a different and somewhat simpler PAM protocol. A promising application of the model is for the prediction of PI-response curves based on PAM fluorometry, together with the long-term prospect of combining it with hydrodynamic and light attenuation models for high-fidelity simulation and optimization of full-scale microalgae production systems.

Keywords:
Microalgae, Dynamic model, PAM fluorometry, Non-photochemical quenching, Nannochloropsis gaditana

1. MODELING THE FLUORESCENCE AS A TOOL TO PREDICT PHOTOSYNTHETIC EFFICIENCY

Mathematical modeling can be a great help for developing a better understanding, and in turn enabling a better prediction capability, of microalgae culture dynamics. Models that convey state-of-the-art scientific knowledge are invaluable tools for unveiling and untangling the underlying photosynthetic and metabolic mechanisms. These models can be used to guide the design of dedicated, information-rich experiments or to improve the design, operation and control of a microalgae culture system in order to enable and sustain a higher productivity or TAG content (Cornet et al., 1992).

Microalgae exhibit a remarkable biological complexity due to the interaction with light that span multiple time scales, ranging from milliseconds to days. Light is used to drive photosynthetic reactions (photoproduction) but when in excess can be deleterious for the organisms (phoinhibition). Therefore microalgae have evolved photoprotective mechanisms suitable for short- and long- term-responses to light variations (see Section A, paragraph 4). Among the available experimental tools to study the afore-mentioned processes, the use of chlorophyll-a fluorescence with PAM instrument has led to important discoveries over the past 40 years (Baker, 2008). Traditionally, a number of fluorescence indexes, such as the realized quantum yield of photosynthesis (ϕ_{PSII}) or the NPQ index, have been used for monitoring photosynthetic efficiency, by qualitatively relating these mechanisms to the measured fluorescence fluxes (Roháček). In contrast, little effort has been devoted to quantifying these relations in the form of mathematical models, which would enable accurate predictions of the quantum yield of photosynthesis and in particular of its dynamic response to variable light conditions.

This paper proposes a mathematical model for *N. gaditana* describing the key photosynthetic mechanisms triggered by variable light conditions and its validation using PAM fluorescence experiments. The dynamic fluorescence model proposed relies on the combination of fast photosynthetic mechanisms with slower photoprotective mechanisms.

2. A DYNAMIC MODEL OF FLUORESCENCE THAT ACCOUNTS FOR PHOTOREGULATION IN MICROALGAE

The building block of our model is the well-accepted Han model that represents the effects of photoproduction and photoinhibition on the fluorescence flux (Han, 2002). The description of photoproduction and photoinhibition in the Han model assumes that the RCII (PSII reaction center) of a photosynthetic unit can be in either one of three states: open (A), ready to accept an electron; closed (B), already occupied by electrons; damaged (C), non-functional. As depicted in Figure 1, each RCII can transit from one state to another depending on the light irradiance I. Photoproduction is described by the transition from A to B. Photoinhibition, on the other hand, corresponds to the transition from B to C, while the reverse transition from C to B describes repair of the damaged RCII by enzymatic processes.

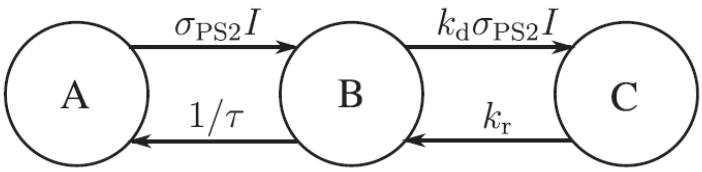

Figure 1. Schematic representation of the Han model.

An important limitation of the Han model in the context of PAM fluorometry is that it does not consider photoregulation mechanisms that may vary some of its parameters on the timescale of minutes. Starting from this, we develop an extension of this model in order to encompass two types of photoregulation, namely qE-quenching and qI-quenching (see Section A, paragraph 4.1). The former, related to heat dissipation, evolves within seconds resulting in up to 90% reduction in fluorescence (Li et al., 2009), whereas the latter, related to photoinhibition, evolves in a time scale of minutes to hours resulting in up to 40% reduction in fluorescence (Falkowski, 1993).

The light protocol and fluorescence measurements used for purpose of model calibration are shown in Figure 2A (gray-shaded area and points with error bars, respectively). The first part of the experiment performed in *N. gaditana* shows a gradual increase of the actinic light intensity in stages of 1 min (Simionato et al., 2011). At the end of the treatment light is switched off for 3 min to follow the fluorescence recovery in dark. The fluorescence fluxes used to calculate fluorescence parameters are the following: F' (light-adapted, steady-state fluorescence), F'_m (light-adapted, maximum fluorescence) and F'_0 (light-adapted, minimum fluorescence). The fits of these fluxes predicted by the model against the fluxes recorded by a PAM fluorometer are shown in Figure 2A. Note that the predicted fluorescence fluxes are in excellent agreement with the measured fluxes.

Besides predicting the fluorescence fluxes well, the ability of the model to predict the fluorescence indexes q_L, ϕ_{PSII} and q_{NPQ} is depicted in Figure 2B-C. The index ϕ_{PSII} and q_L is predicted quite accurately by the model throughout the entire time horizon. Finally, the accurate predictions of q_{NPQ} in Figure 2C provide another confirmation that the NPQ regulation is captured adequately by the selected model structure.

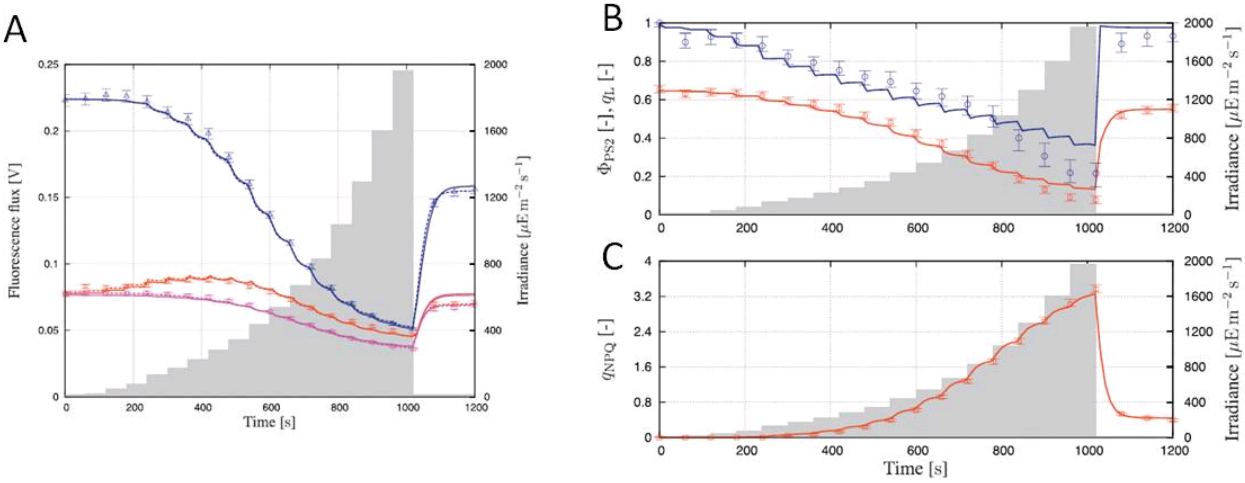

Figure 2. Comparison between the predicted and measured fluorescence fluxes F'_m (blue lines, triangles), F'_0 (purple lines, circles) and F' (red lines, square) in response to various actinic light levels I (gray-shaded area) for the calibration experiment. B-C) comparison between the predicted and measured fluorescence

indexes ϕ_{PSII} (red lines, square), q_L (blue lines, circles) (B) and q_{NPQ} (C) at various actinic light levels I (grey-shaded area).

The foregoing results suggest that the proposed fluorescence model for *N. gaditana* is capable of quantitative predictions of the state of the photosynthetic apparatus under varying light conditions. To confirm it, we carry out a validation experiment for an (unusually) challenging PAM experiment, as shown in gray-shaded area in Figure 3. The corresponding model predictions are compared to the actual flux measurements (Figure 3). Although calibrated for a quite different and somewhat simpler PAM protocol, the calibrated model remains capable of reliable quantitative predictions of the fluorescence fluxes. Deviations are observed in various parts of the response flux profiles, which are possibly due to effects and processes not accounted for in the proposed model, yet these deviation remain small, within 10-20%.

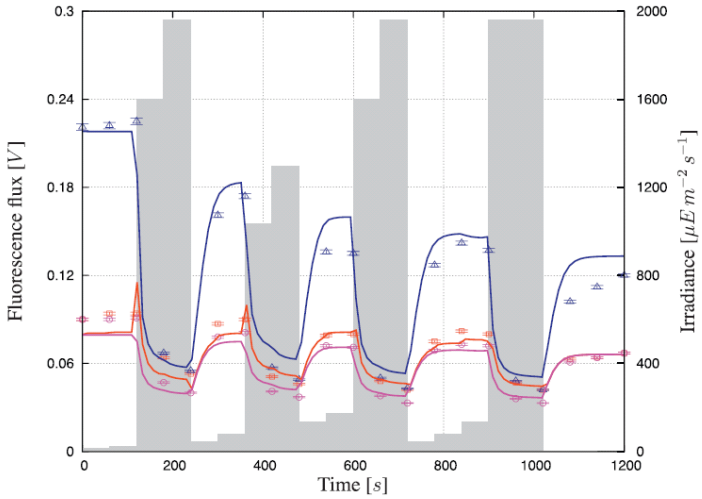

Figure 3. Comparison between the predicted and measured fluorescence fluxes F'_m (blue lines, triangles), F'_0 (purple lines, circles) and F'(red lines, square) in response to various actinic light levels I (gray-shaded area) for the validation experiment.

A careful calibration and sub-sequent validation against multiple experimental data sets shows that the model is capable of quantitative predictions of the state of the photosynthetic apparatus in terms of its open, closed and damaged reaction center. This makes it the first model of its kind capable of reliable predictions of the levels of photoinhibition and NPQ activity, while retaining a low complexity and a small dimensionality.

References

Baker, N.R. (2008). Chlorophyll fluorescence: a probe of photosynthesis in vivo. Annu. Rev. Plant Biol. **59**: 89–113.

Cornet, J.F., Dussap, C.G., Cluzel, P., and Dubertret, G. (1992). A structured model for simulation of cultures of the cyanobacterium Spirulina platensis in photobioreactors: II. Identification of

kinetic parameters under light and mineral limitations. Biotechnol. Bioeng. **40**: 826–34.

Falkowski, P.G.. G.R.. K.Z. (1993). Light utilization and photoinhibition of photosynthesis in marine phytoplankton.

Han, B.-P. (2002). A mechanistic model of algal photoinhibition induced by photodamage to photosystem-II. J. Theor. Biol. **214**: 519–27.

Li, Z., Wakao, S., Fischer, B.B., and Niyogi, K.K. (2009). Sensing and responding to excess light. Annu. Rev. Plant Biol. **60**: 239–60.

Roháček, K. Chlorophyll Fluorescence Parameters: The Definitions, Photosynthetic Meaning, and Mutual Relationships. Photosynthetica **40**: 13–29.

Simionato, D., Sforza, E., Corteggiani Carpinelli, E., Bertucco, A., Giacometti, G.M., and Morosinotto, T. (2011). Acclimation of Nannochloropsis gaditana to different illumination regimes: effects on lipids accumulation. Bioresour. Technol. **102**: 6026–32.

CHAPTER C2

HIGH-FIDELITY MODELING METHODOLOGY OF LIGHT-LIMITED PHOTOSYNTHETIC PRODUCTION IN MICROALGAE

Submitted in
PLoS ONE

HIGH-FIDELITY MODELING METHODOLOGY OF LIGHT-LIMITED PHOTOSYNTHETIC PRODUCTION IN MICROALGAE

Andrea Bernardi[1], Andreas Nikolaou[2], Andrea Meneghesso[3], Tomas Morosinotto[3], Benoit Chachuat[2], Fabrizio Bezzo[1,*]

1 CAPE-Lab (Computer-Aided Process Engineering Laboratory) and PAR-Lab (Padova Algae Research Laboratory), Department of Industrial Engineering, University of Padova, Italy
2 Centre for Process Systems Engineering, Department of Chemical Engineering, Imperial College London, UK
3 PAR-Lab (Padova Algae Research Laboratory), Department of Biology, University of Padova, Italy

Abstract

Reliable quantitative description of light-limited growth in microalgae is key to improving the design and operation of industrial production systems. This article shows how the capability to predict photosynthetic processes can benefit from a synergy between mathematical modeling and lab-scale experiments using systematic design of experiment techniques. A model of chlorophyll fluorescence developed by the authors (Nikolaou et al., 2015) is used as starting point, whereby the representation of non-photochemical-quenching (NPQ) process is refined for biological consistency. This model spans multiple time scales ranging from milliseconds to hours, thus calling for a combination of various experimental techniques in order to arrive at a sufficiently rich data set and determine statistically meaningful estimates for the model parameters. The methodology is demonstrated for the microalga *Nannochloropsis gaditana* by combining pulse amplitude modulation (PAM) fluorescence, photosynthesis rate and antenna size measurements. The results show that the calibrated model is capable of accurate quantitative predictions under a wide range of transient light conditions. Moreover, this work provides an experimental validation of the link between fluorescence and photosynthesis-irradiance (PI) curves which had been theorized.

1. A MATHEMATICAL MODEL FOR *N. GADITANA* TO DESCRIBE COMPLEX PHOTOSYNTHETIC MECHANISMS

The gap between maximal theoretical biomass productivity (or even lab-scale realized productivity) and the actual biomass productivity in large scale production systems is still a big issue for microalgal exploitation. To meet this objective, models capable of reliable and quantitative prediction of all key phenomena affecting microalgae growth, particularly photosynthetic efficiency, can be a great help to improve our understanding as well as optimize process design and operation (Bernard et al., 2016; Simionato et al., 2013a).

Chlorophyll-a fluorescence is a widely used experimental tool that allows to study photosynthetic processes in a non-invasive and fast way (Baker, 2008). Recently, Nikolaou et al. (Nikolaou et al., 2015) have proposed a semi-mechanistic model for *N. gaditana* capable of quantitative prediction of the flux of fluorescence by taking into account three distinct processes acting on different time scales: photoproduction, photoinhibition and photoregulation (see Section A, paragraph 4). It was established through this work that the dynamics of chlorophyll-a fluorescence can help provide good predictions of the photosynthetic response under variable light conditions, thus allowing for the mathematical modeling of key photosynthetic mechanisms. However, it has recently been found that this fluorescence model may not describe photoregulation adequately over long-term experiments, thus advocating for a more detailed and biologically consistent representation.
In the model by Nikolaou et al. (Nikolaou et al., 2015) the complex NPQ processes were lumped into a single first order process. This approximation of the actual biological mechanism may lead to poor prediction of the fluorescence fluxes, for instance in experiments where the actinic light is kept constant for several minutes. This is illustrated in Figure 1, where the model predictions significantly deviate from the data generated by an experiment with a constant actinic light applied for 600 s, followed by a recovery period of 3600 s.

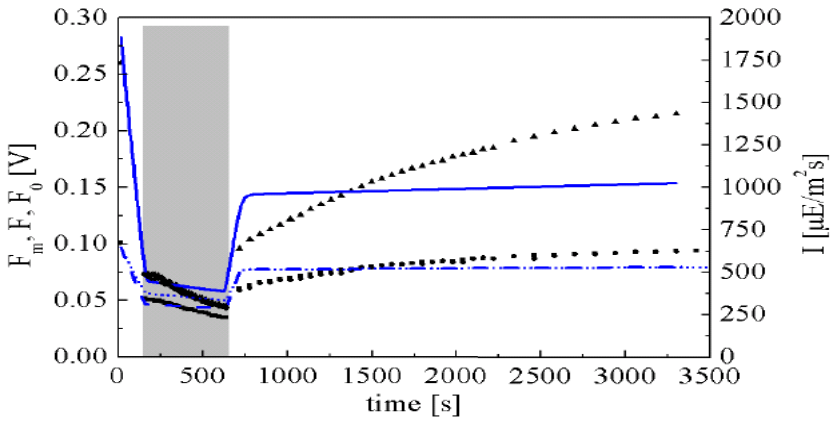

Figure 1. Constant actinic light PAM experiment. Comparison between the predicted (blue lines) and measured fluorescence fluxes F'_m (triangles), F'_0(squares) and F' (circles) in response to a constant light experiment. The grey-shaded area represents the light intensity.

Experimental evidence (Pinnola et al., 2013; Müller et al., 2001) suggests that photoregulation mechanisms involves at least two interdependent processes, which calls for a more complex NPQ representation in this model. The first one is a fast process involving the LHCSR protein, with a time constant of seconds for both its activation and relaxation (Peers et al., 2009). The second one is related to the xanthophyll cycle and acts on a time scale of minutes. More specifically, zeaxanthin can have a complex effect on the NPQ activity as it both enhances the quenching effect of LHCSR and acts as an additional quencher (Pinnola et al., 2013).
In this work we develop the model for *N. gaditana* from (Nikolaou et al., 2015) in order to encompass the combined effect of LHCSR protein and zeaxanthin on the NPQ dynamics. The proposed model, in addition to the PAM fluorescence experiments, incorporates also antenna size and photosynthetic rate measurements in order to provide a more detailed and biologically

consistent representation of the photosynthetic mechanisms. In the microalga *N. gaditana* antenna size measurements, used to study the saturation dynamics of PSII, are performed assessing fluorescence induction kinetics measured with a Joliot-type spectrophotometer (Simionato et al., 2013b; Perin et al., 2015). Photosynthetic rate derives from measurements of the maximal rate of photosynthetic oxygen evolution at a specific actinic light using a Clark electrode. The oxygen evolution measurements are performed at different actinic light to point out the correlation between Photosynthesis rate and Irradiance (PI curve) (Perin et al., 2015).

2. MODEL VALIDATION

Three additional PAM experiments are considered in order to validate the model for the microalga *N. gaditana*. The validation set includes one constant light experiment (Figure 2A) and two different variable light experiments (Figure 2B-C) where the sample is subject to complex actinic light profiles. The predicted fluorescence fluxes along with the experimental data are shown in Figure 2. The model predicts all three validation experiments in a very satisfactory way and is capable of capturing the variations in photosynthetic response triggered by different light dynamics. In particular, it is important to note that the model predictions remain accurate even for PAM protocols very different from the ones used in the calibration set, that is when the model is used for extrapolation.

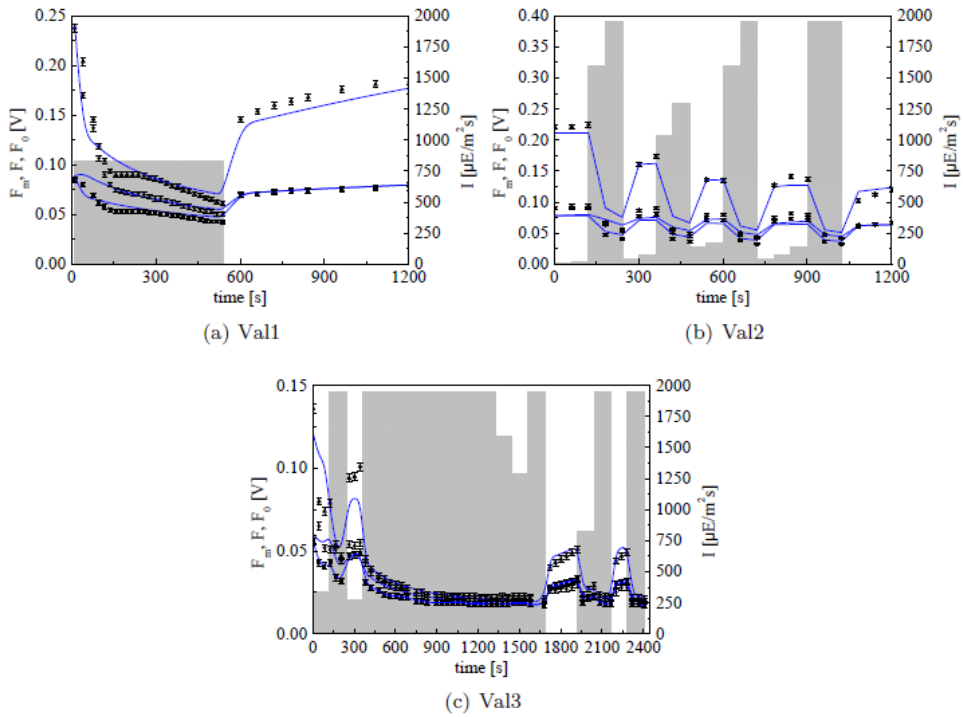

Figure 2. Model validation results. PAM fluorescence profiles along with the model predictions (blue solid lines) corresponding to three validation experiments. a) constant light experiment. b-c) variable light experiments. The grey-shaded area represents the light intensity.

Moreover, two additional PI experiments are used for validation purposes. The measured values are compared with the PI curve simulated by the model, as shown in Figure 3. The model gives accurate prediction of photosynthesis rate measurements. This confirms that the model provides an effective tool to predict PI curves without the use of classical measuring techniques that take time and resources to implement.

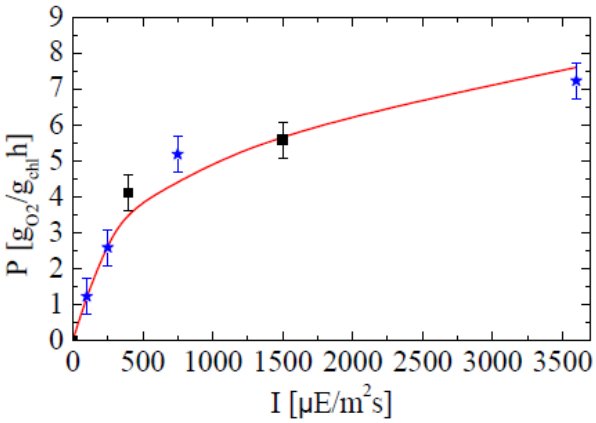

Figure 3. Model validation results. Experimental PI measurements along with model prediction. The solid red line represents the model predicted PI curve; the black squares and the blue stars represent two PSI experiments used for model validation.

The results show that the model is able to represent chlorophyll fluorescence and photosynthesis rate with a good accuracy under a large variety of light conditions for *N. Gaditana*, thus paving the way towards a more reliable and realistic description of the effects of light dynamics on microalgae growth. Furthermore, the connection between PI curves and fluorescence has been verified practically, which could prove beneficial for reducing the experimental effort relative to PI curves experiments.

References

Baker, N.R. (2008). Chlorophyll fluorescence: a probe of photosynthesis in vivo. Annu. Rev. Plant Biol. **59**: 89–113.

Bernard, O., Mairet, F., and Chachuat, B. (2016). Modelling of Microalgae Culture Systems with Applications to Control and Optimization. Adv. Biochem. Eng. Biotechnol. **153**: 59–87.

Müller, P., Li, X.P., and Niyogi, K.K. (2001). Non-photochemical quenching. A response to excess light energy. Plant Physiol. **125**: 1558–1566.

Nikolaou, A., Bernardi, A., Meneghesso, A., Bezzo, F., Morosinotto, T., and Chachuat, B. (2015). A

model of chlorophyll fluorescence in microalgae integrating photoproduction, photoinhibition and photoregulation. J. Biotechnol. **194**: 91–9.

Peers, G., Truong, T.B., Ostendorf, E., Busch, A., Elrad, D., Grossman, A.R., Hippler, M., and Niyogi, K.K. (2009). An ancient light-harvesting protein is critical for the regulation of algal photosynthesis. Nature **462**: 518–21.

Perin, G., Bellan, A., Segalla, A., Meneghesso, A., Alboresi, A., and Morosinotto, T. (2015). Generation of random mutants to improve light-use efficiency of Nannochloropsis gaditana cultures for biofuel production. Biotechnol. Biofuels **8**: 161.

Pinnola, A., Dall'Osto, L., Gerotto, C., Morosinotto, T., Bassi, R., and Alboresi, A. (2013). Zeaxanthin binds to light-harvesting complex stress-related protein to enhance nonphotochemical quenching in Physcomitrella patens. Plant Cell **25**: 3519–34.

Simionato, D., Basso, S., Giacometti, G.M., and Morosinotto, T. (2013a). Optimization of light use efficiency for biofuel production in algae. Biophys. Chem. **182**: 71–8.

Simionato, D., Block, M.A., La Rocca, N., Jouhet, J., Maréchal, E., Finazzi, G., and Morosinotto, T. (2013b). The response of Nannochloropsis gaditana to nitrogen starvation includes de novo biosynthesis of triacylglycerols, a decrease of chloroplast galactolipids, and reorganization of the photosynthetic apparatus. Eukaryot. Cell **12**: 665–76.

CHAPTER C3

PERSPECTIVES ON IMPROVING LIGHT USE EFFICIENCY IN MICROALGAE CULTURES USING COMPUTATIONAL MODELS

PERSPECTIVES ON IMPROVING LIGHT USE EFFICIENCY IN MICROALGAE CULTURES USING COMPUTATIONAL MODELS

Andrea Meneghesso [a], Andrea Bernardi [b], Andreas Nikolaou [c], Giorgio Perin [a], Benoît Chachuat [c], Fabrizio Bezzo [b] and Tomas Morosinotto [a,*]

[a] PAR-Lab: Padova Algae Research Laboratory, Department of Biology, University of Padova, Italy
[b]CAPE-Lab: Computer-Aided Process Engineering Laboratory and PAR-Lab: Padova Algae Research Laboratory, Department of Industrial Engineering, University of Padova, Italy
[c]Centre for Process Systems Engineering, Department of Chemical Engineering, Imperial College London, UK

Abstract

The need for finding economically competitive and renewable energy sources as a substitute to fossil fuels is becoming ever more pressing. Unicellular algae are a promising feedstock for the production of biodiesel on account of their ability to accumulate large amounts of lipids. Nonetheless, much research is still needed in order for algal-derived biofuel to become a reality, starting with making large-scale microalgae cultivation both economically and energetically sustainable. Sunlight provides the energy to support microalgae growth and this energy must therefore be exploited with the highest possible efficiency for optimizing productivity. Algae efficiency in converting solar radiation, however, depends on many environmental factors, including light intensity, temperature, and nutrient availability. Photobioreactor's design and operation too can play a major role as the culture's concentration, depth and mixing can all affect light use efficiency, and therefore productivity. Optimizing microalgae productivity in such a complex environment hinges on our ability to describe, in a quantitative manner, the effect of these various parameters as well as their mutual interactions. This paper argues for the development and widespread application of computational models that are capable of quantitative predictions. Such models prove especially useful in identifying which parameters have the largest impact on productivity, thereby providing a means for enhancing growth through design and operational changes. They can also provide guidance for genetic engineering by identifying those modifications having the largest potential impact on productivity.

This paper has been submitted

1. LIGHT USE EFFICIENCY: A KEY PARAMETER FOR ALGAE-BASED BIOTECHNOLOGICAL APPLICATIONS

Photosynthetic organisms have the ability to convert light energy and CO_2 into high energy molecules such as carbohydrates and lipids, which in turn can be converted into biofuels. The development of fuels from a biological source is particularly promising to displace, or at least to complement, liquid fuels of fossil origin, for instance in the transportation sector where renewable electric power is not (yet) widely applicable (Chisti, 2007). Among the possible photosynthetic organisms, microalgae are particularly interesting for these applications because of their fast growth rates and their ability to accumulate large amounts of lipids, especially under stress conditions (Mutanda et al., 2011). They are considered a viable alternative to crops because of their higher biomass productivity, reduced footprint and water demand, and the absence of competition with food or feed production. Microalgae culture systems may also be coupled with wastewater treatment or used for the production of high added value molecules such as omega-3 fatty acids or pigments (Pulz and Gross, 2004; Del Campo et al., 2007; Guedes et al., 2011; Lubián et al., 2000), with many other biotechnological applications, beyond biofuels production, likely to be identified in the future.

Despite a recognized potential, sustainable production of algal-derived biofuels is still not a reality at the industrial scale, for both economic and energetic reasons. Critical issues that need to be addressed include the development of efficient biomass harvesting and product extraction technologies as well as engineering approaches to intensify microalgae culture (Chisti and Yan, 2011; Amaro et al., 2011; Malcata, 2011). The maximal biomass productivities in the field not only remain far below theoretical estimations, but are also significantly lower than productivities achieved on lab-scale experiments, in particular regarding solar-to-biomass conversion (Melis, 2009). Since the energy to support microalgae growth in large-scale cultivation systems is provided by direct sunlight, the solar-to-biomass conversion efficiency has a key influence on productivity (Simionato et al., 2013). It should be clear in this context that maximizing the solar-to-biomass conversion efficiency is paramount to developing sustainable industrial microalgae production systems, also justifying why this issue receives a high priority in many public or private research efforts for the development of algae-based biotechnological applications.

The effect of light on microalgae culture systems is intricate. Besides providing the energy needed to drive CO_2 fixation, when the incoming irradiance exceeds cell's capacity to perform photochemistry light can be responsible for the production of reactive oxygen species and lead to a loss of photosynthetic production, a phenomenon known as photoinhibition. The main target of photoinhibition is Photosystem II (PSII) and more specifically the D1 protein that disrupts the electron transport chain when damaged (Vass, 2012). The continuous repair of damaged D1 proteins allows microalgae to cope with very high light irradiance. While this is an effective mechanism to ensure algae survival, yet this strategy requires continuous protein synthesis, which incurs a significant energetic penalty and requires large amounts of nutrients (MARSHALL et al., 2000; Loebl et al., 2010).

PSII protein repair is not the only mechanism influencing light use efficiency. Microalgae have evolved by developing a complex system of regulatory mechanisms to protect their

photosynthetic apparatus via dissipating excess energy as heat. This thermal dissipation, called non-photochemical quenching (NPQ), is triggered by fluctuations in light and can be activated on a timescale of seconds or minutes. It provides microalgae with an effective protection against photo-oxidative damage, even in the case of drastic variations in light irradiance (Peers et al., 2009). NPQ is activated when light absorption exceeds the light utilization capacity, a situation that leads to the accumulation of protons in the thylakoids lumen. The proteins in the antenna proteins, also called light harvesting complexes (LHC), undergo a conformational change in response to lumenal pH variations, which can result in up to 80% of the total absorbed energy being diverted as heat (Barber and Andersson, 1992). Even though it is crucial for microalgae to protect themselves from high light irradiance in their natural environment, such a massive energy loss drastically hampers biomass productivity in a photobioreactor and this constitutes a major drawback in biofuel applications, where all energy losses should be minimized.

Another key regulatory mechanism in microalgae is photoacclimation, which relates to a cell's ability to adjust its pigment/protein content and composition to the growth conditions. This slow regulatory mechanism, which act on a timescale of days to weeks, is aimed at optimizing the light-harvesting efficiency on account of physiological needs. When exposed to high light irradiance, for instance, microalgae will reduce their light harvesting efficiency via decreasing the chlorophyll content per cell (Simionato et al., 2011; Bonente et al., 2012). They will also increase their photosynthetic capacity via enhancing the capacity for oxygen evolution, electron transport and CO_2 fixation (Walters, 2005). In addition, long-term and short-term light responses turn out to be inter-dependent and act synergistically. In the process of acclimating to a higher light irradiance, for instance, a cell may increase its capacity to dissipate energy as heat on the short term as well (Gerotto et al., 2011). In a dynamic environment, microalgae must therefore balance out the needs of efficient light harvesting between sustained growth and sufficient protection against light-induced damage. While different microalgae have achieved this balance through a gradual adaptation over eons, their efficiency is not as high when cultivated in environments other than their natural habitats, including industrial ponds and photobioreactors.

2. MODELLING PHOTOSYNTHETIC EFFICIENCY FOR OPTIMIZATION OF ALGAE CULTIVATION

Finding the best compromise between light harvesting efficiency and photo-protection in microalgae cultivation systems calls for a deep understanding of the effect of key parameters on productivity. These effects can be very complex, as illustrated in Figure 1A showing the effect of light irradiance on microalgae growth for *Nannochloropsis*. When the irradiance is below 150 $\mu mol\ m^{-2}\ s^{-1}$, the available energy is the limiting growth factor, and so increasing the irradiance level will enhance growth. Under these conditions the growth rate is thus determined by the incoming irradiance (Sforza et al., 2012b). Above 150 $\mu mol\ m^{-2}\ s^{-1}$ cells photochemical ability is saturated and the effects of photoinhibition on growth come forward together with the activation of NPQ mechanisms reducing growth rate and therefore light use efficiency. The picture becomes even more intricate in considering the lipid content on top of biomass productivity. As shown in Figure 1A, higher light irradiance inhibits biomass growth but stimulates lipids accumulation

(Sforza et al., 2012b). A similar trade-off between biomass growth and lipid productivity could also be observed under other stress conditions such as a nutrient stress (Simionato et al., 2013).
A further complexity comes from the observation that light is not the only parameter influencing microalgae productivity. CO_2 and nutrient availability, for instance, can have a large influence too, as shown in Figure 1B. Here, *Nannochloropsis* cultures exhibit a faster growth rate when supplied with excess CO_2, but the final (steady) biomass concentration remains identical. When additional nitrogen is added to the culture medium, still in the presence of excess CO_2, a much higher steady biomass concentration is obtained, in addition to experiencing faster growth rates.

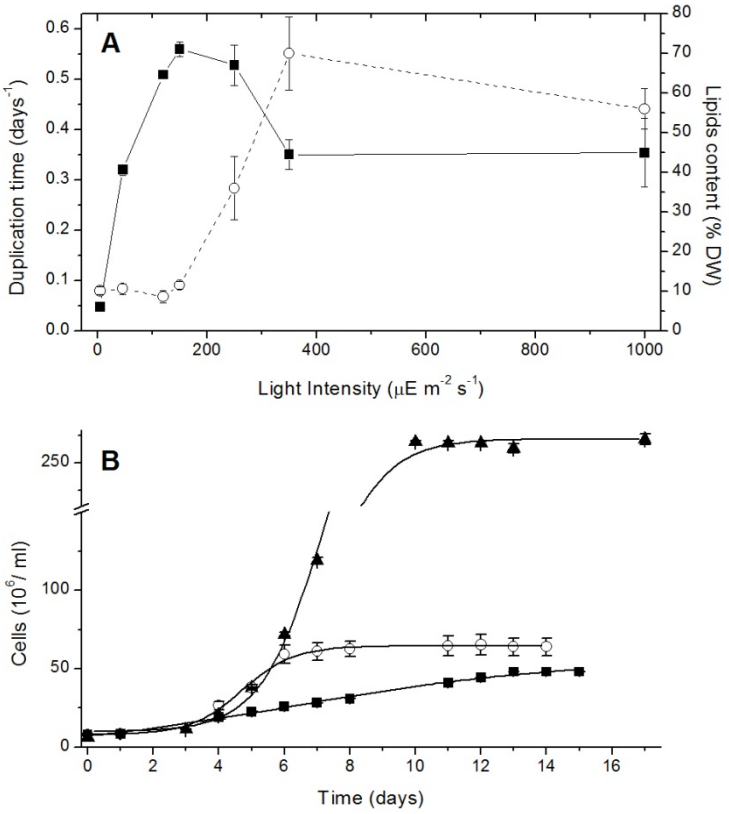

Figure 1. Effect of culture parameters influence on algal biomass and lipids productivity. A) Dependence on growth rate (black squares) and lipids productivity (white circles) from light intensity in *Nannochloropsis salina* cultures. All cultures were in CO_2 excess conditions. Data from (Sforza et al., 2012b). B) Influence of CO_2 and nutrients availability on *Nannochloropsis salina* growth. Growth in f/2 medium in flasks (black squares) is compared with cultures with 5 % CO_2 (white circles) and 5 % CO_2 and medium supplied with 1.5 g/l $NaNO_3$. Data from (Sforza et al., 2012a).

The examples reported in Figure 1 clearly show that microalgae productivity depends on multiple parameters simultaneously. Therefore, optimization of algae productivity calls for a global analysis of all the relevant parameters, as this allows accounting for inter-dependencies and synergies. Even though an increasing amount of information is available in the literature, the effect of multiple parameters is usually analyzed by varying the parameters one-by-one or in simple combinations. Instead, advanced computational tools are highly desirable in order to conduct the analysis. This in turn calls for the development of mathematical models capable of quantitative prediction of the main biological processes at the cells level, including response to light at

different time scales, temperature variations, nutrient availability, and any other relevant parameters.

Computational models are used routinely in chemical engineering for process optimization (Biegler et al., 2014), but their application to microalgae culture systems is made particularly arduous by the large number of governing phenomena, acting on multiple time scales from milliseconds to days: photoproduction, namely the collection of all processes from photons utilization to CO_2 fixation, occurs in a fraction of a second (Williams and Laurens, 2010); NPQ acts on time scales of seconds or minutes (Eberhard et al., 2008); Photoinhibition, on time scales of minutes to hours (Long et al., 1994); Photoacclimation, on time scales of hours to days (MacIntyre et al., 2002); finally, the mechanisms involved in nutrient internalization and their metabolism into useful products occur within hours to days as well (RAVEN and FALKOWSKI, 1999). In addition to these biological effects, microalgae productivity in large-scale culture systems is governed by physical parameters including light attenuation, mixing, temperature, and nutrient mass transfer.

The so-called state models are a particularly useful class of models to describe the effect of light on microalgae growth in engineering applications. These models are based on the concept of photosynthetic unit (PSU), which is comprised of the antenna and the reaction center, together with the associated apparatus that is activated by a given amount of light energy to produce a certain amount of photoproduct. The name 'state models' was coined to reflect that PSUs can be in different states of excitation, and many such models have been proposed over the years, including (but not limited to): (EILERS and PEETERS, 1988; Han, 2001; Pahlow, 2005; Rubio et al., 2003; Baklouti et al., 2006; Papadakis et al., 2012; García-Camacho et al., 2012; Bernardi et al., 2014; Zonneveld, 1998; Wu and Merchuk, 2001). State models can be extended to account for other processes as well. For instance, (Duarte, 1995) describe the effect of temperature on growth by expressing some of the parameters of a state model in the form of Arrhenius-like terms, (Norberg, 2004) and (Bernard and Rémond, 2012) propose other semi-empirical models of the temperature dependence on growth. Recently, multiphysics models have started to appear that integrate these state models within CFD simulation in order to represent the effects of light attenuation and mass-transfer limitation (Nauha and Alopaeus, 2013; Hartmann et al., 2014).

Despite these modeling advances, formulating an overall model that would be capable of accurate prediction of the effect of all major design and operational parameters on microalgae growth remains an ambitious and long-term goal. Intermediate steps towards this objective can nevertheless provide valuable information, e.g. by improving our understanding of the process or by identifying the main bottlenecks for microalgae productivity. Because these models are based on biological assumptions, one may not be able to use them to unravel key biological mechanisms, but they can nonetheless help to quantify certain mechanisms and their influence on productivity. Moreover, the comparison of model predictions with experimental data can help to test various biological hypotheses and decide which ones should be discarded or further refined.

One example illustrating the information that can be gathered from state models is shown in Figure 2, in the case of the microalga *Nannochloropsis*. Under non-limiting nutrient conditions and CO_2 supply and in a situation of minimal cell-shading (Sforza et al., 2012b), the growth model developed by (Bernardi et al., 2014) is capable of accurate prediction of the growth rate at different light intensities (Figure 2A), after calibration. Among the possible uses of this model, one

can estimate the rate of photosynthesis as a function of the light irradiance (Figure 2B), showing a linear increase of the photosynthesis rate at low irradiance before plateauing, as per the expected biological behavior (Gentile and Blanch, 2001). A more informative use of the model involves estimating the energy needed for cell maintenance at different light intensities (Figure 2C), predicting an increase in maintenance energy requirements at higher irradiance, likely caused by a larger repair rate in damaged photosystems. The latter becomes clear in plotting the ratio between the photosynthesis and maintenance rates (Figure 2D). Even though the model by (Bernardi et al., 2014) may not be generally applicable to any microalgae culture since it fails to account for key mechanisms such as nutrients limitation, it nevertheless provides a means for quantifying the weight carried by photoinhibition, clearly suggesting that this mechanism is likely to have a major impact on microalgae productivity at high light irradiance.

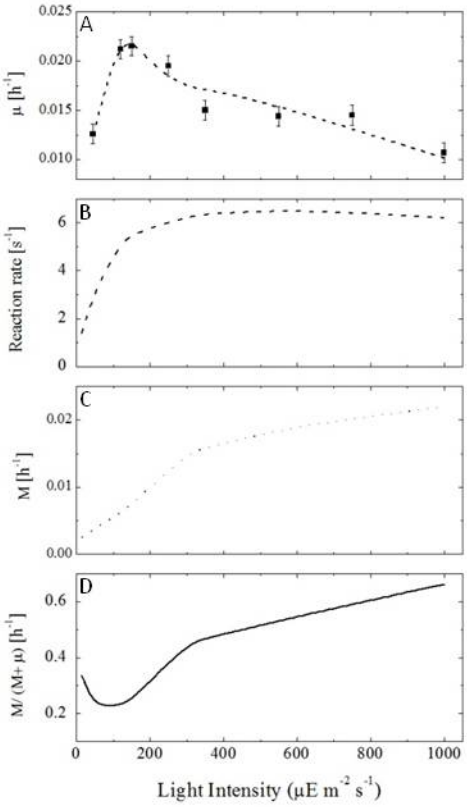

Figure 2. Computational evaluation of photosynthesis and maintenance dependence from light intensity. A) Shows the dependence of *Nannochloropsis salina* net growth rate constant predicted by the model from (Bernardi et al., 2014), a modified version of the model from Camacho-Rubio, (solid line) and experimental values (black squares). B) Reaction rate between closed and open PSU, which represent the photosynthetic electron transport efficiency (dashed line). C) Dependence of the maintenance factor (expressed in h^{-1}) from light intensity. D) Ratio between the maintenance and the gross growth rate (sum of net growth rate with maintenance) dependence from light intensity.

3. MODELS FOR QUANTITATIVE DESCRIPTION OF BIOLOGICAL PHENOMENA

3.1 Predicting Photoinhibition

An important challenge towards the development of a comprehensive model of microalgae growth for quantitative predictions of the biological phenomena lies in the fact that many

biological investigations rely on semi-quantitative or indirect measurements. In the case of the photoinhibition process discussed above, for instance, the use of fluorescence as proxy for evaluating photosystems efficiency is well established in the literature and the Fv/Fm ratio is commonly employed for the evaluation of PSII quantum yield (Maxwell and Johnson, 2000). When cells are exposed to intense light, Fv/Fm decreases as a result of PSII inhibition (Figure 3), and when the cells are moved back to dim light, damaged PSII are repaired and PSII quantum yield returns to its normal level within a few hours. Such a proxy has been extremely helpful in biological investigations of the photoinhibition process, making it possible to isolate the proteins responsible for PSII repair by identifying mutants from their delayed recovery in Fv/Fm after exposure to a high light irradiance (Park et al., 2007). Although precise, the Fv/Fm ratio does not quantify the extent of PSII damage however.

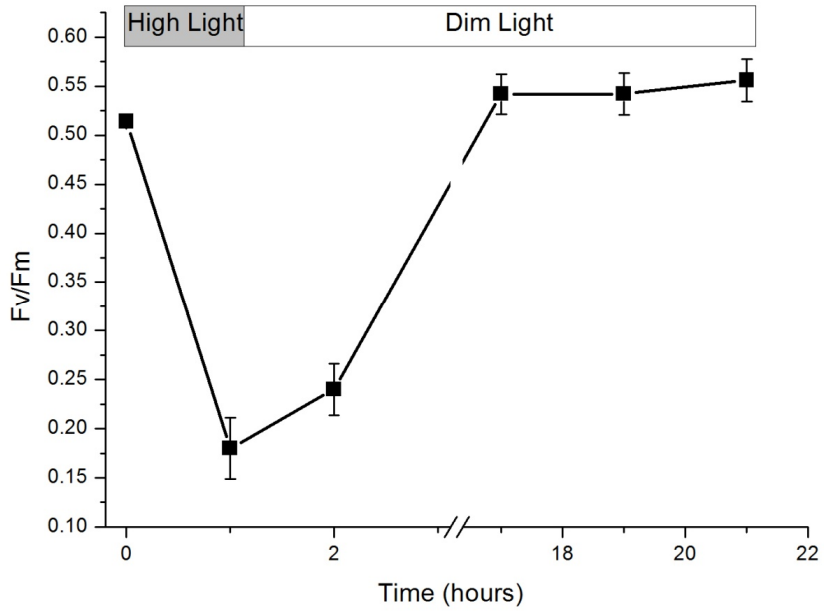

Figure 3. Light induced damages in *Nannochloropsis* cultures. *Nannochloropsis* cells grown at 100 µE m^{-2} s^{-1} were treated for 1 hour of very strong illumination (2000 µE m^{-2} s^{-1}) in atmospheric CO_2 and then allowed for recovery overnight at 10 µE m^{-2} s^{-1}. PSII radiation damages were monitored using in vivo fluorescence

Because photoinhibition has such a large influence on microalgae productivity (see, e.g., Figure 2), it needs to be quantified more accurately. Mathematical models describing fluorescence fluxes can help to unveil the actual relationship between the Fv/Fm measurements and the fraction of inhibited reaction centers. One of such dynamic model of chlorophyll a fluorescence has recently been developed by (Nikolaou et al., 2014) based on the Han model (Han, 2001), which describes photoproduction, photoinhibition and photoregulation in a semi-mechanistic manner. After its calibration and validation using measured fluorescence data, this model can be used to estimate the evolution of PSII damage at various irradiance levels, as illustrated in Figure 4A for *Nannochloropsis* cultures. In turn, the predicted PSII damage levels can be compared with the actual Fv/Fm values determined experimentally at different light intensities. The results in Figure

4B show a clear correlation between these values, allowing for a quantitative evaluation of PSII damage from simple measurements of Fv/Fm.

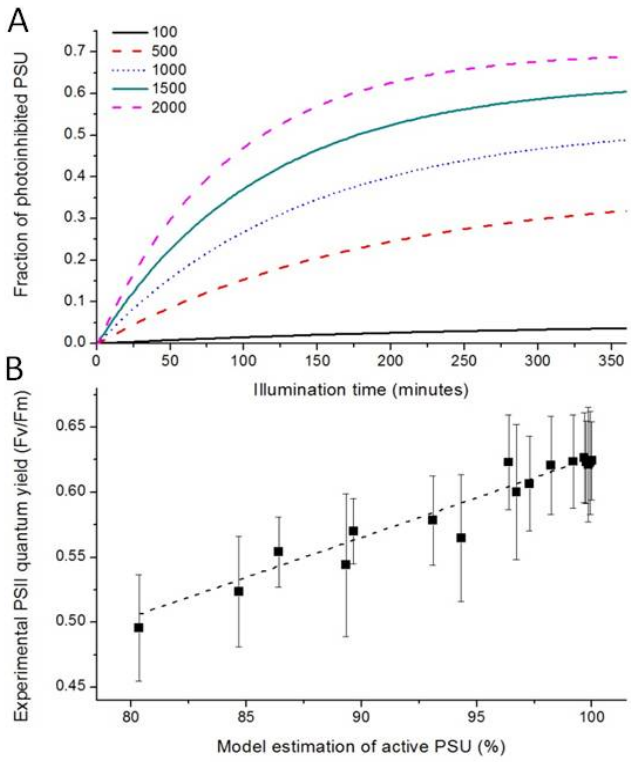

Figure 4. Quantification of Photosystems photoinhibition, comparison between model and experimental values. A) Quantification of PSII photoinhibition in cells exposed to 100, 500, 1000, 1500, 2000 µE m^{-2} s^{-1} exploiting a model describing fluorescence kinetics (Nikolaou et al., 2014). Traces are reported as black solid, red dashed, blue dotted, green solid and pink dashed lines respectively. B) Correlation between model estimation of the fraction of active PSU and the Fv/Fm values experimentally measured on cultures exposed for 5, 10, 15 or 20 minutes at 100, 500, 200, 2700 µE m^{-2} s^{-1}. Data are linearly fitted (dashed line). Fitting parameters are intercept 0.014 ± 0.038; slope 0.612 ± 0.040; r^2 0.93583.

3.2 Predicting Photosynthesis-Irradiance Curves

Photosynthesis-irradiance (PI) response curves provide a practical means of inferring and optimizing productivity in microalgae culture systems (Bernard and Rémond, 2012), yet their accurate representation has been a long-standing challenge since the 1970s. The usual way of representing PI curves is in the form of a static relationship between the light irradiance and the photosynthesis rate; the latter is often expressed in terms of oxygen evolution or CO_2 fixation, as measured using of oxygen electrodes or radioactive carbon tracing. Nonetheless, the inherently dynamic nature of microalgae cultures, together with the experimental protocol used to obtain such PI curves, introduces a great level of uncertainty in the actual measurements and also raise legitimate questions as to the validity of the underlying biological hypothesis of a static model.

In this context too, computational models as the one by (Nikolaou et al., 2014) can help remove much of the uncertainty by discriminating between phenomena acting on disparate time scales.

Specifically, this model can predict the evolution of photosynthetic efficiency (e.g., by means of the Fv/Fm parameter) in response to the actual light intensity profile followed during the PI curve experiment. In turn, the photosynthetic efficiency can be related to the photosynthesis rate, for instance by a theoretical minimum value of 4 mol(e^-)/mol(O_2) as the conversion factor. Figure 5 compares the predicted photosynthesis rates of *Nannochloropsis* (after model calibration) with an experimental PI curve obtained for the same species by (Gentile and Blanch, 2001). The close match over a wide range of light irradiance confirms that the model by (Nikolaou et al., 2014) is capable of quantitative predictions of PI curves based on fast and reliable fluorescence measurement, thereby removing the need for performing time-consuming and potentially inaccurate PI curve experiments. The same model can also be exploited to test the possible influence of different protocols to experimentally assess PI curves, showing that results obtained depends on the exact protocol followed and the initial condition of the photosynthetic apparatus (Bernardi et al., 2015). Precise specification of experimental methods is thus paramount to utilizing PI curves in the assessment of microalgae productivity.

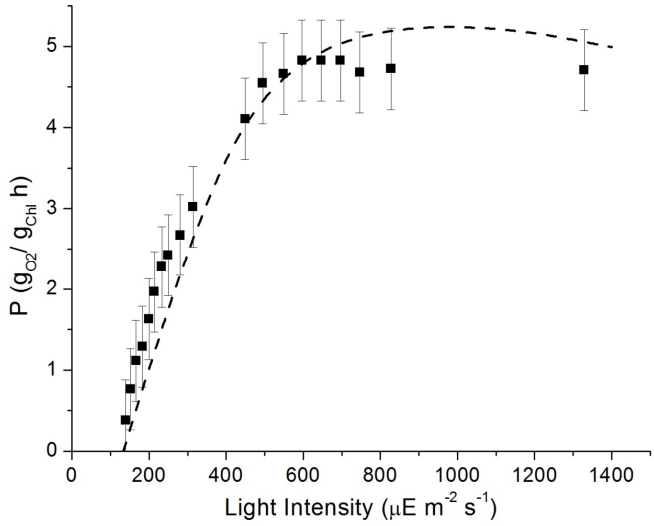

Figure 5: Comparison between model predictions and experimental data of photosynthesis rate vs. irradiance for the microalgae *Nannochloropsis.* Predictions are based on the chlorophyll-a fluorescence model by (Nikolaou et al., 2014). Experimental data are from (Gentile and Blanch, 2001) for a culture preacclimated at 200 μE m^{-2} s^{-1}.

4. FUTURE DIRECTIONS: MODEL ASSISTED EXPERIMENTAL DESIGN AND GENETIC ENGINEERING

In the last section we discuss two promising applications of state models, or more generally semi-mechanistic models, which underpin the need for synergies between modeling and experimental activities in the area of microalgae cultivation. In the first one, we discuss ways that experiments should be designed in order to support a more effective model development; in the second one, we investigate how models may be used to steer experimental investigations, with applications to genetic engineering.

4.1 Model-Assisted Experimental Design

The development of a new model is inherently a complex procedure that requires a sound knowledge of the key physical phenomena at play, the ability to formalize this knowledge into a set of algebraic and differential equations, and of course experimental data to support or reject the modelling assumptions. This procedure may appear obvious since anyone proposing even the simplest regression model does exactly that. If we start going into more details, however, answers to the following few questions may not look so straightforward anymore: how can we discriminate effectively among several modelling hypotheses? How can we guarantee that a model will be identifiable? How can we estimate the model parameters in a statistically meaningful way? How can we deal with uncertainty related to measurement noise, model mismatch, variability in biological responses, etc? And how can we guarantee that a model will be reliable for the purpose of design or operations optimization?

Figure 6 summarizes the basic tasks and flow of information that are needed for an effective model development. The preliminary step involves identifying the phenomena that need describing and the fundamental physical principles to represent them (e.g. the photoproduction and photoinhibition mechanisms). Usually some modelling assumptions are already available, or else preliminary experimental data can be used to decipher correlations among the data and set up a suitable physical interpretation through a mathematical model. In general, there may be competitive modelling approaches at this stage and the ability to discriminate among them clearly depends on the available experimental data. However, the discrimination procedure can be much more effective, in the sense of minimizing the experimental effort or producing sufficiently informative data, if the experiments are suitably designed. Ideally, input-output data should depend *only* on the phenomena that are being investigated and, for this, the interaction between a modelling expert and a biologist is paramount. Moreover, effective discrimination techniques based on advanced methodologies should be considered for the design of such experiments (Chen and Asprey, 2003).

After a suitable candidate model has been selected, the next step involves verifying that the model is identifiable, i.e. that the optimal parameter values are unique and that these values can be determined in a precise way (while still retaining a physically meaning ideally) (Miao et al., 2011). This property is particularly important as multiple parameter combinations may otherwise provide an equally good fit of the experimental data. This would not only lead to a loss of physical significance for the parameters, but a non-identifiable model may turn out to be unreliable when used to simulate or optimize processing/growth conditions differing from the ones used during the calibration. In other words, a non-identifiable model behaves more like an interpolating function and, as such, it may fail to be predictive. Accordingly, the use of such models in assessing design or operational choices is not recommended, even though it may represent some experimental data well. When identifiability issues arise in practice, a first approach to tackle the problem is to re-parameterize the model (Meshkat et al., 2011; Bernardi et al., 2014). If a reparameterization is still not enough, the model structure should then be modified.

Once a candidate model turns out to be identifiable for the available input-output data, one can proceed with the actual parameter estimation. Note that even though a model is structurally identifiable, measurements noise and other uncertainty effects may still hinder its practical

identifiability. Model-based design of experiments (MBDoE) (Franceschini and Macchietto, 2008) is an effective methodology to address this issue in a systematic way, by determining an experiment that contains the maximum possible information based on a mathematical model. Similar to black-box design of experiments, three consecutive steps are needed to determine the model parameters: (i) design of a new set of experiments based on the current knowledge; (ii) execution of the designed experiment and collection of the new data; and (iii) estimation of the new parameter values and statistical assessment (Asprey and Macchietto, 2000). Multiple Iterations between steps 1-3 lead to a reduction of the uncertain parameter region by progressively adding new experimental information. What is specific to MBDoE compared to black-box DoE here is the use of a system model in step 1 to evaluate the experiment design objective function, as part of a systematic optimization framework based on mathematical programming.

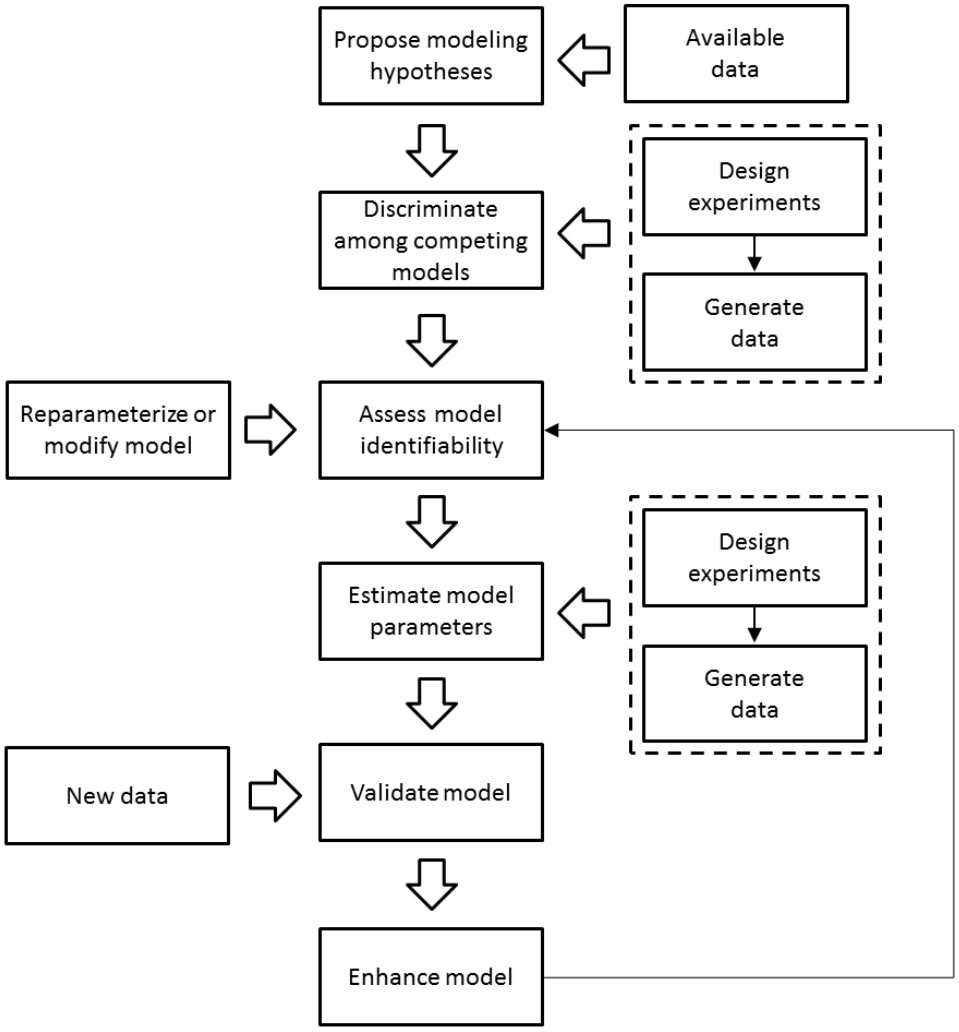

Figure 6. Model development information flow. The block diagram represents the key modeling and experimental activities to be carried for reliable model development.

A number of recent MBDoE techniques, including robust MBDoE techniques (Asprey and Macchietto, 2002) and backoff-based MBDoE techniques (Galvanin et al., 2010), have been developed to preserve the experiment design effectiveness despite the presence of significant uncertainty (possibly due to inherent biological variability), which can be caused by a large uncertain parameter set, measurement noise, or model mismatch. The integration of backoff-based and online MBDoE techniques (Galvanin et al., 2009) allows for an optimal design of dynamic experiments even when limited prior knowledge is available for the system, with great improvement in terms of design efficiency and flexibility of the overall iterative model development scheme.

For instance, Figure 7 shows the outcome of a MBDoE strategy, as applied to the chlorophyll fluorescence model by (Nikolaou et al., 2014). The objective here was to improve a PAM experimental protocol by maximizing the information content in the data, in order for the resulting correlations among the estimated model parameters to be minimal. It has also been established in a related work (Bernardi et al., 2015) that MBDoE techniques allow for a more confident estimation of the uncertain model parameter compared with a calibration based on standard PAM protocols.

Once the final parameter estimation has been performed, different data from the ones used during model calibration should be used to validate the model. Such an interplay between modelling effort and experimental activities allows building-up of model complexity in a controlled manner, keeping in mind the final objective of obtaining a reliable model that can capture the complex multi-scale mechanisms involved in microalgae growth and using this model for optimization and control purposes.

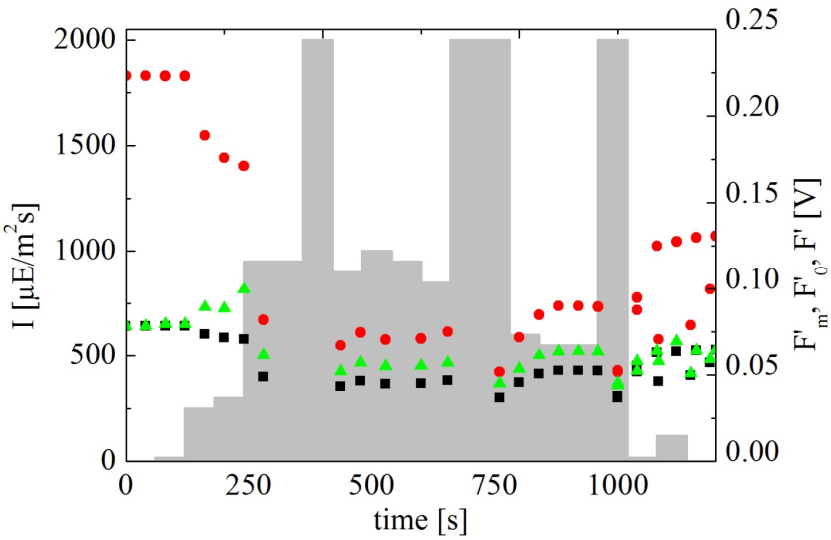

Figure 7. An example of experimental design for model identification. The shaded area represents the actinic light protocol of an optimally designed PAM experiment. At each measurement time, three variables are measured: they correspond to three possible oxidation conditions of PSII: F' (green triangles), is the fluorescence flux at the actual oxidation state of PSII, which depends upon the actinic light; F'_m (red circles), is the maximum fluorescence flux corresponding to an oxidation state where all reaction centers of PSII are closed; and F'_0 (black squares) is the minimum fluorescence flux corresponding to an oxidation state with all open reaction centers.

4.2 Model-Assisted Genetic Engineering

On the path to making large-scale microalgae production for fuel or other applications sustainable the optimization of growth conditions should go in parallel with microalgae genetic modifications to improve productivity (Radakovits et al., 2010). It turns out that certain properties of microalgae, which have been positively selected in wild-type species through evolution, can cause a significantly loss of productivity and are therefore detrimental to large-scale cultivation (Formighieri et al., 2012).

One prototypical example here is the size of the antenna of photosystems, which comprises hundreds of chlorophyll molecules per reaction center in most eukaryotic algae. This large array of pigments maximizing light-harvesting efficiency provide an evolutionary advantage in a natural environment where solar radiation is often limiting for growth (Kirk, 1983) and where the ability to be competitive with other photosynthetic organisms is essential to thrive (Kirst and Melis, 2014). In contrast, such a large antenna is the main cause for non-uniform light distribution in dense microalgae cultures, entailing a significant loss in overall productivity. In fact, the shallow layers are exposed to saturating light and the microalgae present there must activate their protection mechanisms to reduce photo-oxidative damage. Although effective for reducing damages, these mechanisms may end up dissipating up to 80% of the absorbed energy as heat (Peers et al., 2009), strongly reducing light use efficiency in these layers. Then, as most of the light is absorbed in the first few centimeter of the culture, microalgae present in deeper layers become strongly light limited and are therefore at risk of finding themselves below the light compensation point between photosynthesis and respiration (Figure 8).

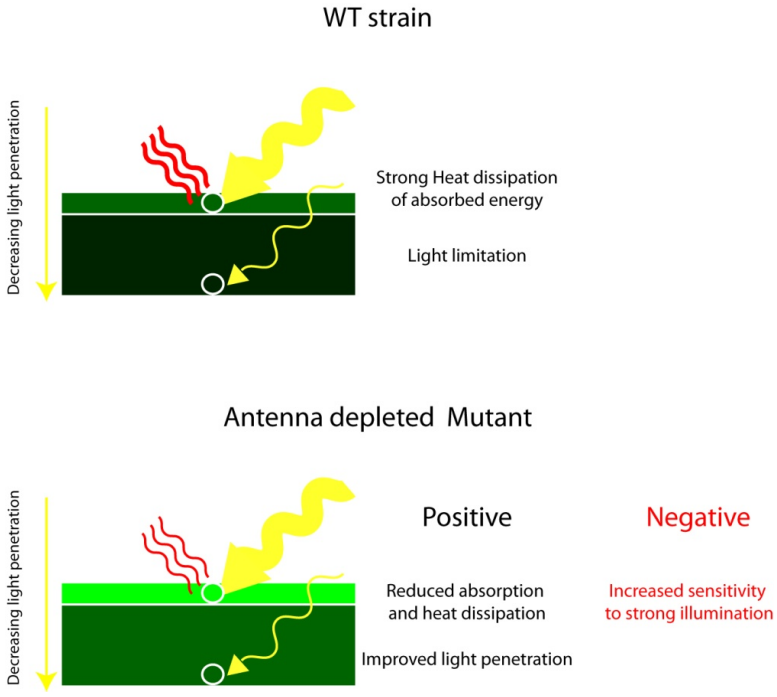

Figure 8. Scheme of potential Advantages vs. Disadvantages of and antenna mutant. WT algal strains are suggested to have limited productivities in a photobioreactor because of a inhomogeneous light distribution. Mutants with reduced antenna have been proposed to provide productivity advantages which however should be weighted with potential disadvantages.

Removing these productivity barriers requires synergies between the development/optimization efforts in photobioreactor design and operation on one hand, and research on genetic modification of microalgae on the other hand. A great deal of research has focused on reengineering the composition and regulation of the photosynthetic apparatus, so that the modified microalgae can grow faster under dense culture conditions in photobioreactors (Wobbe and Remacle, 2014; Simionato et al., 2013). The working hypothesis here is strains with a reduced content in antenna proteins could increase productivity in large-scale systems. As a matter of fact, only about 50 and 90 of the, respectively, 350 and 300 Chl molecules found in each PSII and PSI unit in *C. reinhardtii* are strictly required for the correct assembly of their reaction centers (Melis, 1991). It thus appears possible to greatly reduce the number of LHC units associated to each reaction center, while preserving their whole photochemical capabilities. The expected benefits are two-fold (Simionato et al., 2013): (i) the more exposed layers will absorb less energy, thereby reducing heat dissipation; and (ii) the reduction in light harvesting capacity will lead a more uniform light distribution in the culture medium, thereby promoting growth in deeper layers. Several microalgae strains with reduced antenna content, known as truncated light-harvesting chlorophyll antenna (TLA) mutants, have already been isolated, especially in the model genus *Chlamydomonas reinhardtii* (Nakajima and Ueda, 2000; Nakajima et al., 2001; Nakajima and Itayama, 2003; Bonente et al., 2011b), but also in other species with a greater application potential (Melis et al., 1998; Perin et al., 2014; Cazzaniga et al., 2014). So far, these studies have demonstrated that the chlorophyll content of microalgae can be reduced by targeting multiple different genes. In addition to the genes encoding LHC proteins, alteration of factors involved in either the co-translational or post-translational regulation of antenna proteins, such as the NAB1 repressor (Beckmann et al., 2009; Wobbe et al., 2009), genes involved in the chlorophyll biosynthetic pathway (Polle et al., 2000), or chloroplast signal recognition particles (CpSRPs) (Kirst et al., 2012b, 2012a; Kirst and Melis, 2014) have all proved successful for the generation of TLA mutants (Formighieri et al., 2012). In several studies these TLA mutants have shown an increase in the maximal photosynthesis rate and a higher light saturation limit (Nakajima and Ueda, 2000; Nakajima et al., 2001; Beckmann et al., 2009; Wobbe et al., 2009).

Notwithstanding the promises of TLA mutants, the large-scale testing of these strains in photobioreactors has produced contrasting results (de Mooij et al., 2014). One plausible explanation for this behavior is that the proteins in the antenna play a more complex biological role (Horton and Ruban, 2005) and alteration of their content can lead to unexpected secondary effects. For instance, it is well known that antenna proteins responsible for light harvesting can also play a major role in NPQ photoregulation (Avenson et al., 2008; Bonente et al., 2011a; Elrad, 2002; Horton and Ruban, 2005; Peers et al., 2009). This way, a reduction in light harvesting complexes will also affect the photo-protection capability, leading to increased photoinhibition when the cells are exposed to high irradiance (Figure 8). Secondly, the sole reduction in the photosystem II antenna could decrease the photon use efficiency because a portion of the light-energy absorbed by photosystem I could not be utilized in the linear photosynthetic electron transport process, if this antenna reduction is not balanced by an adjustment in photosystem II/ photosystem I ratio (Polle et al., 2000). Another concern with TLA mutants is their larger respiration rates in low-light regions of dense cultures.

All these potential negative aspects of TLA mutants could hinder the benefits of a more uniform light distribution. In order to effectively improve productivity, it is therefore necessary to balance out the benefits of a reduced light harvesting capacity with the drawbacks of a reduced photo-protection capability (Bonente et al., 2011b; Simionato et al., 2013) (Figure 8). Identifying such a compromise is clearly non-trivial, as it depends on many parameters. Environmental conditions such as light intensity, nutrients availability clearly have a major influence together with parameters related to the photobioreactor design and operation such as light path, culture density and mixing rate. Given this complexity, it is likely that there will be no superior genetically modified strain applicable in all circumstances, but instead the genetic modification ought to be tailored to the local environment and PBR characteristics.

Addressing such a complex problem via trial-and-error approach, as it is done currently, presents many drawbacks and is exposed to many failures. Instead, the availability of reliable and sufficiently detailed models could be a great help in identifying the most promising areas for intervention and driving the overall process, which once again calls for synergies between modelling and biological expertise. These models would allow mapping of biological events and mechanisms to model equations and parameters, thereby creating a correlation between quantitative information (i.e., change in a parameter value) and potential possible genetic intervention (e.g., should we modify the antenna size or rather intervene on quenching mechanisms?). In particular, computer-based approaches based on (global) sensitivity analysis techniques (Saltelli et al., 2007) applied to a multi-scale modelling approach could assess the effect of such parameters on key process outputs (yield, growth rate, concentration, etc) and produce a surface of expected biological behaviors through which one could then conclude whether an intervention line is deemed “safe” (i.e., probably successful) or excessively “risky”. This way, computational models capable of quantitative prediction of the effect of different parameters on algae productivity could also be used for *in silico* comparison of various mutation effects, via the evaluation of their impacts on the light harvesting and photoprotection properties.

This model-based approach could help prevent major mistakes in the prioritization of genetic engineering interventions. But without a reliable simulator than can account for scale-up effects, it may not be possible to predict the effect of a genetic modification on a large-scale culture system reliably. In fact, this has been a common problem with several existing model of TLA mutants when used to predict growth under large-scale culture conditions (Nakajima and Itayama, 2003; Ort and Melis, 2011; de Mooij et al., 2014; Kirst et al., 2014). Although they were developed to predict the biomass specific growth rate and the biomass yield for both wild-type strains and TLA mutants, these simple kinetic models have failed to describe the experimental observations so far (de Mooij et al., 2014). A possible explanation for this mismatch could be that predicting how the light-response curve will change is simply not enough (Stephenson et al., 2011), but additional mechanisms need to be taken into account for accurate prediction of the performance of a large-scale production system, such as the respiratory activity of the TLA mutants, or their photoinhibition and photo-acclimation properties (Formighieri et al., 2012). Due to time and cost constraints, TLA mutants have so far been isolated and selected solely based on their lab-scale behavior, with their performances on larger scale to be tested only in a later stage. The availability of a proper multi-scale and multi-physics model would instead also help steering the selection at a

very early stage. Clearly, the long-term objective here is to use optimization-based techniques to decide which genetic interventions should be carried out to achieve a given performance target. In particular, this will involve determining which *combinations* of modifications are likely to lead to identical/similar performance results at minimum cost, and how to design and operate a photobioreactor in order to get the most out the mutants.

References

Amaro, H.M., Guedes, A.C., and Malcata, F.X. (2011). Advances and perspectives in using microalgae to produce biodiesel. Appl. Energy **88**: 3402–3410.

Asprey, S.P. and Macchietto, S. (2002). Designing robust optimal dynamic experiments. J. Process Control **12**: 545–556.

Asprey, S.P. and Macchietto, S. (2000). Statistical tools for optimal dynamic model building. Comput. Chem. Eng. **24**: 1261–1267.

Avenson, T.J., Ahn, T.K., Zigmantas, D., Niyogi, K.K., Li, Z., Ballottari, M., Bassi, R., and Fleming, G.R. (2008). Zeaxanthin radical cation formation in minor light-harvesting complexes of higher plant antenna. J. Biol. Chem. **283**: 3550–8.

Baklouti, M., Diaz, F., Pinazo, C., Faure, V., and Quéguiner, B. (2006). Investigation of mechanistic formulations depicting phytoplankton dynamics for models of marine pelagic ecosystems and description of a new model. Prog. Oceanogr. **71**: 1–33.

Barber, J. and Andersson, B. (1992). Too much of a good thing: light can be bad for photosynthesis. Trends Biochem. Sci. **17**: 61–66.

Beckmann, J., Lehr, F., Finazzi, G., Hankamer, B., Posten, C., Wobbe, L., and Kruse, O. (2009). Improvement of light to biomass conversion by de-regulation of light-harvesting protein translation in Chlamydomonas reinhardtii. J. Biotechnol. **142**: 70–7.

Bernard, O. and Rémond, B. (2012). Validation of a simple model accounting for light and temperature effect on microalgal growth. Bioresour. Technol. **123**: 520–7.

Bernardi, A., Nikolaou, A., Meneghesso, A., Morosinotto, T., Chachuat, B., and Bezzo, F. (2015). Using fluorescence measurements to model key phenomena in microalgae photosynthetic mechanisms. In Chem. Eng. Trans., p. submitted.

Bernardi, A., Perin, G., Sforza, E., Galvanin, F., Morosinotto, T., and Bezzo, F. (2014). An Identifiable State Model To Describe Light Intensity Influence on Microalgae Growth. Ind. Eng. Chem. Res. **53**: 6738–6749.

Biegler, L.T., Lang, Y., and Lin, W. (2014). Multi-scale optimization for process systems

engineering. Comput. Chem. Eng. **60**: 17–30.

Bonente, G., Ballottari, M., Truong, T.B., Morosinotto, T., Ahn, T.K., Fleming, G.R., Niyogi, K.K., and Bassi, R. (2011a). Analysis of LHcSR3, a protein essential for feedback de-excitation in the green alga Chlamydomonas reinhardtii. PLoS Biol. **9**: e1000577.

Bonente, G., Formighieri, C., Mantelli, M., Catalanotti, C., Giuliano, G., Morosinotto, T., and Bassi, R. (2011b). Mutagenesis and phenotypic selection as a strategy toward domestication of Chlamydomonas reinhardtii strains for improved performance in photobioreactors. Photosynth. Res. **108**: 107–20.

Bonente, G., Pippa, S., Castellano, S., Bassi, R., and Ballottari, M. (2012). Acclimation of Chlamydomonas reinhardtii to different growth irradiances. J. Biol. Chem. **287**: 5833–47.

Del Campo, J.A., García-González, M., and Guerrero, M.G. (2007). Outdoor cultivation of microalgae for carotenoid production: current state and perspectives. Appl. Microbiol. Biotechnol. **74**: 1163–74.

Cazzaniga, S., Dall'Osto, L., Szaub, J., Scibilia, L., Ballottari, M., Purton, S., and Bassi, R. (2014). Domestication of the green alga Chlorella sorokiniana: reduction of antenna size improves light-use efficiency in a photobioreactor. Biotechnol. Biofuels **7**: 157.

Chen, B.H. and Asprey, S.P. (2003). On the design of optimally informative dynamic experiments for model discrimination in multiresponse nonlinear situations. Ind. Eng. Chem. Res. **42**: 1379–1390.

Chisti, Y. (2007). Biodiesel from microalgae. Biotechnol. Adv. **25**: 294–306.

Chisti, Y. and Yan, J. (2011). Energy from algae: Current status and future trends. Appl. Energy **88**: 3277–3279.

Duarte, P. (1995). A mechanistic model of the effects of light and temperature on algal primary productivity. Ecol. Modell. **82**: 151–160.

Eberhard, S., Finazzi, G., and Wollman, F.-A. (2008). The dynamics of photosynthesis. Annu. Rev. Genet. **42**: 463–515.

EILERS, P. and PEETERS, J. (1988). A MODEL FOR THE RELATIONSHIP BETWEEN LIGHT-INTENSITY AND THE RATE OF PHOTOSYNTHESIS IN PHYTOPLANKTON. **42**: 199–215.

Elrad, D. (2002). A Major Light-Harvesting Polypeptide of Photosystem II Functions in Thermal Dissipation. PLANT CELL ONLINE **14**: 1801–1816.

Formighieri, C., Franck, F., and Bassi, R. (2012). Regulation of the pigment optical density of an algal cell: filling the gap between photosynthetic productivity in the laboratory and in mass culture. J. Biotechnol. **162**: 115–23.

Franceschini, G. and Macchietto, S. (2008). Model-based design of experiments for parameter precision: State of the art. Chem. Eng. Sci. **63**: 4846–4872.

Galvanin, F., Barolo, M., and Bezzo, F. (2009). Online Model-Based Redesign of Experiments for Parameter Estimation in Dynamic Systems. Ind. Eng. Chem. Res. **48**: 4415–4427.

Galvanin, F., Barolo, M., Bezzo, F., and Macchietto, S. (2010). A backoff strategy for model-based experiment design under parametric uncertainty. AIChE J. **56**: NA–NA.

García-Camacho, F., Sánchez-Mirón, A., Molina-Grima, E., Camacho-Rubio, F., and Merchuck, J.C. (2012). A mechanistic model of photosynthesis in microalgae including photoacclimation dynamics. J. Theor. Biol. **304**: 1–15.

Gentile, M.P. and Blanch, H.W. (2001). Physiology and xanthophyll cycle activity of Nannochloropsis gaditana. Biotechnol. Bioeng. **75**: 1–12.

Gerotto, C., Alboresi, A., Giacometti, G.M., Bassi, R., and Morosinotto, T. (2011). Role of PSBS and LHCSR in Physcomitrella patens acclimation to high light and low temperature. Plant. Cell Environ. **34**: 922–32.

Guedes, A.C., Amaro, H.M., and Malcata, F.X. (2011). Microalgae as sources of high added-value compounds--a brief review of recent work. Biotechnol. Prog. **27**: 597–613.

Han, B.P. (2001). Photosynthesis-irradiance response at physiological level: a mechanistic model. J. Theor. Biol. **213**: 121–7.

Hartmann, P., Béchet, Q., and Bernard, O. (2014). The effect of photosynthesis time scales on microalgae productivity. Bioprocess Biosyst. Eng. **37**: 17–25.

Horton, P. and Ruban, A. (2005). Molecular design of the photosystem II light-harvesting antenna: photosynthesis and photoprotection. J. Exp. Bot. **56**: 365–73.

Kirk, J.T.O. (1983). Light and photosynthesis in aquatic ecosystems. Light Photosynth. Aquat. Ecosyst.

Kirst, H., Formighieri, C., and Melis, A. (2014). Maximizing photosynthetic efficiency and culture productivity in cyanobacteria upon minimizing the phycobilisome light-harvesting antenna size. Biochim. Biophys. Acta **1837**: 1653–64.

Kirst, H., García-Cerdán, J.G., Zurbriggen, A., and Melis, A. (2012a). Assembly of the light-harvesting chlorophyll antenna in the green alga Chlamydomonas reinhardtii requires expression of the TLA2-CpFTSY gene. Plant Physiol. **158**: 930–45.

Kirst, H., Garcia-Cerdan, J.G., Zurbriggen, A., Ruehle, T., and Melis, A. (2012b). Truncated photosystem chlorophyll antenna size in the green microalga Chlamydomonas reinhardtii upon deletion of the TLA3-CpSRP43 gene. Plant Physiol. **160**: 2251–60.

Kirst, H. and Melis, A. (2014). The chloroplast signal recognition particle (CpSRP) pathway as a tool to minimize chlorophyll antenna size and maximize photosynthetic productivity. Biotechnol. Adv. **32**: 66–72.

Loebl, M., Cockshutt, A.M., Campbell, D.A., and Finkel, Z. V. (2010). Physiological basis for high resistance to photoinhibition under nitrogen depletion in Emiliania huxleyi. Limnol. Oceanogr. **55**: 2150–2160.

Long, S.P., Humphries, S., and Falkowski, P.G. (1994). Photoinhibition of photosynthesis in nature. Annu. PHYSIOL.PLANT MOL.BIOL. **45**: 633–662.

Lubián, L.M., Montero, O., Moreno-Garrido, I., Huertas, I.E., Sobrino, C., González-Del Valle, M., and Parés, G. (2000). Nannochloropsis (Eustigmatophyceae) as source of commercially valuable pigments. In Journal of Applied Phycology, pp. 249–255.

MacIntyre, H.L., Kana, T.M., Anning, T., and Geider, R.J. (2002). PHOTOACCLIMATION OF PHOTOSYNTHESIS IRRADIANCE RESPONSE CURVES AND PHOTOSYNTHETIC PIGMENTS IN MICROALGAE AND CYANOBACTERIA1. J. Phycol. **38**: 17–38.

Malcata, F.X. (2011). Microalgae and biofuels: a promising partnership? Trends Biotechnol. **29**: 542–9.

MARSHALL, H.L., GEIDER, R.J., and FLYNN, K.J. (2000). A mechanistic model of photoinhibition. New Phytol. **145**: 347–359.

Maxwell, K. and Johnson, G.N. (2000). Chlorophyll fluorescence - A practical guide. J. Exp. Bot. **51**: 659–668.

Melis, A. (1991). Dynamics of photosynthetic membrane composition and function. BBA - Bioenerg. **1058**: 87–106.

Melis, A. (2009). Solar energy conversion efficiencies in photosynthesis: Minimizing the chlorophyll antennae to maximize efficiency. Plant Sci. **177**: 272–280.

Melis, A., Neidhardt, J., and Benemann, J.R. (1998). Dunaliella salina (Chlorophyta) with small chlorophyll antenna sizes exhibit higher photosynthetic productivities and photon use efficiencies than normally pigmented cells. J. Appl. Phycol. **10**: 515–525.

Meshkat, N., Anderson, C., and Distefano, J.J. (2011). Finding identifiable parameter combinations in nonlinear ODE models and the rational reparameterization of their input-output equations. Math. Biosci. **233**: 19–31.

Miao, H., Xia, X., Perelson, A.S., and Wu, H. (2011). ON IDENTIFIABILITY OF NONLINEAR ODE MODELS AND APPLICATIONS IN VIRAL DYNAMICS. SIAM Rev. Soc. Ind. Appl. Math. **53**: 3–39.

de Mooij, T., Janssen, M., Cerezo-Chinarro, O., Mussgnug, J.H., Kruse, O., Ballottari, M., Bassi, R., Bujaldon, S., Wollman, F.-A., and Wijffels, R.H. (2014). Antenna size reduction as a strategy

to increase biomass productivity: a great potential not yet realized. J. Appl. Phycol.

Mutanda, T., Ramesh, D., Karthikeyan, S., Kumari, S., Anandraj, A., and Bux, F. (2011). Bioprospecting for hyper-lipid producing microalgal strains for sustainable biofuel production. Bioresour. Technol. **102**: 57–70.

Nakajima, Y. and Itayama, T. (2003). Analysis of photosynthetic productivity of microalgal mass cultures. J. Appl. Phycol. **15**: 497–505.

Nakajima, Y., Tsuzuki, M., and Ueda, R. (2001). Improved productivity by reduction of the content of light-harvesting pigment in Chlamydomonas perigranulata. J. Appl. Phycol. **13**: 95–101.

Nakajima, Y. and Ueda, R. (2000). The effect of reducing light-harvesting pigment on marine microalgal productivity. In Journal of Applied Phycology, pp. 285–290.

Nauha, E.K. and Alopaeus, V. (2013). Modeling method for combining fluid dynamics and algal growth in a bubble column photobioreactor. Chem. Eng. J. **229**: 559–568.

Nikolaou, A., Bernardi, A., Bezzo, F., Morosinotto, T., and Chachuat, B. (2014). A Dynamic Model of Photoproduction, Photoregulation and Photoinhibition in Microalgae Using Chlorophyll Fluorescence. In World Congress, pp. 4370–4375.

Norberg, J. (2004). Biodiversity and ecosystem functioning: A complex adaptive systems approach. Limnol. Oceanogr. **49**: 1269–1277.

Ort, D.R. and Melis, A. (2011). Optimizing antenna size to maximize photosynthetic efficiency. Plant Physiol. **155**: 79–85.

Pahlow, M. (2005). Linking chlorophyll-nutrient dynamics to the Redfield N:C ratio with a model of optimal phytoplankton growth. Mar. Ecol. Prog. Ser. **287**: 33–43.

Papadakis, I.A., Kotzabasis, K., and Lika, K. (2012). Modeling the dynamic modulation of light energy in photosynthetic algae. J. Theor. Biol. **300**: 254–64.

Park, S., Khamai, P., Garcia-Cerdan, J.G., and Melis, A. (2007). REP27, a Tetratricopeptide Repeat Nuclear-Encoded and Chloroplast-Localized Protein, Functions in D1/32-kD Reaction Center Protein Turnover and Photosystem II Repair from Photodamage. PLANT Physiol. **143**: 1547–1560.

Peers, G., Truong, T.B., Ostendorf, E., Busch, A., Elrad, D., Grossman, A.R., Hippler, M., and Niyogi, K.K. (2009). An ancient light-harvesting protein is critical for the regulation of algal photosynthesis. Nature **462**: 518–21.

Perin, G., Segalla, A., Basso, S., Simionato, D., Meneghesso, A., Sforza, E., Bertucco, A., and Morosinotto, T. (2014). Biotechnological optimization of light use efficiency in nannochloropsis cultures for biodiesel production. Chem. Eng. Trans. **37**: 763–768.

Polle, J.E., Benemann, J.R., Tanaka, A., and Melis, A. (2000). Photosynthetic apparatus organization and function in the wild type and a chlorophyll b-less mutant of Chlamydomonas reinhardtii. Dependence on carbon source. Planta **211**: 335–44.

Pulz, O. and Gross, W. (2004). Valuable products from biotechnology of microalgae. Appl. Microbiol. Biotechnol. **65**: 635–48.

Radakovits, R., Jinkerson, R.E., Darzins, A., and Posewitz, M.C. (2010). Genetic engineering of algae for enhanced biofuel production. Eukaryot. Cell **9**: 486–501.

RAVEN, J.A. and FALKOWSKI, P.G. (1999). Oceanic sinks for atmospheric CO 2. Plant, Cell Environ. **22**: 741–755.

Rubio, F.C., Camacho, F.G., Sevilla, J.M.F., Chisti, Y., and Grima, E.M. (2003). A mechanistic model of photosynthesis in microalgae. Biotechnol. Bioeng. **81**: 459–73.

Saltelli, A., Ratto, M., Andres, T., Campolongo, F., Cariboni, J., Gatelli, D., Saisana, M., and Tarantola, S. (2007). Global Sensitivity Analysis. The Primer (John Wiley & Sons, Ltd: Chichester, UK).

Sforza, E., Bertucco, A., Morosinotto, T., and Giacometti, G.M. (2012a). Photobioreactors for microalgal growth and oil production with Nannochloropsis salina: From lab-scale experiments to large-scale design. Chem. Eng. Res. Des. **90**: 1151–1158.

Sforza, E., Simionato, D., Giacometti, G.M., Bertucco, A., and Morosinotto, T. (2012b). Adjusted light and dark cycles can optimize photosynthetic efficiency in algae growing in photobioreactors. PLoS One **7**: e38975.

Simionato, D., Basso, S., Giacometti, G.M., and Morosinotto, T. (2013). Optimization of light use efficiency for biofuel production in algae. Biophys. Chem. **182**: 71–8.

Simionato, D., Sforza, E., Corteggiani Carpinelli, E., Bertucco, A., Giacometti, G.M., and Morosinotto, T. (2011). Acclimation of Nannochloropsis gaditana to different illumination regimes: effects on lipids accumulation. Bioresour. Technol. **102**: 6026–32.

Stephenson, P.G., Moore, C.M., Terry, M.J., Zubkov, M. V, and Bibby, T.S. (2011). Improving photosynthesis for algal biofuels: toward a green revolution. Trends Biotechnol. **29**: 615–23.

Vass, I. (2012). Molecular mechanisms of photodamage in the Photosystem II complex. Biochim. Biophys. Acta **1817**: 209–17.

Walters, R.G. (2005). Towards an understanding of photosynthetic acclimation. J. Exp. Bot. **56**: 435–47.

Williams, P.J. le B. and Laurens, L.M.L. (2010). Microalgae as biodiesel & biomass feedstocks: Review & analysis of the biochemistry, energetics & economics. Energy Environ. Sci. **3**: 554.

Wobbe, L., Blifernez, O., Schwarz, C., Mussgnug, J.H., Nickelsen, J., and Kruse, O. (2009). Cysteine modification of a specific repressor protein controls the translational status of nucleus-encoded LHCII mRNAs in Chlamydomonas. Proc. Natl. Acad. Sci. U. S. A. **106**: 13290–5.

Wobbe, L. and Remacle, C. (2014). Improving the sunlight-to-biomass conversion efficiency in microalgal biofactories. J. Biotechnol.

Wu, X. and Merchuk, J.C. (2001). A model integrating fluid dynamics in photosynthesis and photoinhibition processes. Chem. Eng. Sci. **56**: 3527–3538.

Zonneveld, C. (1998). Photoinhibition as Affected by Photoacclimation in Phytoplankton: a Model Approach. J. Theor. Biol. **193**: 115–123.

SECTION D

CHAPTER D1

CROSSTALK WITH MITOCHONDRIA HAS A SEMINAL INFLUENCE ON PHOTOSYNTHESIS REGULATION IN *CHLAMYDOMONAS REINHARDTII*

CROSSTALK WITH MITOCHONDRIA HAS A SEMINAL INFLUENCE ON PHOTOSYNTHESIS REGULATION IN *CHLAMYDOMONAS REINHARDTII* [1]

Abstract

Chloroplast and mitochondria are the organelles responsible of bioenergetics in photosynthetic organisms. Light energy is the primary source of energy for photosynthetic organisms and chloroplast is believed to be the major player in conversion of light into chemical energy. However, there are emerging evidences in different organisms supporting an important role of mitochondria and its crosstalk with chloroplast also in autotrophic metabolism. In this work we show that the introduction of a mitochondrial mutation in *C. reinhardtii* mutants depleted in the chloroplastic PGRL1 rescue its photosensitivity in HL. Detailed functional analysis of these cells showed that the mitochondria mutation alters the electron transport reactions. As a consequence excess light damage targets PSII while in *pgrl1* mutant is mainly PSI. Reduced photosensitivity, thus, is not due to reduced damage but to the fact that cells are more effective in recovering from PSII damages that PSI. This work thus clearly shows how mitochondrial activity play a seminal influence on photosynthesis in algae, affecting photosynthetic electron transport chain.

Introduction

Photosynthetic eukaryotes rely on two specialized organelles, chloroplast and mitochondria, for the synthesis of NAD(P)H and ATP, the molecules fueling their metabolism. Both organelles share common features, such as an array of membrane bounded enzymatic complexes that, by electrons transfer reactions, generate a proton motive force across a membrane to generate ATP. In the chloroplast, light drives a linear electron flow (LEF) from water to $NADP^+$ catalyzed by the two photosystems (PSI and PSII). Electrons, however, can also follow alternative pathways such as cyclic electron flow (CEF) around PSI. In green algae such *as Chlamydomonas reinhardtii* two pathways for CEF have been identified, one depending from an NDA2 NADPH: plastoquinone oxidoreductase (Jans et al., 2008) and one from a PGR5-PGRL1 complex with putative ferredoxin: plastoquinone oxidoreductase activity (Tolleter et al., 2011; Johnson et al., 2014).

---

[1] Mutant lines of *C. reinhardtii* have been generated by Véronique Larosa[a,b] in Claire Remacle laboratory. In this chapter an extract of their physiological characterization is presented. In this project, my work was focused on the application of different spectroscopic techniques to analyze mutants phenotype and this part of the project is the main subject of this chapter. In addition to myself, Véronique Larosa[a,b] and Tomas Morosinotto[a] contributed to the work. The project was also a collaboration with Ildikò Szabo[a] and Claire Remacle[b] .

[a] Department of Biology, University of Padova; [b] Physiology and Genetics of Microalgae Laboratory, University of Liège.

In mitochondria, the oxidative phosphorylation (OXPHOS) consists of an electron-transfer chain driven by substrate (NADH and succinate) oxidation coupled to the synthesis of ATP through an electrochemical transmembrane gradient. OXPHOS is catalyzed by the so-called complexes I, II, III, IV. As in chloroplast, electrons can follow alternative route via an alternative terminal oxidase (Baurain et al., 2003) catalyzing the reduction of molecular oxygen into water bypassing the activities of CIII and CIV or via an alternative NADH dehydrogenase (Lecler et al., 2012) that bypass complex I activity.

In photosynthetic eukaryotes both organelles are present and their activity needs to be tightly regulated to respond to environmental cues and optimize their activity. In diatoms for example the ratio ATP/NADPH is regulated through extensive energetic exchanges between plastids and mitochondria. This energetic coupling is performed by re-routing NADPH and ATP between the two organelles and it is believed to be indispensable to sustain basal metabolisms (Bailleul et al., 2015). Organelles reciprocal influence can be evidenced also in different respiratory or photosynthetic mutants in the microalgae *C. reinhardtii.* As example complex I and III mutants showed reorganization of the photosynthetic apparatus with a transition to state II and increase of CEF around PSI. This switch in the photosynthetic apparatus favoring ATP synthesis over $NADP^+$ reduction in the chloroplast compensate the decrease in ATP synthesis from mitochondria (Cardol et al., 2003, 2009). Also in plants, complex I inhibition leads to a reduction of photosynthetic activity under high light conditions. This suggests that complex I takes a crucial part as regulatory of photosynthesis (Dutilleul et al., 2003). On the other side, *C. reinhardtii* mutants affected in alternative pathway of photosynthesis, such as the mutants of CEF-related PGRL1 protein, showed increased mitochondrial respiration (Petroutsos et al., 2009; Dang et al., 2014). This phenotype is accompanied by an increased photosensitivity in strong light, mainly due to PSI photoinhibition (Tolleter et al., 2011). In addition, these *pgrl1* mutants showed higher sensitivity of photosynthesis to mitochondrial inhibitors highlighting the importance of the cooperation between organelles in these cells (Dang et al., 2014). Available data thus suggest this strain is a suitable system to highlight mitochondrial influence on cell physiology and on photosynthesis.

This study investigate the biological role of the organelles crosstalk by analyzing a double mutant *pgrl1Δnd4* combining mutations on the nuclear gene *PGRL1* and on the mitochondrial complex I gene *nd4*. The latter mutant selected, *Δnd4,* presents a deletion of codons 2-24 of the mitochondrial *nd4* gene that leads to a completely inactivated complex I. Complex I mutants in *C. reinhardtii* show a slower heterotrophic growth compared to the WT (Remacle et al., 2006; Salinas et al., 2014) but are still viable since respiration deficiency is partially compensated by complex II or alternative NADH dehydrogenase or by photosynthesis.

Growth performances WT, *pgrl1*, *Δnd4* and *pgrl1Δnd4* were assessed in agar plate in different growing conditions, varying light and carbon source availability. The different genotypes did not show any major growth defects when grown under control light conditions in photoautotrophy (TMP + light) (Figure 1A). In mixotrophic conditions (TAP + light), in CL typical complex I mutants phenotype is evidenced. Indeed, mutants of complex I always show a reduced growth in heterotrophic and mixotrophic conditions compared to wild type (Salinas et al., 2014). Once exposed to a stronger illumination (starting from 850 $\mu E\ m^{-2}\ s^{-1}$), *pgrl1* showed growth defects and a clear photosensitivity, as previously reported (Dang et al., 2014; Kukuczka et al., 2014). In

the case of the double mutant *Δnd4pgrl1,* the introduction of a mitochondrial mutation surprisingly rescues the *pgrl1* photosensitivity; such mutant could then grow under strong illumination (Figure 1A). Interestingly this rescued ability to survive strong illumination is present both in photoautotrophic and mixotrophic conditions. The surprising growth phenotype was confirmed in liquid cultures grown at different light intensities both in TMP and TAP (Figure 1B-C, only TMP cultures are reported). While growth rate is equivalent for all genotypes at control light in photoautotrophic conditions (Figure 1B), strong illumination affects *pgrl1* mutants while *Δnd4pgrl1* surprisingly performs as well as the WT (Figure 1C). The reasons why a mitochondrial mutation restores the *pgrl1* ability to grow under strong illumination will be investigated in this work using different spectroscopic approach to follow in detail the photosynthetic response.

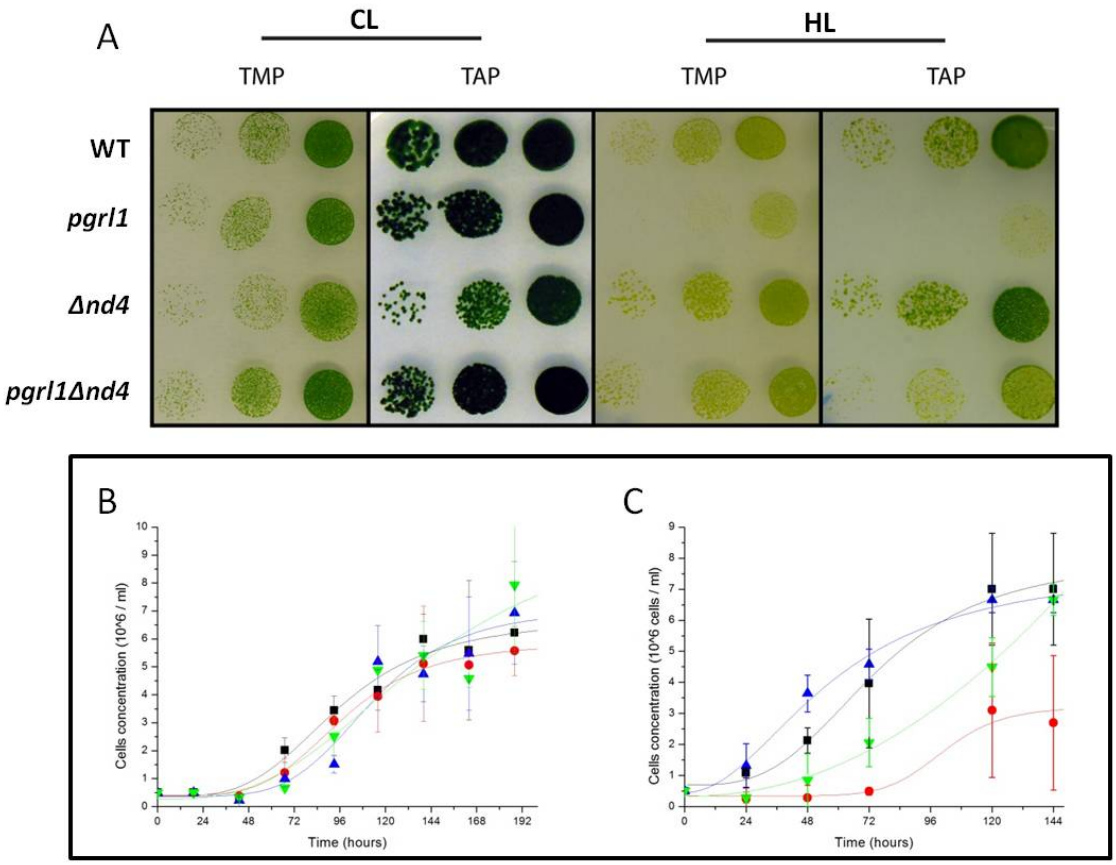

Figure 1. Growth phenotype of the WT, *Δnd4, pgrl1* and the double mutant *Δnd4pgrl1* strains. A) Spot tests in agar plate in photoautotrophic (TMP + light) and mixotrophic (TAP + light) conditions exposed to control light (CL, 50 µE m^{-2} s^{-1}) and high light (HL, 850 µE m^{-2} s^{-1}) intensities. B-C) Growth curves of liquid cultures from WT, *Δnd4, pgrl1* and *Δnd4pgrl1* expressed in counted cell per ml. The different genotypes shown were grown photoautotrophically in TMP medium using (B) control light (70 µE m^{-2} s^{-1}) or (C) high light (1000 µE m^{-2} s^{-1}). WT, *pgrl1*, *Δnd4* and *pgrl1Δnd4* strains are shown as black squares, red circles, blue up triangles and green down triangles, respectively. All growth curves were repeated at least four independent times.

Materials and Methods

Strains and growth conditions. The strains used in this study are derived from the wild-type 137c strain of *C. reinhardtii*. The mitochondrial mutants, *Δnd4*, presents a deletion of codons 2-24 of the mitochondrial *nd4* gene that leads to a loss of complex I activity (Remacle et al., 2006). *C. reinhardtii* cells were grown in liquid cultures (Erlenmeyer flasks) photoautotrophically and mixotrophically using a TMP (Tris-Minimal-Phosphate) and TAP (Tris-Acetate-Phosphate) medium, respectively (Harris et al., 1989). The cultures were exposed to continuous light at control (70 μE m^{-2} s^{-1}) or high (1000 μE m^{-2} s^{-1}) intensities. The temperature was maintained at 25 ± 1 °C in a growth chamber. Algal growth was measured through daily changes in the cell number monitored using a Cellometer Auto X4 cell counter (Nexcelom Bioscience).

Chlorophyll fluorescence measurements. Chlorophyll fluorescence was measured *in vivo* on *C. reinhardtii* cells, using a Dual PAM 100 fluorometer (Walz, Germany). Cells were harvested in the exponential phase and resuspended in TMP and TAP medium at a cell concentration of 10 x 10^6 cells/ml. Afterwards they were dark adapted for 30 minutes keeping them gently mixed. After the dark adaptation photosynthetic parameters were assessed using saturating pulses (200 ms, 9000 μE m^{-2} s^{-1}) during a Light Curve protocol, where the cells were stepwise exposed to increasing light intensities every 1 minute. The parameters Fv/Fm and ϕPSII were calculated as (Fm-Fo)/Fm and (Fm'-F')Fm', respectively (Demmig-Adams et al., 2008). Fm and Fo are the minimal and maximal fluorescence intensity in dark-adapted cells while F' and Fm' are the steady-state and maximum fluorescence intensities during the light treatment.

77 K fluorescence spectra between 650 and 800 nm were recorded with an excitation at 440 nm (Luminescence Spectrometer LS 50, Perkin Elmer). The cells analyzed were previously harvested in the exponential phase of the selected condition (light, carbon source) and resuspended in a buffer containing 60% w/v glycerol. Afterwards they were placed in a special sample holder containing liquid nitrogen. To induce state I the cells were previously treated with DCMU (3-(3,4-dichlorophenyl)-1,1-dimethylurea, 20 μM) and incubated in dim light for 15 minutes. In detail, the inhibitor DCMU blocks the electron flow at the PSII level thus blocking the reduction of the PQ pool. In this scenario PQ pool is over–oxidized by PSI, a signal that induces LHCII migration from PSI to PSII (state I) (Takahashi et al., 2013).

Spectroscopic measurements. The spectroscopic analysis was performed in vivo using a Joliot-type spectrophotometer (JTS-10, Biologic, France). WT, *pgrl1*, *Δnd4*, *Δnd4pgrl1* were harvested in the exponential phase and resuspended in TMP medium supplemented with 20% Ficoll. For these measurements the final cellular concentration was 7 x 10^6 cell/ml for CL-adapted cells and 25 x 10^6 cell/ml for HL-adapted cells. Photosystems stoichiometry and photosynthetic electron flows were performed measuring the Electrochromic Shift (ECS) spectral change in intact cells, representing a shift in the pigment absorption bands associated with changes in the membrane potential and consequently photosystems activity (Bailleul et al, 2010). ECS was measured as the difference between the signals at 520 and 546 nm (the positive and negative peaks of the ECS signal, respectively) to eliminate minor additional spectral changes that were associated with the membrane potential. DCMU (3-(3,4-dichlorophenyl)-1,1-dimethylurea, 20 μM) and HA

(hydroxylamine, 1.5 mM) inhibitors were employed to irreversibly block PSII charge separation, respectively acting as acceptor and donor side inhibitors of PSII. Photosystems (PSI/PSII) ratios were estimated from changes in the amplitude of the fast phase of the ECS signal upon excitation with a saturating single turnover flash. This amplitude recorded at 500 µs evaluate the PSI+PSII and the PSI contribution to the ECS signal in control and in DCMU HA poisoned cells, respectively. PSI was estimated as the fraction of the signal that was insensitive to these inhibitors (Bailleul et al., 2010).

TEF (total electron flow) and AEF (alternative electron flow) were measured assessing the relaxation kinetics of the ECS signal in the dark after a steady-state illumination (Sacksteder et al., 2000; Joliot & Joliot, 2002). In details, cells were illuminated with saturating actinic light until the achievement of an ECS steady-state level (15 sec at 940 µE m^{-2} s^{-1}). The signal at steady state is proportional to transmembrane potential generated by PS II, cytochrome b6f complex, PS I and from transmembrane potential dissipation by the plastid ATP synthase. When light is switched off, PS activities stop immediately, while ATP synthase and cytochrome b6f complex activities remain unchanged. The difference between the slopes of the ECS signal measured in the light (S_L) and after the light is switched off (S_D) is proportional to the rate of PS I and PS II photochemistry (Figure 3A) (Joliot and Joliot, 2002; Alric, 2014). When cell are poisoned with DCMU (20 µM) the difference between the slopes is proportional to the rate of PSI and so is used to estimate AEF activity. The rate calculated from the relaxation kinetics are normalized to the amplitude of one charge separation by PSI and PSII (for the TEF normalization) or by PSI (for the CEF normalization), that can be determined monitoring the ECS absorbance change induced by a single turnover saturating flash in untreated and DCMU+HA-poisoned cells, respectively (Joliot and Joliot, 2002; Bailleul et al., 2015). Data are directly expressed in electrons transferred per second per Photosystem I and II ($e^{-}{\cdot}s^{-1}{\cdot}PS^{-1}$) for TEF and per Photosystem I ($e^{-}{\cdot}s^{-1}{\cdot}PSI^{-1}$) for AEF.

The PSI content was evaluated based on the maximum change in the absorption of P_{700}^{+} in cells treated with DCMU and DBMIB (dibromothymoquinone, 300 µM) at a saturating actinic light (2050 µmoles of photons $m^{-2}s^{-1}$, 630 nm) in an equal number of cells (25 x 10^6 cells/ml). Under these conditions, re-reduction of P_{700}^{+} through photosynthetic electron flow is largely slowed down, thereby allowing to evaluate the full extent of photo-oxidizable P_{700} (Alric et al., 2010).

Results

Photosynthetic efficiency is strongly impaired at high light intensities in Δnd4pgrl1

The first step in this work was to characterize photosynthetic activity in *Δnd4pgrl1,* compared to control strains, in order to start to explain rescued phenotype. For that, different approaches can be employed like the estimation of the maximum quantum yield of PSII (Fv/Fm) and its photochemistry efficiency (ϕPSII) thanks to chlorophyll fluorescence analysis using a pulse modulated amplitude fluorometer (Dual PAM). Fv/Fm is an indicator of photosynthetic performance that can estimate the extent of PSII photoinhibition and ϕPSII measures the proportion of the light absorbed by PSII used in photochemistry and so is an indicator of the overall photosynthetic efficiency (Maxwell and Johnson, 2000).

The maximal photochemical efficiency of PSII for dark-adapted cells (Fv/Fm) grown at control light intensities shows a slight decrease in both *pgrl1* and *Δnd4*, as observed also in previous studies at least for *pgrl1* (Tolleter et al., 2011; Kukuczka et al., 2014; Dang et al., 2014). In the double mutant *Δnd4pgrl1* the decrease is larger than in *pgrl1* and similar to that observed in Δ*nd4* mutant (Figure 2A). The same measurement for cells grown at high light intensities showed a decrease in Fv/Fm in all genotypes due to PSII photoinhibition caused by the strong illumination. This effect however is more evident in single mutants than in WT and was especially strong for *Δnd4pgrl1* where the decrease is particularly important showing an additive effect of the two mutations (Figure 2B).
When ϕPSII was measured in CL cells the values observed at different light intensity were comparable between all genotypes (Figure 2C). On the contrary, in cells grown at HL, ϕPSII was drastically different in the various genotypes analyzed. Interestingly, the most drastic phenotype is observed for Δ*nd4pgrl1* where ϕPSII is very low at all illumination intensities considered (Figure 2D). For single mutants, Δ*nd4* and *pgrl*1, a reduced photosynthetic efficiency is noticed with a stronger decrease for *pgrl1*. According to these results, in HL, Δ*nd4pgrl1* Fv/Fm and ϕPSII surprising did not correlate with the growth phenotype.

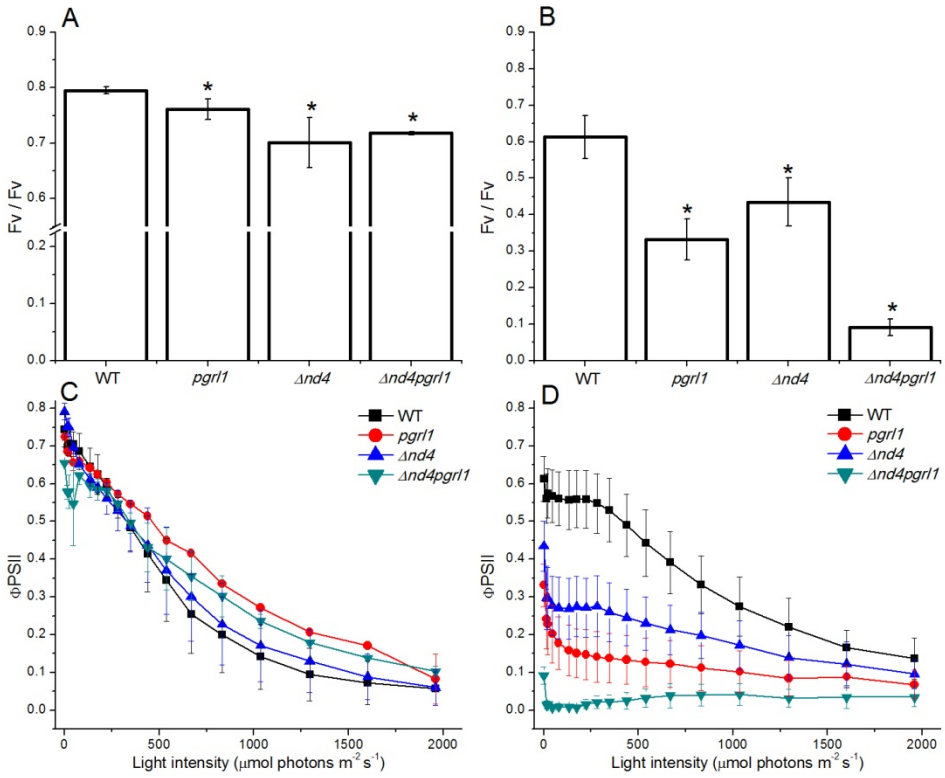

Figure 2. Photosystem II functionality monitored with PAM fluorometry. A-B) Maximum photosystem II quantum yield (Fv/Fm) measured after 30 minutes of dark adaptation of WT, *pgrl1*, *Δnd4* and Δ*nd4pgrl1* strains grown photoautotrophically in CL (A) and HL (B) conditions. Data are expressed as the means ±SD, n = 4. Values that significantly differ from WT are marked with an asterisk (ANOVA, p value <0.05). C-D) Dependence of photochemical efficiency, estimated as the parameter ϕPSII, on illumination intensity for WT, *pgrl1*, *Δnd4* and Δ*nd4pgrl1* strains grown photoautotrophically in CL (C) and HL (D) conditions. The measurements were performed using one-minute steps of increasing light intensity (n = 4 ± SD). WT is represents by black squares , *pgrl1* by red circles , *Δnd4* by blue up triangles and Δ*nd4pgrl1* by green down triangles.

Alternative Electron transports are increased in Δnd4pgrl1

As efficiency of PSII is completely down, the question is which compensation of photosynthetic pathway is involved in the rescue phenotype. Another possibility to measure photosynthetic efficiency is to assess electron transfer rate (ETR) across the thylakoid membrane. This is possible using a technique that measures changes in the carotenoid electrochromic band shift (ECS). A steady-state level of the ECS signal was reached pre-illuminating the samples for 15 sec with saturating light (940 μE m^{-2} s^{-1}). At the end of this light treatment the post-illumination decay rate was analyzed (Figure 3A). The contribution of alternative electron transports to the total ETR can be evaluated as the fraction of electron flow that was insensitive to DCMU addition (see Materials and Methods) (Joliot and Joliot, 2002; Allorent et al., 2015).

This technique compared to fluorescence technique, has the advantage to allow assessing electron transports from both photosystems and to quantifying their contribution to the total transport. Using this approach the total electron flow (TEF) in CL cells is shown to only have slight differences in all genotypes (Figure 3B), as estimated above from the PSII activity. In particular the same TEF was observed in WT and *Δnd4pgrl1* while *Δnd4* showed significantly higher value compared to WT. These measurements, however, allowed us observing that in *Δnd4pgrl1* alternative electron transports, independent from PSII, are more active than in the other genotypes.

These same measurements showed interesting features when performed in the different genotypes grown at HL intensities. Both *pgrl1* and *Δnd4* TEF and AEF did not show significant differences with WT. On the contrary, *Δnd4pgrl1* showed a higher total electron flow than all other genotypes and this is largely due to an increased alternative electron flow (Figure 3C). Also *pgrl1* showed high PSII independent ETR, consistently with their low ϕPSII. On the contrary WT and *Δnd4* showed significant contribution of PSII dependent ETR.

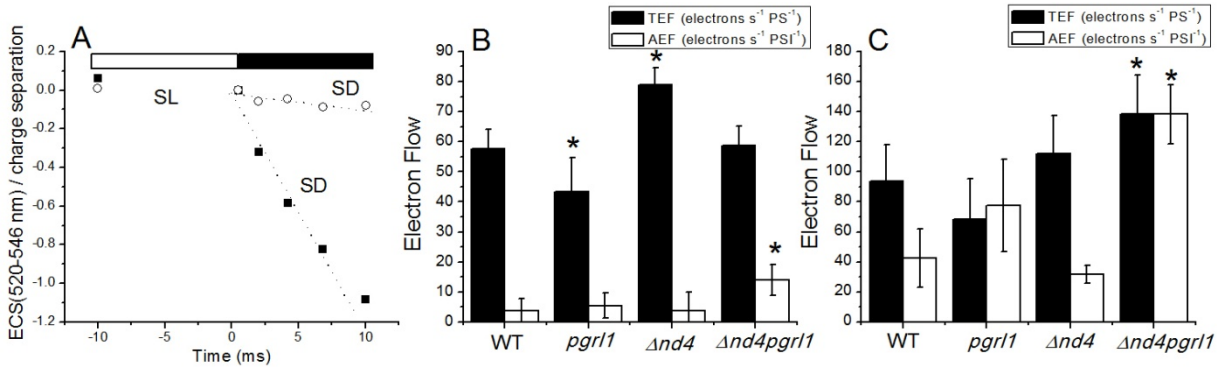

Figure 3. Electron transport rate measured by ECS. A) Changes in the electrochromic shift (ECS) signal measured at 520 - 546 nm during a transition from light to dark in *C. reinhardtii* intact cells. Total (TEF) and alternative electron flow (AEF) activities were measured by following ECS relaxation without (black square) and after addition of DCMU (white circles) to the samples. The difference between the slope in the light (S_L) and the slope in the dark (S_D) is used to measure the different electron transport rate. B-C) Electron transport rates evaluated from ECS relaxation kinetics. The rates are normalized to the amplitude of one charge separation by PSI and PSII (TEF, black bar) or by PSI (AEF, white bar). The data refer to the rates measured in WT, *pgrl1*, *Δnd4* and *Δnd4pgrl1* strains grown photoautotrophically in CL (n = 6 ± SD) (B) and in HL condition (n = 4 ± SD) (C). Values that significantly differ from WT are marked with an asterisk (ANOVA, p value <0.05).

Composition of the photosynthetic apparatus

In order to investigate the mutations effect on composition of the photosynthetic apparatus we quantified PSI/PSII ratio in vivo monitoring the ECS absorbance change induced by a single turnover saturating flash in the presence of untreated and DCMU+HA-poisoned cells (Figure 4A) (Bailleul et al., 2010). In addition, we compared these results to the value obtained from PSI quantification, measured in vivo using P700 absorbance in the presence of DBMIB, DCMU and saturating light (Figure 5A).

In CL condition, *Δnd4pgrl1* PSI/PSII ratio was increased compared to other strains (Figure 4B). However, PSI quantification measurements showed that the absolute amount of PSI was slightly decreased compared to WT (Figure 5B). This suggests that the alteration of PSI/PSII ratio is attributable to a PSII decrease, as suggested also by Fv/Fm decrease (Figure 2) and this already at CL intensities. The same consideration can be done also for the *Δnd4* single mutant although it showed a lower PSI/PSII ratio compared to the double mutant. Additionally the *pgrl1* mutant showed a significant decrease in the ratio compared to other genotypes, probably related to the strong decrease in the total amount of PSI observed (Figure 5B).

In HL, PSI/PSII decreased till reaching 1 : 1 ratio in *pgrl1* and *Δnd4pgrl1* mutant while it remained similar to WT in the *Δnd4* mutant (Figure 4C). In *pgrl1* and *Δnd4pgrl1* PSI quantity dropped considerably in strong irradiation (Figure 5C). It's worth mentioning that in *Δnd4pgrl1* the strong decrease in PSI total amount was accompanied by a severe impairment of the PSII efficiency compared to other strains. Despite this *Δnd4pgrl1* had better growing performance in HL conditions and an alternative electron flow increased.

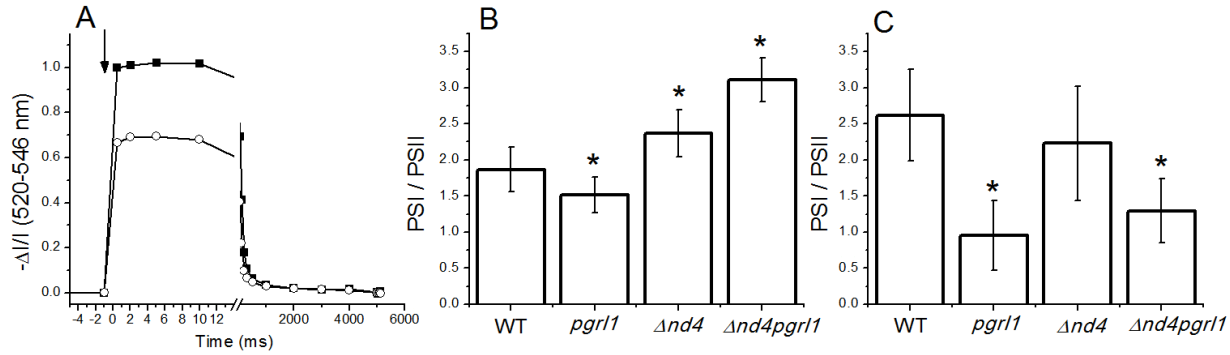

Figure 4. Evaluation of the PSII/PSI ratio in *C. reinhardtii* intact cells based on the ECS signal. A) ECS kinetics in WT *C. reinhardtii* intact cells grown in photoautotrophy and in CL. The ECS signal is presented as the 520 nm minus the 546 nm absorption signal. The signal was induced using a saturating flash (arrow). The solid squares and empty circles represent, respectively, the kinetics of untreated cells (where PSII and PSI both contribute to the ECS signal) and of DCMU and HA-poisoned cells (where only PSI is responsible for the ECS signal). B-C) PSII/PSI ratio obtained from the ECS signal in WT, *pgrl1*, *Δnd4* and *Δnd4pgrl1* strains grown in photoautotrophy and (B) CL (n = 7 ± SD) or in (C) in HL (n = 5 ± SD). Values that significantly differ from WT are marked with an asterisk (ANOVA, p value <0.05).

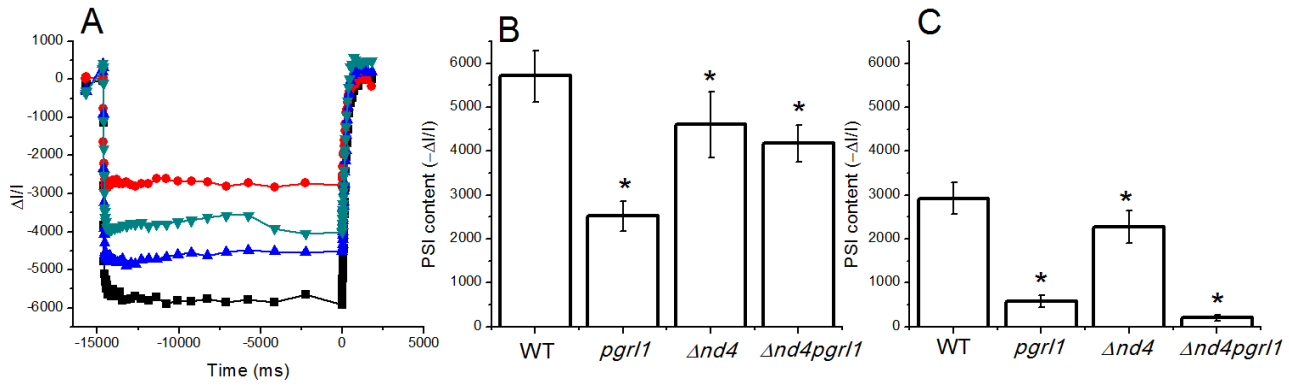

Figure 5. PSI quantification in *C. reinhardtii* intact cells based on the P700 signal. A) Representative traces of PSI quantification from oxidized P700 in the presence of DCMU and DBMIB and a saturating light of 940 µE m^{-2} s^{-1}. The measurements were performed considering an equal number of cells. The different genotypes shown were grown photoautotrophically in CL TMP condition. WT (black squares), *pgrl1* (red circles), *Δnd4* (blue up triangles) and *Δnd4pgrl1* (green down triangles). PSI content obtained from the P700 signal in cells grown in TMP medium in CL condition (B) and HL conditions (C). The data are expressed as the means ±SD, n = 4. Values that significantly differ from WT are marked with an asterisk (ANOVA, p value <0.05).

Another confirmation about the ratio of each photosystem could be exemplified with the 77K fluorescence analysis (Figure 6). Indeed, the fluorescence at liquid nitrogen temperature from algal cells shows distinct spectral bands for chlorophyll linked in PSII or in PSI. Such differences can give important information regarding the amount of the two photosystems but also the identification of state transitions, which is a regulatory mechanism for balancing the distribution of light energy between the photosystems.

Data from 77K fluorescence analysis measured in *Δnd4pgrl* in CL conditions showed a strong increase in the absorption cross section of *Δnd4pgrl1* PSI compared to the other genotypes (Figure 6A). This results was in part expected considering the higher PSI/PSII ratio already measured for the double mutant in CL (Figure 4B). To distinguish between the contribution of PS stoichiometry and state transition in such fluorescence peak we performed the same measurements in the presence of DCMU to favor state I and so enhance LHCII migration from PSI to PSII (Figure 6B). Also in the DCMU-treated condition *Δnd4pgrl1* maintained an higher fluorescence peak related to PSI compared to other genotypes confirming the higher PSI/PSII ratio data derived from ECS measurements. However the variation in the PSI fluorescence emission evidenced comparing untreated and DCMU treated 77K spectra in *Δnd4pgrl1* was higher compared to the slight variations found in single mutants (Figure 6B). This observation suggests the presence in *Δnd4pgrl1* of a stronger DCMU-induced LHCII migration that could imply a state transition favored in state II in the double mutant grown at CL. In HL conditions all the genotypes except WT showed a decreased PSI fluorescence emission peak compared to CL (Figure 6C), consistent with the already described decrease in PSI/PSII ratio (Figure 4C) and PSI total amount (Figure 5C). Moreover also in HL *Δnd4pgrl1* showed the higher PSI fluorescence peak. This is presumably related to a strong LCHII association to PSI (state II) considering that in this condition its PSI/PSII ratio is almost

equal to 1. *pgrl1* and *Δnd4* mutants, instead, despite displaying a PSI/PSII ratio respectively equal and higher than *Δnd4pgrl1* in HL, showed a low PSI fluorescence peak suggesting the presence of state I.

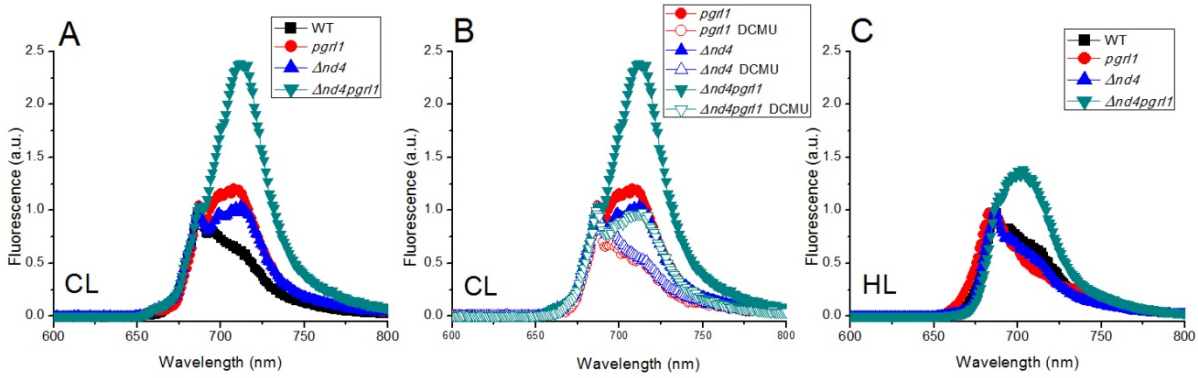

Figure 6. Relative absorption cross section of PSI and II monitored with low-temperature emission spectra. The 77 K fluorescence spectra have been normalized to their amplitude at 685 nm. Two mains peaks are resolved at 685 nm and in the 710 nm region, which respectively correspond to fluorescence by PSII and PSI. A) The 77 K fluorescence spectra of the different genotypes grown photoautotrophically in CL are shown. B) Comparison between the 77 K fluorescence spectra in untreated (filled symbols) and DCMU-poisoned (empty symbols) cells grown in CL. C) The 77 K fluorescence spectra of the different genotypes grown photoautotrophically in HL are shown. WT (black squares), pgrl1 (red circles), Δnd4 (blue up triangles) and Δnd4pgrl1 (green down triangles).

Discussion and Conclusions

Light energy is the primary source of energy for photosynthetic organisms and chloroplast is supposed to be the major player in conversion of light into chemical energy. However, there are emerging evidences in different organisms supporting an important role of organelles crosstalk in metabolism regulation. In this work we show that the addition of a mitochondrial mutation in a *C. reinhardtii* mutant already affected in the chloroplastic pathway such as PGRL1 rescues their photosensitivity in HL. Growth curves clearly show that *Δnd4pgrl1* double mutant grown photoautotrophically in HL conditions presents higher growth rate if compared with the *pgrl1* single mutant (Figure 1C). Interestingly the growth phenotypes don't correlate with the fluorescence measurements, focused mostly on the PSII performance (Figure 2). Fv/Fm and ϕPSII fluorescence parameters, indeed, are strongly decreased in Δ*nd4pgrl1* grown in HL at difference with the other genotypes. Thus, despite the mitochondrial mutation rescues the growth phenotype in HL, the double mutant presents an extensive impairment of the PSII activity.

How the double mutant could grow in this complex scenario is explained observing the different electron transport rate using ECS measurements. *Δnd4pgrl1* in CL and HL presents higher AEF compared with the other genotypes. In HL almost all the TEF measured is composed of alternative transport, with no PSII-related electron transport (Figure 3C). Moreover this increased electron transport around PSI seems to be confirmed by 77K data which suggest a strong LHCII association

to PSI (state II) in the double mutant both in CL and HL conditions (Figure 6). The extent of such association seems to be even higher than that already described for mitochondrial mutants (Cardol et al., 2009). Therefore the introduction of *Δnd4* mutation affects strongly the photosynthetic electron transport and the balance between PSII and I activity. In particular the photosynthetic system in the double mutants seems to rely mostly on PSI activity. The increase in the PSI/PSII ratio in the double mutant grown in CL seems to account for this acclimation to a PSI-related photosynthesis while in HL this is not observed due to the strong photosystems photoinhibition (Figure 5).

Interestingly it is shown that when the double mutant is grown in CL condition PSII rather than PSI is damaged at difference from what observed in the *pgrl1* (Figure 2-5). High light condition, instead, induces a similar PSI inhibitory effect on *Δnd4pgrl1* and *pgrl1* (Figure 5C) but at the same time has a stronger detrimental effect on the PSII of single rather than double mutant (Figure 2). Despite the strongly compromised photosystems efficiency *Δnd4pgrl1* manages to survive showing better growing performance in HL conditions. These results suggest that the few active PSI measured in HL conditions can be involved in an increased AEF able to efficiently replace the PSII-related electron flow. Also the *pgrl1* mutant in HL shows higher AEF/TEF ratio even if with lower values if compared to *Δnd4pgrl1.* Despite this, *pgrl1* photosynthesis remains still partially related to PSII activity, as shown by Fv/Fm and ϕPSII parameters (Figure 2). The only partial switch to a PSI-related photosynthesis in HL pgrl1 mutant and the needs to continuously recover PSII light-damage to foster PSII activity could be the reason why this mutant shows worst growing performance.

These evidences clearly show how mitochondria plays a seminal influence on photosynthetic efficiency, playing a major influence in photosynthetic electron transport chain. The principal actors of this crosstalk are still under debate and could be related likely to reducing power trafficking from mitochondrion to chloroplast.

References

Allorent, G., Osorio, S., Vu, J.L., Falconet, D., Jouhet, J., Kuntz, M., Fernie, A.R., Lerbs-Mache, S., Macherel, D., Courtois, F., and Finazzi, G. (2015). Adjustments of embryonic photosynthetic activity modulate seed fitness in Arabidopsis thaliana. New Phytol. **205**: 707–19.

Alric, J. (2014). Redox and ATP control of photosynthetic cyclic electron flow in Chlamydomonas reinhardtii: (II) involvement of the PGR5-PGRL1 pathway under anaerobic conditions. Biochim. Biophys. Acta **1837**: 825–34.

Alric, J., Lavergne, J., and Rappaport, F. (2010). Redox and ATP control of photosynthetic cyclic electron flow in Chlamydomonas reinhardtii (I) aerobic conditions. Biochim. Biophys. Acta **1797**: 44–51.

Bailleul, B. et al. (2015). Energetic coupling between plastids and mitochondria drives CO2 assimilation in diatoms. Nature **524**: 366–9.

Bailleul, B., Cardol, P., Breyton, C., and Finazzi, G. (2010). Electrochromism: A useful probe to study algal photosynthesis. Photosynth. Res. **106**: 179–189.

Baurain, D., Dinant, M., Coosemans, N., and Matagne, R.F. (2003). Regulation of the alternative oxidase Aox1 gene in Chlamydomonas reinhardtii. Role of the nitrogen source on the expression of a reporter gene under the control of the Aox1 promoter. Plant Physiol. **131**: 1418–30.

Cardol, P., Alric, J., Girard-Bascou, J., Franck, F., Wollman, F.-A., and Finazzi, G. (2009). Impaired respiration discloses the physiological significance of state transitions in Chlamydomonas. Proc. Natl. Acad. Sci. U. S. A. **106**: 15979–84.

Cardol, P., Gloire, G., Havaux, M., Remacle, C., Matagne, R., and Franck, F. (2003). Photosynthesis and state transitions in mitochondrial mutants of Chlamydomonas reinhardtii affected in respiration. Plant Physiol. **133**: 2010–20.

Dang, K.-V., Plet, J., Tolleter, D., Jokel, M., Cuiné, S., Carrier, P., Auroy, P., Richaud, P., Johnson, X., Alric, J., Allahverdiyeva, Y., and Peltier, G. (2014). Combined increases in mitochondrial cooperation and oxygen photoreduction compensate for deficiency in cyclic electron flow in Chlamydomonas reinhardtii. Plant Cell **26**: 3036–50.

Demmig-Adams, B., Adams III, W.W., Barker, D.H., Logan, B.A., Bowling, D.R., and Verhoeven, A.S. (2008). Using chlorophyll fluorescence to assess the fraction of absorbed light allocated to thermal dissipation of excess excitation. Physiol. Plant. **98**: 253–264.

Dutilleul, C., Driscoll, S., Cornic, G., De Paepe, R., Foyer, C.H., and Noctor, G. (2003). Functional mitochondrial complex I is required by tobacco leaves for optimal photosynthetic performance in photorespiratory conditions and during transients. Plant Physiol. **131**: 264–75.

Harris, E., Stern, D., and Witman, G. (1989). The chlamydomonas sourcebook.

Jans, F., Mignolet, E., Houyoux, P.-A., Cardol, P., Ghysels, B., Cuiné, S., Cournac, L., Peltier, G., Remacle, C., and Franck, F. (2008). A type II NAD(P)H dehydrogenase mediates light-independent plastoquinone reduction in the chloroplast of Chlamydomonas. Proc. Natl. Acad. Sci. U. S. A. **105**: 20546–51.

Johnson, X. et al. (2014). Proton gradient regulation 5-mediated cyclic electron flow under ATP- or redox-limited conditions: a study of ΔATpase pgr5 and ΔrbcL pgr5 mutants in the green alga Chlamydomonas reinhardtii. Plant Physiol. **165**: 438–52.

Joliot, P. and Joliot, A. (2002). Cyclic electron transfer in plant leaf. Proc. Natl. Acad. Sci. U. S. A. **99**: 10209–14.

Kukuczka, B., Magneschi, L., Petroutsos, D., Steinbeck, J., Bald, T., Powikrowska, M., Fufezan, C., Finazzi, G., and Hippler, M. (2014). Proton Gradient Regulation5-Like1-Mediated Cyclic

Electron Flow Is Crucial for Acclimation to Anoxia and Complementary to Nonphotochemical Quenching in Stress Adaptation. Plant Physiol. **165**: 1604–1617.

Lecler, R., Vigeolas, H., Emonds-Alt, B., Cardol, P., and Remacle, C. (2012). Characterization of an internal type-II NADH dehydrogenase from Chlamydomonas reinhardtii mitochondria. Curr. Genet. **58**: 205–16.

Maxwell, K. and Johnson, G.N. (2000). Chlorophyll fluorescence - A practical guide. J. Exp. Bot. **51**: 659–668.

Petroutsos, D., Terauchi, A.M., Busch, A., Hirschmann, I., Merchant, S.S., Finazzi, G., and Hippler, M. (2009). PGRL1 participates in iron-induced remodeling of the photosynthetic apparatus and in energy metabolism in Chlamydomonas reinhardtii. J. Biol. Chem. **284**: 32770–81.

Remacle, C., Cardol, P., Coosemans, N., Gaisne, M., and Bonnefoy, N. (2006). High-efficiency biolistic transformation of Chlamydomonas mitochondria can be used to insert mutations in complex I genes. Proc. Natl. Acad. Sci. U. S. A. **103**: 4771–6.

Salinas, T., Larosa, V., Cardol, P., Maréchal-Drouard, L., and Remacle, C. (2014). Respiratory-deficient mutants of the unicellular green alga Chlamydomonas: a review. Biochimie **100**: 207–18.

Takahashi, H., Clowez, S., Wollman, F.-A., Vallon, O., and Rappaport, F. (2013). Cyclic electron flow is redox-controlled but independent of state transition. Nat. Commun. **4**: 1954.

Tikkanen, M., Mekala, N.R., and Aro, E.-M. (2014). Photosystem II photoinhibition-repair cycle protects Photosystem I from irreversible damage. Biochim. Biophys. Acta **1837**: 210–5.

Tolleter, D. et al. (2011). Control of hydrogen photoproduction by the proton gradient generated by cyclic electron flow in Chlamydomonas reinhardtii. Plant Cell **23**: 2619–30.

CHAPTER D2

FLAVODIIRON PROTEINS IN *PHYSCOMITRELLA PATENS* FUNCTION AS AN ELECTRON SINK PROTECTING PHOTOSYSTEM I FROM PHOTOINHIBITION

FLAVODIIRON PROTEINS IN *PHYSCOMITRELLA PATENS* FUNCTION AS AN ELECTRON SINK PROTECTING PHOTOSYSTEM I FROM PHOTOINHIBITION [1]

Abstract

Photosynthetic organisms harvest sunlight to fuel the photosynthetic electron transport, producing NADPH and ATP to support the cell metabolism. In a highly dynamic natural environment photosynthetic organisms evolved multiple mechanisms to modulate flow of excitation energy and electrons. Flavodiiron (FLV) proteins in cyanobacteria use electrons from the photosynthetic transport to reduce oxygen and play a role in protection from light stress. These proteins were lost during evolution of land plants but are still present in non vascular plants, as the moss *Physcomitrella patens*. We generated *P. patens* mutants depleted in FLV and showed these proteins are active as an electron sink downstream of Photosystem I. Measurement of electron transport showed that they play a major role particularly in the first seconds after a sudden change in light intensity, when for a few seconds they are the major sink for electrons from PSI. When exposed to fluctuating light FLV mutants showed light sensitivity and PSI photoinhibition, demonstrating their biological role as a safety valve for excess electrons in dynamic light. FLV absence in mutants was, in part, compensated by increased cyclic electron flow, suggesting that their biological role may have been substituted in vascular plants by this other mechanism of alterative electron flow.

Introduction

In oxygenic photosynthesis, light energy absorbed by the two photosystems (PSI and PSII) drives a linear electron flow (LEF) powering the transfer of electrons from water to $NADP^+$, generating NADPH. This is also coupled with the generation of an electrochemical proton gradient across the thylakoid membranes which leads to the synthesis of ATP that, together with NADPH, is then used for downstream carbon fixation reactions. In a highly dynamic natural environment photosynthetic organisms evolved multiple mechanisms to modulate the flow of electrons, diverting them from LEF to other electron pathways according to metabolic constraints (Külheim et al., 2002; Allahverdiyeva et al., 2015b).

[1] In the lab *flv* KO lines of the moss *P. patens* have been generated and the physiological role of FLV proteins in *P. patens* has been characterized. In this project, my work was mainly focused on the application of ECS techniques to analyze *flv* KO mutants phenotype and this part of the project is the main subject of this chapter.
In addition to myself, Caterina Gerotto, Alessandro Alboresi and Tomas Morosinotto contributed to the work (Department of Biology, University of Padova). The *P .patens* FLV project was also a collaboration with Eva-Mari Aro lab (Department of Biochemistry, Molecular Plant Biology, University of Turku, Finland).

These alternative pathways most likely modulate ATP/NADPH ratio depending on metabolic demand and have been also suggested to create futile cycles which avoid over-reduction of photosynthetic electron transport chain, preventing photo-damage in case of excess light intensity (Peltier et al., 2010). The cyclic electron transport, for example, redirects electrons from PSI to PQ or Cytb6f (Arnon and Chain, 1975), contributing to proton gradient and therefore to ATP synthesis. In cyanobacteria Flavodiiron proteins (known as FLV in photosynthetic organisms) have been identified as an additional component involved in electron transport. The model species *Synechocystis*, for example, harbors four FLV proteins which work as FLV1/3 and FLV2/4 heterodimers. FLV1 and FLV3 proteins function in the light-dependent reduction of O2, using NADPH and producing water, a process also known as the Mehler-like reaction (Helman et al., 2003; Allahverdiyeva et al., 2013). They were found crucial for protecting photosynthetic apparatus, and PSI in particular, under a light regime mimicking natural light conditions (Allahverdiyeva et al., 2013). On the contrary, FLV2 and FLV4 function in the photo-protection of PSII and are not involved in O2 photo-reduction (Zhang et al., 2009, 2012; Bersanini et al., 2014; Helman et al., 2003). FLV were found expressed also in Chlamydomonas reinhardtii where their accumulation was up-regulated in WT and pgrl1 depleted cells upon changes in CO2 and/or light intensities (Dang et al., 2014; Jokel et al., 2015). Despite their crucial role in photoprotection in cyanobacteria, *FLV* genes were lost during evolution of land plants (Zhang et al., 2009; Peltier et al., 2010; Allahverdiyeva et al., 2015a) but they are still found in some non vascular land plants such as in the moss *Physcomitrella patens.* In *P. patens* two coding sequences for FLV proteins, named FLVA and FLVB (Zhang et al., 2009; Peltier et al., 2010), are present in the genome. When compared to *Synechocystis* sequences, *P. patens* FLV protein sequences showed high similarity with cyanobacterial isoforms, particularly FLV1/3 isoforms (Helman et al., 2003). Mosses diverged from vascular plants early after land colonization and for this reason they are considered a model organism also to study the evolution of photosynthetic organisms (Rensing et al., 2008). In order to investigate FLV biological function and obtain insights on the evolution of alternative electron transports upon land colonization, *P. patens* mutants depleted in FLVA and FLVB proteins have been generated.

Materials and Methods

Plant growth and light treatment

Protonemal tissue of *P. patens*, Gransden wild-type (WT) strain, *flva* KO, *flvb* KO and *flva/b* double knock-out (KO) lines were grown in minimum PpNO3 media in controlled conditions : 24°C, 16 h light/8 h dark photoperiod and a light intensity of 50 µE m^{-2} s^{-1} (Control Light, CL), and analyzed after 10 days of growth. For fluctuating light treatment, 3 days old plates grown in CL were moved to a fluctuating light regime (cycles of 5 minutes at 25 µE m^{-2} s^{-1} and 1 minute at 800 µE m^{-2} s^{-1}) during the light phase of photoperiod and analyzed after 7 days in FL (10 days old plates).

Fluorescence and P700 measurement with Dual-PAM

In vivo chlorophyll fluorescence and oxidized $P700^+$ absorption signals were measured simultaneously at room temperature with a Dual PAM-100 fluorometer (Walz) in *P. patens* WT and mutant tissues grown for 10 days in minimum medium. Before measurements, plates were dark-adapted for 40 minutes at room temperature and the maximum fluorescence signal (Fm) and Fv/Fm were determined applying a saturating light pulse (6000 µmol m^{-2} s^{-1}). The detection of maximum $P700^+$ signal (Pm value) was determined with 10 sec of FR light followed by saturation pulse application. For induction/recovery kinetics actinic light was set to 540 µmol m^{-2} s^{-1} (saturating actinic light), 175 µmol m^{-2} s^{-1} or 50 µmol m^{-2} s^{-1}. PSII and PSI parameters were calculated as following: Fv/Fm as (Fm-Fo)/Fm, Y(II) as (Fm'-F)/Fm', relative QA reduction as F'/Fm, Y(I) as 1 - Y(ND) - Y(NA), Y(NA) as (Pm-Pm')/Pm.

Spectroscopic analysis

Spectroscopic analysis on WT, *flva* KO and *flvb* KO lines was performed on 10-day old intact tissues in vivo using a JTS-10 spectrophotometer (Biologic, France). Before measurements, plates were dark-adapted for 40 minutes at room temperature. Relative amount of functional photosynthetic complexes and electron transport rate were evaluated measuring the Electrochromic Shift (ECS) spectral change (Bailleul et al., 2010). ECS is a shift in the pigment absorption bands that is linearly correlated to the number of light-induced charge separations within the reaction centers (Witt, 1979). PSI and PSII content was estimated from changes in the amplitude of the ECS signal (at 520 minus 546 nm) upon excitation with a single turnover xenon flash. After recording the ECS signal of the sample in Hepes 20mM pH 7.5/KCl 10mM buffer, PSII contribution was evaluated from the decrease in the amplitude of the signal in samples poisoned with DCMU (3-(3,4-dichlorophenyl)-1,1-dimethylurea, 80µM) and HA (hydroxylamine, 4mM) which irreversibly block PSII charge separation. PSI was instead estimated as the fraction of the signal that was insensitive to these inhibitors, allowing the calculation of the relative PSI/PSII ratio (Figure 6A) (Simionato et al., 2013).

Total electron transport was instead evaluated from the relaxation of ECS signal in the dark after a light treatment with saturating light (940 µE m^{-2} s^{-2}) (Allorent et al., 2015). Saturating actinic light was given for about 5 minutes but it was temporarily switched off for 30 ms several times to allow an estimation of the slopes of ECS changes in the light (S_L) and in the dark (S_D) and consequently the photosynthetic rate at different time points during the illumination period (Figure 1A) (Joliot and Joliot, 2002). ECS in fact depends on trans-thylakoid membrane potential that under light treatments is positively sustained by the activity of PSII, cytb6f and PSI and negatively counteracted by ATPase proton pumping. Once in the dark PSII and PSI are almost immediately inactivated and therefore the direct comparison between the ECS in the light and in the dark provide information on the electron transport rate (Figure 1B). The total electron transport is therefore calculated by S_L-S_D divided for PSI turnovers measured assessing fast ECS signal after single-turnover flash, as described previously for the photosystems stoichiometry technique. The same electron transport rate measurement was also performed in DCMU treated samples, to inhibit PSII activity and evaluated the contribution of CEF (Figure 1).

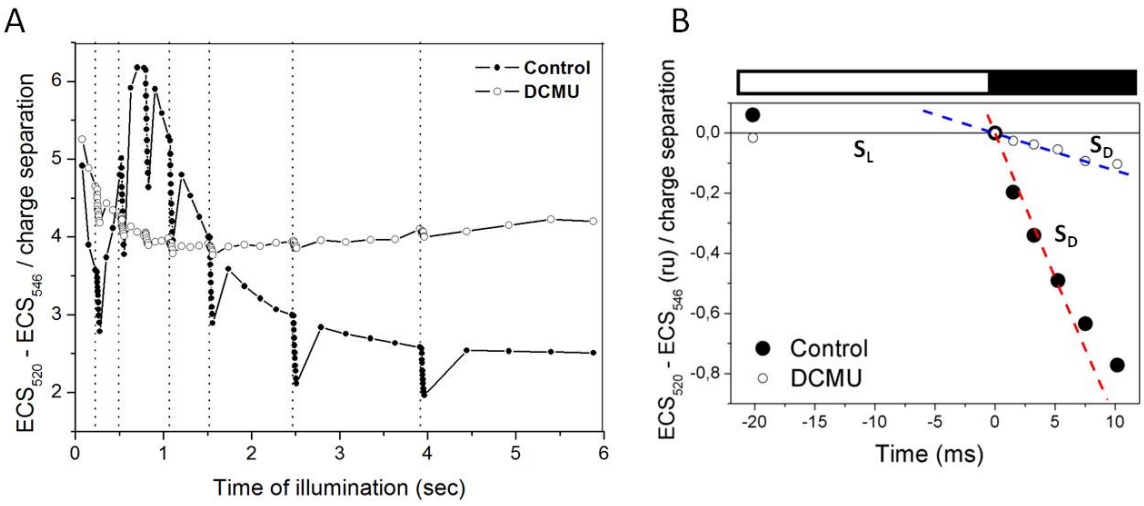

Figure 1. Kinetics of membrane potential measured by ECS spectral changes. A) Example of ECS kinetic employed for calculation of ETR in *P. patens*. ECS was measured at 940 µE m^{-2} s^{-2} as the difference between ECS values at 520 and 546nm and normalized for PSI turnover. Detail of the first 6 seconds of the kinetic of WT untreated (Control, filled circles) and DCMU-treated (DCMU, empty circles) is shown. Dotted vertical lines indicate the time points where actinic light was temporarily switched off for 30ms to allow S_L and S_D calculation. B) Detail of S_L and S_D calculation. The difference between the slope in the light (S_L) and the slope in the dark (S_D) normalized to PSI turnover in Control sample is used to measure the total electron transport rate (black circles, red dotted line). The analyses were repeated in DCMU treated samples (empty circles, blue dotted line), where PSII is inactivated and therefore the difference in ECS is exclusively PSI-dependent and reflects the cyclic electron transport rates.

Results

Photosynthetic efficiency of flv KO lines

Molecular characterization of *P. patens flva* KO and *flvb* KO mutants showed that depletion in FLVA or FLVB strongly affected also the accumulation of the other isoform at the protein level. This strongly suggests that *P. patens* FLVA and FLVB form a heterodimer, as their cyanobacteria homologues (Allahverdiyeva et al., 2013). Despite this similarity, nothing is still known about the biological role of FLV proteins in photosynthetic eukaryotes as *P. patens*. In order to shed light on this mechanisms, *P. patens* mutants depleted in FLV proteins were grown in control light conditions (CL, 50 µE m^{-2} s^{-1}) and the photosynthetic efficiency of both photosystems was analyzed. It should be first mentioned that *flva* KO and *flvb* KO showed no major differences in their growth, pigments content nor photosynthetic quantum yield evaluated as variable fluorescence from dark adapted tissues (Fv/Fm) with respect to WT (Table 1).

Table 1. Fv/Fm and pigment content of WT and *flva* KO and *flvb* KO lines grown in CL conditions.

	Fv/Fm	**Chla/b**	**Chl/Car**
WT CL	0.79 ± 0.02	2.51 ±0.07	3.64 ± 0.1
***Flva* KO line CL**	0.78 ±0.02	2.57 ±0.11	3.34 ±0.1
***Flvb* KO line CL**	0.78 ±0.01	2.60 ±0.09	3.56 ±0.14

A powerful method to assess PSII photosynthetic activity *in vivo* is the analyses of Chl fluorescence quenching kinetics with PAM device during a treatment with saturating light (540 µE m^{-2} s^{-2}). In the

mutants, PSII yield, determined as Y(II) (Figure 2A), was decreased with respect to WT upon actinic light was switched on, but differences gradually disappeared during the illumination period and no more significant differences were found after 1 minute of light treatment. The relative QA (PSII primary electron acceptor) reduction in non steady-state condition was also calculated from Chl fluorescence (Grieco et al., 2012; Suorsa et al., 2012). In *flv* KO samples after 30 seconds of illumination QA pool appeared more reduced than in the WT suggesting an higher reduction of the electron transport chain (Figure 2B). Conversely, during steady state illumination, no major differences were detected among the 3 genotypes tested. The same PAM device can be also used to analyze simultaneously PSI efficiency monitoring $P700^{+}$ absorption signal (Grieco et al., 2012). Also PSI quantum yield, Y(I), evaluated during the light-induction kinetic, was impaired in *flva* KO and *flvb* KO when actinic light was turned on (Figure 2C). The decreased PSI yield was most likely the result of a strong acceptor side limitation in FLV depleted strains, as observed from the higher Y(NA) values at the beginning of illumination in *flv* KO lines (Figure 2D). This result indicates that the electrons carriers downstream of PSI are in a reduced form and cannot accept electron from PSI. As above for PSII, the alterations in PSI parameters with respect to WT occurred at the beginning of light exposure but were progressively recovered during illumination. The same differences in PSII and PSI related parameters were also detected when analyses were performed employing dim actinic light (50 µE m^{-2} s^{-2}) (data not shown), suggesting that FLV absence causes a temporary decrease in photosynthetic efficiency which is mainly a consequence of a dark-to-light transition regardless the light intensity applied.

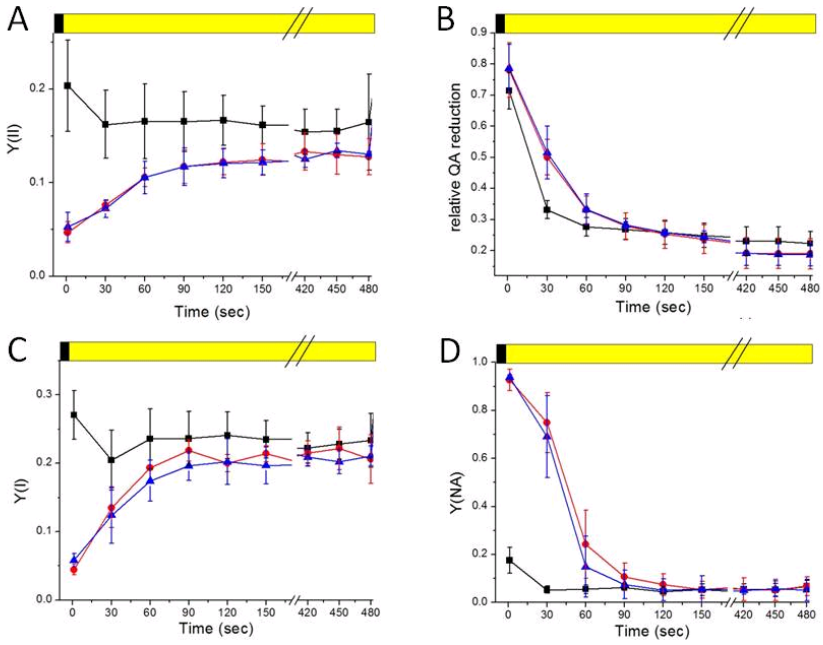

Figure 2. Evaluation of PSII and PSI efficiency in WT, *flva* KO and *flvb* KO *P. patens* lines grown in CL. A-B) Chl fluorescence kinetics were used to calculate parameters describing PSII photosynthetic efficiency. A) Y(II) represents the PSII quantum yield, B) the relative QA reduction parameter. C-D) $P700^{+}$ absorption signal was recorded simultaneously with the Chl fluorescence. C) Y(I) and D) Y(NA) parameters, showing PSI quantum yield of energy conversion and acceptor side limitation, respectively, are reported. In all panels, WT is shown in black, *flva* KO line in red and *flvb* KO line in blue. Upper yellow bar indicate the period where actinic light is on (540 µE m^{-2} s^{-2} in this analyses), black bar the period of dark. Data are reported as average ± SD of 3 independent biological replicates.

flv KO lines showed altered electron transport at the onset of illumination

The results previously described clearly shown that in FLV depleted lines grown in CL conditions the photosynthetic efficiency of the two photosystems was strongly compromised in the first seconds after the onset of illumination. This was mostly due to an over-reduction of the electrons acceptors downstream of the two photosystems that reduce the electron flow compared to WT (Figure 1). Therefore, In order to get a deeper view on the photosynthetic efficiency in the complex scenario of FLV depleted lines, we investigated photosynthetic electron transport rate (ETR) in the different genotypes. A powerful method to evaluate ETR is the analyses of electrochromic shift (ECS), following an approach employed in different photosynthetic organisms including *P. patens* (Bailleul et al., 2010; Kukuczka et al., 2014; Allorent et al., 2015; Joliot and Joliot, 2002). Usually, ETR is measured from dark relaxation kinetics of the ECS signal after a steady-state illumination as also reported in this thesis in Chapter D1. Here instead we need a time-resolved kinetics to better evaluated the differences of electron transport also at the very beginning of illumination. Therefore, we employ a protocol already used for plants (Joliot and Joliot, 2002) which allows ETR calculation at several points during illumination. To this aim, light was temporary switched off for a very short time period (30ms) during actinic light treatment allowing to calculate S_L and S_D and therefore ETR as detailed in Materials and Methods and Fig.1.

In WT plants, ETR showed a peak at approximately 1 second from the beginning of the actinic light treatment (Figure 3). This peak showed a dependence on the actinic light intensity employed in the analyses and, while it was hardly detectable using a very dim light (45 µE m^{-2} s^{-1}), it reached the highest values using saturating light intensities (940 µE m^{-2} s^{-1}). After this fast peak in electron transport, in WT ETR steadily increased during the illumination, likely following the activation of the Calvin-Benson cycle, and reached a final value of ≈ 65 e-/s^{-1} after 5 minutes of illumination with 940 µE m^{-2} s^{-1} (Figure 3A). This steady state value decreased with light, reaching ≈ 40 and 20 e-/s^{-1} after 5 minutes at 150 and 45 µE m^{-2} s^{-1}, respectively.

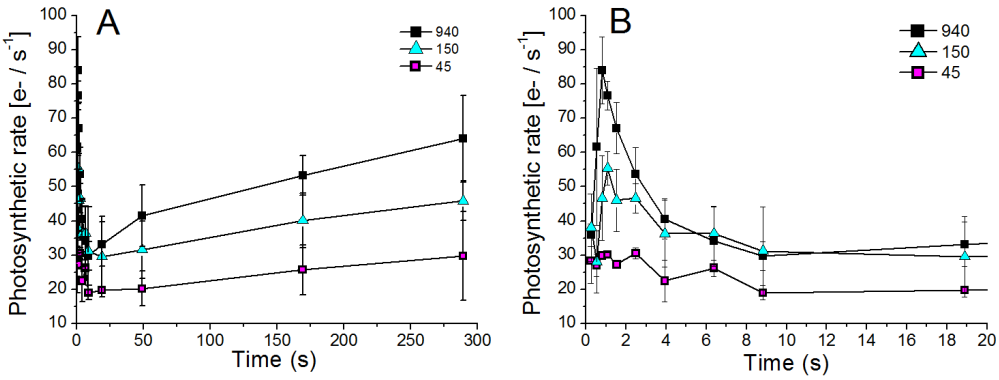

Figure 3. Photosynthetic electron transport rate calculated from ECS analyses at different actinic light in intact tissues of WT *P. patens*. A) Total photosynthetic rates was measured using three different actinic lights, 45 (pink squares), 150 (light blue triangles) and 940 µE m^{-2} s^{-1} actinic light (black squares) on dark-adapted WT plants grown under control light conditions. B) Detail of the first 20 seconds of illumination. The different samples are normalized to PSI turnovers. Data are average ±SD of three independent biological replicates.

When the same measurement was performed on *flva* KO and *flvb* KO plants, this first peak of ETR was completely absent even employing the saturating light (940 µE m^{-2} s^{-1}, Figure 4A-B). After 5 seconds from the beginning of the actinic light treatment, however, there was no more significant difference in ETR between the three genotypes. *flva* and *flvb* KO showed the same progressive increase of ETR as WT plants, reaching the same value after 5 minutes of illumination (Figure 4A). The same analyses were also performed in the presence of DCMU, which inhibits PSII activity and therefore allows to evaluate cyclic electron transport rates around PSI (CEF) (Joliot and Joliot, 2002; Allorent et al., 2015) (Figure 4C-D). In WT DCMU-treated plants ETR is very low while, on the contrary, *flva* KO and *flvb* KO lines showed for the first 20 seconds of illumination a sustained electron transport activity (Figure 4D). In the following phase, instead, the three genotypes showed an equal steady state electron transport with CEF representing less than 10% of total electron transport (≈ 2-5 e-/sec) at the end of the light period (Figure 4C), a value consistent with analyses already performed in other plant species and *P. patens* (Bendall and Manasse, 1995; Joliot and Joliot, 2002; Kukuczka et al., 2014).

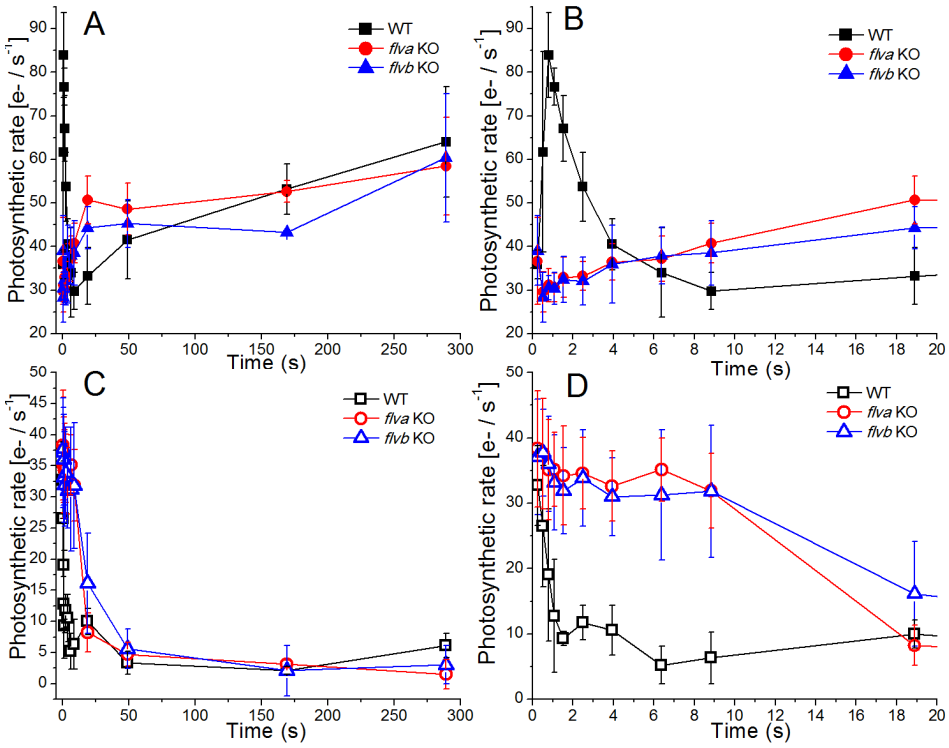

Figure 4. Photosynthetic electron transport rate calculated from ECS analyses in WT, *flva* KO and *flvb* KO *P. patens* lines. Photosynthetic rate was measured using an actinic light at 940 µE m^{-2} s^{-1} in lines grown in CL conditions. A-B) Comparison of total electron transport rate measured in untreated samples of the three different lines. Complete kinetic and the first 20 seconds of these kinetics are shown in A and B, respectively. C-D) Cyclic electron transport rate measured in the presence of DCMU. Complete kinetic and the first 20 seconds of these kinetics are shown in C and D, respectively. WT (black squares), *flva* KO (red circles) and *flvb* KO (blue triangles). Filled symbols: no-add sample, empty symbols: DCMU-treated samples. The different samples are normalized to PSI turnovers. Data are average ±SD of three independent biological replicates.

The direct comparison of untreated and DCMU treated samples of the same genotype (Figure 5), allowed an estimation of CEF contribution in the total electron flow (TEF) measured in the untreated samples. In the first 20 seconds of illumination in WT CEF represents only a small fraction of TEF. The remaining main portion is related to the linear electron flow coming from PSII (Figure 5A). On the contrary, in *flva* KO and *flvb* KO CEF is the main electron pathway in the first 10 seconds of illuminations representing the majority of TEF (Figure 5B). After this high CEF contribution decreases reaching the same WT values. This evidence suggests FLV absence in mutants is, in part, compensated by increased cyclic electron flow.

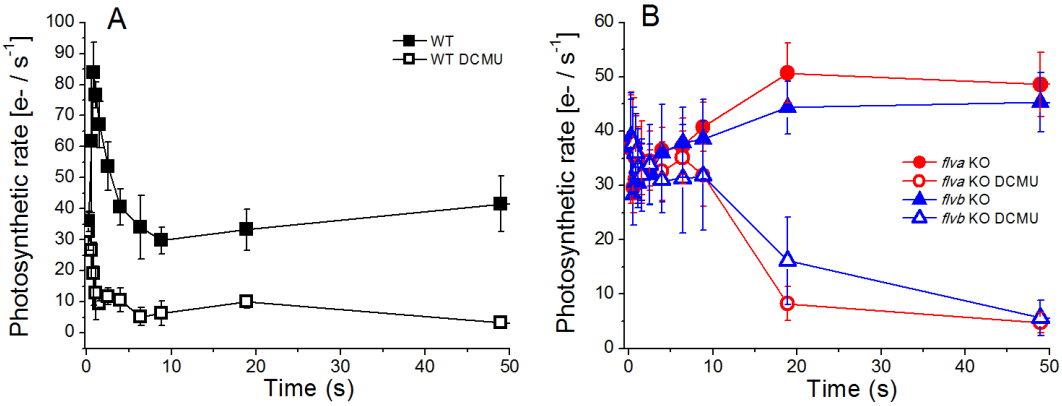

Figure 5. Comparison between TEF and CEF of the same genotype in *P. patens*. Photosynthetic rate was measured using an actinic light at 940 µE m^{-2} s^{-1} in lines grown in CL conditions. The detail of the first 50 seconds of illumination is shown. Comparison between ETR measured in untreated and DCMU-treated in WT lines (A) and *flv* KO lines (B). WT (black squares), *flva* KO (red circles) and *flvb* KO (blue triangles). Filled symbols: no-add sample, empty symbols: DCMU-treated samples. Samples are normalized to PSI turnover. Note the different Y-axis in the different panels. Data are average ±SD of 3 independent replicates.

flv KO show increased PSI photodamage in fluctuating light

Results above clearly shows that FLV proteins play a fundamental role in the light phase following a dark-to-light transition. Additional analyses with Dual PAM device also showed that the same alterations in PSI and PSII parameters were detected in case of a switch from low to high light intensities. Therefore, to further investigate the physiological relevance of FLV in terms of protection from light stress, WT, *flva* KO and *flvb* KO mosses grown for 3 days in control light conditions (CL) were moved to a light regime, called fluctuating light (FL), where treatment with saturating light (1 minute at 800 µE m^{-2} s^{-1} every 6 minutes) were regularly provided during growth at LL (25 µE m^{-2} s^{-1}). After 7 days of growth in FL the functional status of photosystems was evaluated quantifying both PSII yield (Fv/Fm parameter) and photosystems stoichiometry, estimated using electrochromic shift (ECS) after a single turnover flash (Figure 6) (Bailleul et al., 2010), as detailed in Materials and Methods. In control samples grown in constant control light, the 3 genotypes showed no significant differences in PSII efficiency or in PSI/PSII ratio. Upon growth in FL, WT maintained its PSII efficiency while PSI/PSII ratio slightly diminished (Figure 6B-C). On the contrary, *flva* KO and *flvb* KO plants in FL showed a lower PSII efficiency compared to WT. The most striking difference, however, was on PSI/PSII ratio, which was dramatically decreased for both *flva* KO and *flvb* KO (Figure 6B), from ≈1.3 in CL to ≈0.4. Given the slight decrease of PSII

efficiency, the strong decrease in PSI/PSII ratio suggests an even higher reduction in PSI activity, likely damaged by the light treatment. This idea was confirmed by western blot analysis, showing D1 amount, the subunit which is the main target of photoinhibition in PSII core, was almost unaffected while PsaD immunodetected bands were fainter in *flv* KO plants grown in FL compared to WT FL and samples grown in CL, suggesting a partial degradation of the damaged PSI (Figure 6D).

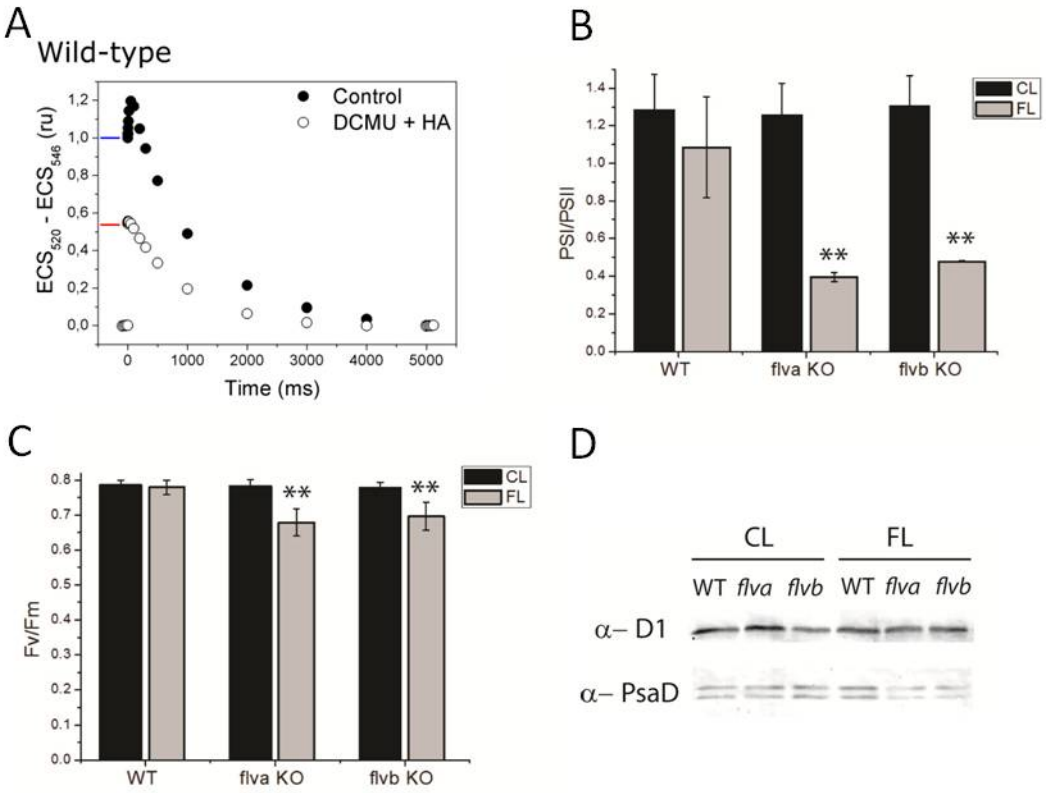

Figure 6: Evaluation of PSI/PSII ratio and Fv/Fm after fluctuating light growth. A) Representative kinetics of the ECS measured in intact tissues of WT *P. patens* grown under fluctuating light. The single-turnover xenon flash was applied at time t = 0 ms. Black dots are untreated samples. White dots are samples treated with DCMU and hydroxylamine (HA). The blue lines indicate the level of PSII + PSI charge separation in control samples and the red lines indicate the level PSI charge separation in treated samples. Those values were used to calculate the photosystems stoichiometry. B-C) PSI/PSII ratio assayed by ECS spectral changes after single turnover xenon flashes and Fv/Fm ratio determined with a Dual Pam 100 (B) of CL and FL growth plates. ** indicates values significantly different from WT CL (t test, p>0.01). D) Western blot quantifications of PSII core subunit D1 and PSI core subunit PsaD on thylakoids extracts from CL and FL grown plates of WT and *flva* KO and *flvb* KO genotypes. The same Chl amount is loaded in each lane (1 Chl µg).

Discussion and Conclusions

FLV are a major electron sink at the onset of light protecting PSI from light induced damage

To face with natural variable light condition and avoid photodamage, photosynthetic organisms have to modulate light harvesting and electron transport reactions to maintain an optimal compromise between photosynthetic efficiency and protection from light excess. This picture is

true for all oxygenic photosynthetic organisms although they use differentiated mechanisms. FLV proteins, for example, play a prominent role in photosynthesis regulation in cyanobacteria. However, they disappeared during evolution of vascular plants but they are still found expressed in green algae (Dang et al., 2014; Jokel et al., 2015) and in the moss *P. patens*. Mosses diverged from vascular plants early after land colonization and have received an increasing attention as model organisms because they represent the evolutionary link between algae and plants (Rensing et al., 2008). In this work we investigate the physiological role of FLV proteins in *P. patens* exploiting the availability of mutants depleted either in FLVA or FLVB proteins.

We show that *P. patens* FLV-depleted lines grown in constant optimal light showed no distinguishable phenotype in photosynthetic apparatus pigmentation and functionality compared to WT mosses (Table 1). Conversely, in case of a sudden change in light irradiation, such as a dark-light transition, *flva* and *flvb* KO are characterized by a strong PSI acceptor side limitation with the consequent decrease of PSI yield in the first minute after the onset of illumination (Figure 2C-D). These results suggest a possible role of FLV in *P. patens* as electron sink downstream of PSI. This is further confirmed by measurement of ETR, showing a peak of electron transport in WT at the onset of illumination which is completely absent in *flv* KO lines (Figure 4). FLV therefore acts as the main pathway aimed at consuming the reducing power and thus downsizing the NAPH/$NADP^+$ ratio (Figure 7A) in case of an abrupt light increase, as a dark-light transition. Conversely, if FLV are absent (figure 7B), the lack of this sink leads to an over-reduction of the PSI downstream pathways lowering the ability to oxidize P700. The consequence is that LEF is temporally blocked, as confirmed by the ETR measurements in *flv* KO lines (Figure 4B), leading to an over-reduction of the whole transport chain which has a negative effect also in the PSII photosynthetic efficiency. This is highlighted by the transient lowering of PSII yield, Y(II), and the reduced redox status of PQ pool (Figure 2A-B), as already suggested in other species (Allahverdiyeva et al., 2013). Noteworthy FLV role seems to be restricted to situations in which the Calvin–Benson cycle is partially inactivated and therefore alternative electron acceptors after PSI are needed, as in a dark-light transition or in abrupt increase in illumination. Under steady state illumination (fig 7C-D), instead, once the Calvin Benson cycle is activated, the consumption of ATP and reducing power by this pathway allowed the recovery of electron transport, abolishing the differences among WT and *flv* KO (Figure 4). This is confirmed also by the fact that in all the analyses performed (Figure 2-5) no differences were retrieved between WT and mutant lines in steady state illumination, nor alterations in growth in constant control light (CL). On the contrary, the deleterious effects of photosynthetic electron chain saturation and the role of FLV in protecting PSI from light induced damage is clear when mutants are obliged to grown in a dynamic light regime (FL). Indeed, *flv* KO lines manifest a slight decrease in PSII efficiency (Fv/Fm) but at the same time a strong decrease in PSI/PSII ratio (Figure 6). These results suggest that the main target of photoinhibition in these conditions is PSI, as confirmed by western blot analysis showing a partial PSI degradation (Figure 6D). Therefore FLV pathway, reducing PSI acceptor side limitation, contributes to limit the light induced damage on PSI. This photoprotective activity is fundamental considering that PSI has not an efficient repair mechanism, such as PSII, and in excess light conditions can be irreversibly damaged.

It is worth mentioning that the ETR in the first seconds of illumination is also qualitatively different in *flv* KO with respect to WT. While in the latter LEF has the major contribution in total electron

transport from the beginning of the illumination, as demonstrated by the very low activity of CEF (Figure 5A), in *flv* KO CEF is sustained for the first 10 seconds of illumination and represent the greatest part of electron transport (Figure 5B). Therefore the sustained activity of CEF in mutants, exactly when FLV proteins should manifest their higher activity, suggests that this alternative pathway could act compensating the absence of FLV proteins in *P. patens.* Thus FLV and CEF electron pathway seems to play a similar role as electron sink downstream PSI. This partial redundancy in a moss, a species representing and intermediate step during evolution going from cyanobacteria, where FLV have a key role in protection from light stress, to vascular plants, which lost FLV genes, provides further proofs supporting the hypothesis that during evolution of land plants FLV role was substituted by PGR5/PGRL1 mediated CEF, an idea already suggested in recent literature (Allahverdiyeva et al., 2015b).

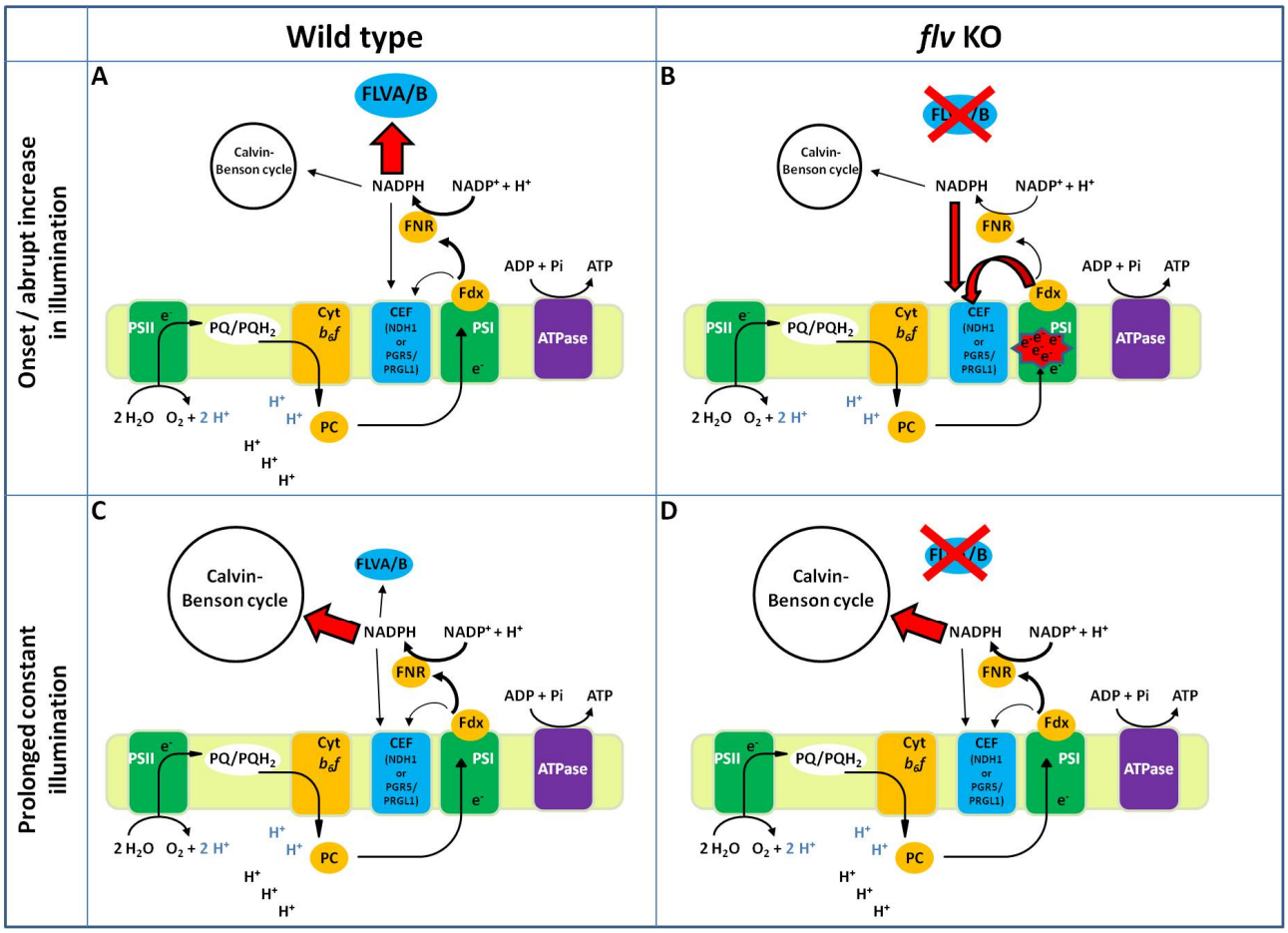

Figure 7: Schematic model representing FLV role in the photosynthetic apparatus in Wild type and *flv* KO *P. patens* lines. A-B) Mechanism of action during the first seconds after the onset of illumination or after an abrupt increase in illumination. C-D) Mechanism of action during a prolonged constant illumination.

References

Allahverdiyeva, Y., Isojärvi, J., Zhang, P., and Aro, E.-M. (2015a). Cyanobacterial Oxygenic Photosynthesis is Protected by Flavodiiron Proteins. Life **5**: 716–743.

Allahverdiyeva, Y., Mustila, H., Ermakova, M., Bersanini, L., Richaud, P., Ajlani, G., Battchikova, N., Cournac, L., and Aro, E.-M. (2013). Flavodiiron proteins Flv1 and Flv3 enable cyanobacterial growth and photosynthesis under fluctuating light. Proc. Natl. Acad. Sci. U. S. A. **110**: 4111–6.

Allahverdiyeva, Y., Suorsa, M., Tikkanen, M., and Aro, E.-M. (2015b). Photoprotection of photosystems in fluctuating light intensities. J. Exp. Bot. **66**: 2427–36.

Allorent, G., Osorio, S., Vu, J.L., Falconet, D., Jouhet, J., Kuntz, M., Fernie, A.R., Lerbs-Mache, S., Macherel, D., Courtois, F., and Finazzi, G. (2015). Adjustments of embryonic photosynthetic activity modulate seed fitness in Arabidopsis thaliana. New Phytol. **205**: 707–19.

Arnon, D.I. and Chain, R.K. (1975). Regulation of ferredoxin-catalyzed photosynthetic phosphorylations. Proc. Natl. Acad. Sci. U. S. A. **72**: 4961–5.

Bailleul, B., Cardol, P., Breyton, C., and Finazzi, G. (2010). Electrochromism: A useful probe to study algal photosynthesis. Photosynth. Res. **106**: 179–189.

Bendall, D.S. and Manasse, R.S. (1995). Cyclic photophosphorylation and electron transport. Biochim. Biophys. Acta - Bioenerg. **1229**: 23–38.

Bersanini, L., Battchikova, N., Jokel, M., Rehman, A., Vass, I., Allahverdiyeva, Y., and Aro, E.-M. (2014). Flavodiiron protein Flv2/Flv4-related photoprotective mechanism dissipates excitation pressure of PSII in cooperation with phycobilisomes in Cyanobacteria. Plant Physiol. **164**: 805–18.

Dang, K.-V., Plet, J., Tolleter, D., Jokel, M., Cuiné, S., Carrier, P., Auroy, P., Richaud, P., Johnson, X., Alric, J., Allahverdiyeva, Y., and Peltier, G. (2014). Combined increases in mitochondrial cooperation and oxygen photoreduction compensate for deficiency in cyclic electron flow in Chlamydomonas reinhardtii. Plant Cell **26**: 3036–50.

Grieco, M., Tikkanen, M., Paakkarinen, V., Kangasjärvi, S., and Aro, E.-M. (2012). Steady-state phosphorylation of light-harvesting complex II proteins preserves photosystem I under fluctuating white light. Plant Physiol. **160**: 1896–910.

Helman, Y., Tchernov, D., Reinhold, L., Shibata, M., Ogawa, T., Schwarz, R., Ohad, I., and Kaplan, A. (2003). Genes Encoding A-Type Flavoproteins Are Essential for Photoreduction of O2 in Cyanobacteria. Curr. Biol. **13**: 230–235.

Jokel, M., Kosourov, S., Battchikova, N., Tsygankov, A.A., Aro, E.M., and Allahverdiyeva, Y.

(2015). Chlamydomonas Flavodiiron Proteins Facilitate Acclimation to Anoxia During Sulfur Deprivation. Plant Cell Physiol. **56**: 1598–607.

Joliot, P. and Joliot, A. (2002). Cyclic electron transfer in plant leaf. Proc. Natl. Acad. Sci. U. S. A. **99**: 10209–14.

Kukuczka, B., Magneschi, L., Petroutsos, D., Steinbeck, J., Bald, T., Powikrowska, M., Fufezan, C., Finazzi, G., and Hippler, M. (2014). Proton Gradient Regulation5-Like1-Mediated Cyclic Electron Flow Is Crucial for Acclimation to Anoxia and Complementary to Nonphotochemical Quenching in Stress Adaptation. Plant Physiol. **165**: 1604–1617.

Külheim, C., Agren, J., and Jansson, S. (2002). Rapid regulation of light harvesting and plant fitness in the field. Science **297**: 91–3.

Peltier, G., Tolleter, D., Billon, E., and Cournac, L. (2010). Auxiliary electron transport pathways in chloroplasts of microalgae. Photosynth. Res. **106**: 19–31.

Rensing, S.A. et al. (2008). The Physcomitrella genome reveals evolutionary insights into the conquest of land by plants. Science **319**: 64–9.

Simionato, D., Block, M.A., La Rocca, N., Jouhet, J., Maréchal, E., Finazzi, G., and Morosinotto, T. (2013). The response of Nannochloropsis gaditana to nitrogen starvation includes de novo biosynthesis of triacylglycerols, a decrease of chloroplast galactolipids, and reorganization of the photosynthetic apparatus. Eukaryot. Cell **12**: 665–76.

Suorsa, M., Järvi, S., Grieco, M., Nurmi, M., Pietrzykowska, M., Rantala, M., Kangasjärvi, S., Paakkarinen, V., Tikkanen, M., Jansson, S., and Aro, E.-M. (2012). PROTON GRADIENT REGULATION5 is essential for proper acclimation of Arabidopsis photosystem I to naturally and artificially fluctuating light conditions. Plant Cell **24**: 2934–48.

Witt, H.T. (1979). Energy conversion in the functional membrane of photosynthesis. Analysis by light pulse and electric pulse methods. The central role of the electric field. BBA Rev. Bioenerg. **505**: 355–427.

Zhang, P., Allahverdiyeva, Y., Eisenhut, M., and Aro, E.-M. (2009). Flavodiiron proteins in oxygenic photosynthetic organisms: photoprotection of photosystem II by Flv2 and Flv4 in Synechocystis sp. PCC 6803. PLoS One **4**: e5331.

Zhang, P., Eisenhut, M., Brandt, A.-M., Carmel, D., Silén, H.M., Vass, I., Allahverdiyeva, Y., Salminen, T.A., and Aro, E.-M. (2012). Operon flv4-flv2 provides cyanobacterial photosystem II with flexibility of electron transfer. Plant Cell **24**: 1952–71.

CHAPTER D3

PHOTOSYNTHESIS IN EXTREME ENVIRONMENTS: RESPONSES TO DIFFERENT LIGHT REGIMES IN THE ANTARCTIC ALGA *KOLIELLA ANTARCTICA*

Published in
Physiologia Plantarum

PHOTOSYNTHESIS IN EXTREME ENVIRONMENTS: RESPONSES TO DIFFERENT LIGHT REGIMES IN THE ANTARCTIC ALGA *KOLIELLA ANTARCTICA*

Nicoletta La Rocca*, Katia Sciuto, Andrea Meneghesso, Isabella Moro, Nicoletta Rascio and Tomas Morosinotto

Dipartimento di Biologia, Università di Padova, Padova 35121, Italy
*Corresponding author, e-mail: nicoletta.larocca@unipd.it
Received 8 April 2014; revised 7 July 2014 doi:10.1111/ppl.12273

Abstract

Antarctic algae play a fundamental role in polar ecosystem thanks to their ability to grow in an extreme environment characterized by low temperatures and variable illumination. Here, for prolonged periods, irradiation is extremely low and algae must be able to harvest light as efficiently as possible. On the other side, at low temperatures even dim irradiances can saturate photosynthesis and drive to the formation of reactive oxygen species. Colonization of this extreme environment necessarily required the optimization of photosynthesis regulation mechanisms by algal organisms. In order to investigate these adaptations we analyzed the time course of physiological and morphological responses to different irradiances in *Koliella antarctica*, a green microalga isolated from Ross Sea (Antarctica). *Koliella antarctica* not only modulates cell morphology and composition of its photosynthetic apparatus on a long-term acclimation, but also shows the ability of a very fast response to light fluctuations. *Koliella antarctica* controls the activity of two xanthophyll cycles. The first, involving lutein epoxide and lutein, may be important for the growth under very low irradiances. The second, involving conversion of violaxanthin to antheraxanthin and zeaxanthin, is relevant to induce a fast and particularly strong non-photochemical quenching, when the alga is exposed to higher light intensities. Globally *K. antarctica* thus shows the ability to activate a palette of responses of the photosynthetic apparatus optimized for survival in its natural extreme environment.

1. ANTARCTIC ALGA AND ITS EXTREME VARIABLE ENVIRONMENT

Antarctic sea ice may appear, at first glance, as a frozen white desert devoid of life. However, this harsh environment represents a unique habitat colonized by both autotrophic and heterotrophic extremophile microorganisms such as bacteria, algae and animals. Different microalgal species can thrive in this hard habitat and during the summer their blooms represent the energy base of the marine food chain, thus playing a fundamental role in the carbon cycle for the polar ecosystems (Andreoli et al., 2000; Anesio and Laybourn-Parry, 2012). In the Antarctic summer algae are exposed to almost constant water temperature (between +5 and −1.8°C) and salinity (34.4‰),

while light irradiance can be highly variable going from very low in the water column under the ice sheets (<10 μE m^{-2} s^{-1}) to much higher intensities (250 μE m^{-2} s^{-1}) within the shallowly mixed water of the sea (Mock and Valentin, 2004; Arrigo et al., 2010). When the sea water surface freezes in autumn, planktonic organisms are trapped in the high salty water within the brine channels generated from expelled salts during ice crystal formation. During winter season this microbial community therefore lives in the interstices of ice semisolid matrix. This leads microorganisms to be almost confined to an habitat quite different from the one of the summer sea water, characterized by low temperature (between −10 and −1.8°C), high salinity (from 35 to 150‰) and very low light (even less than 1 μE m^{-2} s^{-1}) (Thomas and Dieckmann, 2002). Growth or even survival in this extreme habitat requires a complex set of physiological and metabolic adaptations, which, in the case of algae, necessarily affect also the photosynthetic apparatus. As for all photosynthetic organisms, light is an environmental parameter with a major relevance as it provides all the energy supporting metabolism, but it may also represent a source of stress in unfavorable conditions (Li et al., 2009). In particular, antarctic algae must have not only adapted to efficiently capture and use the scarce radiation during winter, but also to acclimate to higher and fluctuating illumination during the summer. In addition very low temperatures decrease efficiency of key steps of photosynthesis such as diffusion of electron transporters and carbon fixation and, as a consequence, even a dim illumination can be in excess with respect to the photochemical ability and it drives to the formation of reactive oxygen species (ROS) leading to oxidative stress (Takahashi and Murata, 2008).

In this work we investigated the long- and short- term responses to variations of irradiance intensity in the green microalga *Koliella antarctica* that was isolated from samples of sea water collected at 3m of depth near the Italian Station of Terra Nova Bay (Ross Sea, Antarctica) (ANDREOLI et al., 1991). Previous studies showed the high morphological and physiological plasticity of *K. antarctica* and its ability to cope with wide ranges of different physical environmental parameters such as temperature (from −2°C to over 20°C, with maximum growth rate at 15°C), salinity (from 0 to 70‰) and light (from 8 to 60 μmol photons m−2 s−1) (Fogliano et al., 2010), as well as its capability to survive for a long time (over 60 days) in the dark (Baldisserotto and Ferroni, 2005). We analyzed the response of this microalga to exposure to different light intensities, evidencing several responses activated with a different timescales.

2. *KOLIELLA ANTARCTICA* ACCLIMATED TO DIFFERENT LIGHT REGIMES

In order to investigate the acclimation response in the microalga *K. antarctica* its growth performances at different light intensity were assessed. Growth kinetics obtained were slightly different, with HLc (high light culture, 150 μE m^{-2} s^{-2}) growing slower than LLc (low light culture, 15 μE m^{-2} s^{-2}) (Figure 1A). In both cases, after 9 weeks from the inoculum cultures were still in a linear growth phase with a very low specific growth rate (μ =0.022 and 0.021 for LLc and HLc, respectively). Analyses with electron microscopy (Figure 1B-C) also showed morphological differences depending on growth light intensity evidencing in HL cells the presence of a thicker cell wall and smaller chloroplasts with a lower number of thylakoid membranes compared with LL acclimated cells (Figure 1B-C). Moreover, cells of HLc showed the presence of large storage bodies

with low electron-density which suggested a lipid nature, as confirmed by fluorescence microscopy experiments after cell incubation with lipid specific Nile red dye (data not shown).

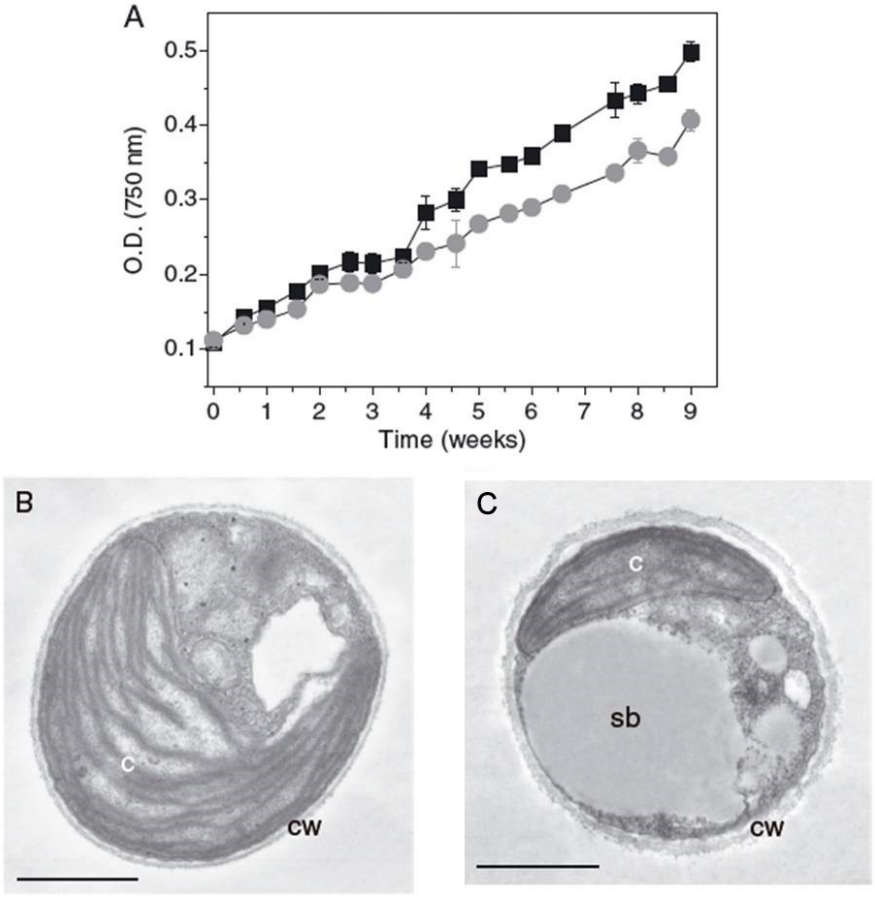

Figure 1. (A) Growth kinetics of *Koliella antarctica* cultures acclimated to the two different light intensities, LL (black squares) and HL (gray circles) (n=4). B-C) Micrographs at the transmission electron microscope of *Koliella antarctica* cells acclimated to LL (B) or to HL (C). HLc show smaller chloroplasts (c), thicker cell wall (cw) and the presence of large storage bodies (sb) if compared with LLc (scale bars=1 μm).

3. LONG-TERM ACCLIMATION OF PHOTOSYNTHETIC APPARATUS TO DIFFERENT ILLUMINATION

Electron microscopy clearly evidenced a reduction in the number of thylakoid membranes in HLc in comparison with LLc. This was confirmed by Chl content in the cells, four times higher in LL compared with HL (Table 1A). It was interesting to observe that Chl a/b ratio was higher in HLc cells, suggesting a decreased number of antenna proteins associated to photosystems. Strong illumination also induced a higher relative Car accumulation, as shown by the increase in Car/Chl ratio. Car composition analyzed by HPLC showed the rise especially of anteraxanthin and zeaxanthin, suggesting the presence of an active violaxanthin cycle in *K. antarctica* (Table 1B). The content of other Car was either roughly constant (lutein and β-carotene) or even decreased (neoxanthin and lutein epoxide) in HLc. The presence of large amounts of lutein epoxide in LL acclimated cells suggested the existence of a second xanthophyll cycle, as found in some shade adapted plants (Matsubara et al., 2003, 2007). The modifications in composition of the

photosynthetic apparatus have been assessed also through Western blot analyses. As presented in Figure 2A LHCII showed a relative decrease in HLc, suggesting a reduction in antenna size. On the contrary LHCSR, a LHC-like protein known to be involved in the activation of NPQ, was slightly increased under the higher irradiance. RuBisCO, the enzyme catalyzing the rate limiting step for carbon fixation, had an increased signal in HLc supporting the idea that this alga was capable of acclimating to different light conditions by modulating its ability to fix carbon dioxide. This was confirmed by measuring qP, a fluorescence parameter which allows estimating photochemical efficiency (Maxwell and Johnson, 2000; Baker, 2008). When all absorbed energy is exploited for photochemistry the value of qP is 1, while when photosynthesis is saturated qP tends to 0. The qP dependence from actinic light intensity was monitored in different cultures and data in Figure 2B show that HLc upon illumination had a higher qP in comparison with those of culture grown under lower light intensity where photosynthesis was saturated sooner. This result clearly suggested that cells adapted to high light could exploit a larger fraction of incident light for photochemistry compared with cells acclimated to low light.

Table 1. Photosynthetic pigment composition of *K. antarctica* cells acclimated to LL and HL. Values are reported as mean ± SD (n=6). B) Car composition expressed as percentage of total car (n=4).

A	LL	HL
Chl ($a+b$) (mg g^{-1})	3.75 ± 0.26	0.93 ± 0.17
Chl a/b	2.08 ± 0.03	2.49 ± 0.16
Car/Chl	0.21 ± 0.01	0.35 ± 0.03

B	LL	HL
Neoxanthin	11.89 ± 1.55	7.83 ± 0.90
Violaxanthin	14.18 ± 2.06	13.94 ± 1.73
Lutein epoxide	4.74 ± 1.03	1.31 ± 0.29
Anteraxanthin	0.92 ± 0.73	6.92 ± 0.73
Lutein	53.30 ± 1.86	57.33 ± 0.89
Zeaxanthin	1.60 ± 0.32	4.89 ± 0.99
β-Carotene	12.12 ± 5.32	9.08 ± 0.66

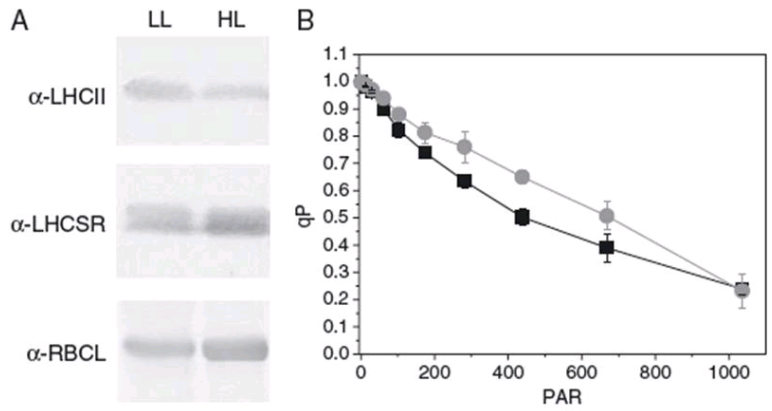

Figure 2. (A) Western blot analyses of LHCII, LHCSR protein and RuBisCO in LL and HL acclimated *K. antarctica* cells. Samples were loaded in gels on the base of chlorophyll contents. The experiment was repeated four times. (B) Dependence of photochemical activity (evaluated by the fluorescence parameter qP) from incident light in *K. antarctica* acclimated to LL (black square) and HL (gray circles) (n=4).

4. FASTER PHOTOPROTECTIVE MECHANISMS IN *KOLIELLA ANTARCTICA*

NPQ Regulation of photosynthesis in respect to environmental conditions does not only involve acclimation and modulation of photosynthetic apparatus composition, but also include other mechanisms activated in a shorter timescale such as NPQ. *Koliella antarctica* ability to activate a NPQ response was monitored in both LL and HL acclimated cells. As shown in Figure 3A we observed a strong NPQ response in both conditions, as shown by the comparison with the kinetics for the model plant *A. thaliana*. It is clear that the response by *K. antarctica* was more intense even if actinic light employed during the measurement was lower than for plants (540 vs 1200 μE m^{-2} s^{-1}). While a significant NPQ response was present in *K. antarctica* constitutively, HLc cells showed a further major increase suggesting the ability to modulate this response in different environmental conditions. It is also important to underline that such a strong NPQ was not due to photoinhibition during measurements, but was mostly represented by the fastest qE component that is rapidly deactivated after a few seconds in the dark. This suggests that *K. antarctica* is capable of activating a strong NPQ and dissipate a large fraction of absorbed energy as heat in a few seconds after the exposure to strong illumination.

Although it took several weeks for LLc cells to acclimate to HL by altering their morphology and Chl content, when LLc cells were moved to stronger illumination for few hours NPQ response intensity was increased very fast reaching values close to the ones found in HLc cells after only 8 h of exposition (Figure 3B). This suggests that one of the first responses by cells to stronger illumination exposition is the enhancement of NPQ ability. It is also interesting to point out that we observed no increase in LHCSR (Figure 3C) in this timeframe, while on the contrary antheraxanthin and zeaxanthin content rapidly increased and reached the content of HLc cells (Figure 3D), suggesting that this may be correlated with the observed NPQ increase.

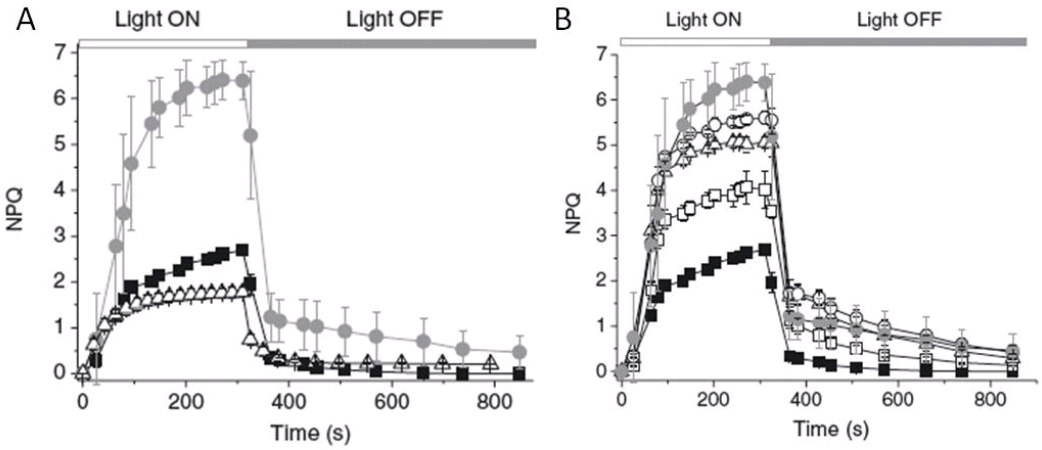

	4h	8h
Neoxanthin	11.57 ± 0.04	7.92 ± 0.91
Violaxanthin	5.27 ± 1.20	6.06 ± 1.14
Lutein epoxide	1.74 ± 0.70	1.28 ± 0.39
Anteraxanthin	6.56 ± 0.82	7.62 ± 1.59
Lutein	56.64 ± 1.11	56.49 ± 1.02
Zeaxanthin	3.63 ± 0.89	4.45 ± 0.71
β-carotene	13.58 ± 3.00	12.18 ± 2.98

Figure 3. A) NPQ kinetics in LL and HL acclimated cells. Fluorescence kinetics of cells acclimated to different light conditions in their exponential growth phase have been measured using an actinic light of 540 µE m^{-2} s^{-1}. NPQ kinetics for LL (black squares), HL (gray circles). Arabidopsis thaliana is also reported in white triangles as comparison (n=4). B) NPQ kinetics after 4 h (white squares), 8 h (white triangles) and 24 h (white circles) exposure of LLc to HL. Kinetics are compared with those of LL (black squares) and HL (gray circles) acclimated cells (n=4). (C) Western blotting against LHCSR showing no increased expression of this protein during the first 8 h of HL exposure. The experiment was repeated three times. (D) Percentages of carotenoid composition of LLc exposed for 4 and 8 h to HL (n=3).

Antheraxanthin and zeaxanthin are well known to have an enhancing effect in NPQ in several organisms both algae and plants (Goss et al., 1998; Niyogi et al., 1998; Pinnola et al., 2013). Results presented above suggested an influence of zeaxanthin in NPQ activation in *K. antarctica*. On the contrary, there was no observable conversion of lutein epoxide into lutein, suggesting a little influence of this second xanthophyll cycle in NPQ kinetics.

In conclusion *K. antarctica*, despite its very low growth rate, showed high plasticity in the regulation of its photosynthetic apparatus allowing the survival in its harsh environment. This plasticity is represented by the ability to acclimate to different illumination intensities with effects on pigments, protein content and morphology, but also the ability to activate a particularly strong NPQ, which allowed for an efficient response to fast fluctuations in illumination.

References

Andreoli, C., Moro, I., and Rocca, N. La (2000). Ecological, physiological, and biomolecular surveys on microalgae from Ross Sea (Antarctica). Ital. J. ….

ANDREOLI, C., S, S., C, G., and L, S. (1991). A preliminary survey on a Green Microalga of the Antarctic Sea. G. Bot. Ital. **125**: 959–960.

Anesio, A.M. and Laybourn-Parry, J. (2012). Glaciers and ice sheets as a biome. Trends Ecol. Evol. **27**: 219–25.

Arrigo, K.R., Mills, M.M., Kropuenske, L.R., van Dijken, G.L., Alderkamp, A.-C., and Robinson, D.H. (2010). Photophysiology in two major southern ocean phytoplankton taxa: photosynthesis and growth of Phaeocystis antarctica and Fragilariopsis cylindrus under different irradiance levels. Integr. Comp. Biol. **50**: 950–66.

Baker, N.R. (2008). Chlorophyll fluorescence: a probe of photosynthesis in vivo. Annu. Rev. Plant Biol. **59**: 89–113.

Baldisserotto, C. and Ferroni, L. (2005). Dark-acclimation of the chloroplast in Koliella antarctica exposed to a simulated austral night condition. Arctic, Antarct. ….

Fogliano, V., Andreoli, C., and Martello, A. (2010). Functional ingredients produced by culture of Koliella antarctica. Aquaculture.

Goss, R., Böhme, K., and Wilhelm, C. (1998). The xanthophyll cycle of Mantoniella squamata converts violaxanthin into antheraxanthin but not to zeaxanthin: consequences for the mechanism of enhanced non-photochemical energy dissipation. Planta **205**: 613–621.

Li, Z., Wakao, S., Fischer, B.B., and Niyogi, K.K. (2009). Sensing and responding to excess light. Annu. Rev. Plant Biol. **60**: 239–60.

Matsubara, S., Morosinotto, T., Bassi, R., Christian, A.-L.L., Fischer-Schliebs, E., Lüttge, U., Orthen, B., Franco, A.C., Scarano, F.R., Förster, B., Pogson, B.J., and Osmond, C.B. (2003). Occurrence of the lutein-epoxide cycle in mistletoes of the Loranthaceae and Viscaceae. Planta **217**: 868–879.

Matsubara, S., Morosinotto, T., Osmond, C.B., and Bassi, R. (2007). Short- and long-term operation of the lutein-epoxide cycle in light-harvesting antenna complexes. Plant Physiol. **144**: 926–941.

Maxwell, K. and Johnson, G.N. (2000). Chlorophyll fluorescence - A practical guide. J. Exp. Bot. **51**: 659–668.

Mock, T. and Valentin, K. (2004). PHOTOSYNTHESIS AND COLD ACCLIMATION: MOLECULAR EVIDENCE FROM A POLAR DIATOM1. J. Phycol.

Niyogi, K.K., Grossman, A.R., and Björkman, O. (1998). Arabidopsis mutants define a central role for the xanthophyll cycle in the regulation of photosynthetic energy conversion. Plant Cell **10**: 1121–1134.

Pinnola, A., Dall'Osto, L., Gerotto, C., Morosinotto, T., Bassi, R., and Alboresi, A. (2013). Zeaxanthin binds to light-harvesting complex stress-related protein to enhance nonphotochemical quenching in Physcomitrella patens. Plant Cell **25**: 3519–34.

Takahashi, S. and Murata, N. (2008). How do environmental stresses accelerate photoinhibition? Trends Plant Sci.

Thomas, D.N. and Dieckmann, G.S. (2002). Antarctic Sea ice--a habitat for extremophiles. Science **295**: 641–4.

APPENDIX

GENERATION OF RANDOM MUTANTS TO IMPROVE LIGHT-USE EFFICIENCY OF *NANNOCHLOROPSIS GADITANA* CULTURES FOR BIOFUEL PRODUCTION

Giorgio Perin[1], Alessandra Bellan[1,2], Anna Segalla[1], Andrea Meneghesso[1], Alessandro Alboresi[1] and Tomas Morosinotto[1]

*Correspondence: tomas.morosiotto@unipd.it
[1] Dipartimento di Biologia, Università di Padova, Via U. Bassi 58/B, 35121 Padua, Italy

Perin *et al. Biotechnol Biofuels (2015) 8:161* DOI 10.1186/s13068-015-0337-5

Abstract

Background: The productivity of an algal culture depends on how efficiently it converts sunlight into biomass and lipids. Wild-type algae in their natural environment evolved to compete for light energy and maximize individual cell growth; however, in a photobioreactor, global productivity should be maximized. Improving light use efficiency is one of the primary aims of algae biotechnological research, and genetic engineering can play a major role in attaining this goal.
Results: In this work, we generated a collection of Nannochloropsis gaditana mutant strains and screened them for alterations in the photosynthetic apparatus. The selected mutant strains exhibited diverse phenotypes, some of which are potentially beneficial under the specific artificial conditions of a photobioreactor. Particular attention was given to strains showing reduced cellular pigment contents, and further characterization revealed that some of the selected strains exhibited improved photosynthetic activity; in at least one case, this trait corresponded to improved biomass productivity in lab-scale cultures.
Conclusions: This work demonstrates that genetic modification of N. gaditana has the potential to generate strains with improved biomass productivity when cultivated under the artificial conditions of a photobioreactor.

Keywords:
Photosynthesis, Nannochloropsis, Mutants, EMS, Insertional mutagenesis, Biodiesel, Algae

This article was published in Biotechnology for Biofuels.

LIGHT REMODELS LIPID BIOSYNTHESIS IN NANNOCHLOROPSIS GADITANA BY MODULATING CARBON PARTITIONING BETWEEN ORGANELLES

Alessandro Alboresi[1*], Giorgio Perin[1*], Nicola Vitulo[3], Gianfranco Diretto[4], Maryse Block[2], Juliette Jouhet[2], Andrea Meneghesso[1], Giorgio Valle[3], Giovanni Giuliano[4], Eric Maréchal[2] and Tomas Morosinotto[1]

[1]PAR-Lab_Padua Algae Research Laboratory, Department of Biology, University of Padova, Via U. Bassi 58/B, 35121 Padova, Italy
[2]Laboratoire de Biologie Cellulaire et Végétale, UMR 5168 CNRS – CEA - INRA – Université Grenoble Alpes, BIG, CEA-Grenoble, 17 rue Des Martyrs, 38054 Grenoble, Cedex 9, France
[3]Innovative Biotechnologies Interdepartmental Research Center (CRIBI), University of Padova, Via U. Bassi 58/B, 35121 Padova, Italy
[4]Italian National Agency for New Technologies, Energy, and Sustainable Development (ENEA), Casaccia Research Centre, Via Anguillarese 301, 00123 Roma, Italy

Abstract

The seawater microalga *Nannochloropsis gaditana* is capable of accumulating a large fraction of reduced carbon as lipids. To clarify the molecular bases of this metabolic feature, we investigated light-driven lipid biosynthesis in *Nannochloropsis gaditana* cultures combining the analysis of photosynthetic functionality with transcriptomic, lipidomic and metabolomic approaches.
Light-dependent alterations are observed in amino acid, isoprenoid, nucleic acid and vitamin biosynthesis, suggesting a deep remodeling in the microalgal metabolism triggered by photoadaptation. In particular, high light intensity is shown to affect lipid biosynthesis, inducing the accumulation of diacylglyceryl-N,N,N-trimethylhomoserine (DGTS) and triacylglycerols (TAGs), together with the up-regulation of genes involved in their biosynthesis. Concurrently, chloroplast polar lipids are instead decreased. This situation correlates with the induction of genes coding for a putative cytosolic fatty acid synthase of type 1 (*FAS1*) and polyketide synthase (*PKS*) and the downregulation of the chloroplast fatty acid synthase of type 2 (*FAS2*). Lipid accumulation is accompanied by the regulation of triose phosphate/inorganic phosphate transport across the chloroplast membranes, tuning the carbon metabolic allocation between cell compartments, favoring the cytoplasm and endoplasmic reticulum at the expense of the chloroplast.
These results highlight the high flexibility of lipid biosynthesis in *Nannochloropsis gaditana* and also indicate a mechanism for the regulation of primary carbon partitioning by controlling metabolite allocation at the sub-cellular level.

This paper has been submitted in PLOS BIOLOGY

ABBREVIATIONS

^{1}Chl*: singlet Chl excited molecules

$^1O_2$: singlet oxygen

^{3}Chl*: Chl triplets

AEF, alternative electron flow;

Arabidopsis, A. thaliana, At: Arabidopsis thaliana;

Car, Carotenoid;

CEF, cyclic electron flow;

Chl, Chlorophyll;

Chlamydomonas, C. reinhardtii: Chlamydomonas reinhardtii.

Cyt, Cytochrome;

DBMIB, dibromothymoquinone;

DCMU, 3-(3,4-dichlorophenyl)-1,1-dimethylurea;

DTT, dithiotreitol;

ECS; electrochromic shift;

ETR, electron transport rate;

F_0, minimal fluorescence of dark adapted sample;

Fd, ferredoxin;

FDP, flavodiiron protein;

FLV, flavodiiron;

Fm, maximal fluorescence of dark adapted sample

Fm', maximal fluorescence of light exposed sample

FNR, Ferredoxin NADP+ reductase;

Fv/Fm, ratio between variable fluorescence and maximal fluorescence of dark adapted sample

KO, knock-out;

Koliella, K. antarctica: Koliella antarctica

HA, hydroxylamine;

LEF, linear electron flow;

LHC, Light harvesting complex;

Lhca, antenna polypeptides of Photosystem I;

Lhcb, antenna polypeptides of Photosystem II;

LHCI, antenna system of Photosystem I;

LHCII, Major antenna complex of Photosystem II;

LHCF, FCP fucoxanthin chlorophyll a/c-binding protein;

LHCSR, Lhc-like protein Stress Related (previously called Li818).

Nannochloropsis, N. gaditana: Nannochloropsis gaditana;

NPQ, Non Photochemical Quenching;

P700, chl a special pair in PSI;

P680, chl a special pair in PSII;

PC, plastocyanin;

PGR5, Proton Gradient Regulation 5;

PGRL1, PGR5-Like 1;

Physcomitrella, P. patens; Pp: Physcomitrella patens;

PQ/PQH2, plastoquinone/plastoquinol;

PSBS photosystem II subunit S;

PSII (PSI): photosystem II (I);

qE, Energy-dependent component of NPQ*;*

qI, photo-Inhibitory quenching*,* component of NPQ*;*

qT, component of NPQ related to State transition

ROS, Reactive oxygen species;

RuBisCO, ribulosio 1,5biphosphate carbossilase-oxygenase*;*

S_L and S_D, slope of ECS signal during and after light treatment;

TEF, total electron flow;

TAP, Tris-Acetate-Phosphate medium;

TMP, Tris-Minimal-Phosphate medium;

VDE, Violaxanthin de-epoxidase*;*

viola, violaxanthin;

WB, western blot;

WT, wild type.

YII or ϕPSII, quantum yield of Photosystem II;

ZE, Zeaxanthin epoxidase

zea, zeaxanthin;

ΔpH: pH gradient